SRR-CWDA-2016-00004
Revision 1

Comment Response Matrix for U.S. Nuclear Regulatory Commission Staff Request for Additional Information on the Fiscal Year 2014 Special Analysis for the Saltstone Disposal Facility at the Savannah River Site

March 2016

Prepared by: Savannah River Remediation LLC
Waste Disposal Authority
Aiken, SC 29808

Prepared for U.S. Department of Energy Under Contract No. DE-AC09-09SR22505

APPROVALS

Preparer:

_____ _____

David Watkins Date
Waste Disposal Authority (WDA) Closure and Disposal Assessments
Savannah River Remediation LLC

Reviewer (per S4 ENG.51):

_____ _____

Steve Hommel Date
WDA Closure and Disposal Determinations
Savannah River Remediation LLC

Management Review:

_____ _____

Kent Rosenberger Date
WDA Closure and Disposal Assessments
Savannah River Remediation LLC

REVISION SUMMARY

REV. #	DESCRIPTION	DATE OF ISSUE
0	Initial Issue	February 2016
1	Revision to address comments from DOE-SR	March 2016

TABLE OF CONTENTS

LIST OF FIGURES

LIST OF TABLES

ACRONYMS/ABBREVIATIONS

ALARA	As Low As Reasonably Achievable
CBP	Cementitious Barriers Partnership
CC	Clarifying Comment
CFR	Code of Federal Regulations
CPT	Cone Penetrometer Test
DLL	Dynamic Link Library
DO	Dissolved Oxygen
DOE	U.S. Department of Energy
DSP	Disposal Structure Performance
EIS	Environmental Impact Statement
FDC	Future Disposal Cell
FFT	Far-Field Transport
FTF	F-Area Tank Farm
FTR	Fractional Transfer Rate
FY	Fiscal Year
GCL	Geosynthetic Clay Liner
GSA	General Separations Area
GUI	Graphic User Interface
GWB	Geochemist's Workbench
HDPE	High Density Polyethylene
HELP	Hydrologic Evaluation of Landfill Performance
HTF	H-Area Tank Farm
IEC	Infiltration and Erosion Control
K_d	Sorption Coefficient
LAZ	Lower Aquifer Zone of the Upper Three Runs Aquifer
MOP	Member of the Public
MSL	Mean Sea Level
NDAA	Ronald W. Reagan National Defense Authorization Act for Fiscal Year 2005
NERP	National Environmental Research Park
NRC	U.S. Nuclear Regulatory Commission
PA	Performance Assessment
PAM	Performance Assessment Method
RAI	Request for Additional Information

SA	Special Analysis
SDF	Saltstone Disposal Facility
SDU	Saltstone Disposal Unit
SP	Saltstone Performance
SRNL	Savannah River National Laboratory
SRS	Savannah River Site
SZ	Saturated Zone
TCCZ	Tan Clay Confining Zone
TER	Technical Evaluation Report
UAZ	Upper Aquifer Zone of the Upper Three Runs Aquifer
UMM	Upper Mud Mat
UTR	Upper Three Runs
UZ	Unsaturated Zone
WDA	Waste Disposal Authority

EXECUTIVE SUMMARY

The *Performance Assessment for the Saltstone Disposal Facility at the Savannah River Site* (SRR-CWDA-2009-00017) was prepared to inform decisions regarding the pertinent requirements of the U.S. Department of Energy's (DOE) Manual 435.1-1, *Radioactive Waste Management,* and *Title 10 Code of Federal Regulations* (CFR) *Part 61, Licensing Requirements for Land Disposal of Radioactive Waste,* Subpart C as required by the *Ronald W. Reagan National Defense Authorization Act for Fiscal* (FY) *Year 2005* (NDAA), Section 3116 (NDAA_3116). Requirements in DOE M 435.1-1 and 10 CFR 61 stipulate that a PA should provide reasonable expectation/assurance that disposal of low-level waste will comply with specified performance objectives. DOE M 435.1-1 also requires assessments for impacts to water resources.

The Saltstone Disposal Facility (SDF) Performance Assessment (PA) serves as the primary long-term risk assessment tool to determine that performance objectives will be met following closure of the SDF. The SDF PA is a performance-based, risk-informed analysis of the fate and transport of SDF waste following final closure of SDF. The DOE used what is referred to as a "hybrid approach" involving a combination of deterministic and probabilistic models to develop this level of assurance. The foundation of the SDF assessment is the "Base Case" model, a deterministic analysis of post-SDF closure that utilizes the most probable and defensible values for the parameters within the SDF PORFLOW model whenever possible. This deterministic analysis produces a single discrete value at each point of assessment that, in turn, can be compared directly to the DOE M 435.1-1 and10 CFR 61.41 performance objective of 25 mrem/yr peak dose and the 10 CFR 61.42 inadvertent intruder dose. The understanding of the results of the SDF PA is further enhanced through an extensive series of uncertainty analyses and sensitivity analyses.

The deterministic Base Case of the SDF PA was developed using reasonably conservative, best-estimate assumptions (i.e., most probable modeling parameters) whenever possible. As a hybrid approach, the deterministic Base Case model is accompanied by the probabilistic model and deterministic alternative modeling cases, which are provided as tools to inform on uncertainty associated with the Base Case as a whole. These additional models employed assumptions that were possible on an individual assumption basis (although less probable than the Base Case and often non-mechanistic when coupled with other assumptions) to assess the effects of deviations from the Base Case assumptions. The fact that Base Case values have uncertainty associated with them does not *a priori* make them incorrect or any less probable. Substituting only pessimistic values for every assumption to account for uncertainty would undercut the intent of the Base Case in supporting risk-based decision making and would likely result in little, if any, real risk reduction, in needless expenditures, exposure to the current Savannah River Site (SRS) workforce, and delays in risk-reducing waste tank closure activities. The application of the hybrid approach to PA development (i.e., including a probabilistic model and deterministic alternative modeling cases) was to allow for the less probable, but still possible, assumptions to be modeled, improving overall understanding of the SDF system.

For the SDF system, DOE M 435.1-1 (page IV-11) requires PAs to "include calculations for a 1,000-year period after closure…" and a period of 10,000 years was utilized for

assessing/understanding long-term impacts of disposal operations as they relate to the 10 CFR 61, Subpart C performance objectives for future hypothetical members of the public and inadvertent intruders. To further account for variability and uncertainty regarding the timing of barrier failures, DOE provided extensive discussion on doses for periods up to 20,000 years following closure of the SDF and performed analyses beyond 20,000 years to gain a better understanding of the closed system performance and radionuclide transport.

As described above, in developing the deterministic Base Case assumptions, DOE sought to develop a conceptual model of the SDF system and surrounding General Separations Area (GSA) that reflects the best available or best estimate values, and includes reasonably conservative modeling assumptions and inventory assignments. In developing these values, DOE did not seek to create artificially pessimistic assumptions that bound possible, but not probable, scenarios. Instead, DOE sought a risk-informed analysis that provides information to feed critical closure decisions associated with the SDF.

In support of the development of the SDF PA, DOE has made a significant investment in parameter research and conceptual model development, utilizing nationally recognized experts in their respective fields including cementitious materials, hydrogeology, and modeling of environmental transport. The fate and transport modeling in the SDF PA reflects approximately 60 years of study of the subsurface of the GSA. It is this strong foundation of research and study that provides DOE reasonable expectation/assurance that the DOE M 435.1-1, as well as 10 CFR 61.41 and 10 CFR 61.42, performance objectives will be met.

Some perspective should be put on the 25 mrem/yr dose objective used to demonstrate compliance with the performance objectives for the protection of the general population from releases of radioactivity (DOE M 435.1 and 10 CFR 61.41). It should be noted that the average annual dose to a United States citizen in 2007 was 620 millirems, approximately 25 times higher than the performance objective. Figure ES-1 provides a breakdown of the exposure sources that make up the average dose of 620 millirems. If an individual moves from the area surrounding SRS to Denver, Colorado, their annual dose from just cosmic and terrestrial background radiation alone will increase by more than 100 millirem; a value four times the performance objective. [NCRP-160] Further, as noted in the U.S. Nuclear Regulatory Commission (NRC) Fact Sheet on Biological Effects on Radiation, “Those people living in areas having high levels of background radiation – above 1,000 mrem (10 mSv) per year – such as Denver, Colorado, have shown no adverse biological effects.” [NRC_01-01-2011] A background dose of 1,000 mrem/yr represents a dose 40 times greater than the performance objective.

Figure ES-1: Major Sources of Radiation Exposure to the Average US Citizen

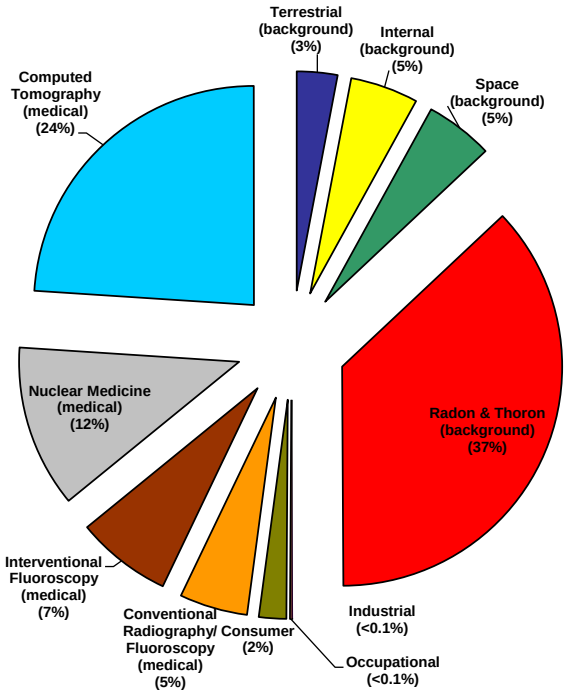

[NCRP-160]

DOE acknowledges that the PA and the associated Special Analyses (SAs) should contain adequate technical bases to support the Base Case (or Evaluation Case) being the most likely modeling case and that the PA should appropriately reflect uncertainties to demonstrate with reasonable expectation/assurance that the performance objectives can be met. DOE believes that the PA provides information regarding both the expected (i.e., probable) results (reflected in the Base Case analyses) and the alternative cases (reflected in the sensitivity analyses). The SDF system has defense-in-depth through multiple barriers that provide reasonable expectation/assurance that compliance with the performance objectives will be achieved. DOE clarifies that reasonable expectation/assurance is based on evaluations of how the facility is expected to perform as well as alternative system performance evaluations (i.e., less likely) that encompass uncertainty and variability (uncertainty and sensitivity analyses).

DOE M 435.1-1, *Radioactive Waste Management*, outlines a comprehensive program to maintain PAs. The program is in place to evaluate changes (e.g., new information, changing facility conditions) that could impact the inputs, results, or conclusions of a DOE PA such as the SDF PA. The program requires that PAs be formally reviewed on an annual basis and revised when changes in radionuclide inventories or facility design are identified or new information on key parameters becomes available through continued research and study. On an annual basis, the adequacy of the SDF PA is assessed and, when warranted, will be revised and shared with the NRC through the NDAA Section 3116(b) monitoring protocols.

Recently, two SAs have been developed as part of such PA maintenance. The first SA, the *FY2013 Special Analysis for the Saltstone Disposal Facility at the Savannah River Site* (hereinafter the FY2013 SDF SA), was developed to evaluate the significance of new

information or new analytical methods on the conclusions reached based on the approved SDF PA. [SRR-CWDA-2013-00062]

Following this, the *FY2014 Special Analysis for the Saltstone Disposal Facility at the Savannah River Site* (hereinafter the FY2014 SDF SA), was developed to reflect a change in future disposal unit design from 150-foot diameter future disposal cells to 375-foot diameter Saltstone Disposal Units (SDUs) (e.g., SDU 6). [SRR-CWDA-2014-00006] During development of the FY2014 SDF SA, the NRC provided a set of Requests for Additional Information (RAIs) and associated Clarifying Comments (CCs) based upon the FY2013 SDF SA, via the *U.S. Nuclear Regulatory Commission Staff Comments and Requests for Additional Information on the Fiscal Year 2013 Special Analysis for the Saltstone Disposal Facility at the Savannah River Site, SRR-CWDA-2013-00062, Revision 2*, dated June 13, 2014. [ML14148A153] In response to the RAIs on the FY2013 SDF SA, C*omment Response Matrix for NRC RAIs on the FY2013 SDF SA*, SRR-CWDA-2014-00099, was prepared and submitted to the NRC in January 2015 with individual responses from DOE. The responses also contained a series of recommendations for potential future work that could potentially further inform the model and understanding of the SDF disposal system with respect to the isolation of waste and future performance.

The NRC provided a set of RAIs and CCs based upon the FY2014 SDF SA, via the *U.S. Nuclear Regulatory Commission Staff Comments and Requests for Additional Information on the Fiscal Year 2014 Special Analysis for the Saltstone Disposal Facility at the Savannah River Site, SRR-CWDA-2014-00006, Revision 2*, dated June 26, 2015. [ML15161A541] This document provides detailed responses to these RAIs and CCs.

Each response begins with the RAI or CC from the NRC, followed by the DOE response.

PERFORMANCE ASSESSMENT METHODS (PAM)

PAM-1

PAM-1	**Question:** A new up-to-date analysis is needed for how the DOE demonstrates that doses to the off-site members of the public be maintained As Low As Reasonably Achievable (ALARA), as required by §61.41 (Protection of the General Population from Releases of Radioactivity).
	Basis: In Section 2.12.2 (NRC Evaluation – ALARA analysis) of the NRC 2012 SDF Technical Evaluation Report (TER), the NRC staff evaluated the DOE ALARA analysis using information from Section 5.7 (ALARA Analysis) of the DOE 2009 SDF Performance Assessment (2009 SDF PA) and the DOE responses to the NRC RAIs on the DOE 2009 SDF PA. That combined DOE ALARA analysis was based on information about the FDCs, PA models based on the FDCs, and dose calculations with an Evaluation Case using those PA models based on the FDCs. In Section 5.7 (ALARA Analysis) of the DOE FY13 SDF Special Analysis document, the DOE included that: "The ALARA information presented in the [2009] SDF PA is not affected by the new information presented in this [document]." It is not clear to the NRC staff how that could be true because the DOE FY13 SDF Special Analysis document supplements the DOE 2009 SDF PA, including new information about the FDCs, new radionuclide inventories in the FDCs, and new dose calculations with a new Evaluation Case based on the new information about the FDCs. In Section 5.7 (ALARA Analysis) of the DOE FY14 SDF Special Analysis document, the DOE included that: "The ALARA information presented in the [2009] SDF PA is not affected by the new information presented in this [document]." It is not clear to the NRC staff how that could be true because the DOE FY14 SDF Special Analysis document supplements both the DOE 2009 SDF PA and the DOE FY13 SDF Special Analysis document, including information about the 375-foot disposal structures, new radionuclide inventories in the FDCs, and new dose calculations with a new Evaluation Case based on both the FDCs and the 375-foot disposal structures.
	Path Forward: Provide the current DOE information that replaces the collection of information in the DOE ALARA analyses in: (1) Section 5.7 of the DOE 2009 SDF PA, (2) the DOE responses to the NRC RAIs on the DOE 2009 SDF PA, (3) Section 5.7 of the DOE FY13 SDF Special Analysis document, (4) the DOE 2015 Response to the NRC 2014 RAI Comments, and (5) Section 5.7 of the DOE FY14 SDF Special Analysis document. Without that current DOE ALARA analysis information, the NRC staff cannot make a determination in a TER about the DOE ALARA analysis.

DOE Response to PAM-1

Since the SDF PA was approved, DOE has issued a new DOE ALARA Handbook (*DOE Handbook, Optimizing Radiation Protection of the Public and the Environment for Use with DOE O 458.1, ALARA Requirements*, DOE-HDBK-1215-2014). The ALARA Handbook provides information to assist DOE program and field offices in understanding what is necessary and acceptable for implementing the ALARA provisions of *Radiation Protection of the Public and the Environment* (DOE O 458.1, Chg. 3). The ALARA Handbook identifies the goals,

requirements and issues that need to be addressed when developing ALARA analyses for optimization of various programs to support DOE's diverse missions.

According to the Director of the South Carolina Department of Health and Environmental Control, the "high level radioactive liquid waste stored [at the SRS] … poses the single largest environmental threat in South Carolina." [DHEC-OS-08-28-2013-01] The SDF is a key component in supporting the application of ALARA with respect to waste removal and treatment operations at the SRS tank farms. Liquid wastes removed from the tank farms undergo treatment processes (to separate high level wastes from low level wastes), and the low level wastes are sent to the SDF for permanent disposal. Therefore, the SDF actually functions as a feature of the radiation protection systems for the SRS tank farms. Regardless, rigorous ALARA processes are applied throughout the waste disposal processes according to the *SRS ALARA Program*, Manual SCD-6 and Manual E7-1, Procedure DE-DP-384, *ALARA Design Considerations and Reviews*.

Consistent with the *SRS ALARA Program*, an ALARA Design Review was completed to evaluate the design of SDU 6. [SRR-SDU-2012-00052; N-CLC-Z-00027] Based upon this analysis, specific operational controls shall be applied to mitigate risks to workers. These controls will begin at the start of waste disposal operations at SDU 6 and will continue as long as institutional controls remain in effect.

The following is an update to the SDF PA, Section 5.7:

DOE's approach to radiation protection for low level waste disposal is based on the performance objectives listed in DOE M 435.1-1, which specify maximum doses for various pathways, and on the ALARA principle, which requires doses to be maintained *"As Low As Reasonably Achievable."* The ALARA requirement in DOE M 435.1-1 states, "*Performance assessments shall include a determination that projected releases of radionuclides to the environment shall be maintained as low as reasonably achievable (ALARA).*"

The SRS has an ALARA program and processes established in company-level policies and procedures for the protection of workers that are well documented. [Manual SCD-6 and Manual E7-1, Procedure DE-DP-384] Some of the existing controls to minimize the dose to workers include the remote handling of materials, shielding transfer lines as well as utilizing structural shielding, and sampling of feed material to ensure activity limits are met. The goal of the ALARA process is attainment of the lowest practical dose after taking into account the social, technical, economic, and public policy considerations.

Depending on the situation, the ALARA analysis can range from simple qualitative statements evaluating different operation and disposal options to rigorous quantitative analyses that consider individual and collective doses to the member of the public (MOP). The rigor of the ALARA analysis should be commensurate with the magnitude of the calculated dose and the decisions to be made regarding the disposal facility.

An alternative to disposing of low level waste at the SDF is to ship the solidified saltstone waste offsite. Public perceptions and resulting concerns about shipping waste to an off-site facility have the potential to affect the social, political, and economic costs of such actions. Proposed actions that are considered unacceptable by an element of society often face significant opposition that increases the time and cost required to complete each step of the decision-making and implementation processes. This can lead to large cost-uncertainty associated with shipping

waste off-site. Therefore, any potential collective dose reduction from shipping the waste off-site is unlikely to outweigh the cost-benefits of processing and disposing of the salt solution waste stream on-site at the SDF.

Based on Table 9.0-1 of the FY2014 SDF SA, the estimated dose pathways evaluated in the FY2014 SDF SA in 1,000 years are less than the SDF PA and well below the performance objectives. In addition, the estimated dose pathways evaluated in the FY2014 SDF SA in 10,000 years are higher than the SDF PA but below the performance objectives. Therefore, a qualitative assessment of disposal alternatives is justified. Additionally, an in-depth ALARA cost-benefit analysis is not appropriate at this time, because the cost of new technology and personnel exposures will not be available until following final waste removal and salt processing operations. Furthermore, historic doses have been well below DOE administrative limits and have met very conservative ALARA goals. Future source terms (i.e., inventory) are expected to have low concentrations of key dose drivers.

The ALARA process is applied to the SDF in several ways: 1) making conservative assumptions when modeling SDF radionuclide inventory, releases, and dose to receptors, 2) evaluating disposal cell design and alternatives, and 3) evaluating and implementing alternative salt processing that could reduce the inventory disposed at SDF. Other technologies for salt processing that could potentially reduce the inventory disposed at the SDF will be evaluated as the technologies emerge.

Social, technical, economic and public policy aspects were most recently considered in the alternative processing analysis included in the Environmental Impact Statement (EIS) for salt processing alternatives. [DOE/EIS-0082-S2] In June 2001, DOE issued the EIS on salt processing alternatives. DOE studied four alternatives:

1. Small Tank Precipitation
2. Ion Exchange
3. Solvent Extraction
4. Direct Disposal in Grout

In 2006, DOE selected the “Solvent Extraction” as the preferred option with the best approach to minimize human health and safety risks associated with salt processing. [DOE/EIS-0082-S2-SA-01] This represents the best available technology to minimize the inventory sent to SDF.

Additional technologies continue to be studied for improvements or enhancements to salt waste processing. For example, the use of Next Generation Solvent has successfully demonstrated an increased decontamination factor for cesium (i.e., Cs-137 and Cs-135). [X-ESR-H-00665] Further, the formula for saltstone was specifically designed to incorporate reducing properties to retard the release of Tc-99.

In summary, the analysis of alternative salt processing techniques; the evaluation of emerging technologies for salt processing and disposal cell design; and meeting the performance objectives of DOE M 435.1-1 and 10 CFR 61 are all evidence of the application of ALARA in limiting the release of radionuclides into the environment. Therefore, the principle of ALARA is satisfied.

The 150-foot diameter SDUs (SDU 2A/2B, 3A/3B, and 5A/5B) were designed to improve the ALARA position of the SDF as compared to the construction of SDUs 1 and 4. The 150-foot diameter SDUs were built with the following ALARA-type design elements:

- Carbon steel walls to ensure watertight containment and designed to help prevent water seepage out of the concrete disposal units over the life of typical concrete water storage tanks
- Minimum 8-inch thick pre-cast walls of Class III sulfate resistant concrete
- Interior coating to mitigate sulfate attack from short-term saltstone bleed water penetration (through surface cracks and by capillary suction), and diffusion of sulfate from the pore fluid of the cured saltstone (such a coating should be chemical, radiation, pH, and hydroxide resistant)
- A geosynthetic clay liner (GCL) consisting of bentonite sandwiched between two geotextiles placed above and below the SDU (the bentonite is expected to remain mineralogically and chemically stable)
- A 100 mil High Density Polyethylene (HDPE) liner with hermetically sealed joints completely surrounding the Future Disposal Cell (FDC)
- 4 inches of Class III sulfate resistant concrete poured on top of the GCL-HDPE in order to protect the GCL-HDPE during construction

More details of the 150-foot diameter SDU design can be found in Section 3.2.1.3 of the SDF PA (referred to as FDCs). These construction details were included in the design of the 150-foot diameter SDUs and enhance the ALARA position of the SDF.

For the FY2014 SDF SA, a 375-foot diameter SDU design was considered. The 375-foot diameter SDUs are designed with the following ALARA-type design elements:

- Controlled compacted backfill soil base
- 4-inch thick lower concrete mud mat
- GCL consisting of a minimum 0.75 lbs/ft^2 sodium bentonite covered by a 100 mil HDPE liner above the lower mud mat
- 6-inch thick upper concrete mud mat
- 12-inch thick cast-in-place floor slab of Class III sulfate-resistant concrete
- Cast-in-place walls of Class III sulfate-resistant concrete having a minimum 10-inch thickness at the roof and 2-foot thickness at the floor
- Shotcrete on the exterior of the walls, reinforcing bar, and the layers of prestressing wire. The shotcrete is applied with a minimum thickness of one and a half to two inches
- Maximum 43 feet of saltstone or other cementitious waste form poured into the disposal unit through a roof penetration
- 12-inch thick roof of Class III sulfate-resistant concrete with a 1.5% slope (in place prior to the saltstone pour)

For the FY2014 SDF SA modeling, a 100-meter buffer zone surrounding SDF was evaluated after an institutional control period of 100 years. Conservatisms in the modeling are summarized in Section 7.2 of the SDF PA and are not revised in either the FY2013 SDF SA or the FY2014 SDF SA. In addition, SRS land use plans indicate that the current SRS boundaries will remain unchanged. Under this plan, the land will remain under the ownership of the federal

government, consistent with the site's designation as a National Environmental Research Park (NERP). In addition, the General Separations Area (GSA) is considered Industrial Use Only with no groundwater usage permitted. Thus, no MOP would have unrestricted access to the SDF. Because the SDF is a much greater distance (approximately five miles) from the site boundary than the 100-meter buffer zone, and groundwater potentially affected by releases from the SDF is completely intercepted by Upper Three Runs (UTR) and McQueen Branch, the FY2014 SDF SA modeling results demonstrate that protection of the public is provided to a much greater degree than the performance measures require. Considerably more dispersion of any radionuclides released to groundwater or air would occur if the closest access point to the disposal facility is SRS site boundary.

The design of future SDUs will be assessed for ALARA improvements, as appropriate, based on new operational and design information as it becomes available.

PAM-2

PAM-2	**Question:** Additional information is needed about parameter values sampled in higher-dose realizations of the uncertainty analysis.
	Basis: Figures 5.6.5-19 and 5.6.5-20 of the DOE FY14 SDF Special Analysis document showed peak doses to an offsite[1] member of the public within 10,000 and 50,000 years of site closure[2], respectively. The description for Figure 5.6.5-19 included that all of the higher-dose realizations between 1,200 and 2,000 years had sampled the highest parameter value for the initial hydraulic conductivity of saltstone. Many other dose peaks after 2,000 years approached 100 mrem/yr. The NRC staff needs to understand the parameters driving risk in those realizations to evaluate the system performance. Figure 5.6.5-20 showed several peak doses of approximately 3 rem/yr and the description included that those doses corresponded to cases in which most of the Technecium-99 (Tc-99) was retained well in saltstone until it was released suddenly. In addition, those cases generally corresponded to low Tc-99 solubility, average infiltration rates, best estimate degradation rates, and high water consumption. However, some of the vertical clusters grouped by degradation rate and infiltration rate spanned approximately two orders of magnitude. The NRC staff needs to understand if variations in the remaining two parameters (i.e., Tc-99 solubility and water consumption) accounted for the majority of that variability or if there were other significant variables that accounted for the higher dose peaks.
	Path Forward: Provide parameter values sampled for several of the greatest dose peaks shown in Figures 5.6.5-19 and 5.6.5-20 of the DOE FY14 SDF Special Analysis document with an explanation why the combinations of the parameter values sampled were unlikely (e.g., similar to the explanation in Section 5.6.4.3 of the DOE FY13 SDF Special Analysis document). For the peaks shown in Figure 5.6.5-19 of the DOE FY14 SDF Special Analysis document, indicate the greatest five (or more) realizations that did not sample the highest initial saturated hydraulic conductivity of saltstone and provide parameter values and an explanation describing those peaks.

DOE Response to PAM-2

This RAI response examines four subsets of data from the multi-realization uncertainty analysis described in Sections 5.6.4 and 5.6.5 of the FY2014 SDF SA. The first subset of data includes the five realizations that exhibited the highest peak doses within 10,000 years. The second subset is similar to the first, in that it presents five realizations that exhibited the highest peak doses within 10,000 years, except this subset excludes all realizations in which the highest initial saturated hydraulic conductivity was sampled. The third subset of data presents the five

[1] In the context of these RAIs and RAI responses, an "offsite member of the public" is a member of the public who makes use of water drawn from a well that is 100-meters from the SDF boundary, as opposed to a member of the public who resides beyond the Savannah River Site boundaries.

[2] In the context of these RAIs and RAI responses, "site closure" refers to facility closure of the Saltstone Disposal Facility and not the closure of the Savannah River Site.

realizations that exhibited the highest peak doses within the entire 50,000-year simulation. Finally, the fourth subset provides a closer examination of one of the "vertical clusters" (specifically, the peak doses that occur at 40,000 years) to identify which parameters are influencing the variability in magnitude of these peaks.

Subset 1: Highest Peak Doses within 10,000 Years

Table PAM-2.1 provides a summary of the five realizations that exhibited the highest peak doses within 10,000 years. Table PAM-2.2 presents a number of the significant parameter values that were sampled, followed by a discussion of how these values influenced these peak doses.

Table PAM-2.1: Summary of Realizations with Highest Peak Doses within 10,000 Years

Realization	Year of Peak Dose	Peak Dose (mrem/yr)	Highest Sector	Most Significant Dose Contributor(s)	Most Significant Dose Pathway(s)
1,176	1,630	145.7	B	I-129	Water Ingestion
1,277	1,500	140.3	B	I-129	Water Ingestion
967	1,500	130.0	K	I-129 and Tc-99	Water Ingestion
382	1,630	120.4	J	I-129 and Tc-99	Water Ingestion
244	1,510	104.0	K	I-129	Water Ingestion

Table PAM-2.2: Parameter Values Associated with Realizations with Highest Peak Doses within 10,000 Years

Parameter	FY2014 SDF SA Eval. Case	Realization				
		1,176	1,277	967	382	244
Saturated Hydraulic Conductivity of Saltstone (1 = 3.9E-10 cm/sec, 2 = 6.4E-09 cm/sec, 3 = 4.5E-07 cm/sec)	2	3	3	3	3	3
Infiltration Rate (1 = Minimum, 2 = Average, 3 = Maximum)	2	2	2	3	3	2
Degradation Rate of Cementitious Materials (1 = Nominal, 2 = Best Estimate)	1	2	1	1	1	2
Technetium Solubility (1 = 1.0E-09 mol/L, 2 = 1.0E-08 mol/L, 3 = 1.0E-07 mol/L)	2	2	2	3	3	1
Primary SDU(s)	**SDU 9**	**SDU 11**	**SDU 11**	**SDU 9**	**SDU 5B**	**SDU 9**
Primary SDU I-129 Inventory (Ci)	1.6	2.56	3.31	2.03	0.44	2.07
Primary SDU Tc-99 Inventory (Ci)	3,700	5,905	8,895	5,061	908	4,693
Secondary SDU	**SDU 6**	**SDU 10**	**SDU 4**	**SDU 6**	**SDU 3B**	**SDU 6**
Secondary SDU I-129 Inventory (Ci)	1.6	2.65	0.31	1.78	0.40	1.17
Secondary SDU Tc-99 Inventory (Ci)	3,700	5,323	640	4,101	908	2,658
Reduced Region II K_d, Iodine (mL/g)	9.0	3.123	2.476	4.016	12.5	2.303
Oxidized Region II K_d, Iodine (mL/g)	15.0	8.702	7.418	19.75	6.798	5.391
Oxidized Region III K_d, Iodine (mL/g)	4.0	2.093	1.849	2.731	3.499	3.338
UZ Thickness, 375-ft diam. SDUs (m)	12.8	9.896*	10.22*	14.75*	13.01	12.10*
UZ Thickness, 150-ft diam. SDUs (m)	12.8	10.64	13.96	13.45	16.52*	15.71
UZ Thickness, SDU 4 (m)	12.2	12.97	12.73	15.55	10.45	16.56
SZ Thickness (m)	20	14.96	16.67	24.95	17.16	16.67
SZ Width, 375-ft diam. SDUs (m)	114.3*	113.1*	124.6*	135.3*	134.2	112.8*
SZ Width, 150-ft diam. SDUs (m)	45.72	43.67	54.75	44.39	38.82*	48.95
SZ Width, SDU 4 (m)	182.8	215.1	160.6	202.2	217.9	199.2
Consumption of Water (Multiplier)	1.0	1.863	1.959	1.631	1.519	1.452

Note: Asterisk (*) indicates saturated zone (SZ) width and unsaturated zone (UZ) thickness that corresponds to the primary SDU.

Figure PAM.2-1 shows the doses to a hypothetical MOP at the 100-meter facility boundary for each of these realizations.

Figure PAM-2.1: MOP Dose from Realizations with Highest Peak Doses within 10,000 Years

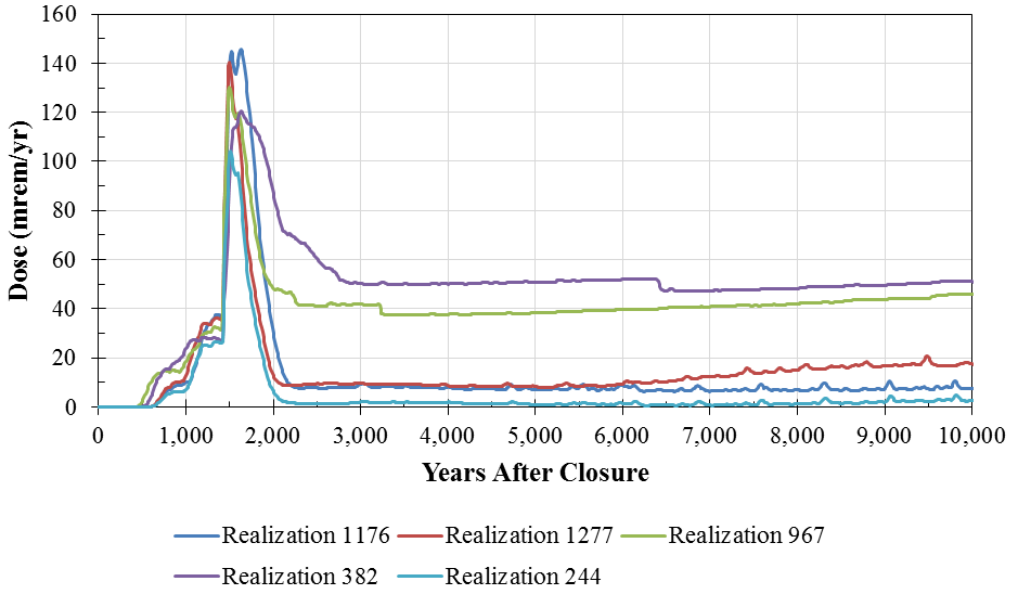

The following provides some additional analysis of each realization. This discussion demonstrates that the relatively high doses exhibited by each of these realizations relied on multiple variables sampling values that were not favorable to the overall system performance. As such, the cumulative impact exaggerates the respective dose peaks.

Realization 1,176

Realization 1,176 sampled the highest initial saturated hydraulic conductivity, which results in faster flow rates. The sampled I-129 inventory was 60% to 70% higher for both SDU 11 and SDU 10 (i.e., the Evaluation Case of the FY2014 SDF SA assumed 1.6 Ci in each SDU, whereas Realization 1,176 sampled 2.65 Ci and 2.56 Ci for these SDUs). All of the iodine cementitious K_ds for iodine were lower than the Evaluation Case (3.1 mL/g versus 9.0 mL/g in Reduced Region II; 8.7 mL/g versus 15 mL/g in Oxidized Region II; and 2.1 mL/g versus 4.0 mL/g in Oxidized Region III), resulting in significantly less retardation. The SZ thickness sampled was approximately 15 m (instead of the 20 m modeled in the Evaluation Case), which increases the concentration of the contaminant plume. Finally, the multiplier for the consumption of water was 1.863 (i.e., the water ingestion dose was increased by more than 85%).

Realization 1,277

Realization 1,277 sampled the highest initial saturated hydraulic conductivity, which results in faster flow rates. The sampled I-129 inventory in SDU 11 was more than double the Evaluation Case inventory (3.31 Ci versus 1.6 Ci), , such that more I-129 was available to contribute to the dose. All of the cementitious K_ds for iodine were lower than the Evaluation Case (2.5 mL/g versus 9.0 mL/g in Reduced Region II; 7.4 mL/g versus 15 mL/g in Oxidized Region II; and 1.8 mL/g versus 4.0 mL/g in Oxidized Region III), resulting in significantly less retardation. The SZ thickness sampled approximately 17 m (instead of the 20 m modeled in the Evaluation Case),

which increases the concentration of the contaminant plume. Finally, the multiplier for the consumption of water was 1.959 (i.e., the water ingestion dose was increased by almost 100%).

Realization 967

Realization 967 sampled the highest initial saturated hydraulic conductivity, which results in faster flow rates. The inventory in SDU 9 was moderately higher for I-129 (from 1.6 Ci in the Evaluation Case to 2.03 Ci in this realization) and for Tc-99 (from 3700 Ci to 5061 Ci). The highest technetium solubility (1.0E-07 mol/L) was sampled, which releases much more Tc-99 than the nominal solubility (1.0E-08 mol/L) assumed in the Evaluation Case, especially when coupled with the higher initial saturated hydraulic conductivity and the maximum infiltration rates (as sampled in this realization). The cementitious K_ds for iodine were lower than the Evaluation Case in Reduced Region II (4.0 mL/g versus 9.0 mL/g), resulting in less retardation. Finally, the multiplier for the consumption of water was 1.631 (i.e., the water ingestion dose increased by more than 60%).

Realization 382

Realization 382 sampled the highest initial saturated hydraulic conductivity, which results in faster flow rates. The highest technetium solubility (1.0E-07 mol/L) was sampled, which releases much more Tc-99. The sampled I-129 inventory was significantly higher for both SDU 5B and SDU 3B (in the Evaluation Case, both SDUs were assumed to have 0.096 Ci, whereas this realization sampled 0.44 Ci in SDU 5B and 0.40 Ci in SDU 3B), such that more I-129 was available to contribute to the dose. For the Tc-99 inventory, both of these SDUs sampled 908 Ci (which is also significantly higher than the 540 Ci assumed in the Evaluation Case), resulting in higher releases, especially when coupled with the higher initial saturated hydraulic conductivity and the maximum infiltration rates (as sampled in this realization). The Oxidized Region II K_d for iodine was lower than the Evaluation Case (6.8 mL/g versus 15 mL/g), resulting in significantly less retardation in saltstone. The SZ thickness sampled approximately 17 m (instead of the 20 m modeled in the Evaluation Case), which increases the concentration of the contaminant plume. Finally, the multiplier for the consumption of water was 1.519 (i.e., the water ingestion dose increased by more than 50%).

Realization 244

Realization 244 sampled the highest initial saturated hydraulic conductivity, which results in faster flow rates. The sampled I-129 inventory was higher for SDU 9 (2.07 Ci in Realization 244 versus 1.6 Ci in the Evaluation Case), such that more I-129 was available to contribute to the dose. All of the cementitious K_ds for iodine were lower than the Evaluation Case (2.3 mL/g versus 9.0 mL/g in Reduced Region II), resulting in significantly less retardation. The SZ thickness sampled was approximately 17 m (instead of the 20 m modeled in the Evaluation Case), which increases the concentration of the contaminant plume. Finally, the multiplier for the consumption of water was 1.452 (i.e., the water ingestion dose was increased by nearly 50%).

Summary of Subset 1 Data

Based on the data provided in Table PAM-2.2, some general observations can be made about these realizations:

- All of these realizations sampled the highest possible initial saturated hydraulic conductivity for saltstone (4.5E-07 cm/sec), resulting in higher flow rates.
- All of these realizations sampled from either the average infiltration rate or the maximum infiltration rate, which increased the flow rates.
- Most of the cementitious iodine K_ds sampled values that were one-half to one-third the values used in the Evaluation Case of the FY2014 SDF SA, resulting in decreased retardation.
- Most of the I-129 inventory values sampled from the relevant SDUs was significantly higher than the I-129 inventory values modeled in the Evaluation Case of the FY2014 SDF SA.
- The two realizations which showed significant Tc-99 dose contributions both sampled the highest possible technetium solubility (1.0E-07 mol/L), the maximum infiltration rate, the nominal cementitious degradation rate, and relatively high UZ thicknesses, indicating that this combination of parameters may influence Tc-99 releases in early times. Both also sampled higher Tc-99 inventories within the relevant SDUs.
- Four of the five realizations sampled smaller SZ thicknesses, which increased the concentration of the contaminant plume.
- The multipliers for water consumption indicated an increase in water consumption of 50% to 100% relative to the Evaluation Case of the FY2014 SDF SA.
- The peak doses for all of these realizations were driven by I-129 and the water ingestion pathway.

Subset 2: Highest Peak Doses within 10,000 Years, Excluding Realizations with Saturated Hydraulic Conductivity = 4.5E-07 cm/sec

Table PAM-2.3 provides a summary of the five realizations that exhibited the highest peak doses within 10,000 years when the data set is screened to exclude realizations with an initial saturated hydraulic conductivity of 4.5E-07 cm/sec. Note that none of these peak doses exceed 75 mrem/yr within 10,000 years of SDF closure. Table PAM-2.4 presents a number of the significant parameter values that were sampled, followed by a discussion of how these values influenced these peak doses.

Table PAM-2.3: Summary of Realizations with Highest Peak Doses within 10,000 Years (Excluding Realizations with High Initial Saturated Hydraulic Conductivity)

Realization	Year of Peak Dose	Peak Dose (mrem/yr)	Highest Sector	Most Significant Dose Contributor(s)	Most Significant Dose Pathway(s)
1,383	9,690	72.44	K	Tc-99	Produce Ingestion
913	5,390	69.36	K	I-129 and Tc-99	Water Ingestion
336	10,000	65.19	K	Tc-99	Water Ingestion
654	4,790	64.12	B	I-129 and Tc-99	Water Ingestion
1,363	10,000	60.25	K	Tc-99	Water and Produce Ingestion

Table PAM-2.4: Parameter Values Associated with Realizations with Highest Peak Doses within 10,000 Years (Excluding Realizations with High Initial Saturated Hydraulic Conductivity)

Parameter	FY2014 SDF SA Eval. Case	Realization				
		1,383	913	336	654	1,363
Saturated Hydraulic Conductivity of Saltstone (1 = 3.9E-10 cm/sec, 2 = 6.4E-09 cm/sec, 3 = 4.5E-07 cm/sec)	2	2	2	1	1	1
Infiltration Rate (1 = Minimum, 2 = Average, 3 = Maximum)	2	2	2	3	2	3
Degradation Rate of Cementitious Materials (1 = Nominal, 2 = Best Estimate)	1	1	1	1	1	1
Technetium Solubility (1 = 1.0E-09 mol/L, 2 = 1.0E-08 mol/L, 3 = 1.0E-07 mol/L)	2	3	3	3	3	3
Primary SDU(s)	**SDU 9**	**SDU 9**	**SDU 9**	**SDU 9**	**SDU 10**	**SDU 9**
Primary SDU I-129 Inventory (Ci)	1.6	1.74	4.51	1.11	2.87	1.87
Primary SDU Tc-99 Inventory (Ci)	3,700	4,336	10,500	2,695	7,031	4,471
Secondary SDU	**SDU 6**	**SDU 6**	**SDU 6**	**SDU 6**	**SDU 11**	**SDU 6**
Secondary SDU I-129 Inventory (Ci)	1.6	1.34	1.09	2.03	2.19	1.07
Secondary SDU Tc-99 Inventory (Ci)	3,700	3,627	2,738	4,433	5,614	2,906
Reduced Region II K_d, Iodine (mL/g)	9.0	11.04	10.19	12.85	4.56	11.38
Oxidized Region II K_d, Iodine (mL/g)	15.0	25.8	5.142	9.491	24.43	20.55
Oxidized Region III K_d, Iodine (mL/g)	4.0	5.139	2.348	3.649	5.945	4.099
UZ Thickness, 375-ft diam. SDUs (m)	12.8	15.42	14.39	12.94	11.58	15.26
SZ Thickness (m)	20	25.25	21.4	17.94	17.81	20.92
SZ Width, 375-ft diam. SDUs (m)	114.3	100.5	127.2	132.9	96.83	130.9
Consumption of Water (Multiplier)	1.0	0.4502	1.645	2.267	2.205	1.071
Consumption of Produce (Multiplier)	1.0	2.070	0.4314	1.272	0.3733	1.461
Soil-to-Plant Uptake Ratio	1.0	44.42	0.8043	1.826	0.1399	22.47

Figure PAM.2-2 shows the doses to a hypothetical MOP at the 100-meter facility boundary for each of these realizations.

Figure PAM-2.2: MOP Dose from Realizations with Highest Peak Doses within 10,000 Years (Excluding Realizations with High Initial Saturated Hydraulic Conductivity)

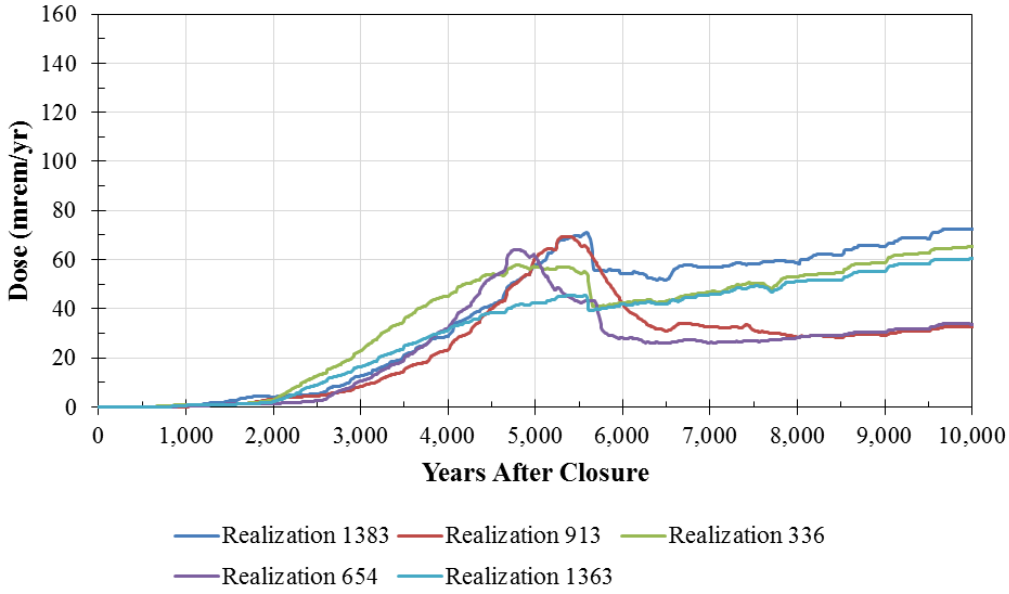

The following provides some additional analysis of each realization. This discussion demonstrates that the relatively high doses exhibited by each of these realizations relied on multiple variable sampling values that were not favorable to the overall system performance. As such, the cumulative impact exaggerates the respective dose peaks.

Realization 1,383

Realization 1,383 is a statistical outlier. Unlike most of the other realizations discussed, the peak dose for this realization is not dominated by the water ingestion pathway. Of the 72 mrem/yr peak dose, only about 8 mrem/yr is from the water ingestion pathway while 60 mrem/yr is attributed to the produce ingestion pathway. The multiplier for the soil-to-plant uptake ratio sampled a value near the extreme upper bound of the sampling range (44.42 on a geometric log-normal distribution with a mean of 1.0 and a maximum of 51.4). The probability of sampling a value this high for the soil-to-plant uptake ratio multiplier was less than 0.06%. The multiplier for the consumption of produce was also high (2.07). The probability of sampling this value was about 11%. Together, these parameters increase the produce ingestion dose pathway by a factor of 92 relative to what the dose would have been had the mean values been used.

This realization also sampled the highest technetium solubility (1.0E-07 mol/L), which releases much more Tc-99. The nominal degradation case was selected, which is conservative relative to the best estimate (or expected) cementitious degradation rate. The sampled Tc-99 inventory was higher for SDU 9 (4,336 Ci in Realization 1,383 versus 3,700 Ci in the Evaluation Case), such that more Tc-99 was available to contribute to the dose. The SZ width associated with SDU 9 is also 14% smaller; conceptually, the smaller width creates a “funneling” affect in which the mass occupies a smaller area, thus increasing the concentration of Tc-99.

Realization 913

Realization 913 also sampled the highest technetium solubility (1.0E-07 mol/L) and the nominal degradation rate. In SDU 9, the sampled I-129 and Tc-99 inventories were significantly higher than the values in the Evaluation Case (4.51 Ci of I-129 versus 1.6 Ci and 10,500 Ci of Tc-99 versus 3,700 Ci), such that more inventory was available to contribute to the dose. The oxidized cementitious K_ds for iodine were lower than the Evaluation Case (5.14 mL/g versus 15 mL/g for Oxidized Region II and 2.35 versus 4.0 for Oxidized Region III), resulting in less retardation in saltstone. Finally, the multiplier for the consumption of water was 1.645 (i.e., the water ingestion dose increased by more than 60%).

Realization 336

Realization 336 also sampled the highest technetium solubility (1.0E-07 mol/L), the nominal degradation rate and the maximum infiltration rate. Additionally, the multiplier for the consumption of water was 2.267 (i.e., the water ingestion dose was increased by more than 120%).

Realization 654

Realization 654 also sampled the highest technetium solubility (1.0E-07 mol/L) and the nominal degradation rate. In SDU 10, the sampled I-129 and Tc-99 inventories were significantly higher than the values modeled in the Evaluation Case (2.87 Ci of I-129 versus 1.6 Ci and 7,031 Ci of Tc-99 versus 3,700 Ci), such that more inventory was available to contribute to the dose. The SZ thickness sampled was approximately 18 m (instead of the 20 m modeled in the Evaluation Case), which increases the concentration of the contaminant plume. Finally, the multiplier for the consumption of water was 2.205 (i.e., the water ingestion dose was increased by more than 120%).

Realization 1,363

Realization 1,363 is a similar to 1,383, but with slightly less extreme sampling. As with Realization 1,383, the peak dose for Realization 1,363 has a significant dose from the produce ingestion pathway (about 28 mrem/yr); however, the contribution from water ingestion is still higher (about 30 mrem/yr). The multiplier for the soil-to-plant uptake ratio sampled a value near the extreme upper bound of the sampling range (22.47 on a geometric log-normal distribution with a mean of 1.0 and a maximum of 51.4). The probability of sampling a value this high for the soil-to-plant uptake ratio multiplier was about 0.8%. The multiplier for the consumption of produce was also higher than the mean (1.46 versus 1.0). Together, these parameters increase the produce ingestion dose pathway by a factor of 33 relative to what the dose would have been had the mean values been used.

Realization 1,363 also sampled the highest technetium solubility (1.0E-07 mol/L), the nominal degradation rate, and the maximum infiltration rate. The Tc-99 inventory for SDU 9 was 4,471 Ci compared to the 3,700 Ci used in the Evaluation Case model.

Summary of Set 2 Data

Based on the data provided in Table PAM-2.4, some general observations can be made about these realizations:

- All of these realizations sampled the highest possible technetium solubility (1.0E-07 mol/L), and most had increased Tc-99 inventories and high multiplier values for the consumption of water, all resulting in significant Tc-99 dose contributions.
- All of these realizations sampled from either the average infiltration rate or the maximum infiltration rate, resulting in increased flow rates.
- All of these realizations sampled the nominal rate for cementitious material degradation, which resulted in higher flow rates than the best estimate (expected) degradation rate.
- Four of the five realizations (Realizations 1,383, 913, 654, and 1,363) sampled significantly higher Tc-99 inventories within the relevant SDUs such that more inventory contributed to dose.
- Three of the five realizations (Realizations 1,383, 913, and 1,363) sampled UZ thicknesses that were significantly larger than the Evaluation Case. , indicating that the longer travel distance in the UZ may result in higher Tc-99 concentrations at the 100-meter boundary.
- Three of the five realizations (Realizations 913, 336, and 654) sampled high multipliers for water consumption resulting in significant increases in the water ingestion dose relative to the Evaluation Case of the FY2014 SDF SA.
- Two of the five realizations (Realizations 1,383 and 1,363) sampled extremely high soil-to-plant uptake ratios (more than an order of magnitude greater than the Evaluation Case) which combined with higher produce consumption multipliers to result in significantly increased produce ingestion doses.

Subset 3: Highest Peak Doses within 50,000 Years

Table PAM-2.5 provides a summary of the five realizations that exhibited the highest peak doses within 50,000 years. Table PAM-2.6 presents a number of the significant parameter values that were sampled, followed by a discussion of how these values influenced these peak doses.

Table PAM-2.5: Summary of Realizations with Highest Peak Doses within 50,000 Years

Realization	Year of Peak Dose	Peak Dose (mrem/yr)	Highest Sector	Most Significant Dose Contributor(s)	Most Significant Dose Pathway(s)
1,272	40,000	3,885	J	Tc-99	Water Ingestion
1,011	39,960	3,598	I	Tc-99	Water and Produce Ingestion
896	39,720	2,946	J	Tc-99	Water Ingestion
433	39,760	2,813	J	Tc-99	Water and Produce Ingestion
490	39,760	2,675	J	Tc-99	Water Ingestion

Table PAM-2.6: Parameter Values Associated with Realizations with Highest Peak Doses within 50,000 Years

Parameter	FY2014 SDF SA Eval. Case	Realization				
		1,272	1,011	896	433	490
Saturated Hydraulic Conductivity of Saltstone (1 = 3.9E-10 cm/sec, 2 = 6.4E-09 cm/sec, 3 = 4.5E-07 cm/sec)	2	1	1	2	2	2
Infiltration Rate (1 = Minimum, 2 = Average, 3 = Maximum)	2	2	2	2	2	2
Degradation Rate of Cementitious Materials (1 = Nominal, 2 = Best Estimate)	1	2	2	2	2	2
Technetium Solubility (1 = 1.0E-09 mol/L, 2 = 1.0E-08 mol/L, 3 = 1.0E-07 mol/L)	2	1	1	2	1	1
Primary SDU(s)	**SDU 3B**	**SDU 3B**	**SDU 3A**	**SDU 3B**	**SDU 3B**	**SDU 3B**
Primary SDU Tc-99 Inventory (Ci)	540	1,165	908	1,165	1,321	1,321
Secondary SDU	**SDU 5B**	**SDU 5B**	**SDU 5A**	**SDU 5B**	**SDU 5B**	**SDU 5B**
Secondary SDU Tc-99 Inventory (Ci)	540	269	908	195	313	427
UZ Thickness, 150-ft diam. SDUs (m)	12.8	12.70	13.81	11.71	14.67	14.14
SZ Darcy Velocity (Multiplier)	1.0	0.7984	1.137	0.9443	0.8832	0.8748
SZ Thickness (m)	20	19.68	17.10	17.95	20.63	15.88
SZ Width, 150-ft diam. SDUs (m)	45.72	41.41	40.90	49.09	43.17	39.46
Consumption of Water (Multiplier)	1.0	2.269	2.225	2.290	1.119	1.412
Consumption of Produce (Multiplier)	1.0	2.377	1.720	2.269	2.295	1.282
Soil-to-Plant Uptake Ratio	1.0	0.929	6.504	0.9358	3.955	0.7169

Figure PAM.2-3 shows the doses to a hypothetical MOP at the 100-meter facility boundary for each of these realizations. Essentially, all five realizations show doses that overlap. To better discern the differences between these realizations, Figure PAM.2-4 expands the relevant time frame and presents the doses on a logarithmic scale. Note that for the first 30,000 years, none of these realizations exceed 20 mrem/yr.

Figure PAM-2.3: MOP Dose from Realizations with Highest Peak Doses within 50,000 Years

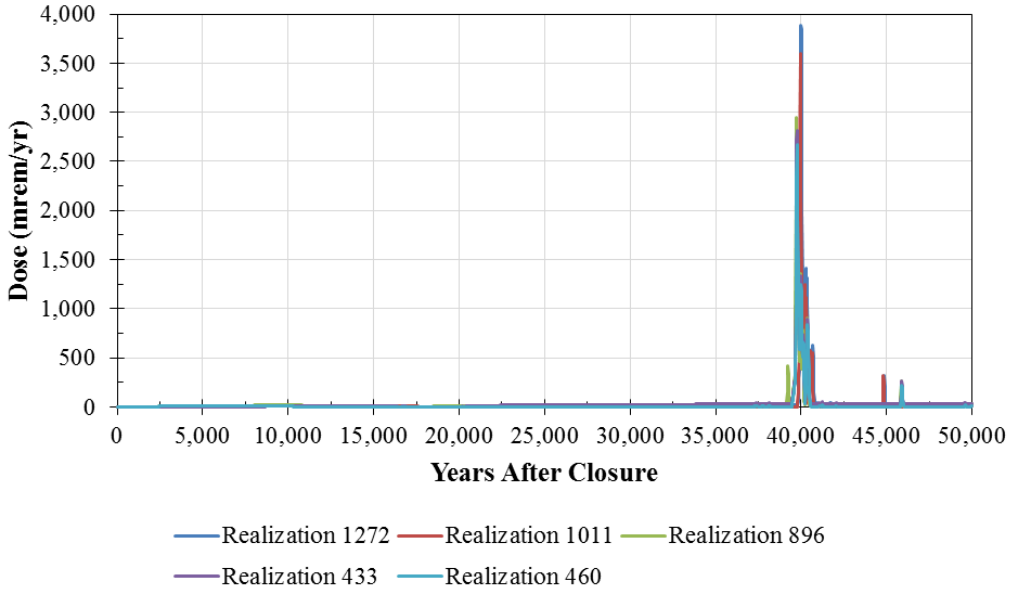

Figure PAM-2.4: MOP Dose from Realizations with Highest Peak Doses within 50,000 Years (Expanded)

The following provides some additional analysis of each realization. This discussion demonstrates that these relatively high doses relied on multiple variable sampling values that were not favorable to the overall system performance. As such, the cumulative impact exaggerates the respective dose peaks.

Realization 1,272

Realization 1,272 sampled the lowest initial saturated hydraulic conductivity and the best estimate degradation rate for cementitious materials. Additionally, the lowest technetium solubility was sampled. This combination significantly reduces the amount of water flow through the saltstone, such that only a minimal amount of Tc-99 is released prior to the "spike" that occurs once the lowest layer of saltstone become oxidized. SDU 3B contains more Tc-99 inventory which contributes to the spike once the significant release event occurs. The inventory in SDU 3B was 1,165 Ci of Tc-99 versus the 540 Ci used in the Evaluation Case. The SZ Darcy velocity multiplier was approximately 0.80, indicating a 20% reduction in the rate of groundwater flow through the SZ. This slows down the transport of Tc-99, such that higher concentrations build up near the 100-meter boundary. The SZ width associated with the 150-foot diameter SDUs is about 10% smaller than the Evaluation Case of the FY2014 SDF SA (41.4 m versus 45.7 m, respectively); conceptually, the smaller width creates a "funneling" affect in which the mass occupies a smaller area, thus increasing the concentration of Tc-99. Finally, the multiplier for the consumption of water was 2.269 (i.e., the water ingestion dose was increased by more than 120%).

Note that the increase in the multiplier for the consumption of produce (2.377 versus 1.0) had a negligible impact relative to the total dose, which was dominated by the water ingestion pathway.

Realization 1,011

Realization 1,011 sampled the lowest initial saturated hydraulic conductivity and the best estimate degradation rate for cementitious materials. Additionally, the lowest technetium solubility was sampled. Together, this combination significantly reduces the amount of water flow through the saltstone, such that only a minimal amount of Tc-99 is released prior to the "spike" that occurs once the lowest layer of saltstone becomes oxidized. The relevant SDUs contain more Tc-99 inventory which contributes to the spike once the significant release event occurs. The inventory in both SDUs (3A and 5A) was sampled at 908 Ci of Tc-99 each, versus the 540 Ci used in the Evaluation Case. The SZ width associated with the 150-foot diameter SDUs is about 11% smaller than the Evaluation Case of the FY2014 SDF SA (40.9 m versus 45.7 m, respectively); conceptually, the smaller width creates a "funneling" affect in which the mass occupies a smaller area, thus increasing the concentration of Tc-99. The SZ thickness sampled approximately 17 m (instead of the 20 m modeled in the Evaluation Case), which increases the concentration of the contaminant plume. The multiplier for the consumption of water was 2.225 (i.e., the water ingestion dose was increased by more than 120%).

In addition, the soil-to-plant uptake ratio sampled a high value (6.504 versus the 1.0 used in the Evaluation Case) as did the consumption of produce (1.72 versus 1.0), resulting in a significant increase to the produce ingestion dose pathway.

Realization 896

Realization 896 sampled many values that were similar to (or the same as) the Evaluation Case of the FY2014 SDF SA. The largest differences were the degradation rate (Realization 896 used the best estimate degradation rate whereas the Evaluation Case used the nominal rate) and the multiplier for the consumption of water (2.290 versus 1.0). The Tc-99 inventory in SDU 3B

(1,165 Ci) was significantly higher than in the Evaluation Case (540 Ci). The SZ Darcy velocity multiplier was about 0.94, indicating a 6% reduction in the rate of groundwater flow through the SZ. This slows down the transport of Tc-99, such that higher concentrations build up near the 100-meter boundary. Also, the SZ thickness sampled approximately 18 m (instead of the 20 m modeled in the Evaluation Case), which increases the concentration of the contaminant plume.

Note that the increase in the multiplier for the consumption of produce (2.269 versus 1.0) had a negligible impact relative to the total dose, which was dominated by the water ingestion pathway.

Realization 433

Realization 433 sampled the nominal initial saturated hydraulic conductivity and the nominal rate for cementitious degradation. More importantly, the lowest technetium solubility was sampled, resulting in less Tc-99 release prior to the oxidation transition. By "holding back" Tc-99, the SDUs contain more inventory which contributes to the spike once the significant release event occurs. The Tc-99 inventory in SDU 3B (1,321 Ci) was significantly higher than in the Evaluation Case (540 Ci). The SZ Darcy velocity multiplier was about 0.88, indicating a 12% reduction in the rate of groundwater flow through the SZ. This slows down the transport of Tc-99, such that higher concentrations build up near the 100-meter boundary. The SZ width associated with the 150-foot diameter SDUs is about 5% smaller than the Evaluation Case of the FY2014 SDF SA (43.2 m versus 45.7 m, respectively) increasing the concentration of Tc-99. The multiplier for the consumption of water was 1.119 (i.e., the water ingestion dose was increased by more than 10%).

In addition, the soil-to-plant uptake ratio sampled a high value (3.955 versus the 1.0 used in the Evaluation Case) as did the consumption of produce (2.30 versus 1.0), resulting in a significant increase to the produce ingestion dose pathway.

Realization 490

Realization 490 sampled the nominal initial saturated hydraulic conductivity and the nominal rate for cementitious degradation. More importantly, the lowest technetium solubility was sampled, resulting in less Tc-99 release prior to the oxidation transition. By "holding back" Tc-99, the SDUs contain more inventory which contributes to the spike once the significant release event occurs. The inventory in SDU 3B (1,321 Ci) was significantly higher than in the Evaluation Case (540 Ci). The SZ Darcy velocity multiplier was about 0.87, indicating a 13% reduction in the rate of groundwater flow through the SZ. This slows down the transport of Tc-99, such that higher concentrations build up near the 100-meter boundary. The SZ width associated with the 150-foot diameter SDUs is about 15% smaller than the Evaluation Case of the FY2014 SDF SA (41.4 m versus 45.7 m, respectively) increasing the concentration of Tc-99. The SZ thickness sampled about 16 m (instead of the 20 m modeled in the Evaluation Case), which increases the concentration of the contaminant plume. Finally, the multiplier for the consumption of water was 1.412 (i.e., the water ingestion dose was increased by more than 40%).

Summary of Subset 3 Data

Based on the data provided in Table PAM-2.2, some general observations can be made about these realizations:

- All of these realizations had peak doses that were dominated by contributions from the 150-foot diameter SDUs.
- All of these realizations sampled either the lowest or the nominal values for the initial saturated hydraulic conductivity (3.9E-10 cm/sec or 6.40E-09 cm/sec, respectively).
- All of these realizations sampled from the average infiltration rate.
- Four out of five of these realizations sampled the lowest possible technetium solubility (1.0E-09 mol/L), which significantly limited the release of Tc-99 prior to the oxidation of saltstone.
- All five realizations sampled values for Tc-99 inventory which were significantly higher than the Evaluation Case within the relevant SDUs.
- Four of the five realizations sampled SZ Darcy velocity multipliers less than 1.0, resulting in slower Tc-99 transport through the SZ, which allows for the concentrations to accumulate more at the 100-meter boundary.
- Four of the five realizations sampled smaller SZ thicknesses which also increased the concentrations.
- Four of the five realizations sampled SZ widths (for the relevant SDUs) with lower values than the value used in the FY2014 SDF SA.
- The multipliers for water consumption indicated an increase in water consumption of 12% to more than 100% relative to the Evaluation Case of the FY2014 SDF SA.
- The peak doses for all of these realizations were driven by Tc-99, mostly via the water ingestion pathway.

Subset 4: Realizations with Peak Doses at 40,000 Years

This final subset provides an analysis of one of the "vertical clusters" observed within the peak doses from the uncertainty analysis (see Figure 5.6.5-20 of the FY2014 SDF SA). For this analysis, the realizations with peak doses occurring at 40,000 years were selected because these realizations have peaks that span about one and a half orders of magnitude (from 98 mrem/yr to 3,885 mrem/yr). Table PAM-2.7 provides a list of all the realizations that showed peak doses occurring at 40,000 years.

Table PAM-2.7: List of Realizations with Highest Peak Doses at 40,000 Years

Realization	Year of Peak	50,000-Year Peak
1,272	40,000	3,885
194	40,000	2,156
725	40,000	1,962
103	40,000	1,850
1,218	40,000	1,103
509	40,000	1,053
1,473	40,000	896
575	40,000	750.6

Realization	Year of Peak	50,000-Year Peak
1,212	40,000	730.5
700	40,000	672.8
211	40,000	646.2
537	40,000	475
870	40,000	188.3
80	40,000	146.6
1,382	40,000	123.2
1,075	40,000	98.23

To identify which parameters influenced the spread of the magnitudes, this analysis focused on the three realizations with the highest peak doses (Realizations 1,272, 194, and 725) and the three realizations with the lowest peak doses (80, 1,382, and 1,075). By focusing on only the realizations that exhibited the highest- and the lowest-magnitude peak doses, rather than a full examination of all sixteen realizations, the similarities and differences between the parameters which influence the magnitudes of these peaks are more easily identified. Table PAM-2.8 provides a summary of these six realizations. Table PAM-2.9 presents a number of the significant parameter values that were sampled, followed by a discussion of how these values influenced these peak doses.

Table PAM-2.8: Summary of Realizations with Highest Peak Doses at 40,000 Years Selected for Analysis

Realization	Year of Peak Dose	Peak Dose (mrem/yr)	Highest Sector	Most Significant Dose Contributor(s)	Most Significant Dose Pathway(s)
1,272	40,000	3,885	J	Tc-99	Water Ingestion
194	40,000	2,156	J	Tc-99	Water Ingestion
725	40,000	1,962	I	Tc-99	Water and Produce Ingestion
80	40,000	146.6	J	Tc-99	Water Ingestion
1,382	40,000	123.2	I	Tc-99	Water Ingestion
1,075	40,000	98.23	J	Tc-99	Water Ingestion

Table PAM-2.9: Parameter Values Associated with Realizations with Highest Peak Doses at 40,000 Years

Parameter	FY2014 SDF SA Eval. Case	Realization					
		Higher Dose Peaks			Lower Dose Peaks		
		1,272	194	725	80	1,382	1,075
Saturated Hydraulic Conductivity of Saltstone (1 = 3.9E-10 cm/sec, 2 = 6.4E-09 cm/sec, 3 = 4.5E-07 cm/sec)	2	1	1	1	1	1	1
Infiltration Rate (1 = Minimum, 2 = Average, 3 = Maximum)	2	2	2	2	2	2	2
Degradation Rate of Cementitious Materials (1 = Nominal, 2 = Best Estimate)	1	2	2	2	2	2	2
Technetium Solubility (1 = 1.0E-09 mol/L, 2 = 1.0E-08 mol/L, 3 = 1.0E-07 mol/L)	2	1	1	1	2	2	1
Primary SDU(s)	**SDU 3B**	**SDU 3B**	**SDU 3B**	**SDU 5A**	**SDU 3B**	**SDU 3A**	**SDU 3B**
Primary SDU Tc-99 Inventory (Ci)	540	1,165	728	1,035	457	391	136
Secondary SDU	**SDU 5B**	**SDU 5B**	**N/A**	**SDU 3A**	**SDU 5B**	**SDU 5A**	**SDU 5B**
Secondary SDU Tc-99 Inventory (Ci)	540	269	N/A	457	81	391	1,321
UZ Thickness, 150-ft diam. SDUs (m)	12.8	12.70	14.59	14.16	12.71	16.83	11.84
SZ Darcy Velocity (Multiplier)	1.0	0.7984	0.9155	1.094	1.036	1.021	1.113
SZ Thickness (m)	20	19.68	21.26	20.96	26.27	17.83	18.42
SZ Width, 150-ft diam. SDUs (m)	45.72	41.41	48.57	45.26	40.28	45.11	48.31
Consumption of Water (Multiplier)	1.0	2.269	2.149	1.895	0.4942	0.6576	0.5741
Consumption of Produce (Multiplier)	1.0	2.377	2.325	0.8079	0.9152	0.3894	0.4766
Soil-to-Plant Uptake Ratio	1.0	0.929	0.1888	12.32	0.7348	0.1891	2.200

N/A = Not Applicable

Figure PAM.2-5 shows the doses to a hypothetical MOP at the 100-meter facility boundary for each of these realizations. As expected, all six realizations show doses that significantly overlap. To better discern the differences between these realizations, Figure PAM.2-6 expands the relevant time frame and presents the doses on a logarithmic scale.

Figure PAM-2.5: MOP Dose from Realizations with Highest Peak Doses at 40,000 Years

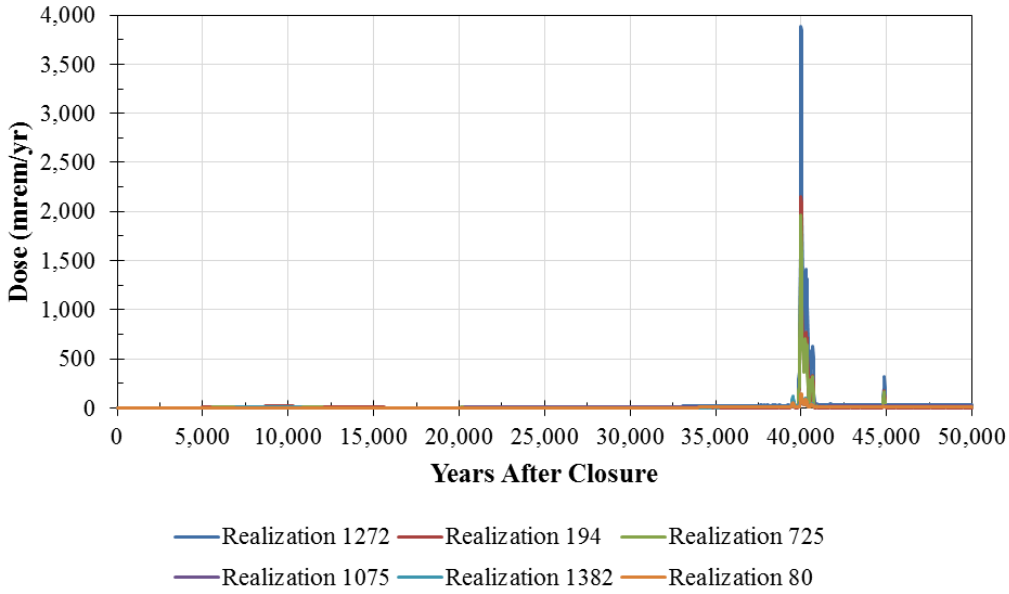

Figure PAM-2.6: MOP Dose from Realizations with Highest Peak Doses at 40,000 Years (Expanded)

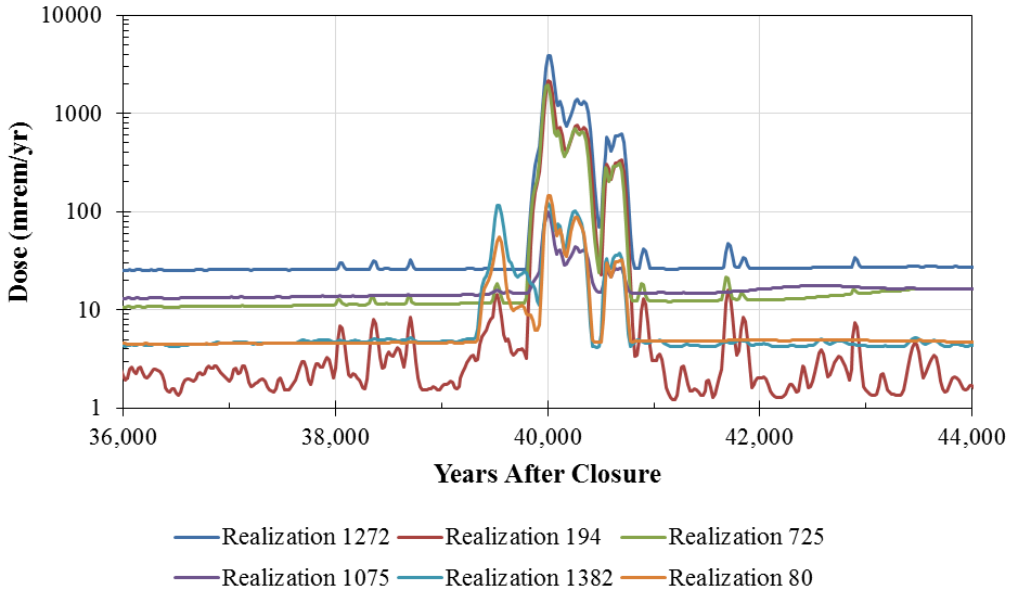

The following provides some additional analysis of these realizations. This discussion explores which parameters are most likely to influence the differences in the magnitudes exhibited between the higher dose and lower dose realizations.

Note that the first three parameters listed in Table PAM-2.9 sampled the same values for all six realizations. These parameters influence the flow field selection, which is what drove the timing of these peak doses to occur at 40,000 years. Of the parameters listed in Table PAM-2.9, there are nine parameters which have the potential to influence the magnitude of the dose:

- Technetium Solubility,
- Tc-99 Inventory (in relevant SDUs),
- UZ Thickness,
- SZ Darcy Velocity,
- SZ Thickness,
- SZ Width,
- Consumption of Water,
- Consumption of Produce, and
- Soil-to-Plant Uptake Ratio.

The following looks at each of these parameters and identifies those which most influenced the respective dose magnitudes.

Realization 1,272 (High Magnitude Peak Dose)

Realization 1,272 sampled the lowest technetium solubility (1.0E-09 mol/L). This reduces the amount of Tc-99 released prior to the "spike" that occurs once the lowest layer of saltstone becomes oxidized. SDU 3B contains more Tc-99 inventory which contributes to the spike once the significant release event occurs. The inventory in SDU 3B was 1,165 Ci of Tc-99 versus the 540 Ci used in the Evaluation Case. The UZ thickness and SZ thickness were not significantly different from the Evaluation Case, indicating that these parameters may not be as important for influencing the magnitude of the peak dose. The SZ Darcy velocity multiplier was approximately 0.80, indicating a 20% reduction in the rate of groundwater flow through the SZ. This slows down the transport of Tc-99, such that higher concentrations build up near the 100-meter boundary. The SZ width associated with the 150-foot diameter SDUs is about 10% smaller than the Evaluation Case of the FY2014 SDF SA (41.4 m versus 45.7 m, respectively); conceptually, the smaller width creates a "funneling" affect in which the mass occupies a smaller area, thus increasing the concentration of Tc-99. Finally, the multiplier for the consumption of water was 2.269 (i.e., the water ingestion dose was increased by more than 120%).

This realization did not show a significant dose contribution via the produce ingestion dose pathway, so the related parameters (i.e., the consumption of produce and the soil-to-plant update ratio) are not considered in the review.

Realization 194 (High Magnitude Peak Dose)

Realization 194 sampled the lowest technetium solubility (1.0E-09 mol/L). This reduces the amount of Tc-99 released prior to the "spike" that occurs once the lowest layer of saltstone becomes oxidized. SDU 3B contains more Tc-99 inventory which contributes to the spike once the significant release event occurs. The inventory in SDU 3B was 728 Ci of Tc-99 versus the 540 Ci used in the Evaluation Case. The UZ thickness and SZ thickness were not significantly different from the Evaluation Case, indicating that these parameters may not be as important for influencing the magnitude of the peak dose. The SZ Darcy velocity multiplier was approximately 0.92, indicating an 8% reduction in the rate of groundwater flow through the SZ,

which further supports the possibility of greater accumulation of Tc-99 at the 100-meter boundary. The SZ width associated with the 150-foot diameter SDUs (48.6 m) was not significantly different from the Evaluation Case of the FY2014 SDF SA (45.7 m). Finally, the multiplier for the consumption of water was 2.149 (i.e., the water ingestion dose was increased by nearly 115%).

This realization did not show a significant dose contribution via the produce ingestion dose pathway, so the related parameters (i.e., the consumption of produce and the soil-to-plant update ratio) are not considered in the review.

Realization 725 (High Magnitude Peak Dose)

Realization 725 sampled the lowest technetium solubility (1.0E-09 mol/L). This reduces the amount of Tc-99 released prior to the "spike" that occurs once the lowest layer of saltstone becomes oxidized. SDU 5A contains more Tc-99 inventory which contributes to the spike once the significant release event occurs. The inventory in SDU 5A was 1,035 Ci of Tc-99 versus the 540 Ci used in the Evaluation Case. The UZ thickness and SZ thickness were not significantly different from the Evaluation Case, indicating that these parameters may not be as important for influencing the magnitude of the peak dose. The SZ Darcy velocity multiplier (1.09) was not significantly different from the Evaluation Case (1.0). The SZ width associated with the 150-foot diameter SDUs (45.3 m) was also not significantly different from the Evaluation Case of the FY2014 SDF SA (45.7 m). The multiplier for the consumption of water was 1.895 (i.e., the water ingestion dose was increased by nearly 90%). Finally, the soil-to-plant update ratio sampled a value (12.32) that was significantly higher than in the Evaluation Case (1.0), resulting in a produce ingestion dose that was approximately an order of magnitude higher.

Realization 80 (Low Magnitude Peak Dose)

Realization 80 sampled the nominal technetium solubility (1.0E-08 mol/L). This solubility value allows a higher amount of Tc-99 to be released prior to the "spike" that occurs once the lowest layer of saltstone becomes oxidized, such that less of the Tc-99 is available to contribute to the peak dose. SDU 5A contains less Tc-99 inventory (209 Ci) than in the Evaluation Case (540 Ci), significantly reducing the magnitude of the spike once the significant release event occurs. The UZ thickness was not significantly different than in the Evaluation Case (14.7 m versus 12.8 m). The SZ thickness (26.3 m) was much higher than in the Evaluation Case (20.0 m), thus expanding the spread of the contaminant plume and reducing the overall concentration. The SZ Darcy velocity multiplier was approximately 1.04, indicating a 4% increase in the rate of groundwater flow through the SZ, which may cause the size of the contaminant plume to expand more, thus reducing the concentration at the 100-meter boundary. The SZ width associated with the 150-foot diameter SDUs (40.3 m) was significantly smaller than the Evaluation Case of the FY2014 SDF SA (45.7 m), which should result in a greater concentration; however, the influence of the other parameters likely overwhelms the impact from this one parameter. Finally, the multiplier for the consumption of water was only 0.49 (i.e., the water ingestion dose was decreased by approximately 50%).

This realization did not show a significant dose contribution via the produce ingestion dose pathway, so the related parameters (i.e., the consumption of produce and the soil-to-plant update ratio) are not considered in the review.

Realization 1,382 (Low Magnitude Peak Dose)

Realization 1,382 sampled the nominal technetium solubility (1.0E-08 mol/L). This solubility value allows a higher amount of Tc-99 to be released prior to the "spike" that occurs once the lowest layer of saltstone becomes oxidized, such that less of the Tc-99 is available to contribute to the peak dose. SDU 3A contains less Tc-99 inventory (391 Ci) than in the Evaluation Case (540 Ci), significantly reducing the magnitude of the spike once the significant release event occurs. The UZ thickness was greater than in the Evaluation Case (16.8 m versus 12.8 m). The SZ thickness (17.8 m) was slightly smaller than in the Evaluation Case (20.0 m), which should result in a greater concentration; however, the influence of the other parameters likely overwhelms the impact from this one parameter. The SZ Darcy velocity multiplier was approximately 1.02, indicating a 2% increase in the rate of groundwater flow through the SZ, which may cause the size of the contaminant plume to expand more, thus reducing the concentration at the 100-meter boundary. The SZ width associated with the 150-foot diameter SDUs (45.1 m) was not significantly different from the Evaluation Case of the FY2014 SDF SA (45.7 m). Finally, the multiplier for the consumption of water was only 0.66 (i.e., the water ingestion dose was decreased by approximately 34%).

This realization did not show a significant dose contribution via the produce ingestion dose pathway, so the related parameters (i.e., the consumption of produce and the soil-to-plant update ratio) are not considered in the review.

Realization 1,075 (Low Magnitude Peak Dose)

Realization 1,075 sampled the lowest technetium solubility (1.0E-09 mol/L). This reduces the amount of Tc-99 released prior to the "spike" that occurs once the lowest layer of saltstone becomes oxidized. Although SDU 5B contains significantly more Tc-99 inventory than in the Evaluation Case (1,321 Ci versus 540 Ci), it is releases from SDU 3B that most influence the peak concentration at Sector J. SDU 3B contains significantly less Tc-99 inventory (136 Ci) than in the Evaluation Case (540 Ci), significantly reducing the magnitude of the spike once the significant release event occurs. The UZ thickness was smaller than in the Evaluation Case (11.8 m versus 12.8 m), as was the SZ thickness (18.4 m versus 20.0 m), which should result in greater concentrations; however, the influence of the other parameters likely overwhelms the impact of these parameters. The SZ Darcy velocity multiplier was approximately 1.11, indicating an 11% increase in the rate of groundwater flow through the SZ, which may cause the size of the contaminant plume to expand more, thus reducing the concentration at the 100-meter boundary. The SZ width associated with the 150-foot diameter SDUs (48.3 m) was greater than in Evaluation Case of the FY2014 SDF SA (45.7 m), thus expanding the thickness of the contamination plume and reducing the overall concentration. Finally, the multiplier for the consumption of water was only 0.57 (i.e., the water ingestion dose was decreased by approximately 43%).

This realization did not show a significant dose contribution via the produce ingestion dose pathway, so the related parameters (i.e., the consumption of produce and the soil-to-plant update ratio) are not considered in the review.

Summary of Subset 4 Data

The three realizations with the highest peak doses (among those realizations with peaks that occur at 40,000 years, as identified in Table PAM-2.7), all sampled the lowest technetium solubility value (1.0E-09 mol/L). This prevents Tc-99 from being released prior to complete saltstone oxidation, such that once the release does occur there is ample inventory available to contribute to the higher dose. Only one of the lower dose realizations (Realization 1,075) sampled this low technetium solubility (Realizations 80 and 1,382 sampled the nominal value of 1.0E-08 mol/L).

Given that all six of these realizations sampled the same flow field parameters, it is clear that the magnitudes of these doses are most significantly influenced by the water consumption multiplier and the initial inventory for the relevant SDU (either SDU 3B or 3A). To a lesser degree, the SZ Darcy velocity multiplier is also important (where a larger multiplier results in decreased concentration), as are the geometry parameters (UZ thickness, SZ thickness, and SZ width) which control the spread of the contaminant plume (i.e., more spreading results in lower concentrations). Finally, whenever an extremely high value is sampled for the soil-to-plant uptake ratio, the produce ingestion pathway becomes more significant (as seen in Realization 725).

General Conclusion

Although this analysis provides some additional detail, the conclusions presented in this RAI response closely reflect the information presented in the probabilistic sensitivity analysis presented in Section 5.6.5.4 of the FY2014 SDF SA.

While the realizations discussed herein provide insight as to which parameters have the greatest influence on the timing and the magnitude of the peak doses, these realizations should not be interpreted as reflective of possible future outcomes. Operational controls (e.g., Waste Acceptance Criteria (X-SD-Z-00001), which limit SDF inventories) shall mitigate uncertainty in the system. Further, all of the peaks described herein relied on multiple parameters being sampled at extreme values. The extreme ranges in many of these parameters do not necessarily reflect the upper or lower bounds of reality, but often only reflect uncertainty in terms of what is known versus unknown. In such cases, DOE erred on the side of conservatism for the purpose of defensibility; however, future PA maintenance activities shall reduce this type of uncertainty and further constrain the range of sampled values.

PAM-3

PAM-3	**Question:** Additional information is needed about the process of benchmarking the deterministic GoldSim model results to the PORFLOW model results.
	Basis: The first three steps of the benchmarking procedure in Section 5.6.2 of the DOE FY14 SDF Special Analysis document compared results from the PORFLOW model and results of deterministic runs of the GoldSim model for: (1) radionuclide fluxes from the unsaturated zone (UZ) to the saturated zone (SZ) for each type of disposal structure; (2) radionuclide concentrations in the SZ at the 100-meter boundary for Sectors B, I, J, and K; and (3) projected dose to a member of the public for Sectors B, I, J, and K. The DOE used GoldSim as a stand-alone model for uncertainty and sensitivity analyses. In addition, the DOE used GoldSim as a dose calculator to compute doses from PORFLOW-generated radionuclide concentrations. Section 5.6.2.1 of the DOE FY14 SDF Special Analysis document states that: "Dose calculations [in the GoldSim model] are performed using the same dose calculations that were used to determine the PORFLOW dose results." If concentrations from both GoldSim and PORFLOW models were transformed into dose with the same dose calculations, then it is not clear to the NRC staff what the difference was between Benchmarking Step 2, where SZ concentrations were compared, and Benchmarking Step 3, where doses were compared. The NRC staff needs to understand the reason for performing Benchmarking Step 3 to ensure our understanding of the overall PA approach and the DOE benchmarking process for GoldSim and PORFLOW.
	Path Forward: Provide an explanation how Benchmarking Step 3 (comparison of projected doses to a member of the public) provided different information than Benchmarking Step 2 (comparison of SZ concentrations at the 100-meter well).

DOE Response to PAM-3

In general terms, Benchmarking Step 2 evaluates how well the GoldSim model approximates radionuclide transport behavior in the saturated zone as compared to the PORFLOW model. This is accomplished through comparison of the GoldSim and PORFLOW models' predicted maximum concentrations for the radionuclides of interest (i.e., Cs-135, I-129, Ra-226, and Tc-99) at various 100-meter points of assessment from 0 to 20,000 years after closure.

Benchmarking Step 3 examines how well the GoldSim model captures MOP dose results predicted by the PORFLOW model. Using total dose as the basis for comparison allows for the fate and transport of essentially all radionuclides to be evaluated. This ensures that the differences from other radionuclides do not exhibit any significant and unexpected impacts on the results, thus providing a more complete comparison when presented in conjunction with Benchmarking Steps 1 and 2.

PAM-4

PAM-4	**Question:** The future climatic or geologic conditions that will prevail at a site are not known, but the PA process requires consideration of possible future conditions. The DOE did not provide in the DOE FY14 SDF Special Analysis document an analysis or evaluation that examined possible future conditions at the site.
	Basis: Sources of uncertainty inherent to waste disposal in the near surface include, but are not limited to incomplete knowledge of the natural system, the natural system's evolution, and the natural system's interactions. The NRC staff previously identified the uncertainties in a PA as: (1) scenario uncertainty; (2) model uncertainty, which spans conceptual model uncertainty and mathematical model uncertainty; and (3) parameter uncertainty (see NUREG/CR-5211 and NUREG/CR-5927). Scenario uncertainty, defined as the consideration of uncertainty in the future evolution of the site, may result in several different conceptual models for the system as distinguished by the effects of phenomena on the system. Uncertainty about the future of the site is the result of an inherent lack of knowledge about how the site will evolve over time. Climatic variation may significantly change groundwater flow pathways over time, which would necessitate changes to the groundwater flow model or the introduction of new parameters.
	Path Forward: Provide an uncertainty analysis that examines possible future conditions at the site (e.g., net depositional or erosional changes at the site or changing climatic conditions within a 10,000-year period).

DOE Response to PAM-4

The water table surface in the vicinity of the SDF mimics surface topography. Based on the location of the SDF at SRS, it is unlikely that future erosion would modify the current conceptual model of hydrologic flow. The only likely scenario that would result in potential impacts to the SDF conceptual model of hydrologic flow would be a significant increase or decrease in rainfall. Either scenario would not alter hydrologic flow patterns, but could impact vadose zone (unsaturated) thickness.

It should be noted that the radionuclides that are the dose drivers for the SDF are I-129 and Tc-99. Both of these radionuclides have very low K_ds, resulting in travel times through the vadose zone in the range of feet per year as opposed to feet per 100 years or 1,000 years. Changes in the thickness of the vadose zone due to climate changes would only be in the range of tens of feet, at the most, because the depth from the bottom of the SDUs to the water table is only 36 feet to 48 feet as described in *Numerical Flow and Transport Simulations Supporting the Saltstone Disposal Facility Performance Assessment.* [SRNL-STI-2009-00115] Therefore, modifying the thickness of the vadose zone would only move travel times to exposure points by a couple of years as opposed to 100s or 1,000s of years.

The *Comment Response Matrix for NRC RAIs on the FY2013 SDF SA* (SRR-CWDA-2014-00099) provided additional information to support the assumed SZ thickness at the SDF. Physically, the thickness of the SZ near the SDF is defined as the vertical distance from the water table (i.e., the top of the SZ aquifer) to the top of the Gordon Aquifer (i.e., the Gordon Confining Unit [Green Clay] that represents the bottom of the SZ aquifer). As described in *Saltstone Disposal Facility Sensitivity Modeling to Address Concerns Related to Saturated Zone Transport*

(SRR-CWDA-2014-00095), the thickness of the saturated zone is estimated to be between 19 meters and 32 meters (62 to 105 feet), based upon local topography. A sensitivity analysis was performed, independently from any specific SDF SA, to assess the relative impact from varying the SZ thickness over the expected range of thickness and found very little impact. Changes to the SZ thickness, based on rainfall changes would inversely impact the thickness of the vadose zone. The modeling used a range of saturated zone thickness from 19 meters to 32 meters (62 to 105 feet). This saturated zone thickness range represents only a 43 foot variance, therefore the vadose zone would vary inversely by the same thickness. Table FFT-1.1 of SRR-CWDA-2014-00099 provides peak dose variability to the MOP based on changes in saturated zone thickness. The peak dose to the MOP in 10,000 years only ranged from 12.6 to 12.8 mrem/yr.

In addition, in the FY2014 SDF SA, various flow cases were evaluated with a range of infiltration rates which would reflect potential changes in climate and rainfall. In Section 5.6.7.3 of the FY2014 SDF SA a flow case sensitivity analysis was performed on four different flow cases. Flow Case F14 represented the most extreme conditions modeled with high infiltration, nominal degradation, and initially high saturated hydraulic conductivity assumed. Given the extreme conditions represented by this flow case (i.e, maximum infiltration rates, nominal degradation of cementitious materials, and an initial saturated hydraulic conductivity of saltstone of 4.5E-07 cm/sec) and the resulting doses, there is a high degree of confidence that the peak dose to the MOP will not exceed 25 mrem/yr within 10,000 years.

SALTSTONE PERFORMANCE (SP)

SP-1

SP-1	**Question:** Additional justification is needed for the DOE assumed change in hydraulic conductivity of saltstone with time, which does not account for the feedback of increasing hydraulic conductivity as decalcification progresses.
	Basis: In Section 4.2.2.3 of the DOE FY14 SDF Special Analysis document, decalcification via advection was assumed to control the degradation of saltstone. The rate of decalcification was assumed to be constant and was based on the initial hydraulic conductivity of saltstone. However, decalcification would result in an increase in the hydraulic conductivity of saltstone and therefore, the rate of decalcification would increase as the hydraulic conductivity in saltstone increases in time. That dependency would create a feedback loop that was not accounted for by the DOE. Including that feedback loop of increasing hydraulic conductivity with decalcification would significantly decrease the amount of time required for complete degradation of saltstone to occur. The DOE evaluated three cases: (1) best estimate, (2) nominal value, and (3) conservative estimate scenarios. Those three cases multiply the initial hydraulic conductivity by factors of 1, 10, and 100, respectively. The purpose of those cases was to account for the potential head gradient in the vadose zone for the saltstone. It is not clear to the NRC staff how much head may accumulate on top of a disposal structures and to what extent that could account for increasing hydraulic conductivity of saltstone with respect to time. The DOE previously indicated that the assumed linear rate of degradation was overly conservative and accounts for other degradation mechanisms. As described in more detail in RAI Question SP-3 – later in these RAI Questions, the DOE basis for the selection of potential degradation mechanisms and justification that the rate of saltstone degradation was conservative is not clear to the NRC staff.
	Path Forward: Provide justification for why the feedback mechanism of increased hydraulic conductivity with time does not need to be accounted for in the degradation analysis. (If that justification includes the conservatism associated with the linear rate of degradation, then it should also account for the NRC staff concern in RAI Question SP-3 – later in these RAI Questions).

DOE Response to SP-1

The NRC's comment that the inclusion of a feedback loop to allow for increasing hydraulic conductivity behind the decalcification front as it moves downward may significantly decrease the amount of time required for complete degradation is true. The reason that DOE feels that the temporal change in hydraulic conductivity due to degradation as used by the PORFLOW model is appropriate as well as conservative is because the hydraulic conductivity is described by a linear change over time from the intact value (6.4E-09 cm/sec) to the fully degraded value (4.1E-05 cm/sec), starting as soon as roof degradation is complete (e.g., 1,413 years after facility closure for the 375-foot diameter SDUs).

Justification for DOE's stance is exhibited by the results of a degradation analysis based on the equation defining the time required for the advection-driven decalcification front to reach the

bottom of the saltstone as presented in Section 4.2.2.3 of the FY2014 SDF SA. For this response, the equation presented in the FY2014 SDF SA is redefined in the form:

$$t = \frac{C_{Ca}}{C_{Ca^{2+}}} \cdot \frac{h}{U(\tau)} \quad (1)$$

Where:

$U(\tau)$	=	Volumetric water flux at time τ [cm/yr]
t	=	Elapsed time [yr]
τ	=	Time [yr]
h	=	Monolith height (or saltstone thickness) [cm/yr]
C_{Ca}	=	Calcium concentration in solid phase [mol/cm^3 total]
C_{Ca}^{+2}	=	Dissolved calcium concentration [mol/cm^3 liquid]

U is a function of time, based on the position of the front.

As with the original analysis, the velocity is defined as U = 1, 10, and 100 times the saturated hydraulic conductivity for the "Best Estimate", "Nominal", and "Conservative" assumptions, respectively, as defined in Section 4.2.2 of the FY2014 SDF SA.

The time-dependent value of the vertical hydraulic conductivity used to derive $U(\tau)$ in Equation (1) is based on the harmonic mean of the hydraulic conductivities for a two-layered system (ISBN: 0-13-365312-9, Equation 2.31) where the two layers represent the saltstone ahead of and behind the decalcification front. The time-dependent value of the hydraulic conductivity can be defined as:

$$K_{eff}(t) = \frac{h}{\frac{d(t)}{K_{deg}} + \frac{h - d(t)}{K_{init}}} \quad (2)$$

Where:

$K_{eff}(t)$	=	Effective saturated hydraulic conductivity at time t [cm/yr]
K_{init}	=	Initial saturated hydraulic conductivity [cm/yr]
K_{deg}	=	Degraded saltstone saturated hydraulic conductivity [cm/yr]
$d(t)$	=	Distance the decalcification front has traveled up until time t [cm]

During the process of saltstone degradation, the saltstone behind the decalcification front becomes highly conductive, but the downward flow of water is still strongly inhibited by the non-degraded saltstone ahead of the front.

As depicted in Figure SP-1.1, which is based on an analysis of a 375-foot diameter SDU, when a "feedback loop" is considered (i.e., the nonlinear curves), the time-dependent effective hydraulic conductivity exhibits an exponential increase over time as opposed to a linear increase such as used in the FY2014 SDF SA models (i.e., the linear curves). In the nonlinear (feedback loop) analysis, the fully degraded hydraulic conductivity is reached in about half the time taken by the

linear model, but in the nonlinear analysis the hydraulic conductivity also remains lower for a significantly longer period of time. In Figure SP-1.1 the nature of the temporal change in hydraulic conductivity can be seen in the Nonlinear and Linear Conservative models (green curves) where the "Conservative, Nonlinear" curve was generated assuming feedback (a change in bulk hydraulic conductivity as the calcification front moves through the saltstone) and the "Conservative, Linear" curve is the linear approximation used in PORFLOW modeling (Figure SP-1.1).

The nature of the temporal change in hydraulic conductivity for the "Best Estimate" and "Nominal" curves, are shown in the Log-Log plot presented in Figure SP-1.2 due to the amount of time required for the calcification front to fully penetrate the saltstone. Note that the delay in the degradation process is not presented in either figure.

As can be seen in Figure SP-1.1, by considering a "feedback loop", which defines the effective hydraulic conductivity as the harmonic mean of the saltstone hydraulic conductivities behind and ahead of the front, the hydraulic conductivity of the "Conservative, Nonlinear" assumption would be lower than the hydraulic conductivity used in the PORFLOW model (i.e., the "Conservative, Linear") for over 20,000 years. Similarly, for the "Best Estimate" and "Nominal" degradation assumptions, the hydraulic conductivities would be lower than those used in the PORFLOW model for over 2,000,000 and 200,000 years, respectively (see Figure SP-1.2). Although we do not model beyond 100,000 years, this process is followed to the extent needed (e.g., greater than 2,000,000 years) to develop the linear relationship, based on initial condition and complete degradation of the material.

Figure SP-1.1: Semi-Log Plot of the Effective Hydraulic Conductivity over Time

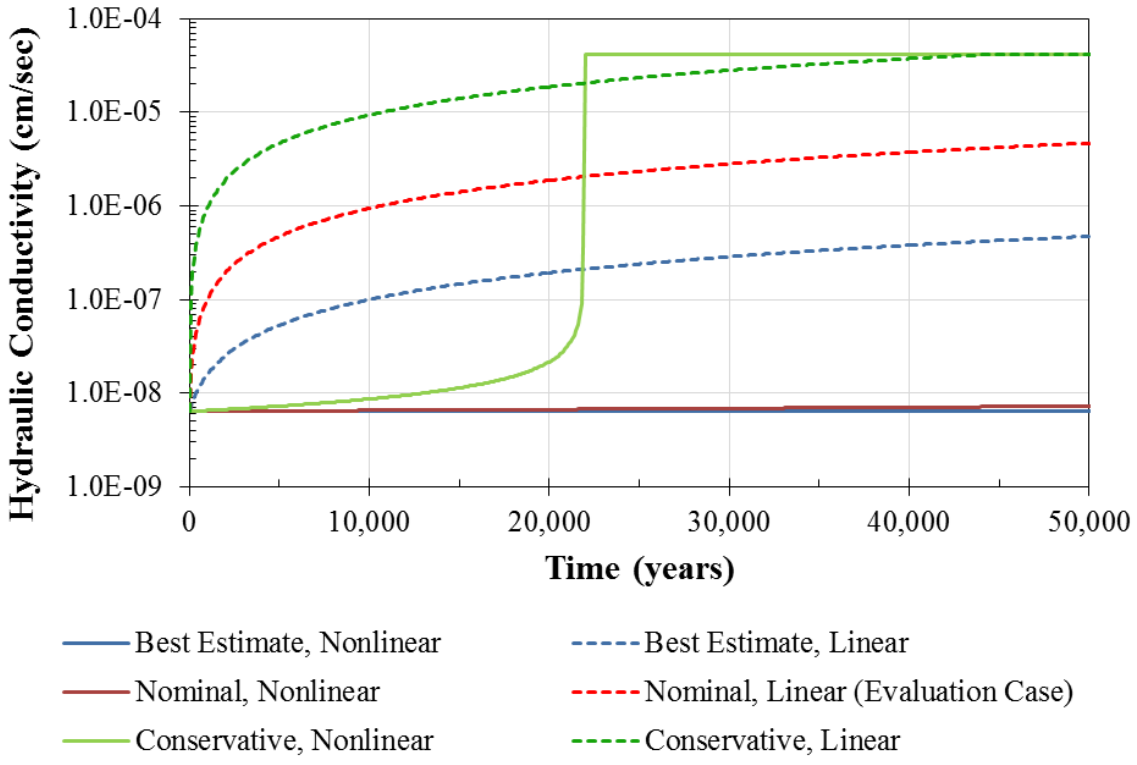

Figure SP-1.2: Log-Log Plot of the Effective Hydraulic Conductivity over Time

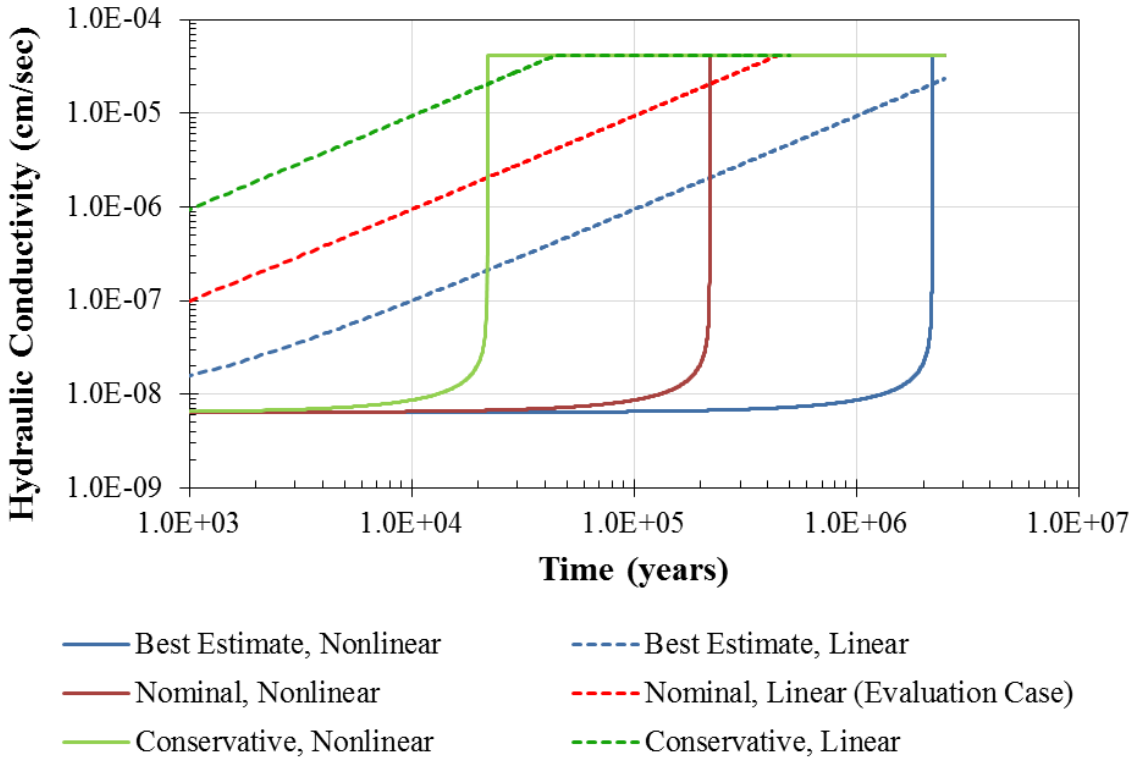

When evaluating whether or not the linear degradation approach used in the FY2014 SDF SA is conservative with respect to system performance, one must consider the influence of the degradation front on horizontal flow. With respect to a more spatially rigorous simulation of radionuclide migration in a nonlinear two-layered system, water entering the saltstone from above would be diverted from vertical flow to horizontal flow, allowing mass to bleed out the sides of the SDU, which would be expected to reduce the rate of decalcification and slow releases relative to the Evaluation Case (which is dominated by vertical/downward flow and release). However, the horizontal release mechanism would tend to provide earlier releases (at lower magnitudes) which are spread out over time, thus providing results that are similar to those represented by the mass-transfer model described in Section 5.6.6.2 of the FY2014 SDF SA. This behavior is expected to effectively decrease peak radionuclide releases. The simpler conceptual model used in the FY2014 SDF SA is therefore conservative.

SP-2

SP-2	**Question:** Additional information is needed regarding the risk associated with gas-phase transport of oxygen into unsaturated fractures.
	Basis: In the DOE 2015 Response to the NRC 2014 RAI Comments (see RAI Comment SP-4 in that document), the DOE indicated that the assumption of linear degradation provided some compensation for the potential effects of mechanical degradation. The DOE expected that degradation rates would initially be much slower and increase more gradually over time. Although the assumed linear degradation rate was more conservative than what the DOE assumed in the DOE 2009 SDF PA, it is not clear to the NRC staff that it is conservative or compensated for the potential effects of mechanical degradation (for more detailed information, see RAI Question SP-3 below). In the DOE FY14 SDF Special Analysis document, the DOE described that the modeled column degradation in the DOE FY13 SDF Special Analysis document and in the DOE 2015 Response to the NRC 2014 RAI Comments (see RAI Comment CC-3 in that document) could be used as an analog for the effect of fractures. However, the DOE did not consider a completely interconnected pathway of oxidation from the top of the roof of a disposal structure, through the saltstone, and down to the floor of the disposal structure to be a credible scenario within the 10,000-year performance period. Degradation of the column forms a complete pathway by 7,200 years in the DOE evaluation case and by 2,000 years in a sensitivity case from the DOE 2015 Response to the NRC 2014 RAI Comments (see RAI Comment CC-3 in that document). In the DOE 2015 Response to the NRC 2014 RAI Comments (see RAI Comment SP-1 in that document), the DOE indicated that the interconnected flow path acted to channel oxygenated water away from the saltstone inventory. Based on the results of those analyses, the DOE assumed that the risks from any potential fractures were not likely to be significant. Although the DOE column degradation analyses provided some insight into the effects of fractures with the through-going fast pathway, it is not clear to the NRC staff that those analyses adequately accounted for the potential effects of fractures. The rate and extent of fracturing of saltstone are not well understood. As such, it is difficult to compare the results from a through-going column analysis to saltstone grout with the potential for interconnected and unsaturated fractures. Although fast pathways can divert water away from the inventory, they can also potentially introduce much more oxygen into the wasteform than oxygen dissolved in water. Unsaturated fractures may have a significantly greater fracture-matrix interfacial area than what the DOE assumed in the column degradation analysis. Accordingly, that gas-phase oxidation may exceed the rate of oxidation assumed in the DOE evaluation case or column degradation sensitivity case. In addition, the potential exists for fractures to result in a pulse-like release of redox-sensitive radionuclides. A fractured region of saltstone may not be hydraulically active; but, it could still be susceptible to gas-phase oxidation. After water is introduced to the oxidized saltstone, redox-sensitive radionuclides could be released within several pore flushes. In addition, the DOE column degradation analysis did not include any inventory for the column, whereas a damaged area of saltstone would contain inventory. Also, a completely interconnected pathway of oxidation from the top of the roof of a disposal structure, through the saltstone, and down to the floor of the disposal structure is not a prerequisite for gas-phase oxidation to occur. A disposal structure is not expected to be airtight. As such, any fracturing that was connected to the exterior of the saltstone grout would be susceptible to gas-phase oxidation.

	Path Forward: Provide additional support for the DOE assumption that saltstone is not susceptible to fracturing and gas-phase oxidation. Model support activities could include degradation analyses that couple chemical and mechanical degradation models to provide a more complete degradation analysis. The NRC staff understands the challenges associated with developing and validating that type of degradation analysis. As such, as part of the model support activities, the DOE could provide a more realistic analysis evaluating the risk associated with fractures and gas-phase oxidation. In the DOE 2015 Response to the NRC 2014 RAI Comments, the DOE proposed a future activity of studying the rates of oxidation in potential unsaturated fractures. That type of information could help support the DOE assumptions regarding the risk-significance of fractures.

DOE Response to SP-2

The DOE does not believe that saltstone will degrade in such a way as to form a significant network of interconnected, unsaturated fractures within 10,000-years performance. The saltstone monolith is completely enclosed within concrete and will be buried and covered with an engineered closure cap. Any fractures that may form are more likely to be narrow, shallow, and unconnected. As such, oxygen sources would be unlikely to channel directly through the entire height of the closure cap and the saltstone monolith to interact with a significant interfacial area as part of a fracture-matrix.

The sensitivity analysis showing Tc-99 releases due to non-depleting oxygen sources within saltstone (see Section 5.6.7.4 of the FY2014 SDF SA) introduces much more oxygen into the waste form than would be expected from infiltrating water. This analysis presents a range of volume-based non-depleting oxygen sources which may be used as a non-mechanistic surrogate for considering the effects of hypothetical unsaturated fracture-matrix interfacial areas. As postulated by the NRC, significantly increasing the oxidation within localized regions of the saltstone monolith results in pulse-like releases of redox-sensitive radionuclides (see Figure 5.6.7-16 of the FY2014 SDF SA).

Note that if oxygen were moving through the saltstone via a network of fractures, it is likely that preferential flow paths would also exist. These preferential flow paths would significantly alter the flow pattern within the modeled system. The DOE believes that such preferential flow paths would limit the interaction between the supply of oxygen and the redox-sensitive radionuclides within the saltstone monolith, resulting in more localized releases (i.e., limiting releases). Further, the amount of oxygen available for transport is expected to be relatively limited given the expected thickness of the assumed closure cap.

In addition to the sensitivity analysis showing Tc-99 releases due to non-depleting oxygen sources within saltstone, the following describes a new probabilistic model developed as part of these RAI responses. This probabilistic model was designed to provide additional understanding of the potential risk significance of parameters related to technetium release. Despite variability and conservatisms within the assumed sampling distributions, the results of this analysis indicate that, within 10,000-years, there is a low probability that Tc-99 releases would increase to a significant magnitude such that changes to the conclusions of the FY2014 SDF SA would be needed. Further, the values assumed for the Evaluation Case nearly maximize the peak release

within the 50,000-year simulation period (i.e., a lower magnitude release is likely if different input values were assumed for the Evaluation Case).

Probabilistic Tc-Ox Model

To better evaluate the parameters related to oxidation and the risks related to the releases of Tc-99, a special probabilistic sensitivity model was developed. As stated in Section 5.6.7.4 of the FY2014 SDF SA, non-depleting sources of oxygen are not expected to be present within saltstone. Oxygen is only expected to enter the SDUs via infiltrating water, as modeled in the SDF PA and the Evaluation Case. Any oxygen sources initially present within saltstone (i.e., air pockets that form during waste disposal) would be quickly depleted. Therefore, the following evaluation is designed only to evaluate the influence of specific parameters but is not designed to be interpreted as being within the bounds of expected future conditions.

For this sensitivity model, the GoldSim SDF Tc-99 Release Model (described in Section 4.4.2 of the FY2014 SDF SA) was modified so that only four stochastic parameters existed within the model: *SLAGRedCap1* (the reducing capacity in saltstone), *SLAGRedCap2* (the reducing capacity in concrete), *Solubility* (the solubility limit for Tc-99 release), and *RemovalPct* (the percentage of Tc-99 mass that applied to the simplified mass bypass model described in Section 4.4.2.2 of the FY2014 SDF SA).

All other stochastic parameters were modified to simply assume the deterministic (Evaluation Case) values. This modified GoldSim SDF Tc-99 Release Model shall hereinafter be referred to as the Probabilistic Tc-Ox Model.

To exaggerate the effect of the *RemovalPct* from the mass bypass, the model was set to allow the specified percentage of the mass to be released from any modeled cell that has become fully oxidized, automatically sending that mass directly to the unsaturated zone. Note that since the Evaluation Case does not explicitly consider saltstone fracturing, the benchmark model (described in Section 5.6.2 of the FY2014 SDF SA), only releases technetium from saltstone at the peripheral interfaces of the walls and the roof-support columns. Alternatively, for this special probabilistic sensitivity model and for the sensitivity evaluation described in Section 5.6.6.2 of the FY2014 SDF SA, technetium may be released from any oxidized area of the saltstone, not just from the oxidized saltstone at the peripheral interfaces. This simplified model was designed to emulate the hypothetical transport of oxidized (previously precipitated) Tc-99 through a saltstone/concrete structure containing ubiquitous fractures with a high degree of connectivity, rather than reconcentrating (i.e., re-reducing) within the intact saltstone matrix.

Each of the four sampled parameters within the Probabilistic Tc-Ox Model was assigned an unrealistically wide range of distribution. The reducing capacity variables (SLAGRedCap1 and SLAGRedCap2) were assigned triangular distributions with a minimum value of 0, a mode equal to the Evaluation Case value, and a maximum equal to double the Evaluation Case value (see Figures SP-2.1 and SP-2.2). Solubility was assigned a log-uniform distribution that varies the technetium solubility by one and a half orders of magnitude above and below the Evaluation Case value of 1E-08 mol/L (see Figure SP-2.3), such that the actual solubility values range from approximately 3E-10 mol/L to approximately 3E-07 mol/L. Finally, the RemovalPct variable was assigned a uniform distribution from 1% to 99% (see Figure SP-2.4).

Figure SP-2.1: Probability Distribution for the Reducing Capacity of Saltstone

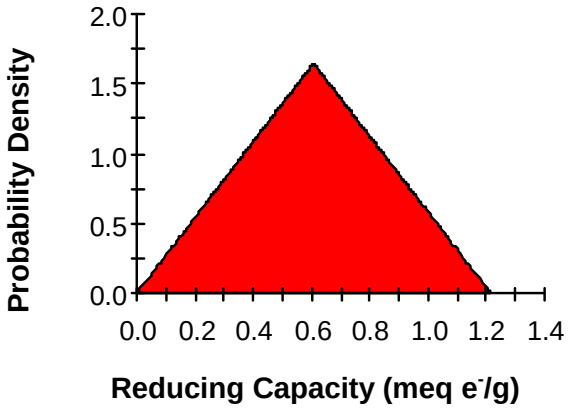

Figure SP-2.2: Probability Distribution for the Reducing Capacity of Concrete

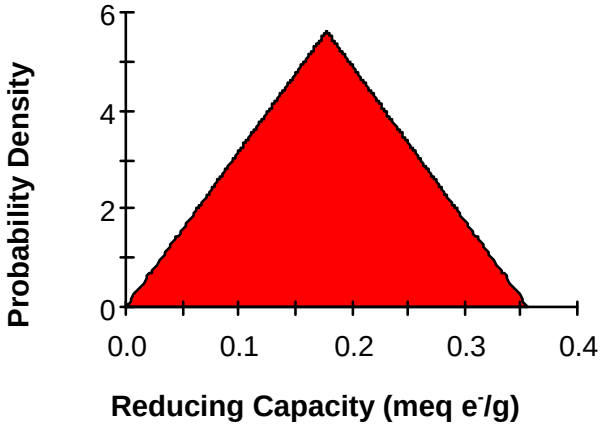

Figure SP-2.3: Cumulative Probability for the Technetium Solubility Multiplier

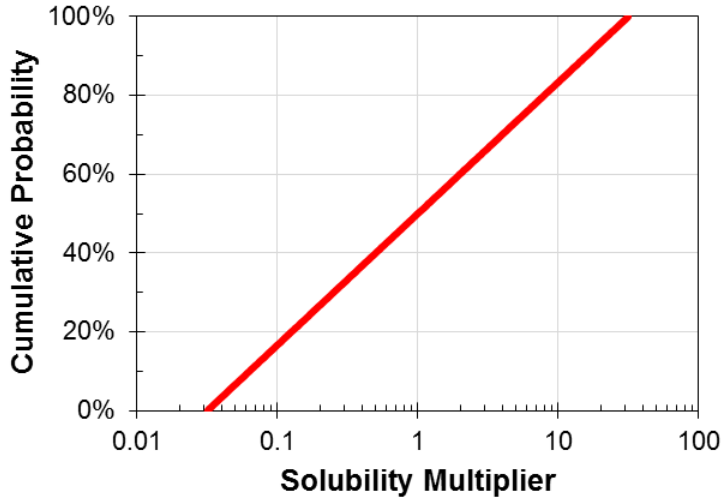

Figure SP-2.4: Probability Distribution for the Simplified Mass Bypass / Removal Percentage

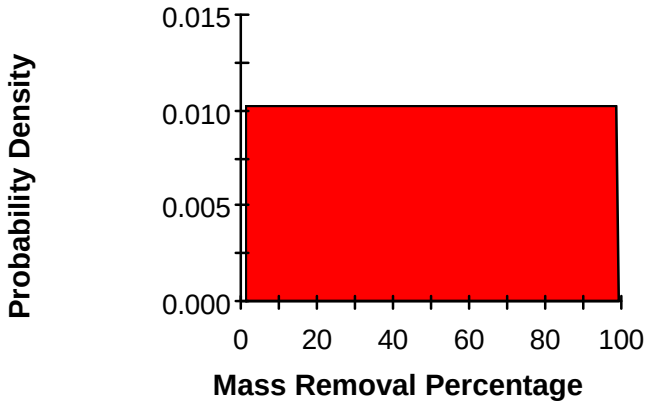

Note that of these four parameters, the solubility multiplier is the only one that was originally sampled for in the probabilistic model used in the FY2014 SDF SA; however, instead of the log-uniform distribution, the original distribution for the solubility multiplier sampled three values: 0.1, 1.0, and 10.0 using a discrete sampling distribution.

To better isolate the impacts of the changes relative to a single disposal unit, the Probabilistic Tc-Ox Model was also setup to only simulate releases from SDU 9. The model was then run for 1,000 realizations to generate a distribution of flux releases to the SZ (see Figure SP-2.5). For the first 7,000 years, the median value and the deterministic Evaluation Case value are nearly identical. The results from the deterministic Evaluation Case and the median value from this unique sensitivity study exhibit similar behavior until about 19,000 years after closure, when the median values begin to decline relative to the Evaluation Case.

Figure SP-2.5: Tc-99 Flux Released to the SZ (via Probabilistic Tc-Ox Model)

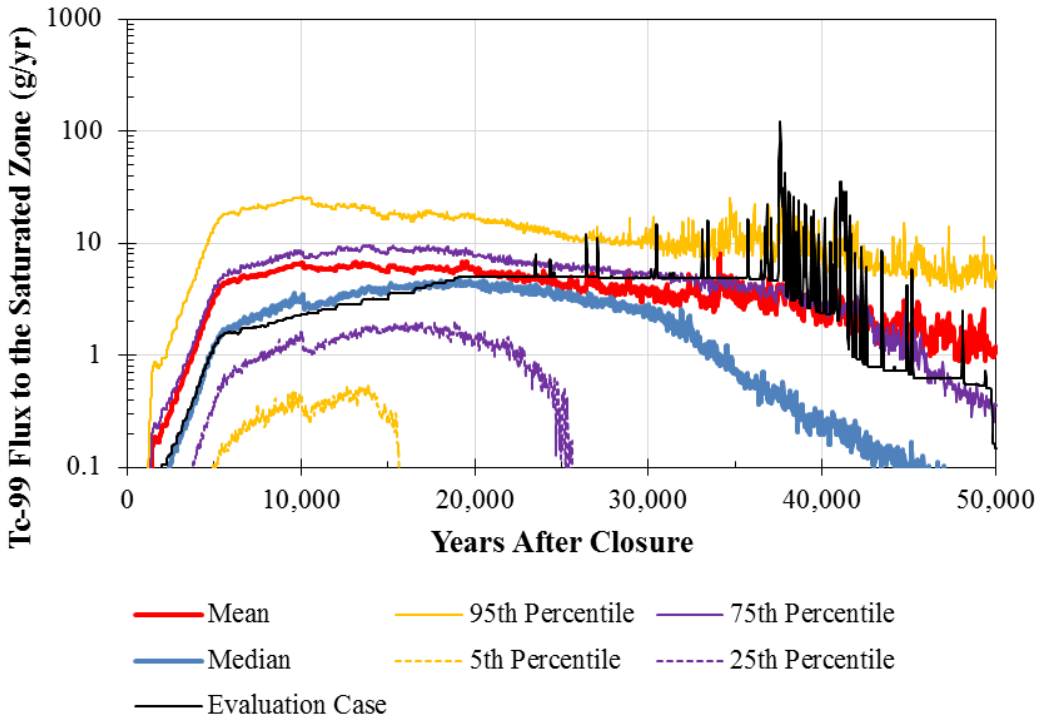

When these releases are applied to the dose calculator the Tc-99 dose results very closely reflect the respective fluxes (see Figure SP-2.6). Within 10,000-years, the dose contributions from Tc-99 are typically highest at or near 10,000 years. However, when the Tc-99 dose contributions are added to the dose contributions from the other radionuclides (see Figure SP-2.7), the peak dose is typically at or near 5,300 years, reflecting the Evaluation Case dose results from Section 5.5 of the FY2014 SDF SA. Note that for these dose contributions the deterministic values from the Evaluation Case were assumed (i.e., the Tc-Ox model did not probabilistically simulate impacts to radionuclides other than Tc-99 releases).

Table SP-2.1 provides the Tc-99 dose contributions for various statistical results according to the Probabilistic Tc-Ox Model. This table also includes the estimates of total doses from summing the Tc-99 doses contributions to the contributions from the other radionuclides (e.g., I-129). Given that the ranges of variability applied to the sampled parameters are wider than expected and that logic for the mass bypass model is not limited to the peripheral zones of saltstone (see the response to RAI CC-3), the data in Table SP-2.1 indicates that it is unlikely that changes to the release of Tc-99 would result in total doses that exceed 25 mrem/yr within 10,000-years.

Figure SP-2.6: Tc-99 Dose Contributions from SDU 9 (via Probabilistic Tc-Ox Model)

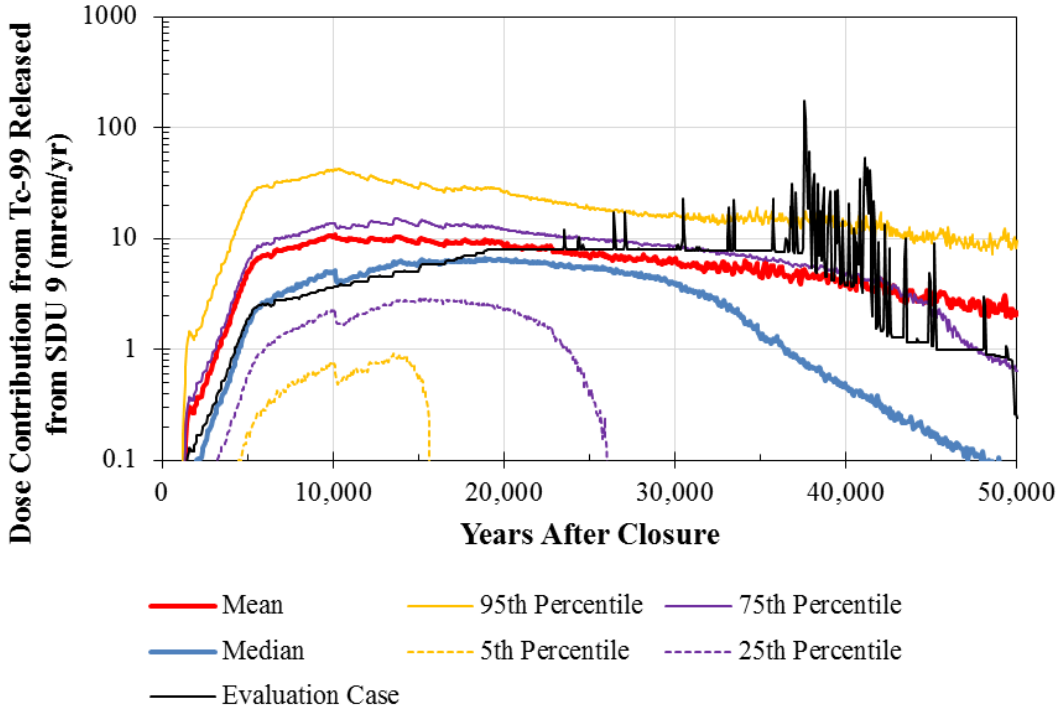

Figure SP-2.7: Total Dose Contributions from SDU 9 (via Probabilistic Tc-Ox Model)

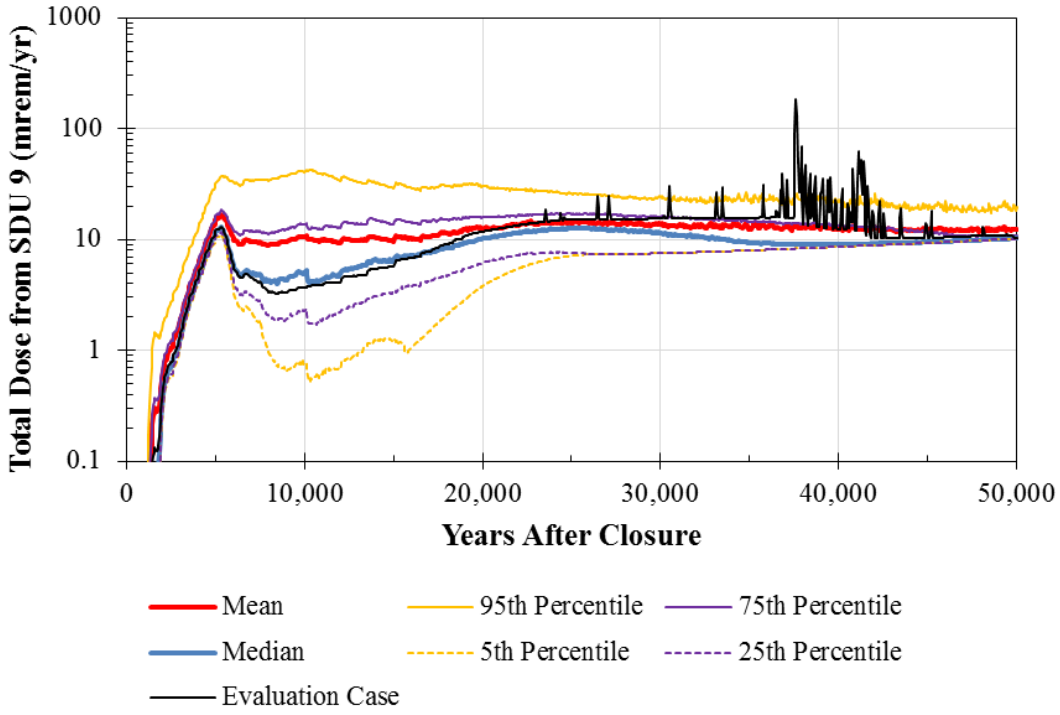

Table SP-2.1: Summary of Tc-99 Dose Contributions at 5,300 Years Based on the Probabilistic Tc-Ox Model

Model	Dose Statistic	Tc-99 Flux to the SZ at 5,300 Years (g/yr)	Tc-99 MOP Dose Contributions (mrem/yr)	Total Dose [a] (mrem/yr)
Evaluation Case (PORFLOW)	Deterministic Value	1.0	1.3	12.5
Probabilistic Tc-Ox Model (GoldSim)	Mean	3.9	5.9	17.1
	95th Percentile	16.5	25.9	37.1
	75th Percentile	4.6	7.5	18.7
	Median	1.5	2.1	13.3
	25th Percentile	0.5	0.7	11.9
	5th Percentile	0.1	0.2	11.3

Notes: (a) Adds the Tc-99 dose contribution to the 11.2 mrem/yr contributed from all other radionuclides at 5,300 years, based on the Evaluation Case results (Section 5.5 of the FY2014 SDF SA).

A statistical analysis of the correlations between the sampled parameters and the peak SZ fluxes of Tc-99 reveals a number of key observations. First, within 10,000 years, the peak flux is not particularly sensitive to the removal percent (mass bypass) or the reducing capacity of concrete. Instead, when the peak SZ flux is greater than about 8.0 g/yr, it is almost entirely dependent on the technetium solubility multiplier and the reducing capacity of saltstone. Figures SP-2.8 and SP-2.9 provide graphical depictions of the correlations between these two key parameters and the peak SZ Tc-99 flux.

Figure SP-2.8: Correlation Between Peak SZ Flux of Tc-99 (Within 10,000 Years) and the Reducing Capacity of Saltstone, Per Technetium Solubility (Probabilistic Tc-Ox Model; 1,000 Realizations)

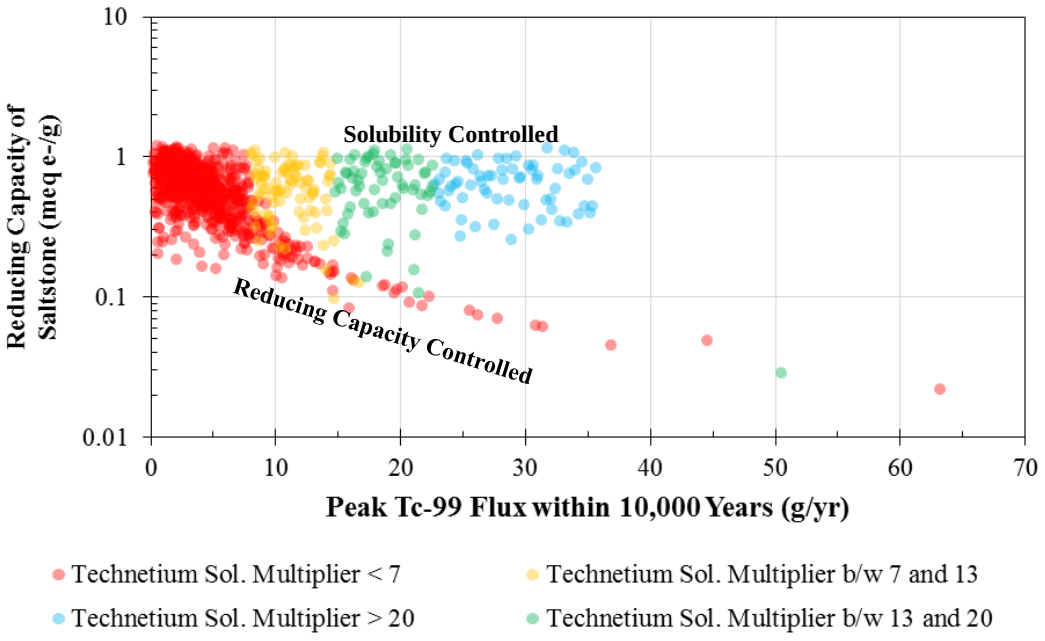

Figure SP-2.9: Correlation Between Peak SZ Flux of Tc-99 (Within 10,000 Years) and the Technetium Solubility Multiplier, Per Reducing Capacity of Saltstone (Probabilistic Tc-Ox Model; 1,000 Realizations)

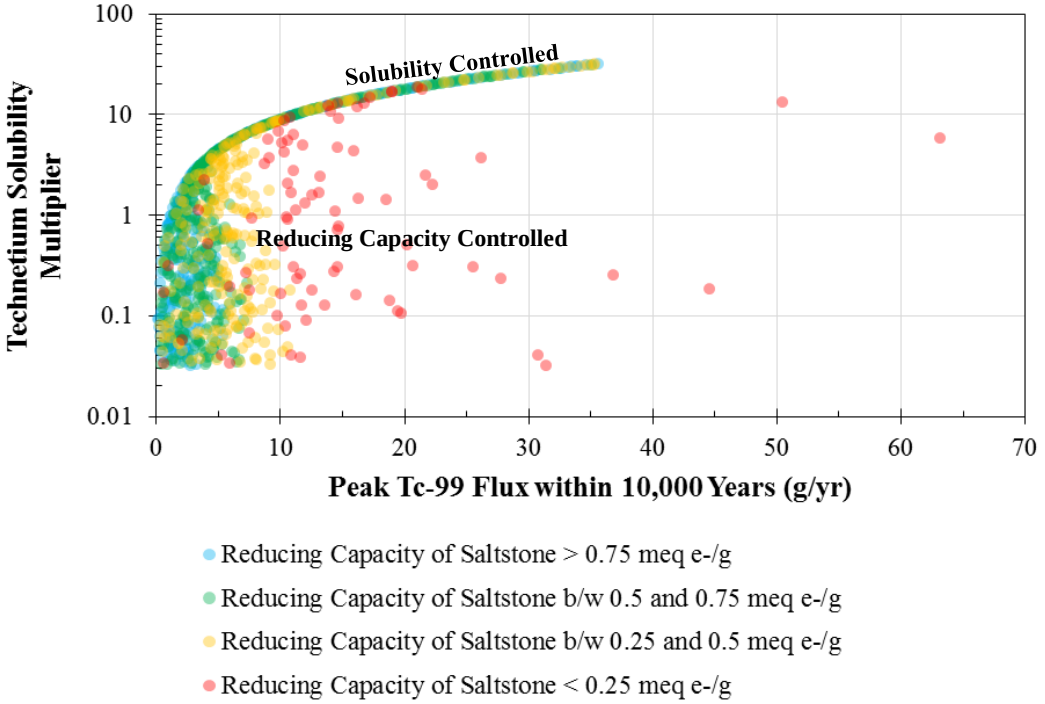

Essentially, these figures show that for the higher flux values, when the technetium solubility multiplier is greater than approximately 7.0 (such that the modeled technetium solubility is greater than 7.0E-08 mol/L), it becomes the dominant controlling parameter. The relationship is positive and almost perfectly linear. When the technetium solubility multiplier is less than 7.0, the reducing capacity of saltstone becomes the dominant controlling parameter. This relationship is negative and logarithmic. While there is a strong relationship between the reducing capacity of saltstone and the SZ flux of Tc-99, it is not as strong as that observed between the technetium solubility and the SZ flux of Tc-99.

This relationship can be observed in Figure SP-2.10, which shows the SZ flux over time for the 250 realizations that exhibited the highest peak fluxes within 10,000 years. In this figure, the flux curves that are distinctively "smooth" (i.e., the dominant band) are showing the release of Tc-99 as a function of the technetium solubility multiplier. The distinctively "spikey" fluxes are showing the release of Tc-99 as a function of the reducing capacity of saltstone. In general, the releases attributed to the reducing capacity were lower than those attributed to the solubility control.

Figure SP-2.10: Time Histories for SZ Flux of Tc-99 for the 250 Realizations with the Highest Flux within 10,000 Years (Probabilistic Tc-Ox Model)

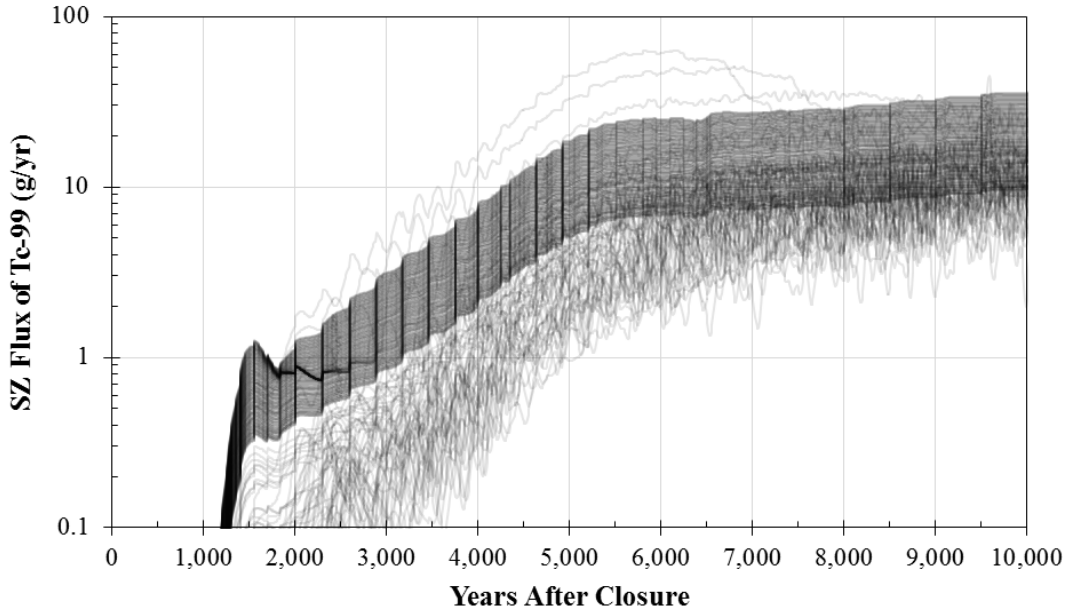

After the first 10,000 years, however, the technetium solubility is significantly less important. Over the 50,000-year simulation period, the technetium solubility is only important when the peak SZ flux is less than about 40 g/yr. Over time, as the magnitude of the peaks increase, the removal percentage (from the mass bypass) becomes increasingly more important. Figures SP-2.11, SP-2.12, and SP-2.13 provide graphical depictions of the relationships between the reducing capacity of saltstone, the removal percentage, technetium solubility, and the peak SZ flux of Tc-99. Figures SP-2.11 and SP-2.12 show the same values (i.e., the correlations between the reducing capacity of saltstone and the Tc-99 flux), but are colored according to the removal

percentage (Figure SP-2.11) and technetium solubility (Figure SP-2.12). Figure SP-2.13 shows the correlations between the removal percentage and the Tc-99 flux.

Figure SP-2.11: Correlation Between Peak SZ Flux of Tc-99 (Within 50,000 Years) and the Reducing Capacity of Saltstone, Per Mass Bypass / Removal Percentage (Probabilistic Tc-Ox Model; 1,000 Realizations)

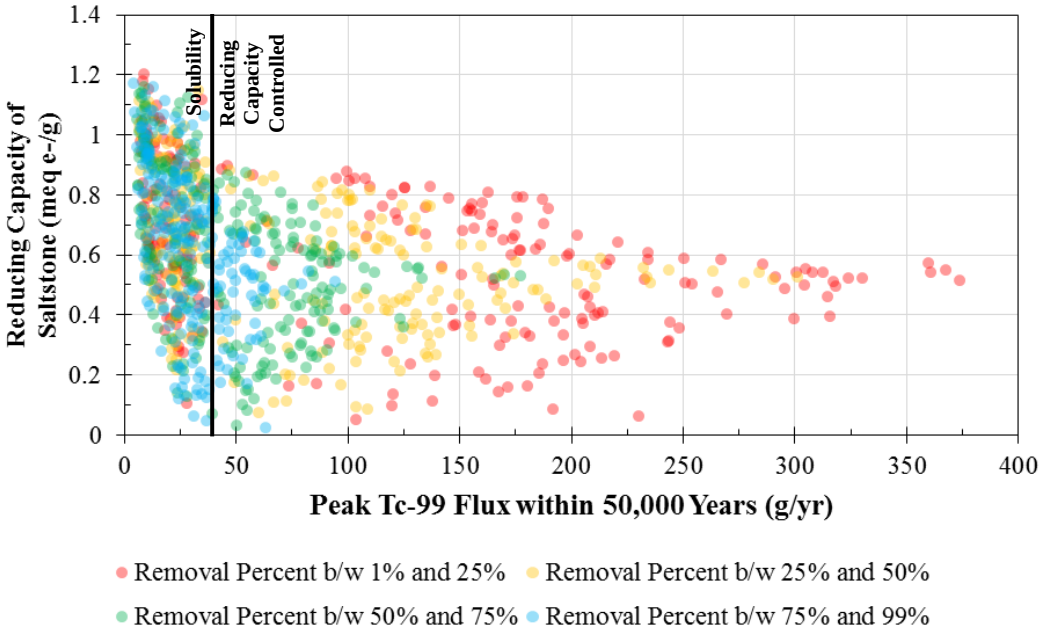

Figure SP-2.12: Correlation Between Peak SZ Flux of Tc-99 (Within 50,000 Years) and the Mass Bypass / Removal Percentage, Per Reducing Capacity of Saltstone (Probabilistic Tc-Ox Model; 1,000 Realizations)

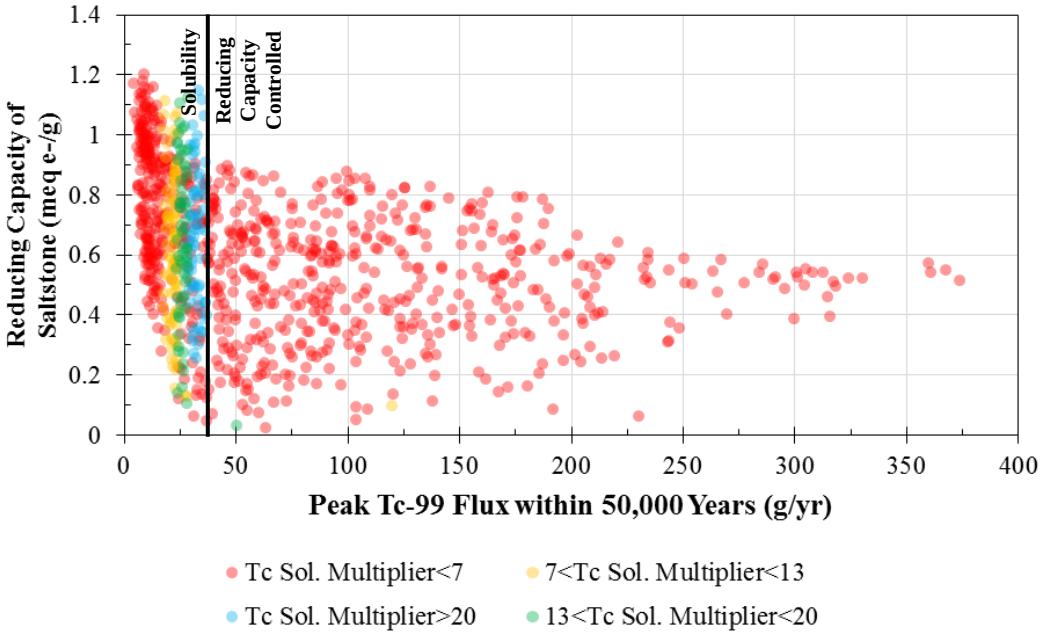

Figure SP-2.13: Correlation Between Peak SZ Flux of Tc-99 (Within 50,000 Years) and the Removal Percentage ("Mass Bypass") (Probabilistic Tc-Ox Model; 1,000 Realizations)

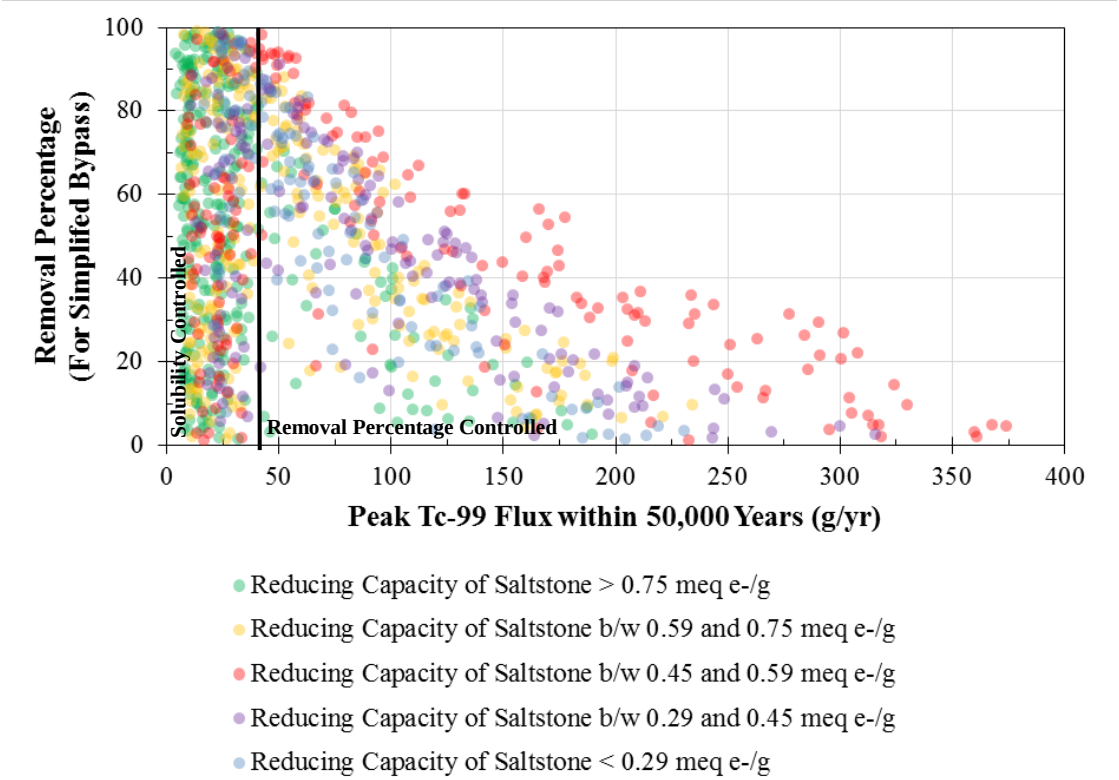

Figures SP-2.11, SP-2.12 and SP-2.13 show that the flux peaks are highest when the removal percentage is low and the reducing capacity of saltstone is between 0.45 and 0.59 meq e^-/g.

When the reducing capacity is lower, saltstone oxidizes more quickly, resulting in earlier Tc-99 releases. Over time, flow rates through saltstone increases as the material undergoes greater hydraulic degradation. If the saltstone oxidizes early in the simulation, the Tc-99 is released but it is not necessarily transported as quickly because flow through the relatively undegraded saltstone is slower.

Alternatively, when the reducing capacity is higher, saltstone takes longer to fully oxidize. If it takes a significantly long time for saltstone to oxidize, releases through the more limited release processes (i.e., solubility controls and the mass bypass removal percentage) will reduce the available inventory of Tc-99 before the oxidation occurs.

To maximize the peak SZ flux of Tc-99 within 50,000 years, the optimal reducing capacity for saltstone is about 0.52 meq e^-/g with no bypass (i.e., removal percentage = 0). Given that the Evaluation Case of the FY2014 SDF SA had very similar values (i.e., a reducing capacity for saltstone of 0.607 meq e^-/g and bypass was assumed along the outer edges of the saltstone), the results of the FY2014 SDF SA are conservative within the 50,000-year simulation period.

Figure SP-2.14 shows the SZ flux over time for the 250 realizations that exhibited the highest peak fluxes within 50,000 years. Because the correlations are not as strong as those observed within the first 10,000 years, the pattern exhibited by these fluxes is not immediately

distinguishable; however, it is noted that most of the fluxes are relatively low (i.e., less than 10 g/yr) for the first 20,000 years.

Figure SP-2.14: Time Histories for SZ Flux of Tc-99 for the 250 Realizations with the Highest Flux within 50,000 Years (Probabilistic Tc-Ox Model)

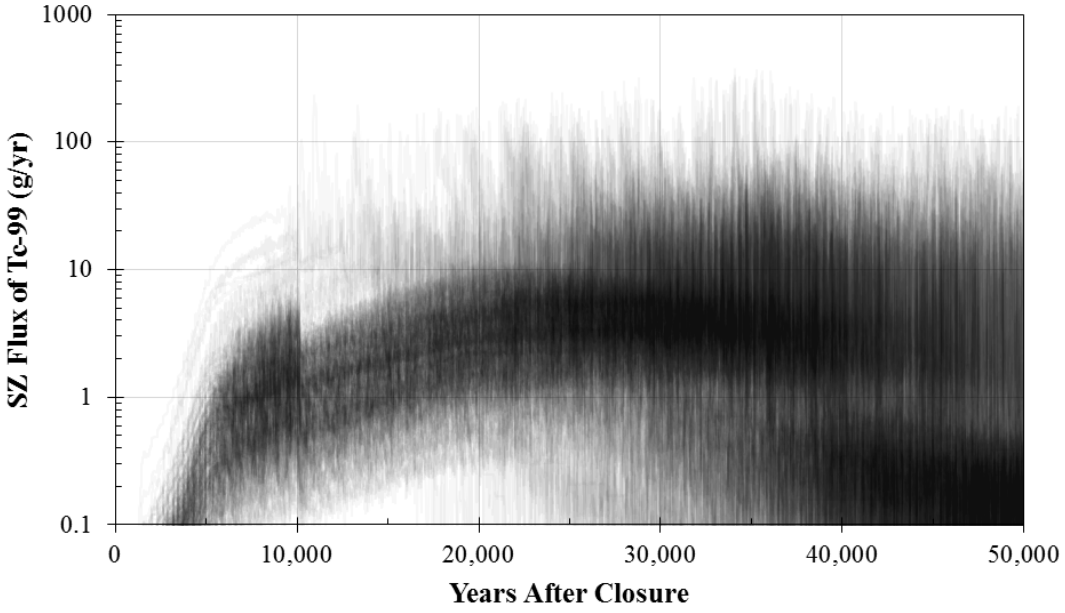

This pattern is more distinguishable in Figure SP-2.15 which only shows the top 50 realizations. In this figure, most of the earlier fluxes are even lower (between 1 and 5 g/yr in the first 20,000 years).

Figure SP-2.15: Time Histories for SZ Flux of Tc-99 for the 50 Realizations with the Highest Flux within 50,000 Years (Probabilistic Tc-Ox Model)

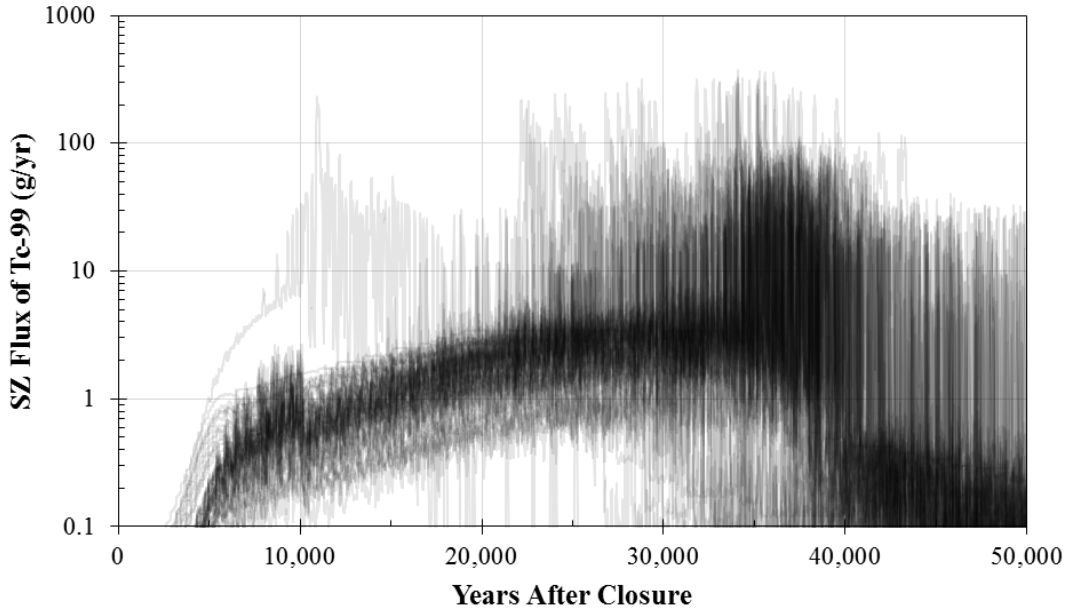

Finally, Figures SP-2.16 through SP-2.20 are provided for informational purposes. Each of these figures shows the magnitude and the timing of the peak Tc-99 fluxes, with varying colors to indicate the respective sampled values. Note that in Figures SP-2.16 and SP-2.17 the multiple peaks occurring at approximately 9,500 years correspond to the timing of the last change to the volumetric flow rate through saltstone within 10,000 years (see Figure 4.4-12 of the FY2014 SDF SA).

Figure SP-2.16: Peak SZ Flux of Tc-99 Within 10,000 Years (Probabilistic Tc-Ox Model; 1,000 Realizations), By Technetium Solubility Multiplier

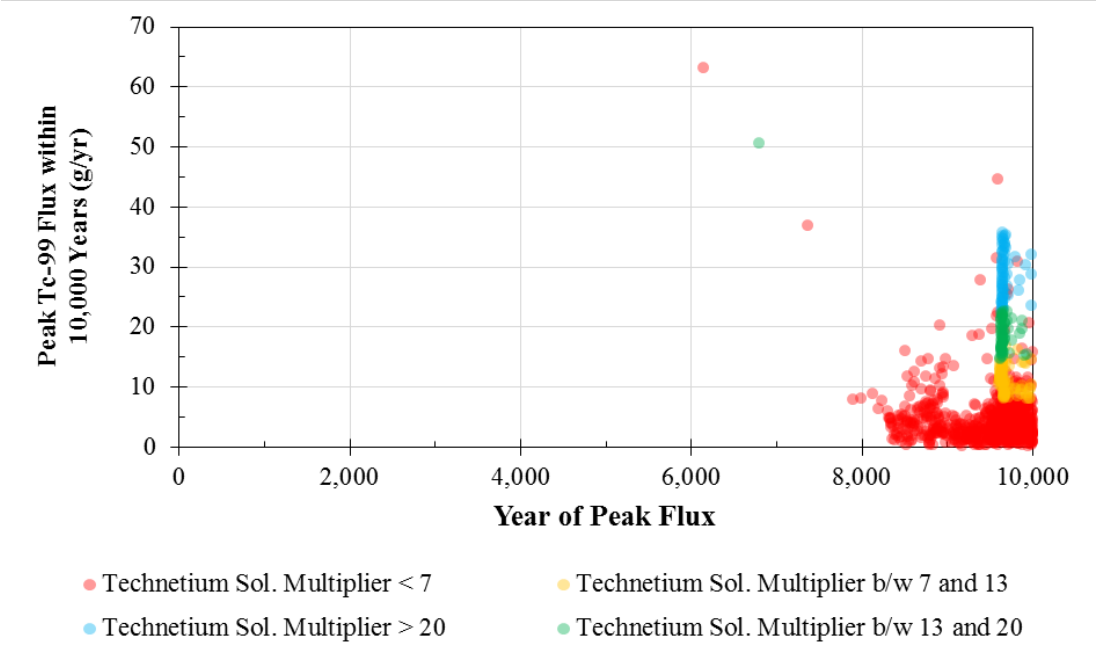

Figure SP-2.17: Peak SZ Flux of Tc-99 Within 10,000 Years (Probabilistic Tc-Ox Model; 1,000 Realizations), By Reducing Capacity of Saltstone

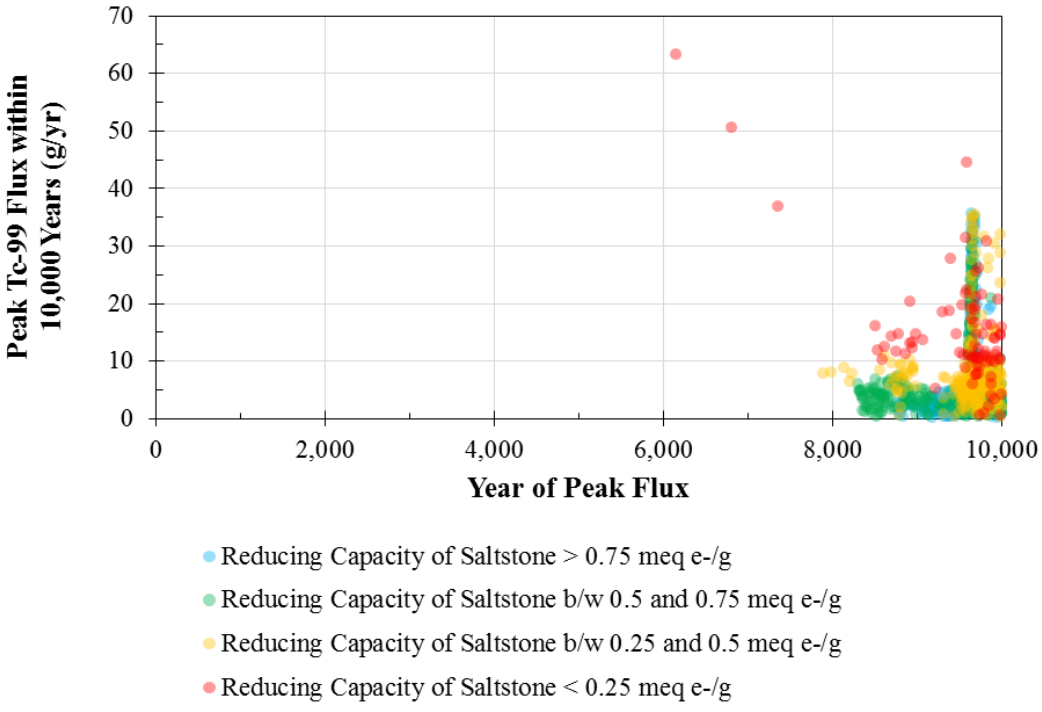

Figure SP-2.18: Peak SZ Flux of Tc-99 Within 50,000 Years (Probabilistic Tc-Ox Model; 1,000 Realizations), By Reducing Capacity of Saltstone

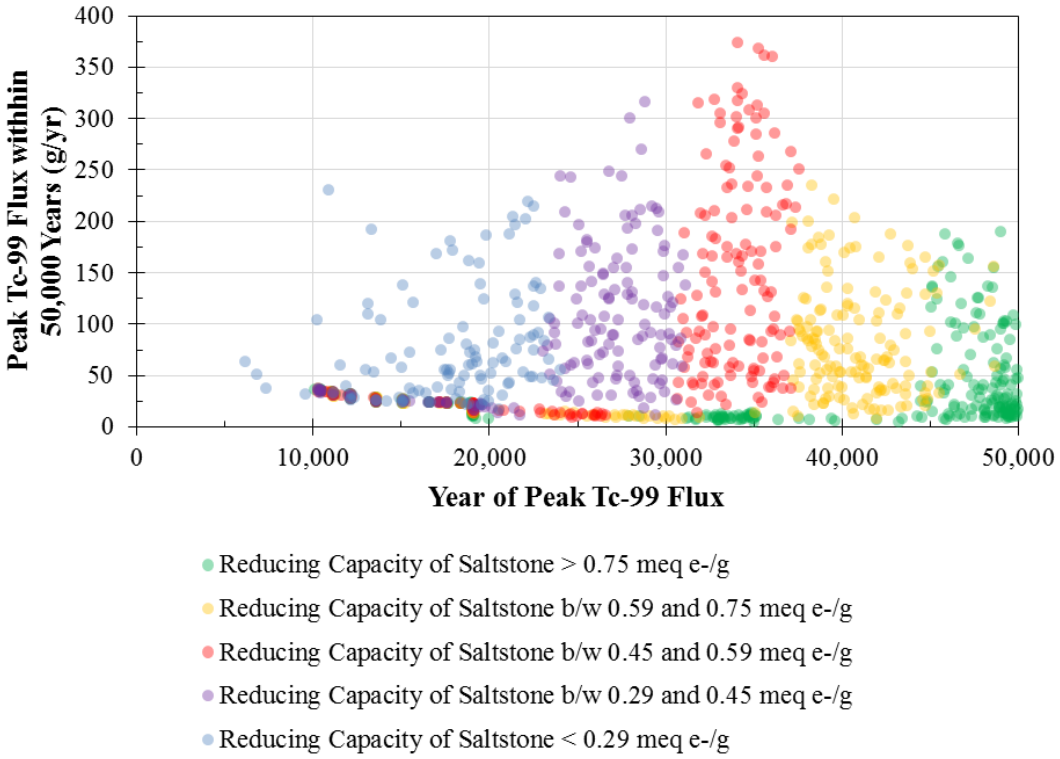

Figure SP-2.19: Peak SZ Flux of Tc-99 Within 50,000 Years (Probabilistic Tc-Ox Model; 1,000 Realizations), By Removal Percentage ("Mass Bypass")

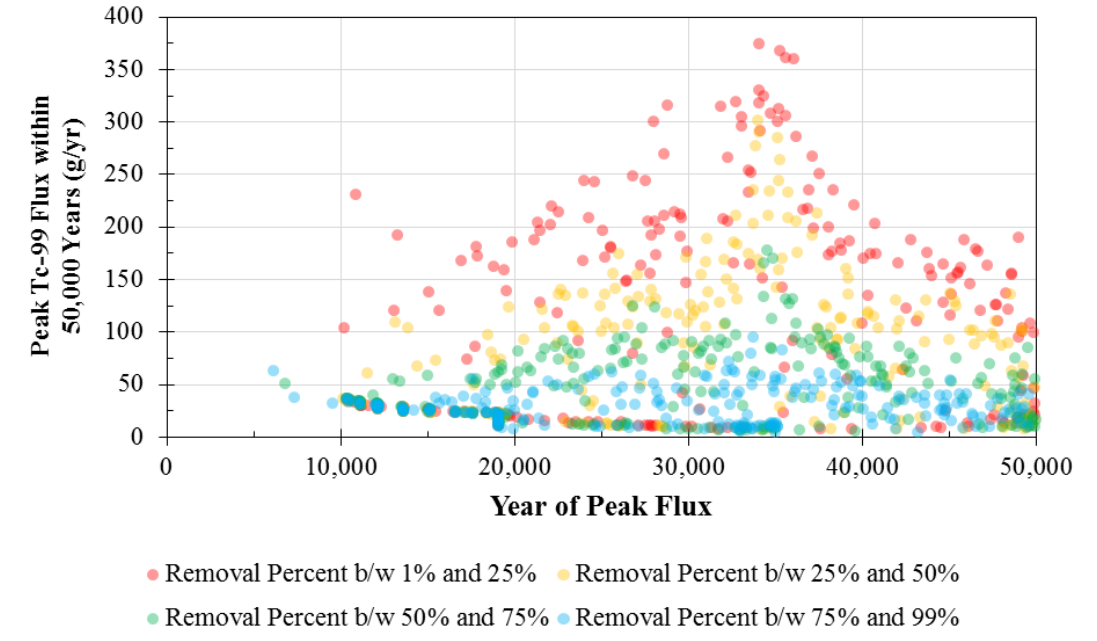

Figure SP-2.20: Peak SZ Flux of Tc-99 Within 50,000 Years (Probabilistic Tc-Ox Model; 1,000 Realizations), By Technetium Solubility Multiplier

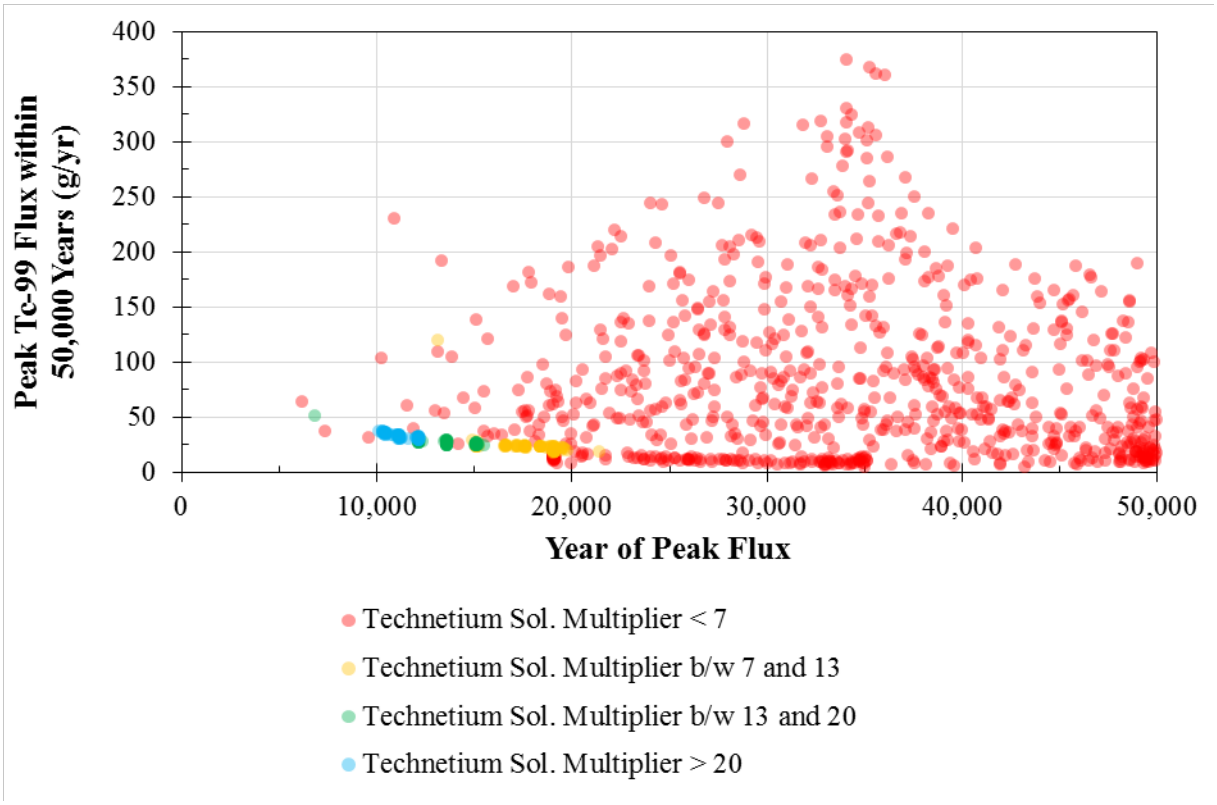

SP-3

SP-3	**Question:** It is not clear to the NRC staff that the DOE assumption of a linear rate of degradation of saltstone is conservative and bounds all potential additional degradation mechanisms.
	Basis: In the DOE 2015 Response to the NRC 2014 RAI Comments (see RAI Comment SP-4 in that document), the DOE indicated that the hydraulic conductivity of the roof of a disposal structure will increase by three orders of magnitude by the end of the 100-year institutional control period. Also, the DOE stated that: "No known degradation mechanisms would have such a substantial impact on the degradation of the cementitious materials." It is not clear to the NRC staff: (1) which degradation mechanism or coupled mechanisms may control the degradation of saltstone, (2) the extent to which saltstone may degrade prior to significant increases in hydraulic properties, and (3) the rate at which saltstone hydraulic properties evolve. Saltstone is a unique cementitious material that is chemically and hydraulically very far from equilibrium with respect to the surrounding natural environment and has a porosity of approximately 60 percent (%). Generally, the further a material is from equilibrium the more quickly its properties evolve to that of the surrounding environment. The hydraulic conductivity of compacted clay barriers have been observed to increase by several orders of magnitude within several years due to the formation of preferential flow paths that controlled the hydraulic conductivity (see NUREG CR-7028, Vol. 1). The NRC staff understands that degradation of cementitious materials will differ from that of clay barriers; however, cementitious materials, in particular saltstone with a porosity of approximately 60%, would appear to be susceptible to the formation of preferential flow paths due to the low, contrasting matrix permeability. Dissolution, cracking, or the combination of those two processes may initially have minimal impact on the hydraulic properties of saltstone until a threshold interconnectivity of pores exists. After that extent of degradation is reached and significant interconnectivity of pores exists, the hydraulic properties could increase at a rate greater than the DOE assumed linear increase in hydraulic conductivity.
	Path Forward: Provide a technical basis to support the DOE assumption that saltstone will either not hydraulically degrade in a non-linear fashion or that the threshold for that degradation would not result in the DOE not meeting the performance objectives of 10 CFR Part 61.

DOE Response to SP-3

The DOE acknowledges that because saltstone is a unique cementitious material, there are no pre-existing man-made or natural materials from which material property tests can be performed. Therefore, the DOE must rely on analytical modeling techniques to predict the long-term performance of saltstone. The DOE shall continue to pursue improvements in this area in collaboration with cementitious material experts (e.g., the DOE Cementitious Barriers Partnership (CBP)).

As explained in Section 4.2.2 of the FY2014 SDF SA, the current degradation model assumes decalcification to be the primary mechanism controlling saltstone degradation. [SRR-CWDA-2014-00006] For greater defensibility, the "best estimate" of the analytical hydraulic

degradation rate was increased by an order of magnitude to create the nominal degradation rate (e.g., for the 375-foot diameter SDUs full degradation of saltstone occurs in about 438,000 years (Nominal) instead of 4,380,000 years (Best Estimate)). Figure SP-3.1 illustrates the significance of this built-in conservatism.

Figure SP-3.1: Saturated Hydraulic Conductivity for the 375-Foot Diameter SDU Saltstone

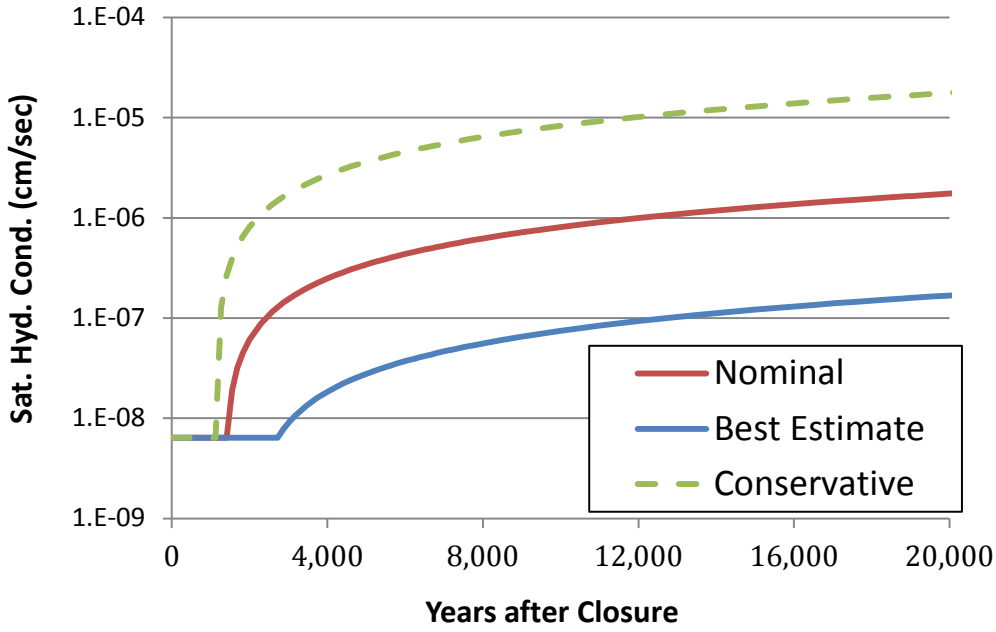

[Source: FY2014 SDF SA, Figure 4.2-19]

The response to RAI SP-1 demonstrated an alternative approach for modeling degradation which incorporated a feedback loop in order to more appropriately consider the effects of the changing hydraulic properties over time. This approach showed that saltstone could take significantly longer than 11,000 years to reach or exceed 8.5E-07 cm/sec (i.e., the Nominal Case took approximately 200,000 years to reach a hydraulic conductivity of 8.5E-07 cm/sec). Therefore, the linear degradation rate is likely conservative, relative to the degradation approach applied in response to RAI SP-1.

Given the available information, the DOE believes that the current approach is conservative with respect to the 1,000-year compliance period (per DOE M 435.1-1) and even with respect to periods 10,000 years and beyond.

SP-4

SP-4	**Question:** The DOE assumption that degradation of saltstone was based on the amount of time for complete decalcification to occur, rather than a progression of increased hydraulic conductivity in the uppermost layer followed by the successive underlying layers, was not justified in either the DOE FY13 or the DOE FY14 SDF Special Analysis documents.
	Basis: In both the DOE FY13 and the DOE FY14 SDF Special Analysis documents, the DOE assumed that saltstone degraded uniformly as an intact monolith with the hydraulic conductivity increasing linearly with respect to time due to decalcification. However, the process of decalcification would tend to result in the preferential removal of calcium from the uppermost layers, followed by removal of calcium in the successive underlying layers. Consequently, the hydraulic conductivity of the uppermost layers would increase more quickly than the underlying layers. It is not clear to the NRC staff how that top-down progression of decalcification and the corresponding hydraulic properties of saltstone impacts the release of radionuclides; in particular as it is coupled with the Tc shrinking core model.
	Path Forward: Provide a basis for why the DOE did not consider the top-down progression of decalcification for the hydraulic degradation of saltstone to be plausible or risk-significant. Alternatively, provide dose results incorporating an analysis with a conceptual model of a top-down progression of decalcification for the hydraulic degradation of saltstone.

DOE Response to SP-4

As discussed in the response to RAI SP-1, DOE does consider the top-down progression of decalcification for the hydraulic degradation of saltstone to be plausible, but does not consider it to be risk-significant. The reason that it is not considered to be risk-significant is because of an offsetting conservatism inherent to the DOE modeling effort. The DOE degradation model solves for the time needed for the decalcification front to reach the bottom of the saltstone assuming advection dominates and using the initial saltstone hydraulic conductivity throughout the calculation. Although the use of this constant hydraulic conductivity generates a conservative (later) time, at which the hydraulic conductivity reaches the fully degraded value, the use of a straight line increase (i.e., linear degradation rate) from initial conductivity to fully degraded conductivity weights the increase in conductivity towards early time.

Because of the highly conservative nature of the linear approximation used to generate hydraulic conductivities used in the PORFLOW simulations, the approximation tends to be conservative as shown in Figures SP-1.1 and SP-1.2. Figures SP-1.1 and SP-1.2 present comparisons of the time-dependent hydraulic conductivities used in the PORFLOW model with effective hydraulic conductivities based on the time-dependent harmonic mean of a two-layered system defined by the saltstone hydraulic conductivities ahead and behind the moving decalcification front. As discussed in RAI SP-1, the saltstone hydraulic conductivities used for the PORFLOW simulations tends to be higher than they would have been if generated assuming a time-dependent hydraulic conductivity based on a moving front.

SP-5

SP-5	**Question:** Additional analysis is needed to demonstrate the effect on dose of removing the modeled delay before saltstone degradation begins.
	Basis: In the DOE FY14 SDF Special Analysis document, the DOE modeled saltstone in the 375-foot disposal structures as beginning to degrade 1,413 years after site closure[1] and the DOE modeled saltstone in the 150-foot disposal structures as beginning to degrade 961 years after site closure. Previously, the DOE modeled saltstone in Saltstone Disposal Structure (SDS) 4 as beginning to degrade 2,112 years after site closure. In each model, the DOE assumed that saltstone degradation would not begin until after the roof was completely degraded by chemical mechanisms. However, saltstone fracturing caused by physical mechanisms could occur prior to complete chemical degradation of a roof. Certain mechanisms, such as shrinkage, cracking, or fracturing due to thermal gradients, could occur within the first year after emplacement. Also, saltstone fractures have occurred in SDS 4 already (see SRNL-ESB-2008-00017). In addition fracturing due to differential settlement could occur within several years after site closure. Degradation of saltstone beginning earlier than DOE assumed could lead to higher hydraulic conductivity during the performance period. In addition, eliminating the DOE assumed degradation period could shift doses due to risk-significant radionuclides, such as Iodine-129, earlier in the performance period.
	Path Forward: Provide an analysis that demonstrates the effects on all three types of disposal structures on dose of removing the delay before saltstone degradation begins.

DOE Response to SP-5

A GoldSim simulation (herein referred to as SP-5 Simulation) was performed to address the NRC's question regarding an earlier onset to saltstone degradation than assumed in the FY2014 SDF SA. [SRR-CWDA-2014-00006] Since GoldSim imports its flow fields from PORFLOW, DOE took a conservative approach and shifted the flows GoldSim was importing from PORFLOW by the degradation delay (see Table SP-5.1) for a given SDU type (i.e., the flow data used by GoldSim at time X was set equal to the PORFLOW flow data at time (X + degradation delay)). In other words, the delay time prior to the start of saltstone degradation was ignored. In so doing, the GoldSim simulations (for the SDF Tc-99 Release Model and SDF All-Species Model) are effectively starting at time zero, but with higher infiltration rates than predicted by the closure cap model and used in PORFLOW.

[1] In the context of these RAIs and RAI responses, "site closure" refers to facility closure of the Saltstone Disposal Facility and not the closure of the Savannah River Site.

Table SP-5.1: Saltstone Degradation Delay for each SDU Type

Disposal Unit	Degradation Delay (yr)
SDU 1	486
SDU 4	2,112
150-ft SDU	961
375-ft SDU	1,413

In the GoldSim SDF All-Species Model (described in the FY2014 SDF SA), chemical transition times are imported from PORFLOW and calculated using a pore-flush model. Since flows in the SP-5 Simulation are shifted relative to PORFLOW, the GoldSim SDF All-Species Model was modified to calculate the chemical transition times directly using the pore-flush model rather than importing the results from PORFLOW. This modification was not necessary for the GoldSim SDF Tc-99 Release Model since transition times in this instance are calculated via the transition time dynamic link library which utilizes a shrinking core model. [SRR-CWDA-2013-00073]

Figure SP-5.1 is included here to show the difference in the saltstone flow rate from the FY2014 SDF SA Evaluation Case and the SP-5 Simulation.

Figure SP-5.1: Comparison of Volumetric Flow (cm^3/yr) through Saltstone

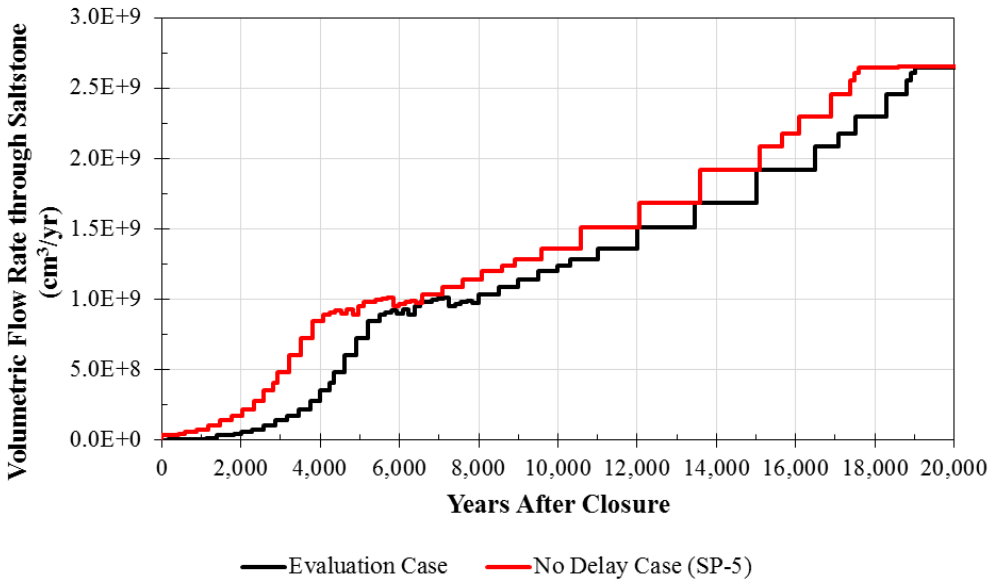

Results comparing the SP-5 Simulation to the FY2014 SDF SA Evaluation Case are presented in Figures SP-5.2 and SP-5.3 and summarized in Table SP-5.2. The results demonstrate that while removal of the degradation delay does shift the peak doses in the 10,000-year and 50,000-year windows to earlier times (1,600 years earlier and 960 years earlier, respectively), the magnitude and shape of the peaks remain largely unchanged and the performance objective is still met. Therefore, the SP-5 Simulation provides reasonable expectation/assurance that if saltstone degradation were to begin without a delay for all SDUs, the peak dose at the 100-meter SDF boundary would remain below 25 mrem/yr through 10,000 years.

Figure SP-5.2: Dose at the 100-meter SDF boundary (10,000 years)

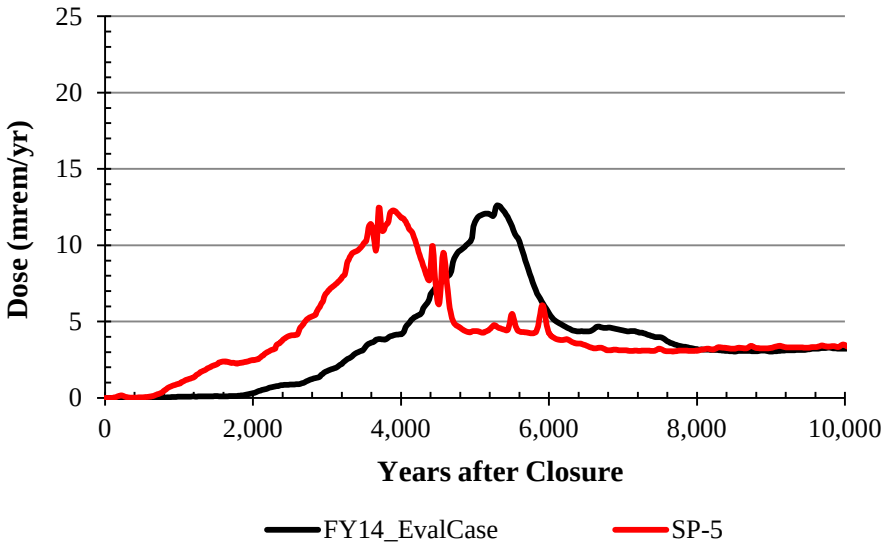

Figure SP-5.3: Dose at the 100-meter SDF boundary (50,000 years)

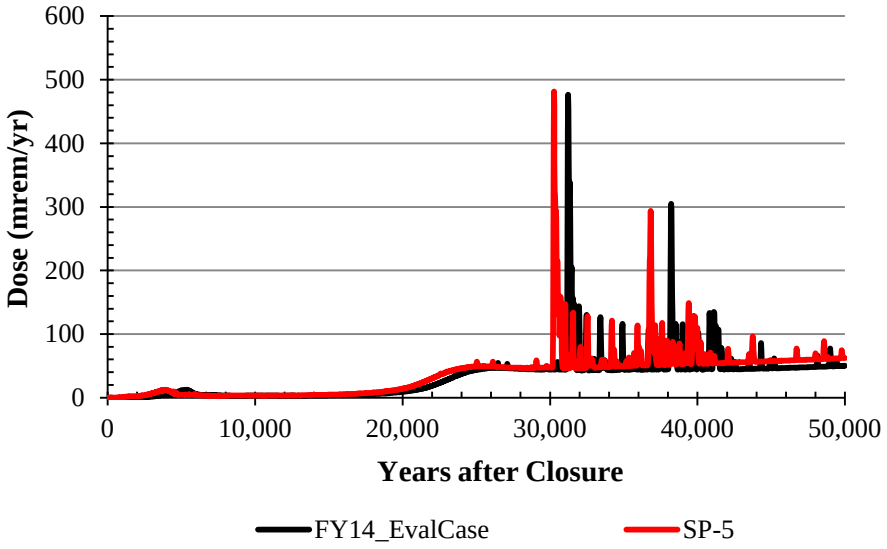

Table SP-5.2: Summary of SP-5 GoldSim Simulation

GoldSim Simulation	Peak Dose (mrem/yr)		Peak Year	
	10,000 yr	50,000 yr	10,000 yr	50,000 yr
FY14_EvalCase	1.26E+01	4.77E+02	5,300	31,220
SP-5	1.25E+01	4.81E+02	3,700	30,260

SP-6

SP-6	**Question:** Additional support is needed to justify the use of residual reducing capacity as a basis for Tc-99 release.
	Basis: As described in the NRC RAI Comment SP-9 on the DOE FY13 SDF Special Analysis document, recent research from Savannah River National Laboratory (SRNL) (SRNL-STI-2013-00541) and the Cementitious Barriers Partnership (CBP) (CBP-TR-2013-002) has called into question the use of reducing capacity as the basis for the DOE Tc-99 release model. The SRNL research indicated that residual reducing capacity does not appear to be well-correlated to Tc-99 mobility in chemically reducing cementitious materials. The reason for the poor correlation between residual reducing capacity and Tc-99 release in the research is not clear to the NRC staff. However, that type of behavior could result if some of the reactions that the DOE modeled as going to equilibrium were kinetically limited. In the DOE 2015 Response to the NRC 2014 RAI Comments (see RAI Comment SP-9 in that document), the DOE referenced the revised Tc-99 release model, which released Tc-99 from each PORFLOW finite element more gradually than the release model used to support the DOE FY13 SDF Special Analysis document. The revised Tc-99 release model was responsive to several different NRC RAI Comments; but did not address the possible poor correlation of Tc oxidation with saltstone residual reducing capacity because the release was still computed as a function of the residual reducing capacity. One implication of a potential poor correlation between Tc chemical reduction and residual reducing capacity in saltstone was to undermine the DOE assumption that Tc would be re-reduced if it was transported into an area of saltstone with residual reducing capacity. In the DOE FY14 SDF Special Analysis document, the DOE performed a sensitivity analysis to demonstrate the effects of modeled re-reduction of Tc-99 when it entered a PORFLOW model finite element with residual reducing capacity. That sensitivity analysis used a simple mass transfer to model the transfer of various fractions of Tc directly into the aquifer when it was oxidized (i.e., eliminating re-reduction for different fractions of Tc). That sensitivity analysis demonstrated increased Tc-99 release before 10,000 years when Tc-99 was assumed not to be re-reduced (i.e., peak release rate increased by a factor of 10 within 10,000 years) and decreased projected peak doses at longer times (i.e., peak release rate decreased by a factor of 15 within 50,000 years). However, that sensitivity analysis did not provide all of the needed information about the potential effects on dose if Tc-99 were oxidized and became mobile before the surrounding residual reducing capacity was consumed because the rate of Tc oxidation was still limited by the modeled progress of the oxidation front in saltstone. In the DOE 2015 Response to the NRC 2014 RAI Comments (see RAI Comment SP-9 in that document), the DOE also referenced planned future research using a dynamic leaching procedure with cores of field-emplaced saltstone. Those experiments may provide important information on the release of Tc from field-emplaced samples. In addition, a sensitivity analysis related to non-depleting oxygen sources in saltstone may provide insight into the potential effects of Tc oxidation in areas of saltstone that still have residual reducing capacity. The DOE originally provided that analysis in the DOE FY13 SDF Special Analysis document and described it further in Section 5.6.7.4 of the DOE FY14 SDF Special Analysis document. Although that sensitivity analysis bases Tc oxidation on the residual reducing capacity in saltstone, it is relevant to concerns about the potentially poor correlation of Tc mobility to saltstone reducing capacity because the non-depleting oxygen

	sources could be interpreted , non-mechanistically as areas where Tc is oxidized prior to being reached by an oxidation front moving through saltstone. In the NRC RAI Comments on the DOE FY13 SDF Special Analysis document, the NRC staff identified that the results of the sensitivity analysis with non-depleting oxygen sources were difficult to interpret because Tc-99 released from areas near the non-depleting oxygen sources was immediately re-reduced by surrounding material. In the DOE FY14 SDF Special Analysis document, the DOE indicated that between 10,000 and 16,000 years after site closure[1], the oxidized areas began to interconnect, which provided connected pathways for Tc-99 migration. The DOE did not provide results in terms of dose for that sensitivity analysis. However, Figure 5.6.7-13 in the DOE FY14 SDF Special Analysis document showed release rates comparable to the release rate in the DOE evaluation case that resulted in a projected dose of 477 mrem/yr approximately 31,000 years after site closure. Figure 5.6.7-13 also showed that increasing the fraction of saltstone represented by non-depleting oxygen sources moved the Tc-99 release significantly forward in time and where 20% of the saltstone was represented with a non-depleting oxygen source, the releases began within 10,000 years of site closure.
	Path Forward: Provide a description of the potential effects on projected performance of an alternative conceptual model where residual reducing capacity of cementitious materials does not govern Tc-99 release. A potential analysis could combine the sensitivity analyses that the DOE conducted with non-mechanistic non-depleting oxygen sources and limited re-reduction. Alternately, the DOE could provide laboratory or field evidence that supports the use of residual reducing capacity as a basis for Tc-99 release. Any evidence supporting the use of residual reducing capacity as a basis for Tc-99 release should address the results of recent research from SRNL (SRNL-STI-2013-00541) and the CBP (CBP-TR-2013-002).

DOE Response to SP-6

DOE's response to RAI SP-2, in particular the section on the probabilistic Tc-Ox Model, provides a basis for additional discussion. Results from the probabilistic Tc-Ox Model utilized in SP-2 illustrate that:

1) If Tc solubility exceeds approximately 7.0E-08 mol/L
   a. The peak Tc flux within 10,000 years and 50,000 years is primarily controlled by Tc solubility
2) If Tc solubility is below approximately 7.0E-08 mol/L
   a. The peak Tc flux within 10,000 years is primarily controlled by saltstone reduction capacity
   b. The peak Tc flux within 50,000 years is controlled by both saltstone reduction capacity and the percentage of Tc mass applied to the simplified mass bypass model

[1] In the context of these RAIs and RAI responses, "site closure" refers to facility closure of the Saltstone Disposal Facility and not the closure of the Savannah River Site.

Scenarios in which Tc solubility varies are considered in further detail in DOE's response to RAI SP-12.

In this response, the impact that reduction capacity and mass bypass have on Tc-99 release is addressed by means of a sensitivity analysis considering ten different scenarios in the GoldSim SDF Tc-99 Release Model (Table SP-6.1). Specifically, two different configurations of saltstone and concrete reducing capacity were considered:

Configuration 1: The FY2014 SDF SA Evaluation Case

Configuration 2: A conservative worst-case scenario assuming saltstone has the reduction capacity of SDU concrete and the SDU concrete has the reduction capacity of SRS sandy sediment

The use of two different material property configurations in this sensitivity analysis was to account for variability in the predicted reduction capacity. Although non-mechanistic non-depleting oxygen sources were not explicitly modeled, the effect of these oxygen sources on reduction capacity and Tc mobility is approximated by Configuration 2. The composition and reduction capacities for the materials considered in this sensitivity analysis are provided in Table SP-6.2.

Table SP-6.1: Sensitivity Cases Considered for SP-6 Response

Configuration	Assigned Reducing Properties		Mass Bypass Removal Percentage				
	Saltstone	**Concrete**	Case A	Case B	Case C	Case D	Case E
1	TR547 Saltstone	SDU 2 Concrete	0%	25%	50%	75%	100%
2	SDU 2 Concrete	Sandy Sediment					

Table SP-6.2: Experimental Reduction Capacities for Materials Related to the SDF

Sample	Composition (dry-wt%)				Reducing Capacity (meq e-/g)	Reference
	Slag	**Portland Cement**	**Fly Ash**	**Aggregate/ sand**		
SDU 2 Concrete	17	13	10	58	1.78E-01	WSRC-RP-2005-01674 and SRNL-STI-2009-00637
TR547 [a]	45	10	45	0	6.07E-01	SRNL-STI-2009-00637
Sandy Sediment[b]	N/A	N/A	N/A	N/A	8.12E-02	SRNS-STI-2008-00045

Notes: (a) Saltstone simulant. All percentages of saltstone formulations are reported on a dry weight percentage basis, that is, the weight of the ingredients before water was added.
(b) SRS subsurface sediment.

Recent research by Savannah River National Laboratory (SRNL) suggests a poor correlation between residual reducing capacity (as measured using the Angus-Glasser Ce(IV)-Fe(II) method) and Tc-99 mobility in chemically reducing cementitious materials. [SRNL-STI-2013-00541] While the results of this research are valuable, it may not be directly applicable to Tc-99 releases from saltstone at the SDF due to the use of an alternative formula for the cementitious waste

form. Similarly, the study from the Cementitious Barriers Partnership (*Effect of Oxidation on Chromium Leaching and Redox Capacity of Slag-Containing Waste Forms*) may not be applicable as it drew conclusions based on chromium releases, but did not explicitly study the effects on technetium. [CBP-TR-2013-002]

Regardless, to account for potential uncertainty in Tc-99 releases, five different mass bypass removal percentages ranging from 0% to 100% were considered in the sensitivity analysis effectively limiting Tc-99 re-reduction. Note, the mass bypass model is described in Section 4.4.2.2 of the FY2014 SDF SA. The results from the sensitivity analysis are presented in Figures SP-6.1 and SP-6.2 and summarized in Table SP-6.3.

Figure SP-6.1: Sensitivity Analysis Peak Dose Results at the 100-Meter Boundary (10,000 Years)

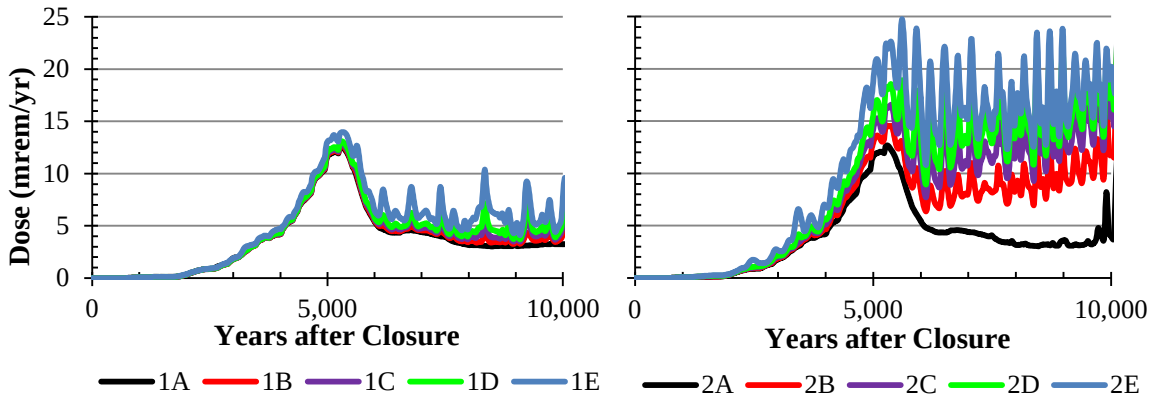

Figure SP-6.2: Sensitivity Analysis Peak Dose Results at the 100-Meter Boundary (50,000 Years)

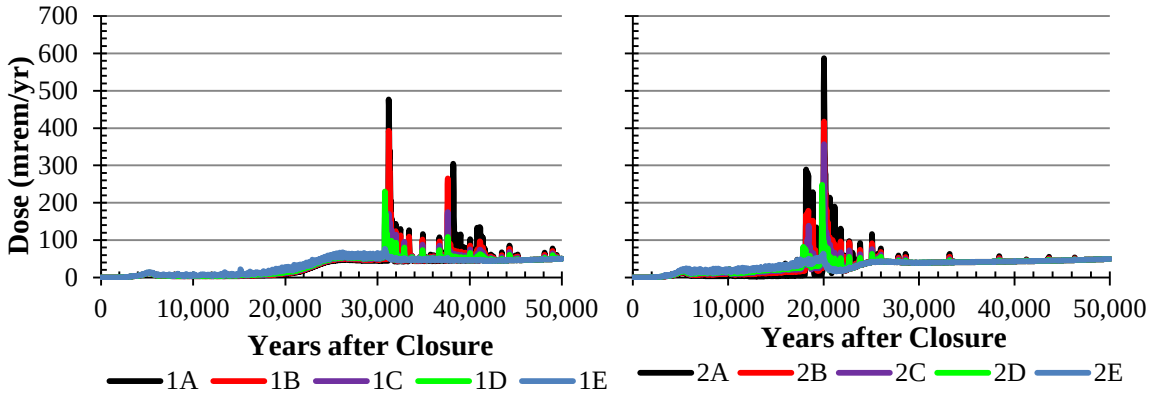

Table SP-6.3: Summary of Sensitivity Analysis Results

Sensitivity Case	Tc Solubility (mol/L)	Assigned Reducing Properties		Mass Bypass Removal Percentage	Peak Dose (mrem/yr)	
		Saltstone	Concrete		10,000 yr	50,000 yr
1A	1.00E-08	TR547 Saltstone	SDU 2 Cement	0%	1.27E+01	4.77E+02
1B				25%	1.28E+01	3.93E+02
1C				50%	1.29E+01	1.76E+02
1D				75%	1.31E+01	2.31E+02
1E				100%	1.40E+01	7.71E+01
2A	1.00E-08	SDU 2 Cement	Sandy Sediment	0%	1.27E+01	5.88E+02
2B				25%	1.61E+01	4.17E+02
2C				50%	1.94E+01	3.57E+02
2D				75%	2.18E+01	2.49E+02
2E				100%	2.48E+01	6.39E+01
2E_HighTcSol	4.20E-08			100%	2.36E+01	7.43E+01

Figure SP-6.1 illustrates that even under the most conservative conditions considered (Sensitivity Case 2E), the peak dose does not exceed 25 mrem/yr within 10,000 years. Put another way, the SDF is predicted to meet the performance objective even when the effects of non-mechanistic, non-depleting oxygen sources are simulated (Configuration 2) and zero Tc-99 re-reduction occurs (100% mass bypass).

An additional sensitivity case was run to determine what impact the anticipated higher Tc solubility for Reduced/Young cementitious material (i.e., 4.2E-08 mol/L, see RAI SP-12 for details) would have on dose under Sensitivity Case 2E conditions. The results of this simulation (Sensitivity Case 2E_HighTcSol) presented in Table SP-6.3 and Figure SP-6.3 reveals that the performance objective is still met under these conditions, and that the increased Tc solubility actually lowers the peak dose within 10,000 years. In summary, this sensitivity analysis provides reasonable expectation/assurance that the SDF will meet the performance objective even if non-mechanistic, non-depleting oxygen sources are present and zero re-reduction occurs.

Figure SP-6.3: Impact of Increased Tc Solubility on Most Conservative Sensitivity Case

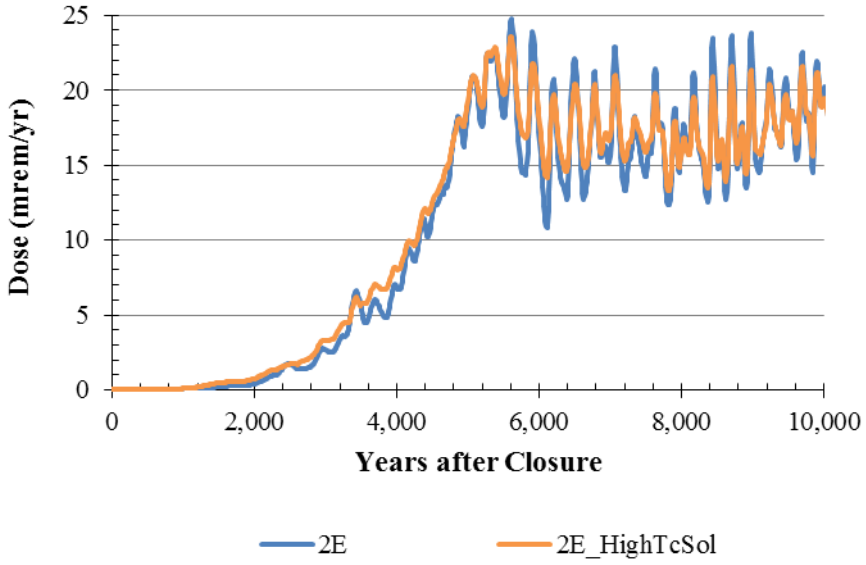

Finally, note that testing is currently being conducted on a laboratory-prepared monolithic sample in which groundwater simulants are forced through a Tc-99 spiked saltstone sample utilizing a positive pressure differential of approximately 12 psi from the sample inlet to the outlet. This testing enables accelerated pore volume exchange (one pore volume per ≈ 1,500 hours) and hence the ability to evaluate the release of Tc-99 from saltstone that results from multiple pore volume exchanges. In addition, DOE is currently planning identical testing to be conducted on an actual sample cored from SDU Cell 2A in April 2015 [SREL Doc: R-16-004]. This will enable a direct comparison of laboratory-prepared and field-emplaced samples with respect to Tc-99 release and the ability to retain a reducing matrix. The intent is to measure the dissolved oxygen (DO) content of the influent to, and the effluent from, the saltstone sample to determine if oxygen is consumed by the assumed surplus reduction capacity of the material. It is anticipated that this testing will provide an enhanced understanding of the time-dependent redox interactions that occur in saltstone and subsequently better inform the simulation model.

SP-7

SP-7	**Question:** If the DOE demonstrates that residual reducing capacity is an appropriate basis for modeling the release of Tc-99 (see RAI Question SP-6 above), then additional justification is needed for the assumed reducing capacity of saltstone.
	Basis: In both the DOE FY13 and the DOE FY14 SDF Special Analysis documents, the DOE assumed that the saltstone has a reducing capacity of 0.607 milliequivalents of electrons per gram. The NRC RAI Comment SP-10 on the DOE FY13 SDF Special analysis document requested that the DOE provide justification of the modeled reducing capacity of saltstone and provided several specific NRC staff concerns with the value used by the DOE. In the DOE 2015 Response to the NRC 2014 RAI Comments (see RAI Comment SP-10 in that document), the DOE addressed the specific NRC staff concern about sulfur solubility by indicating that ferrous iron may be more responsible for the measured reducing capacity of saltstone than sulfide species. The other specific NRC staff concerns in RAI Comment SP-10 on the DOE FY13 SDF Special Analysis document still remain current NRC staff concerns relevant to the DOE FY14 SDF Special Analysis document. In the DOE 2015 Response to the NRC 2014 RAI Comments (see RAI Comment SP-10 in that document), the DOE indicated that future research may be done to address the NRC staff concern that the components of saltstone that supply the measured reducing capacity may not be able to reduce Tc in a cementitious matrix. The NRC staff concern is based on both a CBP report (CBP-RP-2010-013-01) and a Pacific Northwest National Laboratory (PNNL) study (PNNL-22957), which indicated that nitrite was a major contributor to the measured reduction capacity. However, as described in the PNNL report, the reduction potential of nitrite was not sufficient to reduce Tc(VII) to Tc(IV). Accordingly, it may not be appropriate to include the measured reduction capacity of the saltstone simulant, which includes nitrite, in the assumed reducing capacity of saltstone. The PNNL report also demonstrated that the use of the Ce(IV) titration method, which included sulfuric acid, may overestimate the reducing capacity available in saltstone. The PNNL report indicated that the method measured nearly all of the reducing capacity of the solid sample because most of the solids dissolved in the strong acid. The PNNL report indicated that with the Cr(VI) method, which used neutral or alkaline conditions, only the reducing capacity of the solid surface and any internal surface that oxygen can reach in the available contact time was likely to be measured. The formation of a passivation layer on the blast furnace slag was indicated as potentially contributing to the decreased reactivity under the Cr(VI) method. It is not clear to the NRC staff that the DOE use of the Ce(IV) method was appropriate for determining the reducing capacity of saltstone because the conditions for the Cr(VI) method were more consistent with the expected alkaline conditions of saltstone. In addition to the previous NRC staff concerns in RAI Comment SP-10 on the DOE FY13 SDF Special Analysis document, the NRC staff has concerns about the effects of oxygen entrainment during full-scale mixing, pumping, and pouring on the reducing capacity of field-emplaced saltstone.
	Path Forward: Provide justification for the modeled reducing capacity of saltstone available for reaction with infiltrating water, including the following issues: (1) applicability of the measurement method; (2) identity of species supplying the measured reducing capacity and the ability of those species to reduce Tc(VII) to Tc(IV) in a cementitious environment; (3) any

	kinetic limitations caused by the potential formation of a passivation layer on blast furnace slag particles; and (4) the effects of interactions with oxygen and oxygen entrainment during field-scale mixing, pumping, and pouring. Measurements of the reducing capacity of cores of field-emplaced saltstone could address concerns about field-emplaced saltstone but would not necessarily address all of the NRC staff concerns in this RAI Question (e.g., concerns about the applicability of the measurement method).

DOE Response to SP-7

It is acknowledged that there is uncertainty associated with the current reduction capacity measurements. However, sensitivity analyses have been conducted with respect to the uncertainty of the available reduction capacity and have determined that this parameter, under these modeling conditions, is not risk-significant. Despite the complexities inherent in the relationship between the reducing capacity and Tc-99 releases (e.g., speciation, re-reduction, oxygen entrainment, etc.), assuming a different value for the initial reduction capacity provides insight (at a high-level) of the potential impacts from conditions which may deviate from those assumed in the Evaluation Case of the FY2014 SDF SA. [SRR-CWDA-2014-00006] The results from these sensitivity analyses indicate that despite uncertainty relative to reduction capacity, the risk of significant Tc-99 releases (i.e., releases resulting in doses exceeding 25 mrem/yr within 10,000 years) is minimal (see the responses to RAIs SP-2, SP-6, and SP-8).

In an effort to better understand the time-dependent change in the reducing nature of saltstone, testing is currently being conducted on a laboratory-prepared monolithic sample in which groundwater simulants are forced through a Tc-99 spiked saltstone sample utilizing a positive pressure differential of approximately 12 psi from the sample inlet to the outlet. This testing enables accelerated pore volume exchange (one pore volume per ≈ 1,500 hours) and hence the ability to evaluate the release of Tc-99 from saltstone that results from multiple pore volume exchanges. In addition, DOE is currently planning identical testing to be conducted on an actual sample cored from SDU Cell 2A in April 2015 [SREL Doc: R-16-004]. This will enable a direct comparison of laboratory-prepared and field-emplaced samples with respect to Tc-99 release and the ability to retain a reducing matrix. The intent is to measure the DO content of the influent to, and the effluent from, the saltstone sample to determine if oxygen is consumed by the assumed surplus reduction capacity of the material. It is anticipated that this testing will provide an enhanced understanding of the time-dependent redox interactions that occur in saltstone and subsequently better inform the simulation model.

SP-8

SP-8	**Question:** Additional information is needed to demonstrate the effects of uncertainty in modeled chemical reducing capacity in saltstone.
	Basis: Section 5.6.3 of the DOE FY14 SDF Special Analysis document referenced both Section 5.6.3 of the DOE 2009 SDF PA and the DOE FY13 SDF Special Analysis document for the description of variables included in the probabilistic uncertainty analysis. Based on those references, Appendix D of the DOE FY14 SDF Special Analysis document, and the DOE document "Updates to the Saltstone Disposal Facility Stochastic Fate and Transport Model" (SRR-CWDA-2013-00073), it does not appear to the NRC staff that reducing capacity of saltstone was directly included in the DOE probabilistic uncertainty analyses. An alternate value for the residual reducing capacity of saltstone was modeled in the DOE Case K evaluation; however, as described in the NRC 2012 SDF TER, the results of that analysis were difficult to interpret because of modeled hold-up of Tc-99 in the disposal structure floors. The DOE expected the reducing capacity of saltstone to serve as a key chemical barrier to Tc-99 release. Therefore, to evaluate the projected system performance, the NRC staff needs to understand the effects of modeled reducing capacity on the system performance. As described above in RAI Question SP-7, the NRC staff identified sources of uncertainty in the reducing capacity that will be available to reduce Tc(VII) to Tc(IV) in saltstone. Furthermore, as described in NRC RAI Comment SP-10 on the DOE FY13 SDF Special Analysis document, additional uncertainty may be imparted by variability in slag reactivity caused by inherent variability in the slag and variable storage times and storage conditions.
	Path Forward: Provide a sensitivity or uncertainty analysis that demonstrates the effects of uncertainty in saltstone reducing capacity on projected dose from Tc-99. Because many of the factors that affect the available reducing capacity in saltstone are expected to apply to disposal structure concrete, the modeled reducing capacity in saltstone and disposal structure concrete should be correlated (see RAI Question DSP-10 – later in this document). A justification of the sensitivity analysis values used or the probabilistic uncertainty range used should address the issues discussed in RAI Question SP-7 above and additional variability caused by inherent variability in slag reactivity and variable slag storage times and storage conditions.

DOE Response to SP-8

To effectively ascertain the impact that saltstone and concrete reducing capacities (RAI SP-8 and RAI DSP-10, respectively) have on projected dose at the 100-meter points of assessment around the SDF, a sensitivity analysis was performed using the GoldSim SDF Tc-99 Release Model and GoldSim SDF All-Species Model from the FY2014 SDF SA. [SRR-CWDA-2014-00006] Table SP-8.1 presents a summary of the most current experimental reduction capacities determined for materials related to the SDF. Five of the materials presented in Table SP-8.1 were considered in this sensitivity analysis (Table SP-8.2). While some of these materials do not reflect the material properties for actual construction materials for the SDU concrete or the saltstone waste form, the variability represented by this analysis provides additional understanding that is useful for informed decision-making.

Table SP-8.1: Experimental Reduction Capacities for Materials Related to the SDF

Sample	Composition (dry wt-%)				Reducing Capacity (meq e-/g)	Reference
	Slag	Portland Cement	Fly Ash	Aggregate / sand		
Aged Concrete [a]	N/A	N/A	N/A	N/A	8.55E-02	SRNS-STI-2008-00045
SDU 2 Concrete	17	13	10	58	1.78E-01	SRNL-STI-2009-00637
TR547 [b]	45	10	45	0	6.07E-01	SRNL-STI-2009-00637
TR545 [b]	90	10	0	0	6.81E-01	SRNL-STI-2009-00637
Blast Furnace Slag	100	0	0	0	8.22E-01	SRNS-STI-2008-00045; SRNL-STI-2009-00637; WSRC-RP-2005-01674; Lukens, et al (2005)
Portland Cement	0	100	0	0	1.98E-01	SRNL-STI-2009-00637
Fly Ash	0	0	100	0	2.99E-01	SRNL-STI-2009-00637
Red Clay Sediment [c]	N/A	N/A	N/A	N/A	2.44E-02	SRNS-STI-2008-00045
Sandy Sediment [c]	N/A	N/A	N/A	N/A	8.12E-02	SRNS-STI-2008-00045

Notes: (a) Aged Concrete is from 50 year old SRS concrete.
(b) Saltstone simulants. All percentages of saltstone formulations are reported on a dry weight percentage basis, that is, the weight of the ingredients before water was added.
(c) SRS subsurface sediments.

Table SP-8.2: Sensitivity Analysis Nomenclature

Material	Sensitivity Case		Reducing Capacity (meq e-/g)
	Saltstone	Concrete	
Blast Furnace Slag	1	A	8.22E-01
TR547 Saltstone	2	B	6.07E-01
SDU 2 Concrete	3	C	1.78E-01
Aged Concrete (50 yr old)	4	D	8.55E-02
Sandy Sediment	5	E	8.12E-02

The TR547 Saltstone Simulant, SDU 2 Concrete, and Aged Concrete materials were chosen because they best represent the disposal units present at the SDF. Blast Furnace Slag and SRS sediments (both sandy and clayey) were also considered in this analysis not because they are thought to reflect actual disposal conditions within the SDUs, but rather to capture the extremes (i.e., maximum and minimum) of the reduction capacity distribution for all materials present at the SDF. In all, 36 different scenarios were simulated (Table SP-8.2). For example, Sensitivity Case 1A assumes that both saltstone and concrete materials in the SDF have a reduction capacity equal to that of blast furnace slag (0.822 meq e-/g), Sensitivity Case 1B assumes saltstone has a reduction capacity equal to that of blast furnace slag (0.822 meq e-/g) and concrete has a reduction capacity equal to that of the TR547 saltstone simulant (0.607 meq e-/g). It should be noted that Sensitivity Case 2C represents the FY2014 SDF SA Evaluation Case.

The results from this sensitivity analysis are presented to illustrate the effects from changes in saltstone reduction capacity (Figure SP-8.1) and to illustrate the effects from changes in concrete reduction capacity (Figure SP-8.2), relative to predicted dose. Table SP-8.3 provides a summary of the results from the sensitivity analysis.

Figure SP-8.1: Saltstone Reduction Capacity Variability

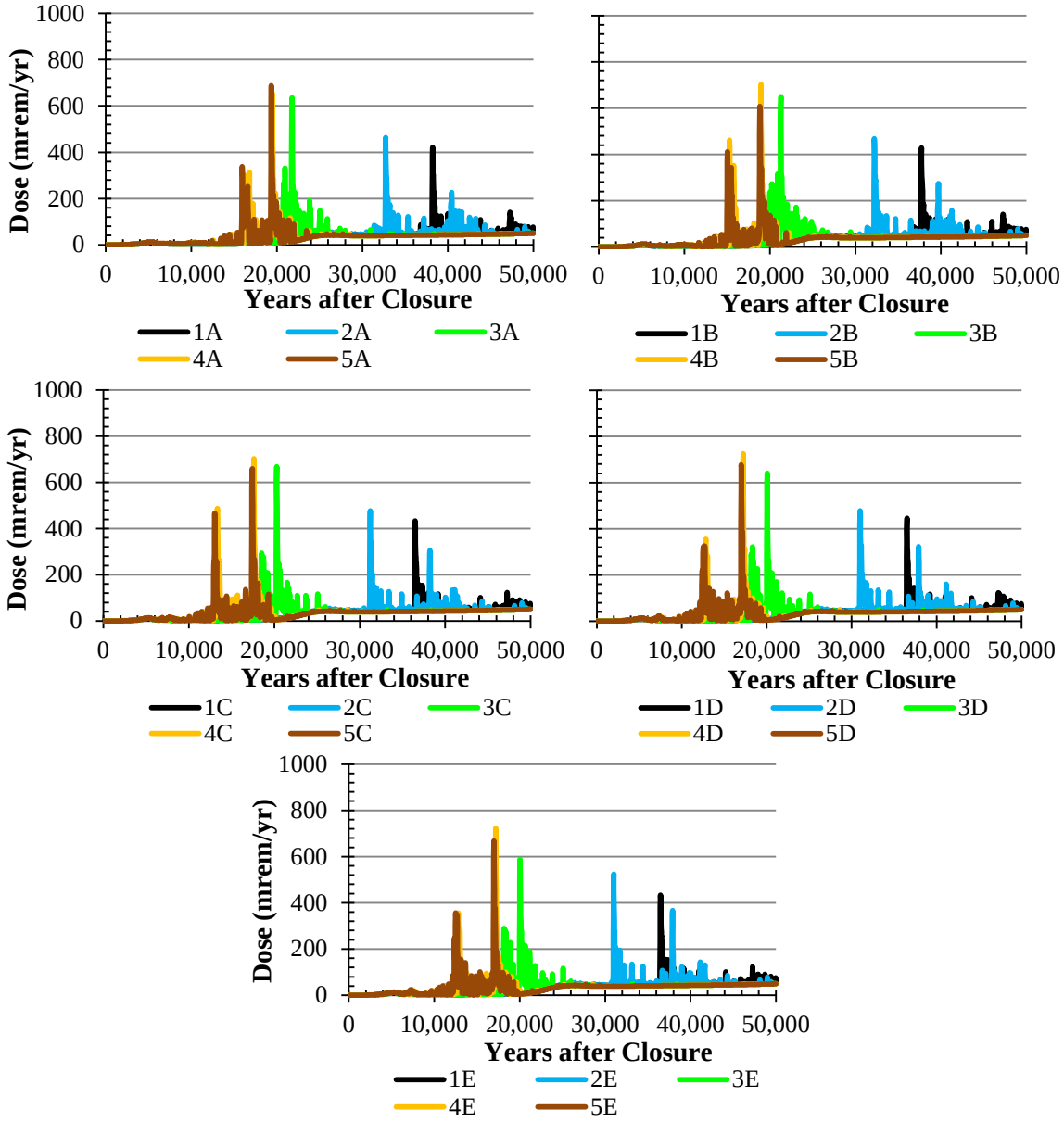

Figure SP-8.2: Concrete Reduction Capacity Variability

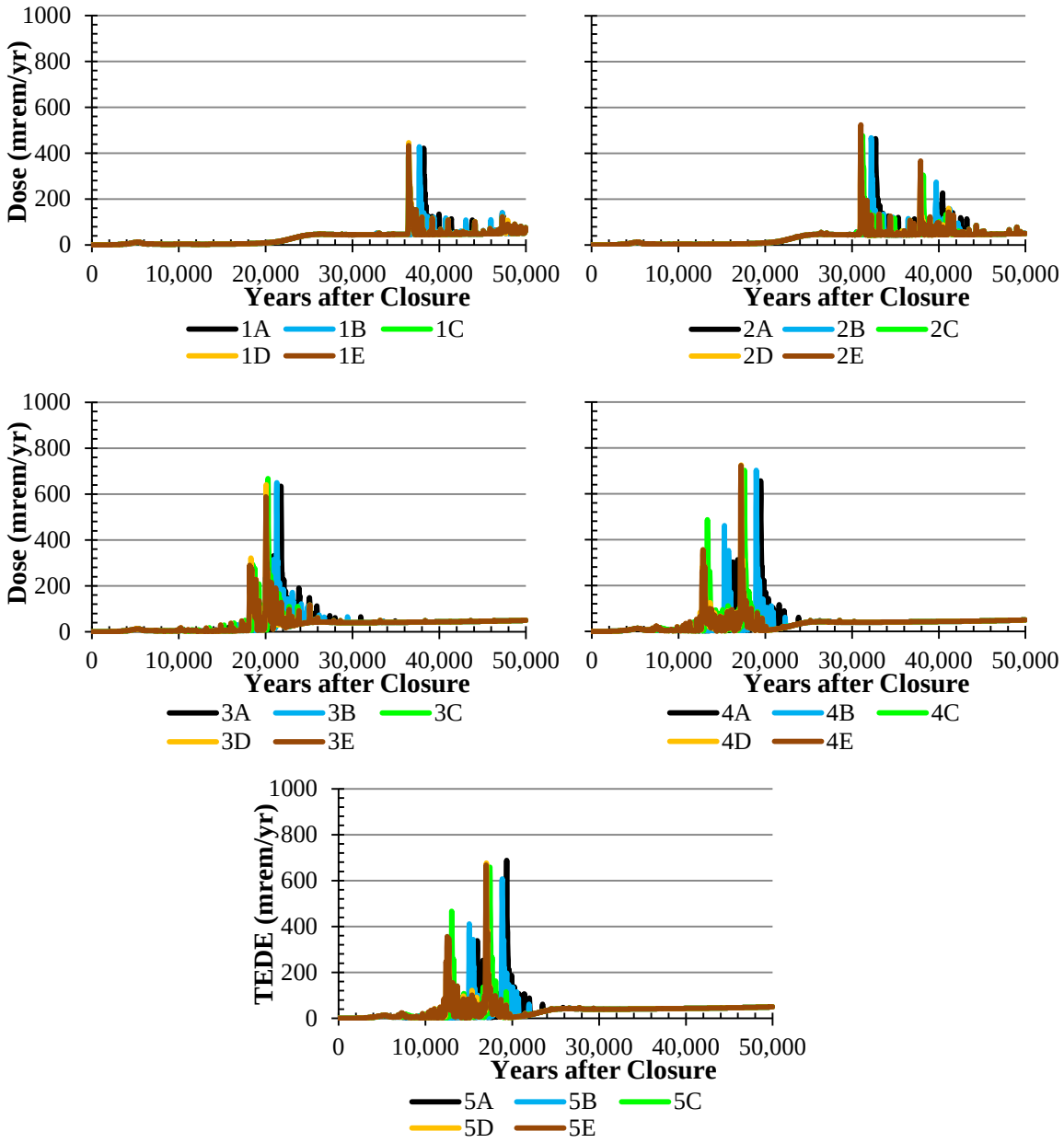

Examination of Figures SP-8.1 and SP-8.2 highlights two points in particular:

1) Variability in saltstone reduction capacity impacts peak dose timing approximately ten times more than variability in concrete reduction capacity.

2) As saltstone reduction capacity decreases, concrete reduction capacity increasingly impacts peak dose timing (e.g., compare scenario A to E in each plot of Figure SP-8.2).

As an interesting aside, when considering saltstone reduction capacity variability (Figure SP-8.1), the timing between the highest and second highest dose peaks is shortest for simulations assuming a saltstone reducing capacity equal to SDU 2 Concrete (Sensitivity Case 3A through

3E). This is due to how closely the Tc-99 release coincides for the 150-foot and 375-foot diameter SDUs in this scenario.

Table SP-8.3: Sensitivity Analysis Results

Sensitivity Case	Assigned Reducing Properties		Peak Dose (mrem/yr)	
	Saltstone	Concrete	10,000 yr	50,000 yr
1A	100% Blast Furnace Slag	100% Blast Furnace Slag	1.27E+01	4.21E+02
1B	100% Blast Furnace Slag	TR547 Saltstone	1.27E+01	4.28E+02
1C	100% Blast Furnace Slag	SDU 2 Concrete	1.27E+01	4.33E+02
1D	100% Blast Furnace Slag	Aged Concrete (50 yr)	1.27E+01	4.46E+02
1E	100% Blast Furnace Slag	SRS Sandy Sediment	1.27E+01	4.33E+02
2A	TR547 Saltstone	100% Blast Furnace Slag	1.27E+01	4.64E+02
2B	TR547 Saltstone	TR547 Saltstone	1.27E+01	4.68E+02
2C [a]	TR547 Saltstone	SDU 2 Concrete	1.27E+01	4.77E+02
2D	TR547 Saltstone	Aged Concrete (50 yr)	1.27E+01	4.78E+02
2E	TR547 Saltstone	SRS Sandy Sediment	1.27E+01	5.24E+02
3A	SDU 2 Concrete	100% Blast Furnace Slag	1.29E+01	6.35E+02
3B	SDU 2 Concrete	TR547 Saltstone	1.29E+01	6.50E+02
3C	SDU 2 Concrete	SDU 2 Concrete	1.30E+01	6.68E+02
3D	SDU 2 Concrete	Aged Concrete (50 yr)	1.31E+01	6.40E+02
3E	SDU 2 Concrete	SRS Sandy Sediment	1.31E+01	5.88E+02
4A	Aged Concrete (50 yr)	100% Blast Furnace Slag	1.35E+01	6.56E+02
4B	Aged Concrete (50 yr)	TR547 Saltstone	1.35E+01	7.02E+02
4C	Aged Concrete (50 yr)	SDU 2 Concrete	1.65E+01	7.02E+02
4D	Aged Concrete (50 yr)	Aged Concrete (50 yr)	2.26E+01	7.25E+02
4E	Aged Concrete (50 yr)	SRS Sandy Sediment	2.34E+01	7.23E+02
5A	SRS Sandy Sediment	100% Blast Furnace Slag	1.30E+01	6.88E+02
5B	SRS Sandy Sediment	TR547 Saltstone	1.30E+01	6.07E+02
5C	SRS Sandy Sediment	SDU 2 Concrete	1.68E+01	6.58E+02
5D	SRS Sandy Sediment	Aged Concrete (50 yr)	2.22E+01	6.77E+02
5E	SRS Sandy Sediment	SRS Sandy Sediment	2.37E+01	6.68E+02

Notes: (a) FY2014 SDF SA Evaluation Case

Sensitivity Case 4D represents a scenario in which both saltstone and concrete have the reduction capacity of Aged Concrete. In this instance, the performance objective is met and the maximum total dose at the 100-meter boundary is below 25 mrem/yr within 10,000 years after closure (Table SP-8.3). In fact, the 25 mrem/yr performance objective is also achieved when the unrealistically conservative Sensitivity Case 5E is considered, in which both saltstone and concrete are assumed to have a reduction capacity equivalent to SRS sandy sediment.

To provide further assurance, two additional model simulations were conducted using Sensitivity Cases 4D and 5E along with a higher Tc solubility of 4.2E-08 mol/L (see SP-12 and Table SP-12.1 for details on the selection of this value). Even under these overly conservative conditions, the peak dose within 10,000 years after facility closure did not exceed 25 mrem/yr (Figure SP-8.3). Therefore, this sensitivity analysis provides reasonable expectation/assurance that the expected variability in saltstone and concrete reduction capacities will not hinder the SDF from meeting performance objectives. This conclusion is consistent with the results of the uncertainty

analyses related to modeled reducing capacities and the release of Tc-99, as presented in the response RAI SP-2.

Figure SP-8.3: Most Conservative Sensitivity Cases with Elevated Tc Solubility

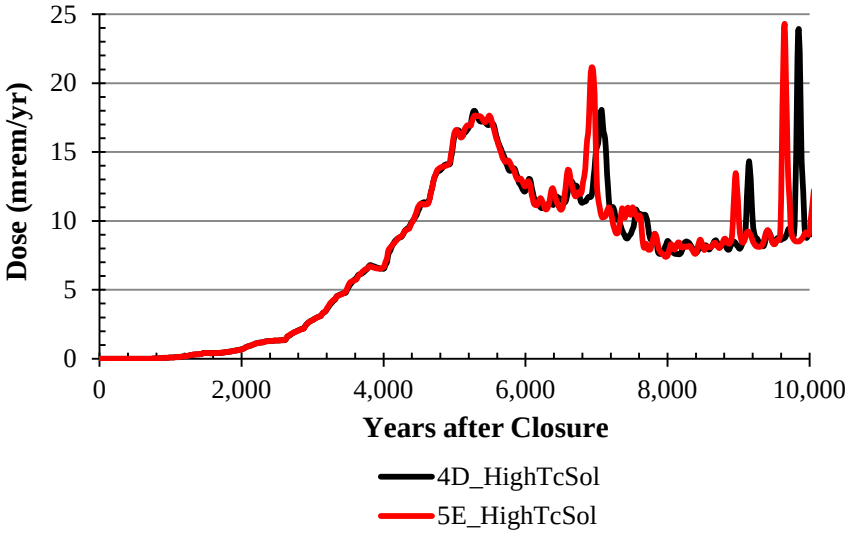

Finally, in an effort to better understand the time-dependent change in the reducing nature of saltstone, testing is currently being conducted on a laboratory-prepared monolithic sample in which groundwater simulants are forced through a Tc-99 spiked saltstone sample using accelerated pore volume exchange to evaluate the release of Tc-99 from saltstone. In addition, DOE is currently planning identical testing to be conducted on an actual sample cored from SDU Cell 2A in April 2015 [SREL Doc: R-16-004]. This will enable a direct comparison of laboratory-prepared and field-emplaced samples with respect to Tc-99 release and the ability to retain a reducing matrix.

SP-9

SP-9	**Question:** Additional information is needed about the sensitivity analysis results regarding increased dispersivity in saltstone.
	Basis: The PORFLOW sensitivity analysis in Section 5.6.7.5 of the DOE FY14 SDF Special Analysis document provided useful information on the effects of increased vertical and lateral dispersivity in saltstone. In particular, that sensitivity analysis addressed some of the NRC staff concerns about the effects of cold joints resulting from multiple saltstone lifts. However, the DOE did not provide a basis for the horizontal and vertical dispersivity values used in that sensitivity analysis. Figure 5.6.7-26 of the DOE FY14 SDF Special Analysis document showed a peak flux of over 200 g/yr for Tc-99 from a 375-foot disposal structure. The DOE did not provide that result in terms of dose. Although that dose peak was projected to occur between 40,000 and 45,000 years after disposal, the NRC staff needs to understand the likelihood of the conditions leading to that projected peak because of the NRC staff concerns about the timing of those projected Tc peaks.
	Path Forward: Provide a basis for the horizontal and dispersivity values used in the sensitivity analysis. The basis should address the potential effects of cold joints between lifts. Provide results in terms of dose of the sensitivity analysis described in Section 5.6.7.5 of the DOE FY14 SDF Special Analysis document.

DOE Response to SP-9

As stated in Section 5.6.7.5 of the FY2014 SDF SA, the dispersivity values used in the sensitivity analysis "were selected for illustrative purposes only because actual dispersivity values within heterogeneous pours of saltstone are expected to be variable and specific to the pour conditions of each SDU." In other words, DOE expects there to be variability in the dispersivity between lifts, but there is no technical basis for the values selected. The analysis was not intended to provide an accurate prediction of expected conditions, but only to convey a general illustration of potential impacts from variable dispersion values. Regardless of the values selected, the results of the analysis in Section 5.6.7.5 of the FY2014 SDF SA demonstrated that applying greater dispersivity does not result in adverse impacts within 10,000 years with respect to the significant dose contributors.

Doses were not provided for this analysis because (1) only a limited set of radionuclides were modeled, and (2) aquifer transport was not modeled. However, the dose from Tc-99 may be estimated using an approach similar to the approach used to estimate doses in the response to RAI SP-10. In that response, a release-to-dose multiplier was estimated for the Tc-99 released from the 150-foot diameter SDUs and from the 375-foot diameter SDUs. For this response, a flux-to-dose multiplier was estimated for the Tc-99 flux from the 150-foot diameter SDUs (1.45 (mrem/yr)/(g/yr)) and from the 375-foot diameter SDUs (4.85 (mrem/yr)/(g/yr)). These multipliers were estimated by scaling the Tc-99 flux (in g/yr) from the Evaluation Case to approximate the resulting Evaluation Case dose peaks (in mrem/yr).

Applying these assumed multipliers to the Tc-99 fluxes shown in Figures 5.6.7-20 and 5.6.7-26 of the FY2014 SDF SA provides an approximate dose contribution from Tc-99. The Tc-99 dose

contribution was then added to the dose contributions for all other radionuclides to provide a peak dose estimate (Figure SP-9.1). Although the increased dispersity of Tc-99 resulted in higher doses than those from the Evaluation Case, the timing of the peaks remains well beyond 10,000 years. Therefore, the conclusions from the FY2014 SDF SA remain unaffected.

Figure SP-9.1: Approximation of Peak Dose to the MOP, With and Without Increased Dispersivity of Tc-99, Within 50,000 Years

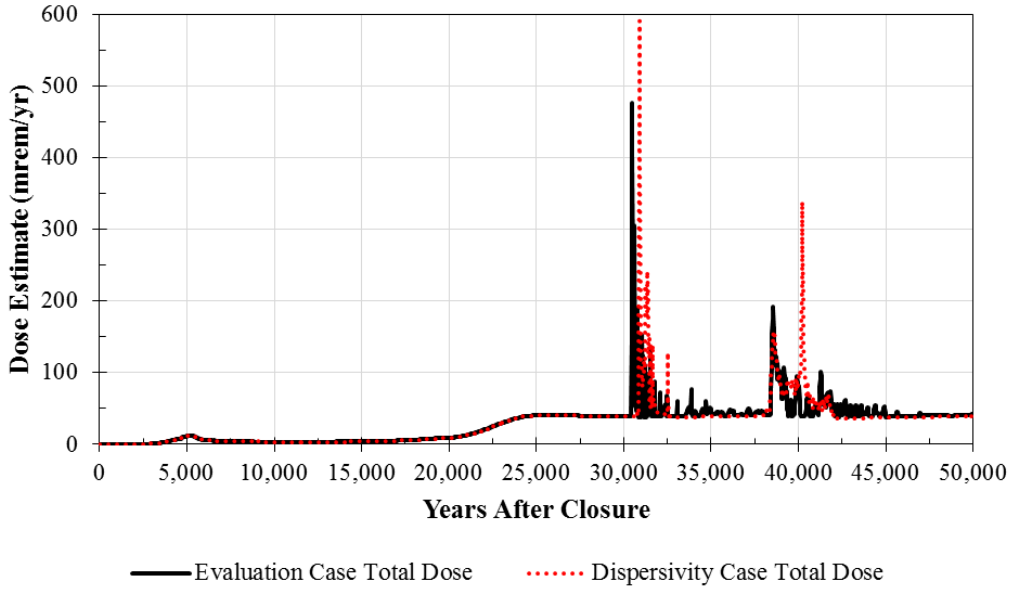

This is a reasonable approach because Tc-99 transports quickly to the 100-meter boundary once it has been released from the SDUs. Comparing the estimated dose of the Evaluation Case (black curve in Figure SP-9.1) to the doses presented in Figure 5.5-9 of the FY2014 SDF SA provides confidence in the dose estimate approach.

SP-10

SP-10	**Question:** Additional information is needed on the results of the sensitivity analysis with non-depleting oxygen sources within saltstone.
	Basis: The PORFLOW sensitivity analysis provided in Section 5.6 7.4 of the DOE FY14 SDF Special Analysis document provided useful information on the hypothetical effects of non-depleting oxygen sources within saltstone. That analysis could be used to non-mechanistically represent several phenomena of concern to the NRC staff, including: the effects of unsaturated fractures (see RAI Question SP-2 above); and the potentially poor correlation between Tc release and consumption of reducing capacity (see RAI Question SP-6 above). Although the cumulative fractional amount of Tc released was provided for 50,000 years, the dose results were provided for only 20,000 years and those results did not capture the Tc-99 peak doses. In addition, those results are difficult to interpret without information on storage in the floor and mud mats. In the DOE FY14 SDF Special Analysis document, the DOE indicated that assumed floor oxidation did not have a significant effect on the results. However, in the DOE 2009 SDF PA, there was a significant effect of retention of Tc-99 in the disposal structure floor in Case K. It is not clear to the NRC staff how retention in the floor and basemat would affect Tc-99 release in the sensitivity analysis provided in the Section 5.6.7.4 of the DOE FY14 SDF Special Analysis document.
	Path Forward: Provide results of the sensitivity analysis described in Section 5.6.7.4 of the DOE FY14 SDF Special Analysis document in terms of dose for 50,000 years. Either show the storage of Tc-99 in the floor and basemats or perform the analysis with oxidized floor and basemats.

DOE Response to SP-10

The aquifer transport of Tc-99 was not modeled beyond 20,000 years for the various non-depleting oxygen sources because the peak releases of Tc-99 from the 375-foot diameter SDUs occurred within 20,000 years for each of the three sensitivity cases identified in Section 5.6.7.4. For the smaller 150-foot diameter SDUs, the peak releases for the 5% and 10% oxygen source cases occurred shortly after 20,000 years, but due to the lower inventory, the release value was low relative to the release values from the larger SDUs. Figures SP-10.1 and SP-10.2 show the releases of Tc-99 from a 150-foot diameter SDU and a 375-foot diameter SDU, respectively, over 50,000 years.

Despite not having modeled the aquifer transport of these releases, total doses can be estimated based on the peak releases from the Evaluation Case. To generate this dose estimate, the Tc-99 releases from the representative 150-foot diameter SDU (Figure SP-10.1) were multiplied by an assumed multiplier (88 (mrem/yr)/Ci) and the releases from the representative 375-foot diameter SDU were multiplied by a different assumed multiplier (283 (mrem/yr)/Ci). These multipliers were determined by scaling the Tc-99 releases (in Ci) from the Evaluation Case to approximate the resulting Evaluation Case dose peaks (in mrem/yr).

The values were added together to give a total Tc-99 dose contribution. The resulting Tc-99 dose was added to the dose contributions from other radionuclides, which were extracted from the 50,000-year results presented in Figure 5.5-9 of the FY2014 SDF SA. The release-to-dose multipliers were subjectively determined based on visually comparing the resulting dose curves

within 20,000 years (Figure SP-10.3) to the doses presented in Figure 5.6.7-16 of the FY2014 SDF SA, which demonstrates that this approach provides a good approximation of the doses within 20,000 years.

Figure SP-10.1: Release of Tc-99 from a 150-Foot Diameter SDU

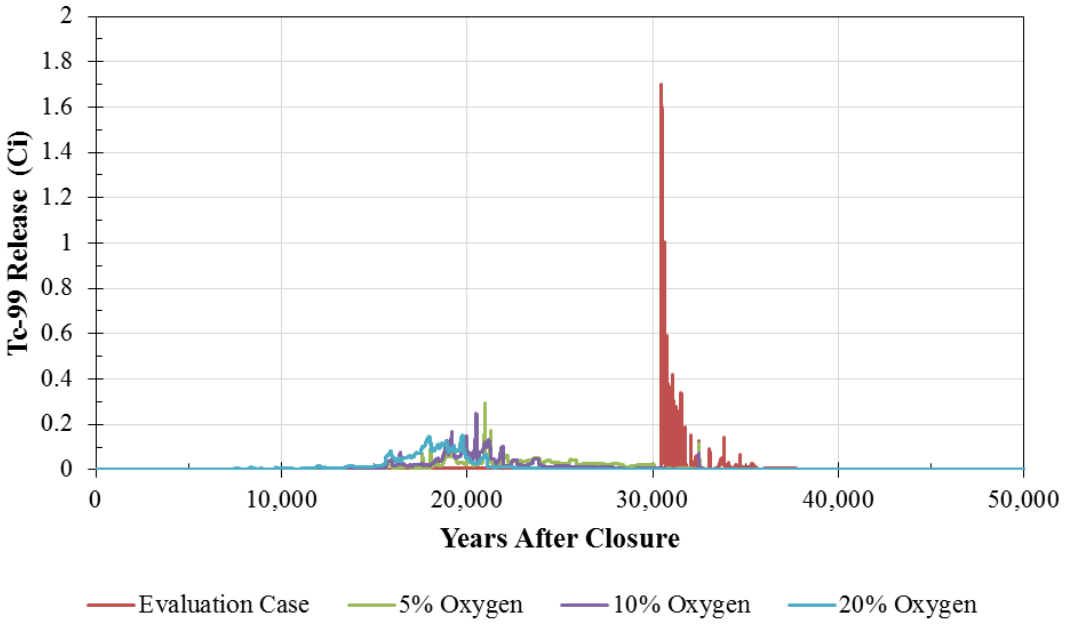

Figure SP-10.2: Release of Tc-99 from a 375-Foot Diameter SDU

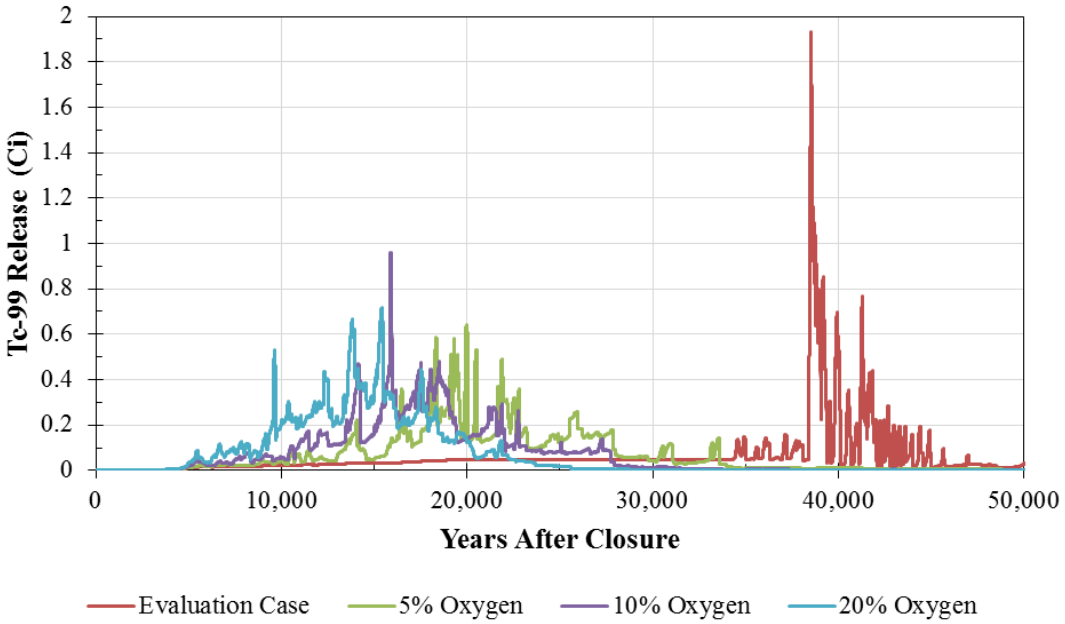

Figure SP-10.3: Approximation of Peak Dose to the MOP, Assuming Non-Depleting Oxygen Sources (0%, 5%, 10%, and 20%), Within 20,000 Years

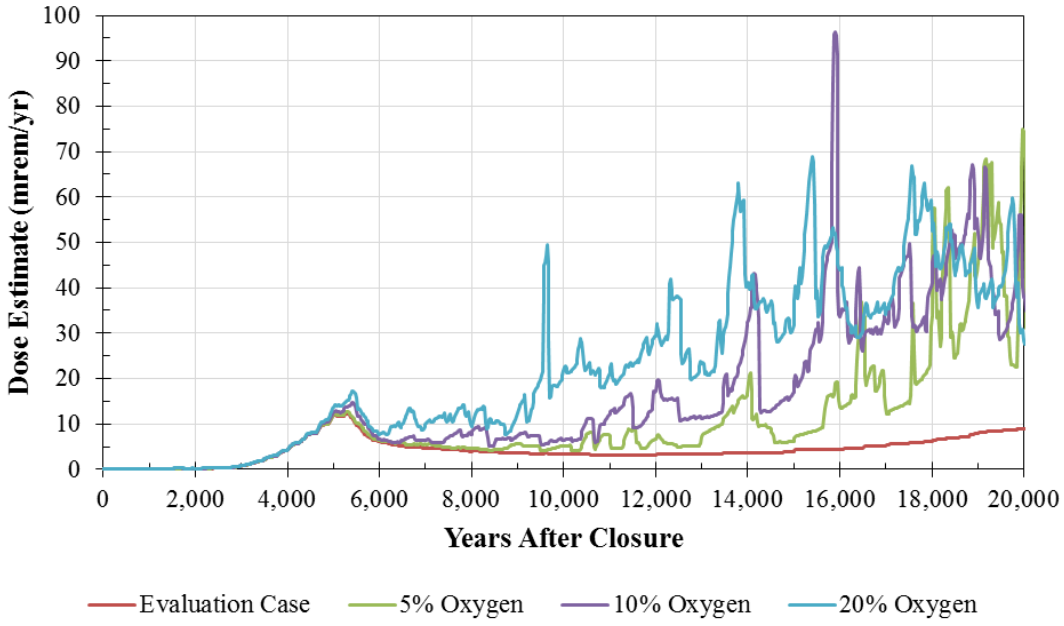

This is a reasonable approach because Tc-99 transports quickly to the 100-meter boundary once it has been released from the SDUs. Using this approach, the peak doses within 50,000 years were estimated (Figure SP-10.4). This figure shows that beyond 20,000 years, the Evaluation Case resulted in the most conservative (i.e., the highest) peak doses. A number of factors contribute to this phenomenon. For example, when transported to the reduction zone, the oxidized Tc-99 is re-reduced, allowing for accumulation that results in significant Tc-99 concentrations. Similarly, as demonstrated in the response to RAI SP-1, the linear degradation rate results in more mass being held within the saltstone matrix (over significantly long time periods); whereas a more gradual release (at negligible magnitudes) may occur if a nonlinear degradation mechanism is applied (such as the decalcification feedback loop described in response to RAI SP-1).

Figure SP-10.4: Approximation of Peak Dose to the MOP, Assuming Non-Depleting Oxygen Sources (0%, 5%, 10%, and 20%), Within 50,000 Years

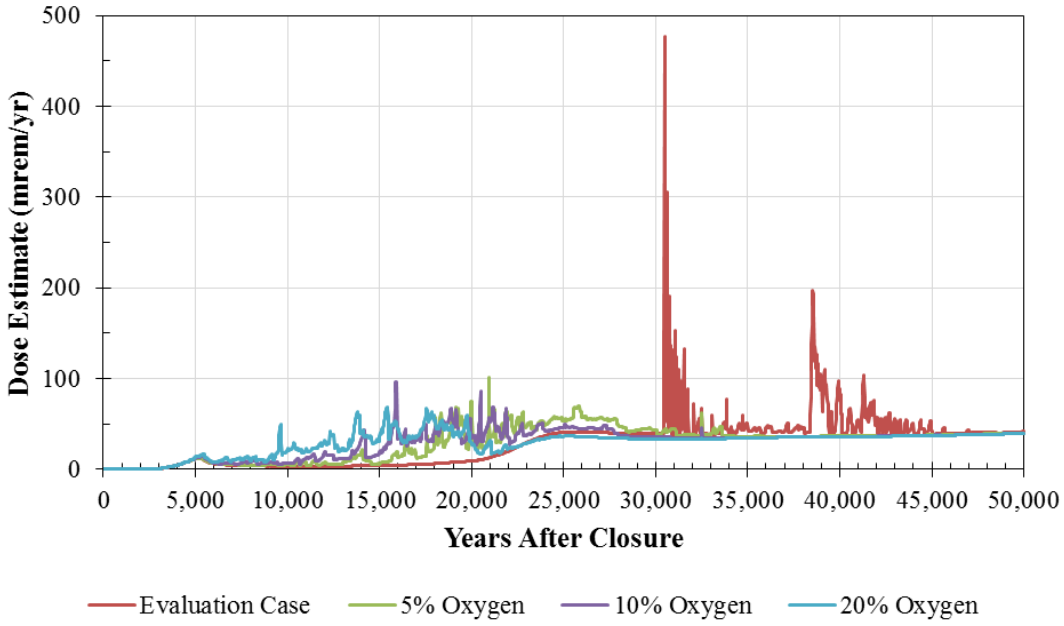

The mud mats are not significant barriers to Tc-99 release, and therefore provide very limited storage. The floor only stores Tc-99 as a function of the reducing capacity of the overlying saltstone. Once the saltstone above the floor is oxidized, the floor is immediately oxidized, thereby releasing all of the available Tc-99.

The response to RAI SP-2 includes a probabilistic simulation of parameters relevant to Tc-99 releases. Analysis of those probabilistic results indicated that the Tc-99 releases are not particularly sensitive to the reducing capacity of concrete (i.e., the floors and mud mats).

Additionally, in an effort to better understand the time-dependent change in the reducing nature of saltstone, testing is currently being conducted on a laboratory-prepared monolithic sample in which groundwater simulants are forced through a Tc-99 spiked saltstone sample using accelerated pore volume exchange to evaluate the release of Tc-99 from saltstone. In addition, DOE is currently planning identical testing to be conducted on an actual sample cored from SDU Cell 2A in April 2015 [SREL Doc: R-16-004]. This will enable a direct comparison of laboratory-prepared and field-emplaced samples with respect to Tc-99 release and the ability to retain a reducing matrix.

SP-11

SP-11	**Question:** Additional justification is needed for the sorption coefficient (K_d) values assumed for risk-significant and potentially risk significant radionuclides in saltstone in the DOE Evaluation Case and the ranges of values used in the sensitivity cases.
	Basis: In the 2012 NRC SDF TER and in the NRC RAI Comments on the DOE FY13 SDF Special Analysis document, the NRC staff indicated that the K_d values assumed for iodine (I), selenium (Se), radium (Ra), and strontium (Sr) in cementitious materials were not adequately supported. Section 5.6.6.4 of the DOE FY14 SDF Special Analysis document showed results from sensitivity analyses that were performed to evaluate the potential effect on the projected dose from the K_d values assumed for cementitious materials. In the sensitivity analyses performed for I, the K_d values were decreased by a factor of two. However, that reduction does not appear to the NRC staff to fully capture the range of potential K_d values for that element. For example, as described in the NRCs 2012 SDF TER, values that are lower than those assumed in that sensitivity analysis have been measured for the sorption of I onto cementitious materials. The basis for the assumed K_d value for I for cementitious materials was also discussed with the DOE during the NRC February 2015 Onsite Observation Visit (see SDF-CY15-01 Report in ADAMS as ML15041A562). In response to Follow Up-Action Item SDF-CY15-01-007, the DOE provided the NRC staff with additional documents related to the sorption of I (see ML15075A111). One of those documents (i.e., Wang et al. (2012)) included a recommendation for the use of a K_d value of 10 mL/g for I in Region II concrete based on expert opinion. However, that document did not provide the experimental data used to derive that value, so the applicability of that value to saltstone is not clear to the NRC staff. In the sensitivity analyses performed for Ra, the K_d values were also decreased by a factor of two. There is limited availability of directly applicable measurements for the sorption of Ra onto cementitious materials. New measurements were reported in the DOE document, "Crosswalk of Select Documents Related to the Monitoring Programs for the Saltstone Disposal Facility,"(SRR-CWDA-2014-00002, Rev. 1) for the K_d of Ra in saltstone materials that were much higher than the values used in the modeling. However, the high values measured could be due to precipitation of the Ra, instead of sorption. Due to the uncertainty in the sorption of Ra onto cementitious materials, the use of a wider range of K*d* values in the sensitivity analysis may be more defensible. The sensitivity analysis performed for the K_d values for the sorption of Se onto cementitious materials included a significant decrease in the assumed K_d values. The values assumed in the sensitivity analysis appear to appropriately bound the potential K_d values for the reduced cementitious materials. However, the values assumed for the oxidized cementitious materials do not include the full range of measured values (i.e., measured K_d values ranging from 29.7 to 78.5 mL/g reported in SRNS-STI-2008-00045). The use of a lower K_d value for the oxidized concrete would be more defensible. Because lower K_d values increase the rate of release of radionuclides from a source, the NRC staff is concerned that use of those K_d values to represent sorption in saltstone could lead to an underestimate of the dose.
	Path Forward: Provide a justification for the K_d values assumed for I, Se, and Ra in saltstone and the ranges used in the sensitivity analyses in the DOE FY14 SDF Special Analysis

	document. Alternately, perform sensitivity analyses that include the range of observed K_d values for those elements to determine the potential effect of those parameters on the projected dose, or else provide a revised analysis that uses more defensible values.

DOE Response to SP-11

This response is organized according to each element identified within SP-11 (i.e., iodine, radium, and selenium), as each shall be addressed independently. Each of these element-specific responses provides sensitivity analyses which use wider ranges for the K_d values than those that were analyzed in the FY2014 SDF SA. Regardless of the results of these sensitivity analyses, studies of K_d values are on-going. Future modeling shall incorporate the most recent and appropriate K_d data available. However, based on the sensitivity evaluations provided below, the DOE believes the K_d data utilized is adequate for addressing risk-significant and potentially risk-significant radionuclides in saltstone.

Iodine

A series of additional sensitivity models were developed within the FY2014 SDF SA GoldSim model to assess the risk significance of iodine K_d values for saltstone. These sensitivity models were developed to provide greater insight than the assessment already provided within Section 5.6.6.4 of the FY2014 SDF SA. [SRR-CWDA-2014-00006] For these new sensitivities, K_ds for iodine within concrete and within saltstone were modified as summarized in Table SP-11.1. This table also identifies the corresponding I-129 dose curves, as depicted in Figure SP-11.1. The FY2014 SDF SA showed that the peak I-129 dose to the MOP at 100 meters was driven by releases from SDU 9; therefore, these sensitivity models only simulated SDU 9 releases and transport.

Table SP-11.1: Summary of Additional Iodine K_d Sensitivities

Curve in Figure SP-11.1	K_ds for Concrete	K_ds For Saltstone
Solid blue	No change [a]	No change [a]
Dashed blue	Set to 0.0 mL/g [b]	No change [a]
Solid orange	No change [a]	Set to 1.0 mL/g [c]
Dashed yellow	Set to 0.0 mL/g [b]	Set to 1.0 mL/g [c]
Solid purple	No change [a]	Set to 0.0 mL/g [b]
Dashed purple	Set to 0.0 mL/g [b]	Set to 0.0 mL/g [b]

Notes: (a) Uses the same values as the FY2014 SDF SA Evaluation Case. [SRR-CWDA-2014-00006]
(b) To prevent a divide-by-zero error within the GoldSim model, a non-zero value was required. An extremely small value (1.0E-30 mL/g) was assumed to be effectively zero. Value applied regardless of the pH or Eh of the cementitious material.
(c) Value applied regardless of the pH or Eh of the cementitious material.

Figure SP-11.1: I-129 Doses from SDU 9 to the 100-Meter MOP, Comparison for Iodine K_d Sensitivity

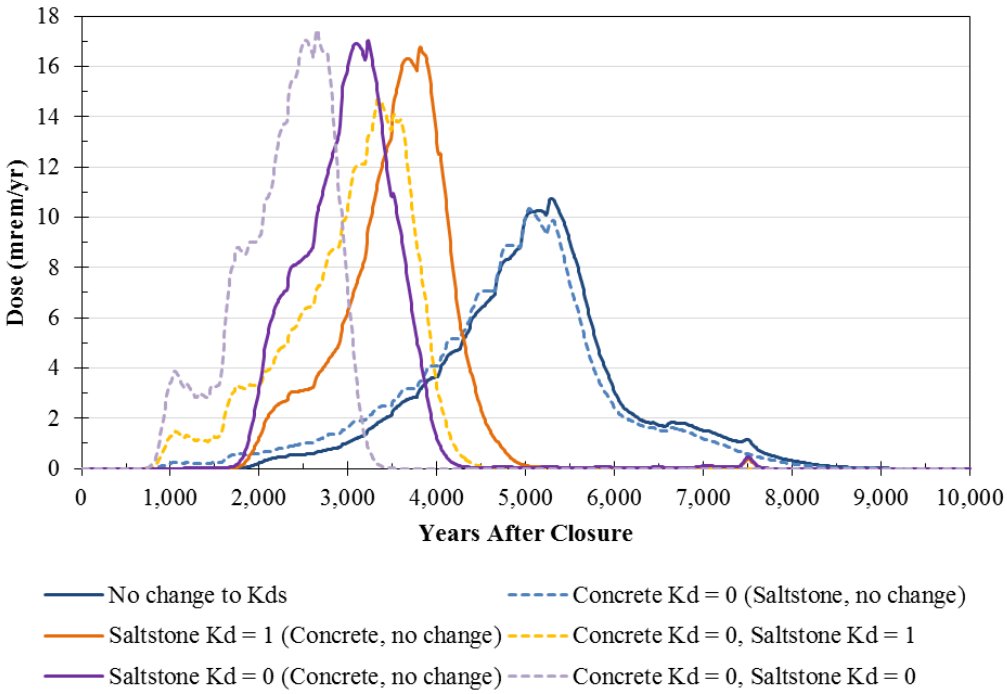

When the concrete K_ds were set to zero (dashed lines), the I-129 doses begin to climb at about 750 years after closure, regardless of the K_ds assumed for saltstone. Similarly, when the concrete K_ds were left unchanged relative to the Evaluation Case of the FY2014 SDF SA (solid lines), the I-129 doses begin to climb at about 1,750 years after closure, regardless of the K_ds assumed for saltstone. Therefore, the concrete K_ds used in the Evaluation Case effectively delay the initial release of I-129 by about 1,000 years.

The timing of the peak I-129 doses is also delayed, primarily as a function of the relationship between the saltstone K_d and the volumetric flow through saltstone. The significance of the saltstone K_d decreases over time, relative to the significance of the volumetric flow, because the volumetric flow through saltstone generally increases over time. To illustrate this relationship, Figures SP-11.2 through SP-11.4 show the same dose curves (from Figure SP-11.1) along with the volumetric flow rates that correspond to the timing of the respective dose peaks. Note that the dose scale remains unchanged, but the scales of the depicted flow rates vary significantly between each figure.

The influence that the K_d values impose on the magnitude of the I-129 dose peak is not as clear as the timings. In general, higher K_d values for iodine provide greater retardation, resulting in lower peak doses; however, Figure SP-11.3 demonstrates an exception to this generalization. Due to the relationship between the saltstone K_d and the volumetric flow through saltstone, when the concrete K_d is assumed to be zero (dashed yellow dose curve), the releases occur earlier while the flow rate is still relatively low. Therefore, the release is more gradual, depleting the available inventory of I-129 over time, such that once the flow rate increases there is less inventory available to contribute to the magnitude of the peak dose. Conversely, when the

concrete K_ds are unchanged relative to the Evaluation Case of the FY2014 SDF SA (solid orange dose curve), the release of I-129 is retarded, leaving significantly more I-129 to contribute to the peak dose as the volumetric flow rate increases.

Figure SP-11.2: I-129 Doses from SDU 9 to the 100-Meter MOP, Iodine K_d in Saltstone = 0 mL/g

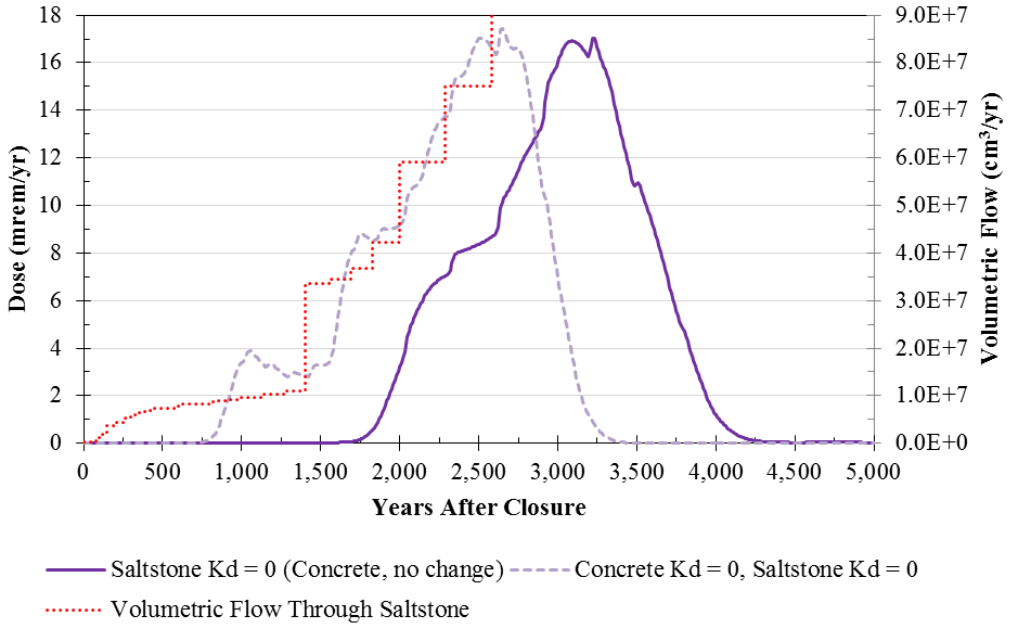

Figure SP-11.3: I-129 Doses from SDU 9 to the 100-Meter MOP, Iodine K_d in Saltstone = 1 mL/g

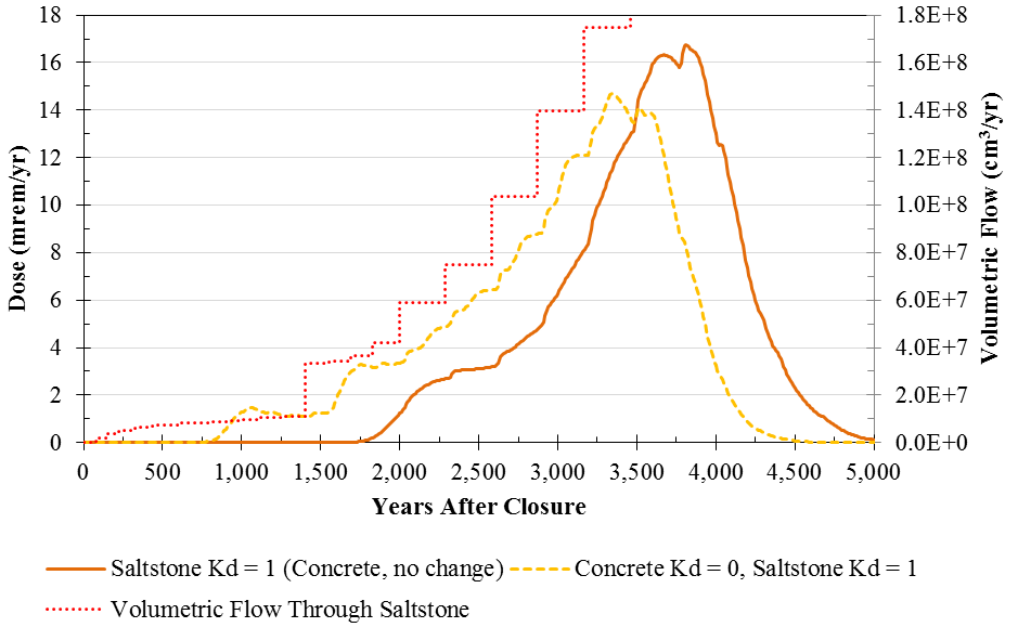

Figure SP-11.4: I-129 Doses from SDU 9 to the 100-Meter MOP, Iodine K_d in Saltstone Same as SA

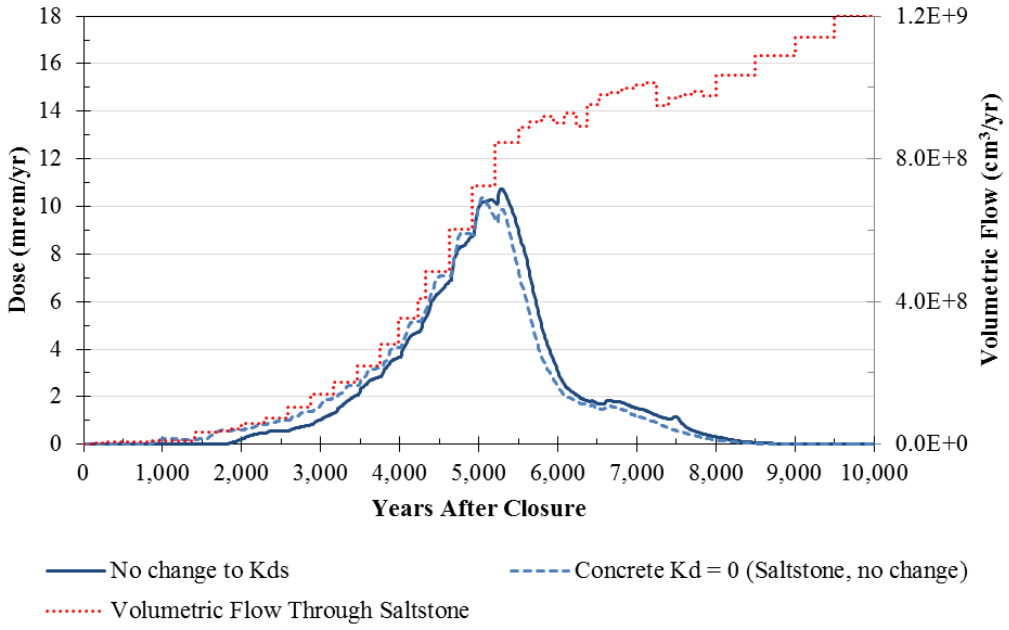

The dashed purple line in Figure SP-11.2 shows, effectively, no retardation of iodine within concrete or saltstone. As such, this is not a realistic representation of potential doses, but it does provide an extreme upper bound for evaluating the risk significance. Dose contributions from other radionuclides at the times of these peaks is less than 1.5 mrem/yr (per Table 5.5-2 and Figure 5.5-4 of the FY2014 SDF SA), such that the total dose to a MOP at 100 meters would be less than the 25 mrem/yr performance objective.

Note that the magnitudes of the peaks provided in both Figures SP-11.2 and SP-11.3 are not significantly higher than the peaks provided in the Iodine K_d Sensitivity study from Section 5.6.6.4 of the FY2014 SDF SA, which assumed that all iodine K_d values were reduced by half relative to the Evaluation Case.

Radium

Despite the questions from the NRC, DOE does not believe that radium K_ds are risk-significant relative to the MOP performance objectives. As identified in Section 3.4 of the FY2014 SDF SA, only Tc-99, I-129, and Cs-135 were considered risk-significant radionuclides.

For the low risk radionuclides (including Ra-226 and its parents) a very conservative approach was assumed for modeling the inventory values. Specifically, each SDU was assumed to contain the entire soluble and insoluble (salt) inventory present in both tank farms. These inventory values are so overly conservative that they do not provide a good indication of expected conditions; therefore, an alternative inventory shall be assumed for the radium K_d sensitivity analysis. Instead of every SDU containing the entire soluble and insoluble inventory present within the tank farms, the tank farm inventory shall be conservatively doubled, then distributed based on volume to each future SDU. This approach is applied to the initial values for Ra-226 and two of its parents (Th-230 and U-234). Similarly, Ra-228 and two of its parents (Th-232 and

U-236) will also be updated. All other radionuclides shall use the same inventory as reported in Table 3.4-1 of the FY2014 SDF SA. Table SP-11.2 provides a summary of the revised inventory values assumed for this set of sensitivity analyses. The inventories for SDUs 1, 4, 2A, and 2B remain unchanged relative to the FY2014 SDF SA.

Table SP-11.2: Revised Inventories Assumed for the Additional Radium K_d Sensitivities

	Approx. Volume (gal)	Percent of Total Volume (%)	Ra-226 (Ci)	Ra-228 (Ci)	Th-230 (Ci)	Th-232 (Ci)	U-234 (Ci)	U-236 (Ci)
Total Tank Farm Inventory			1.33E+01	2.33E-02	1.34E+01	2.31E-01	9.27E+00	4.29E-01
× 2			2.67E+01	4.67E-02	2.67E+01	4.61E-01	1.85E+01	8.58E-01
SDU 3A	2.9E+06	1.15%	3.06E-01	5.36E-04	3.07E-01	5.30E-03	2.13E-01	9.85E-03
SDU 3B	2.9E+06	1.15%	3.06E-01	5.36E-04	3.07E-01	5.30E-03	2.13E-01	9.85E-03
SDU 5A	2.9E+06	1.15%	3.06E-01	5.36E-04	3.07E-01	5.30E-03	2.13E-01	9.85E-03
SDU 5B	2.9E+06	1.15%	3.06E-01	5.36E-04	3.07E-01	5.30E-03	2.13E-01	9.85E-03
SDU 6	3.4E+07	13.63%	3.64E+00	6.36E-03	3.64E+00	6.29E-02	2.53E+00	1.17E-01
SDU 7	3.4E+07	13.63%	3.64E+00	6.36E-03	3.64E+00	6.29E-02	2.53E+00	1.17E-01
SDU 8	3.4E+07	13.63%	3.64E+00	6.36E-03	3.64E+00	6.29E-02	2.53E+00	1.17E-01
SDU 9	3.4E+07	13.63%	3.64E+00	6.36E-03	3.64E+00	6.29E-02	2.53E+00	1.17E-01
SDU 10	3.4E+07	13.63%	3.64E+00	6.36E-03	3.64E+00	6.29E-02	2.53E+00	1.17E-01
SDU 11	3.4E+07	13.63%	3.64E+00	6.36E-03	3.64E+00	6.29E-02	2.53E+00	1.17E-01
SDU 12	3.4E+07	13.63%	3.64E+00	6.36E-03	3.64E+00	6.29E-02	2.53E+00	1.17E-01

Figure SP-11.5 shows Ra-226 contributions to the MOP doses at 100 meters at Sectors J and K, where the solid lines reflect the contributions from the FY2014 SDF SA inventory and the dashed lines reflect the doses resulting from the updated inventory. Note that these inventories are still conservative as they assume a total inventory that is twice the available inventory in the tank farms.

In the FY2014 SDF SA, the Sector J dose contribution is significantly higher than in Sector K. Although the 150-foot diameter SDUs contain significantly less volume than the 375-foot diameter SDUs, the SA assumed the same inventory for each SDU regardless of volume. As such, the 150-foot diameter SDUs (e.g., 3A and 3B) held higher concentrations of Ra-226 and its parents. By distributing the inventory based on relative volume, the doses at Sector J are much closer to those at Sector K (see the dashed lines in Figure SP-11.5).

Figure SP-11.5: Ra-226 Dose Comparison to the 100-Meter MOP, FY2014 SDF SA Inventory versus Revised Inventory

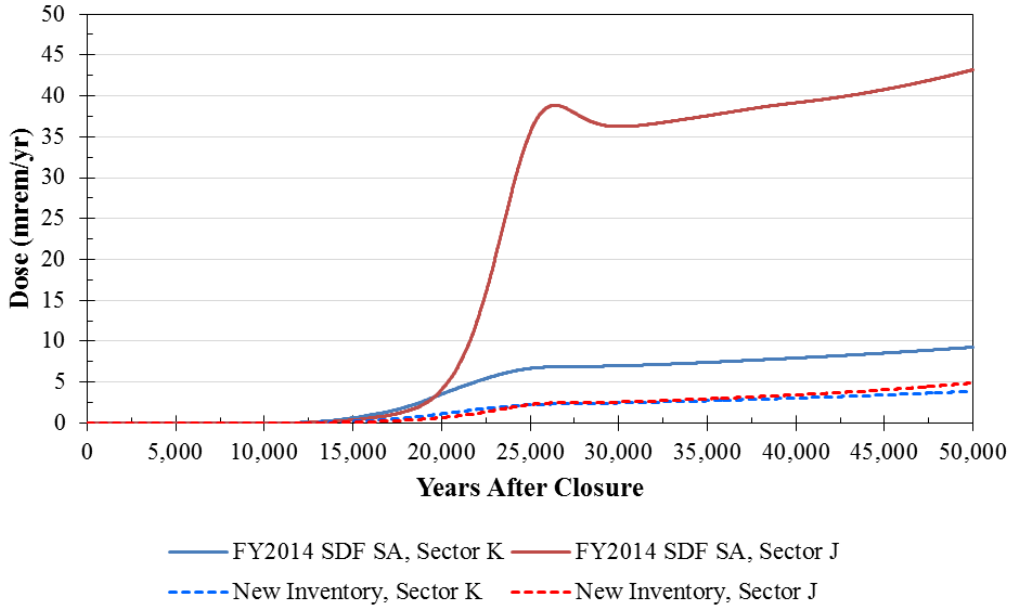

Beginning with the model that used the new inventory, a series of additional sensitivity models were developed to assess the risk significance of radium K_d values for saltstone and concrete. These sensitivity models were developed to provide greater insight than the assessment already provided within Section 5.6.6.4 of the FY2014 SDF SA. [SRR-CWDA-2014-00006] For these new sensitivities, K_ds for radium within concrete and within saltstone were modified as summarized in Table SP-11.3. This table also identifies the corresponding Ra-226 dose curves, as depicted in Figure SP-11.6. The Ra-226 dose contributions at Sector J were slightly higher than at Sector K, so the figure is only showing the Sector J results.

Table SP-11.3: Summary of Additional Radium K_d Sensitivities

Curve in Figure SP-11.6	K_ds For Saltstone	K_ds for Concrete
Red	Set to 0.0 mL/g [b]	Set to 0.0 mL/g [b]
Green	Set to 0.0 mL/g [b]	No change [a]
Yellow	No change [a]	Set to 0.0 mL/g [b]
Blue	No change [a]	No change [a]

Notes: (a) Uses the same values as the FY2014 SDF SA Evaluation Case. [SRR-CWDA-2014-00006]
(b) To prevent a divide-by-zero error within the GoldSim model, a non-zero value was required. An extremely small value (1.0E-30 mL/g) was assumed to be effectively zero. Value applied regardless of the pH or Eh of the cementitious material.

Figure SP-11.6: Ra-226 Doses at Sector J (100-Meter MOP), Comparison for Radium K_d Sensitivity

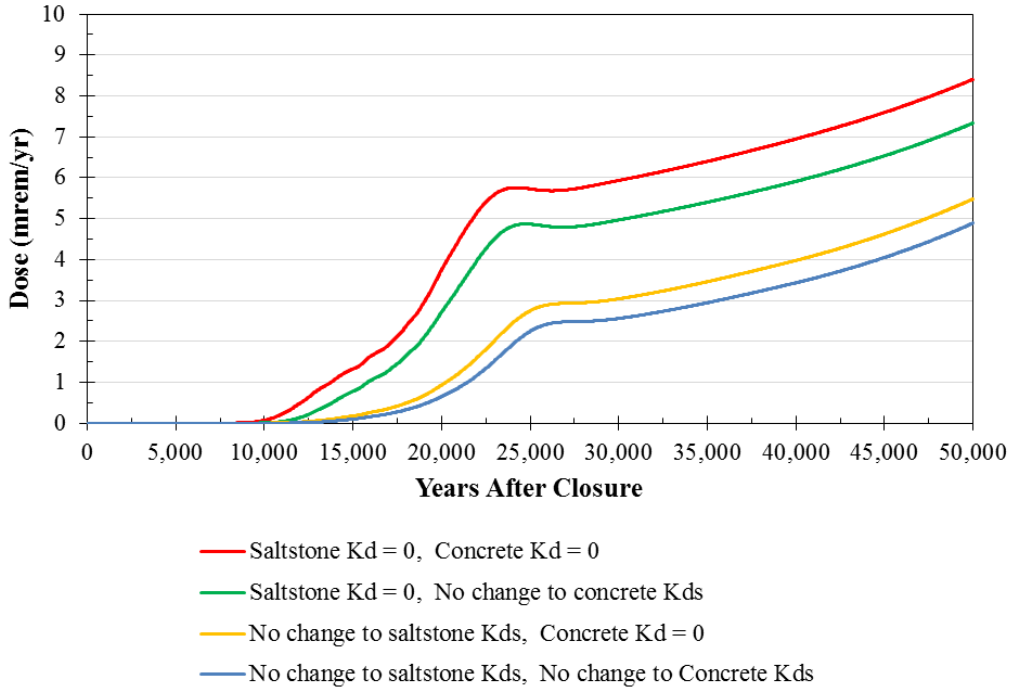

None of the analyses resulted in Ra-228 doses above 1.0E-06 mrem/yr; therefore, Ra-228 is not discussed.

The red line in Figure SP-11.6 shows, effectively, no retardation of radium within concrete or saltstone. As such, this is not a realistic representation of potential doses, but it does provide an extreme upper bound for evaluating the risk significance. For the first 10,000 years, there is effectively no dose contribution from Ra-226. Aside from Ra-226 and Tc-99, there is very little dose contribution from other radionuclides beyond 10,000 years. Within 20,000 years, the Tc-99 releases only contribute about 5 mrem/yr (per Table 5.5-3 and Figure 5.5-5 of the FY2014 SDF SA). As such, the total dose to a MOP at 100 meters would be about 9 mrem/yr within 20,000 years (which is less than the 25 mrem/yr performance objective). Beyond 20,000 years, dose contributions from Tc-99 exceed 200 mrem/yr (near 30,000 years), such that the contribution from Ra-226 is relatively insignificant.

Note that the magnitudes of the peaks provided in Figure SP-11.6 are well below the Ra-226 doses provided in the Radium K_d Sensitivity study from Section 5.6.6.4 of the FY2014 SDF SA, which assumed that all radium K_d values were reduced by half relative to the Evaluation Case. This is attributed to the more reasonable inventory assumptions used in these new analyses and because the most significant K_d with respect to radium transport is not saltstone or cement, but the leachate-impacted sandy soil K_d, as described in Section 5.6.6.4 of the FY2014 SDF SA.

Despite the relative significance of the parameter, no additional sensitivity modeling was performed on the leachate-impacted sandy soil K_d for radium. In the FY2014 SDF SA, this parameter was assumed to have a value of 75 mL/g; however, a recent report indicated that

leachate-impacted sandy soil K_d for radium is significantly higher (> 1500 mL/g). [SREL Doc. R-13-0005]

Selenium

As with radium, the FY2014 SDF SA incorporated extremely conservative assumptions for determining the modeled inventory of selenium. These inventory values are so overly conservative that they do not provide a good indication of expected conditions; therefore, an alternative inventory shall be assumed for the selenium K_d sensitivity analysis. Instead of every SDU containing the entire soluble and insoluble inventory present within the tank farms, the tank farm inventory shall be conservatively doubled, then distributed based on volume to each future SDU. This approach is applied to the initial values for Se-79. All other radionuclides shall use the same inventory as reported in Table 3.4-1 of the FY2014 SDF SA. Table SP-11.4 provides a summary of the revised inventory values assumed for this set of sensitivity analyses. The inventories for SDUs 1, 4, 2A, and 2B remain unchanged relative to the FY2014 SDF SA.

Table SP-11.4: Revised Inventories Assumed for the Additional Selenium K_d Sensitivities

	Approx. Volume (gal)	Percent of Total Volume (%)	Se-79 (Ci)
Total Tank Farm Inventory			8.90E+01
		× 2	1.78E+02
SDU 3A	2.9E+06	1.15%	2.04E+00
SDU 3B	2.9E+06	1.15%	2.04E+00
SDU 5A	2.9E+06	1.15%	2.04E+00
SDU 5B	2.9E+06	1.15%	2.04E+00
SDU 6	3.4E+07	13.63%	2.43E+01
SDU 7	3.4E+07	13.63%	2.43E+01
SDU 8	3.4E+07	13.63%	2.43E+01
SDU 9	3.4E+07	13.63%	2.43E+01
SDU 10	3.4E+07	13.63%	2.43E+01
SDU 11	3.4E+07	13.63%	2.43E+01
SDU 12	3.4E+07	13.63%	2.43E+01

Figure SP-11.7 shows Se-79 contributions to the MOP doses at 100 meters at Sectors J and K, where the solid lines reflect the contributions from the FY2014 SDF SA inventory and the dashed lines reflect the doses resulting from the updated inventory. Note that these inventories are still conservative as they assume a total inventory that is twice the available inventory in the tank farms.

Figure SP-11.7: Se-79 Dose Comparison (100-Meter MOP), FY2014 SDF SA Inventory versus Revised Inventory

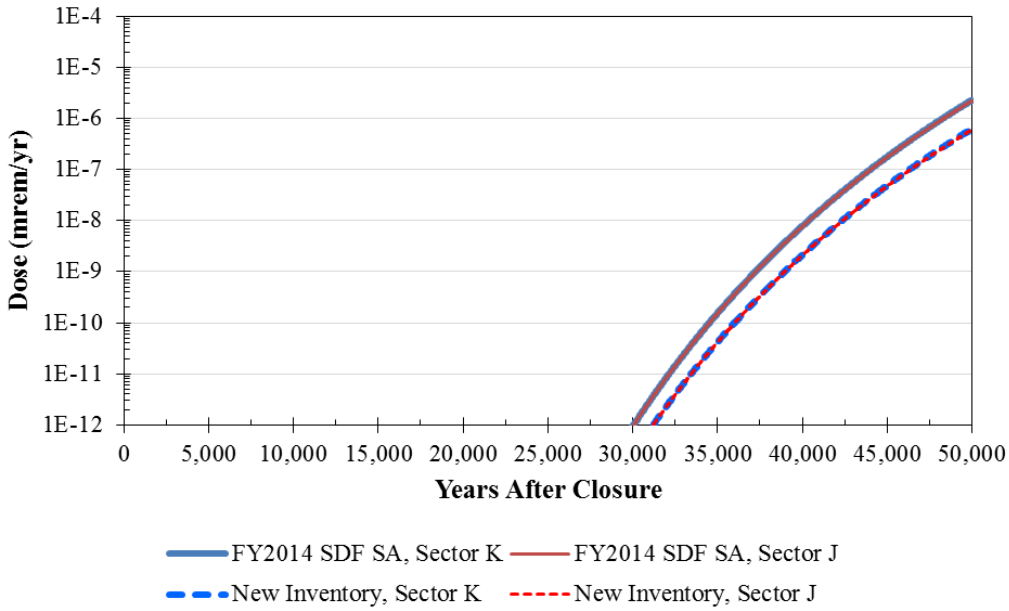

Beginning with the model that used the new inventory, a series of additional sensitivity models were developed to assess the risk significance of selenium K_d values for saltstone and concrete. These sensitivity models were developed to provide greater insight than the assessment already provided within Section 5.6.6.4 of the FY2014 SDF SA. [SRR-CWDA-2014-00006] For these new sensitivities, K_ds for selenium within concrete and within saltstone were modified as summarized in Table SP-11.5. This table also identifies the corresponding Se-79 dose curves, as depicted in Figure SP-11.8. The Se-79 dose contributions at Sector J were slightly higher than at Sector K, so the figure is only showing the Sector J results.

Table SP-11.5: Summary of Additional Selenium K_d Sensitivities

Curve in Figure SP-11.7	K_ds For Saltstone	K_ds for Concrete
Red	Set to 0.0 mL/g [b]	Set to 0.0 mL/g [b]
Green	Set to 0.0 mL/g [b]	No change [a]
Yellow	No change [a]	Set to 0.0 mL/g [b]
Blue	No change [a]	No change [a]

Notes: (a) Uses the same values as the FY2014 SDF SA Evaluation Case. [SRR-CWDA-2014-00006]
(b) To prevent a divide-by-zero error within the GoldSim model, a non-zero value was required. An extremely small value (1.0E-30 mL/g) was assumed to be effectively zero. Value applied regardless of the pH or Eh of the cementitious material.

Figure SP-11.8: Se-79 Doses at Sector J (100-Meter MOP), Comparison for Selenium K_d Sensitivity

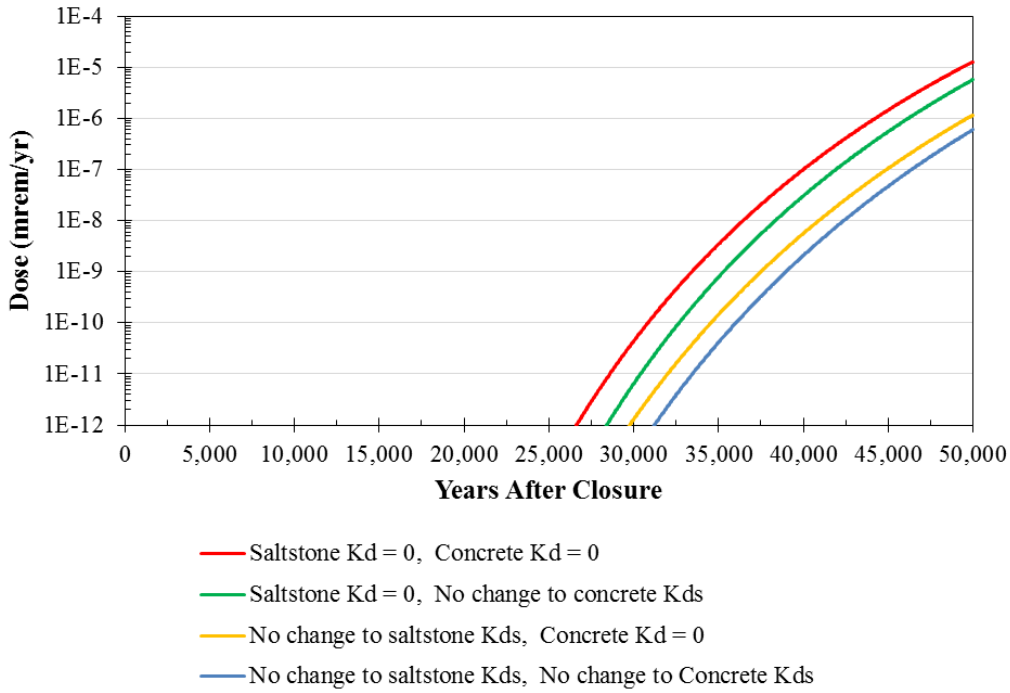

The red line in Figure SP-11.8 shows, effectively, no retardation of selenium within concrete or saltstone. As such, this is not a realistic representation of potential doses, but it does provide an extreme upper bound for evaluating the risk significance. For the first 25,000 to 30,000 years, there is effectively no dose contribution from Se-79. Further, within 50,000 years, the highest dose contribution exhibited from any on these sensitivity models was only about 1.0E-05 mrem/yr. Given that Tc-99 dose contributions exceed 200 mrem/yr (near 30,000 years), the dose contributed from Se-79 is insignificant.

A final additional sensitivity was performed using the model with zero K_d values for concrete and saltstone (red curve in Figure SP-11.8). For this additional analysis, the leachate-impacted sandy soil K_d for selenium was set to 1.0 mL/g. This value represents the lower bound associated with saltstone leachate solution, as reported in the report: *Impact of Cementitious Leachate on Se, Nb and Ra Partitioning* (SREL Doc. R-13-0005). Figure SP-11.9 shows a peak dose contribution from Se-79 that is less than 2 mrem/yr around 17,000 years after closure. Given other dose contributions and the reliance of multiple conservative assumptions to reach this peak, the DOE does not consider Se-79 a significant dose contributor.

Figure SP-11.9: Se-79 Dose at Sector J (100-Meter MOP), Selenium K_d Sensitivity where K_ds in Cementitious Materials = 0 mL/g and K_d in Leachate-Impacted Sandy Soil = 1.0 mL/g

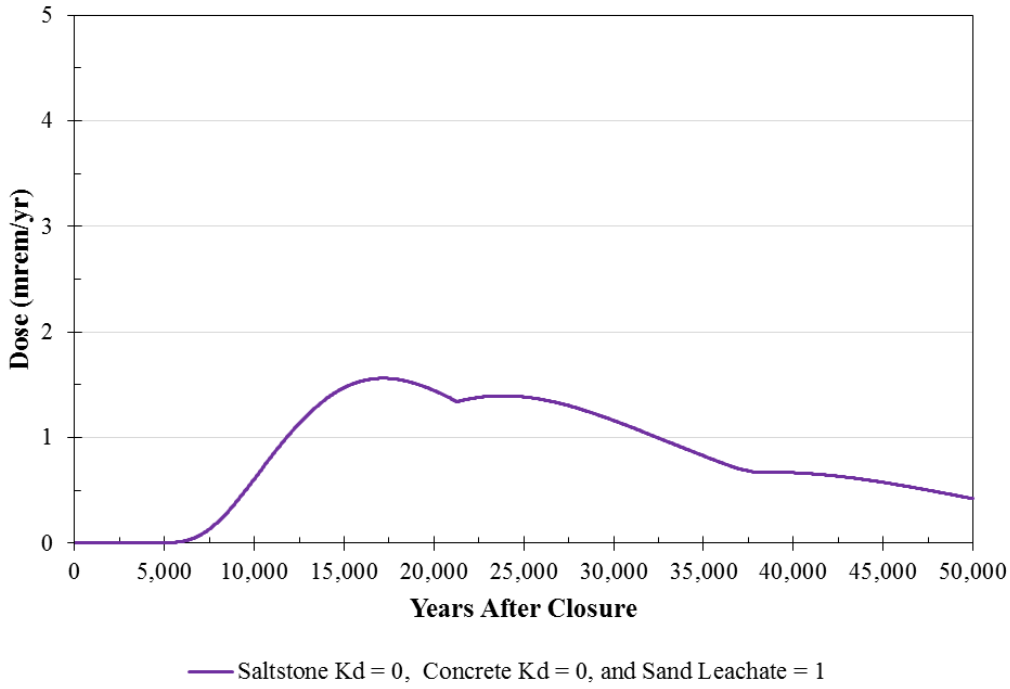

Summary of Iodine, Radium, and Selenium K_d Analyses

The additional analyses demonstrated that I-129 dose contributions are sensitive to the iodine K_ds in saltstone (and concrete, to a much lesser degree), and the degree of this sensitivity is also dependent upon the volumetric flow through saltstone. Even under the most conservative modeling assumptions, the overall magnitude of the I-129 dose contribution is not expected to increase by more than 5 or 6 mrem/yr and thus total doses remain below the 25 mrem/yr MOP performance objective. The analyses also demonstrated that Ra-226 is not a significant dose contributor within the first 10,000 years after SDF closure, regardless of the cementitious K_d values, and is relatively insignificant (when compared to Tc-99 dose contributions) beyond 10,000 years. Finally, the additional analyses also showed that Se-79 is not expected to be a significant dose contributor, even under very conservative cementitious and soil K_d assumptions.

SP-12

SP-12	**Question:** Additional information is needed about the representation of Tc release from young cementitious materials.
	Basis: In NRC RAI Comment SP-8 on the DOE FY13 SDF Special Analysis document, the NRC staff was concerned about the value of $1x10^{-8}$ moles/liter used by the DOE to represent Tc solubility in saltstone. The NRC staff specifically cited higher solubility values (i.e., approximately $1x10^{-6}$ moles/liter) observed by Cantrell and Williams in the PNNL-21723 report from 2012 and questioned how those results were incorporated into the DOE analysis. During the NRC May 2014 Onsite Observation Visit (see SDF-CY14-01 Report in ADAMS as ML14199A219), the DOE explained that those values were measured at a higher pH than anticipated in moderately-aged saltstone (i.e., approximately 10.5). Section 4.1.2 of the DOE FY14 SDF Special Analysis document included the following: "Under reducing conditions (Eh < -0.38 V), the calculated technetium solubility decreased as the pH decreased. For example, when pH changed from 12.7 to 10.5 (the approximate pH decrease between the young and moderately-aged saltstone stages used in [this document]) at a fixed Eh of -0.38 V, the calculated solubility of TcO2·1.6H2O is predicted to significantly decrease from 6.3E-07 M to 5.2E-09 M." However, the DOE FY14 SDF Special Analysis document did not address how the higher solubility representative of young concrete was represented in the model, which used a value of 1×10^{-8} moles/liter for the entire 10,000 year performance period.
	Path Forward: Perform an analysis and provide results that project Tc-99 release during the time period when saltstone has a pH higher than moderately-aged cementitious material (i.e., higher than a pH of 10.5), including considering the higher Tc solubility expected at those pH values.

DOE Response to SP-12

The progression of saltstone aging can be summarized as follows: Reduced/Young → Reduced/Moderate → Oxidized/Moderate → Oxidized/Aged. [SRNL-STI-2014-00083] In December of 2012, SRNL released a report comparing "thermodynamic modeling results to recent laboratory measurements to provide estimates for technetium geochemical input values for transport modeling." [SRNL-STI-2012-00769] The report concluded that a hydrated technetium dioxide phase (likely $TcO_2 \cdot 1.6H_2O$) controlled technetium solubility in saltstone leachate under reducing conditions (Eh < -0.38 V). Furthermore, it was established that within this reducing environment, the solubility of technetium dioxide phases decreases with increasing acidity (Table SP-12.1).

Table SP-12.1: Solubility of $TcO_2 \cdot 1.6H_2O$ under reducing conditions (Eh < -0.38V)

pH	Tc Solubility (mol/L)
12.7	6.3E-07
11.8	4.2E-08
11.0	9.4E-09
10.5	5.2E-09

[SRNL-STI-2012-00769]

Based on this data, the pH-to-technetium solubility may be reasonably approximated with the following exponential formula:

$$Sol_{Tc} = (3.909 \times 10^{-19})e^{(2.190 \times pH)} \qquad \text{(Eq. SP-12.1)}$$

where Sol_{Tc} is the solubility of technetium (mol/L).

The data from Table SP-12.1 and the curve resulting from Equation SP-12.1 are displayed in Figure SP-12.1. Using this relationship, technetium solubility may be modeled based on the evolution of the pH of pore water as it moves through saltstone.

Figure SP-12.1: Relationship of pH to Tc Solubility

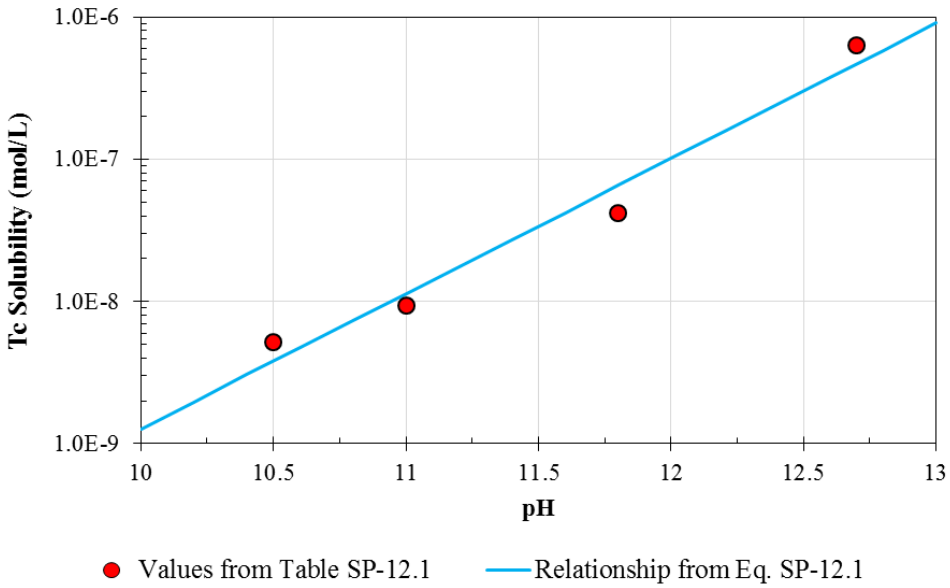

To determine the pH of the pore water within reducing cementitious materials, DOE uses Geochemist's Workbench® (GWB) modeling software. Results from GWB simulations used for the SDF PA and SA modeling of saltstone degradation illustrate that infiltrate reacting with saltstone begins near pH 11.8 and drops to a pH of 11 between 10 to 50 pore volumes (shown in Figures SP-12.2 and SP-12.3). [SRR-CWDA-2011-00044]

Based on the GWB chemical degradation models shown in Figures SP-12.2 and SP-12.3, the highest predicted pH value in saltstone is approximately 11.8. According to Table SP-12.1, the pH of 11.8 corresponds to a technetium solubility of 4.20E-08 mol/L; however, the estimated solubility, when applying a pH of 11.8 to Equation SP-12.1, is closer to 6.5E-08 mol/L. Because the technetium solubility of 6.5E-08 mol/L would release more Tc-99 in early times (relative to a solubility of 4.20E-08 mol/L), it is considered more conservative and will be assumed as the initial solubility value for sensitivity modeling. Therefore, within the cementitious environment, the Reduced/Young → Reduced/Moderate transition shall be simulated by decreasing the technetium solubility value from 6.5E-08 mol/L to 1.0E-08 mol/L (see FY2014 SDF SA, Section 4.4.1.3) due to the pH decreasing from 11.8 to 10.

Figure SP-12.2: Mineralogical Controls on Eh and pH Transitions

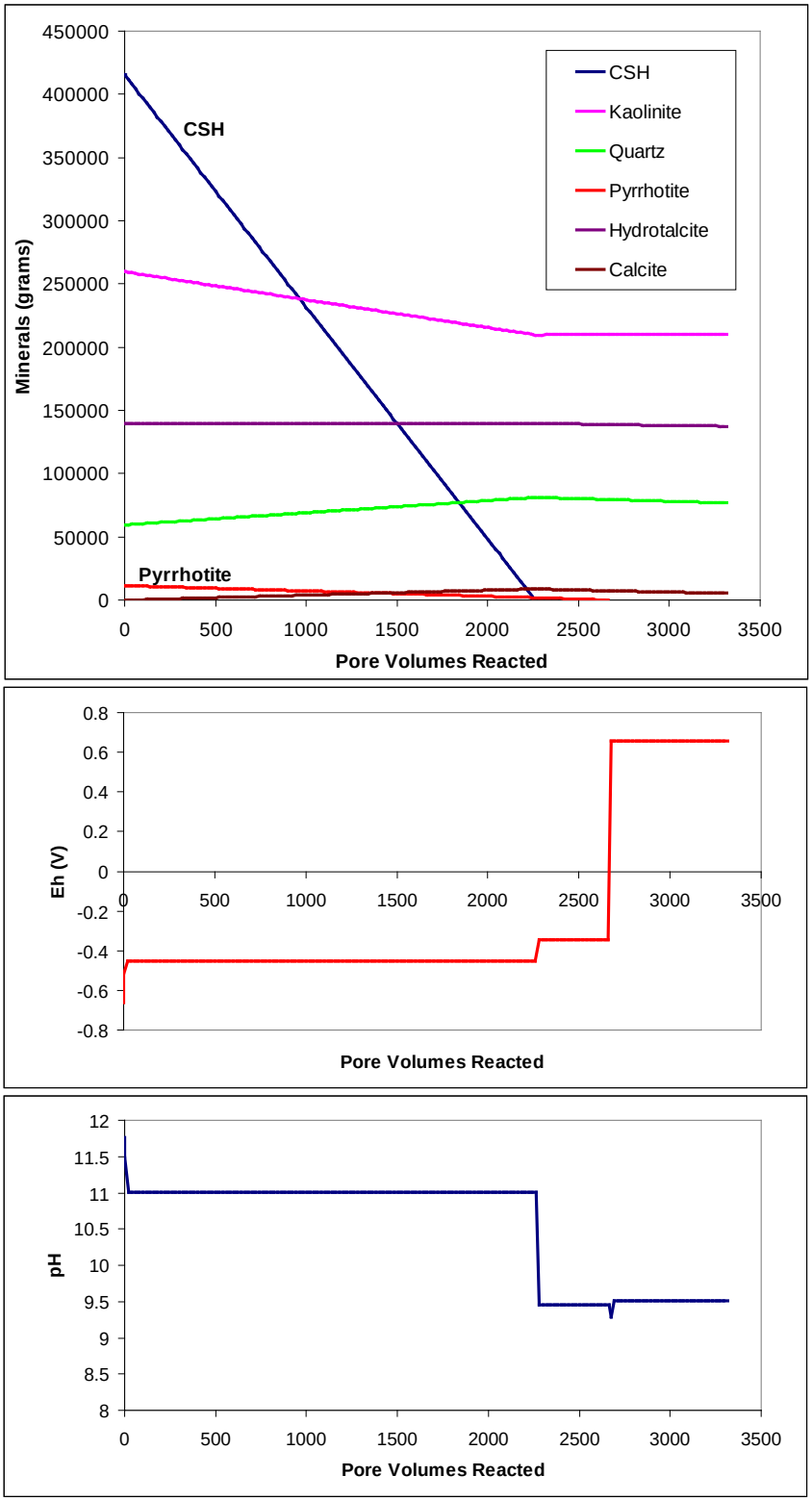

[Figure SP-8.1 in SRR-CWDA-2011-00044]

Figure SP-12.3: Reaction Paths of Saltstone with Similar Formula but Differing Bulk Densities and Porosities; Saltstone Assumed to React with Groundwater

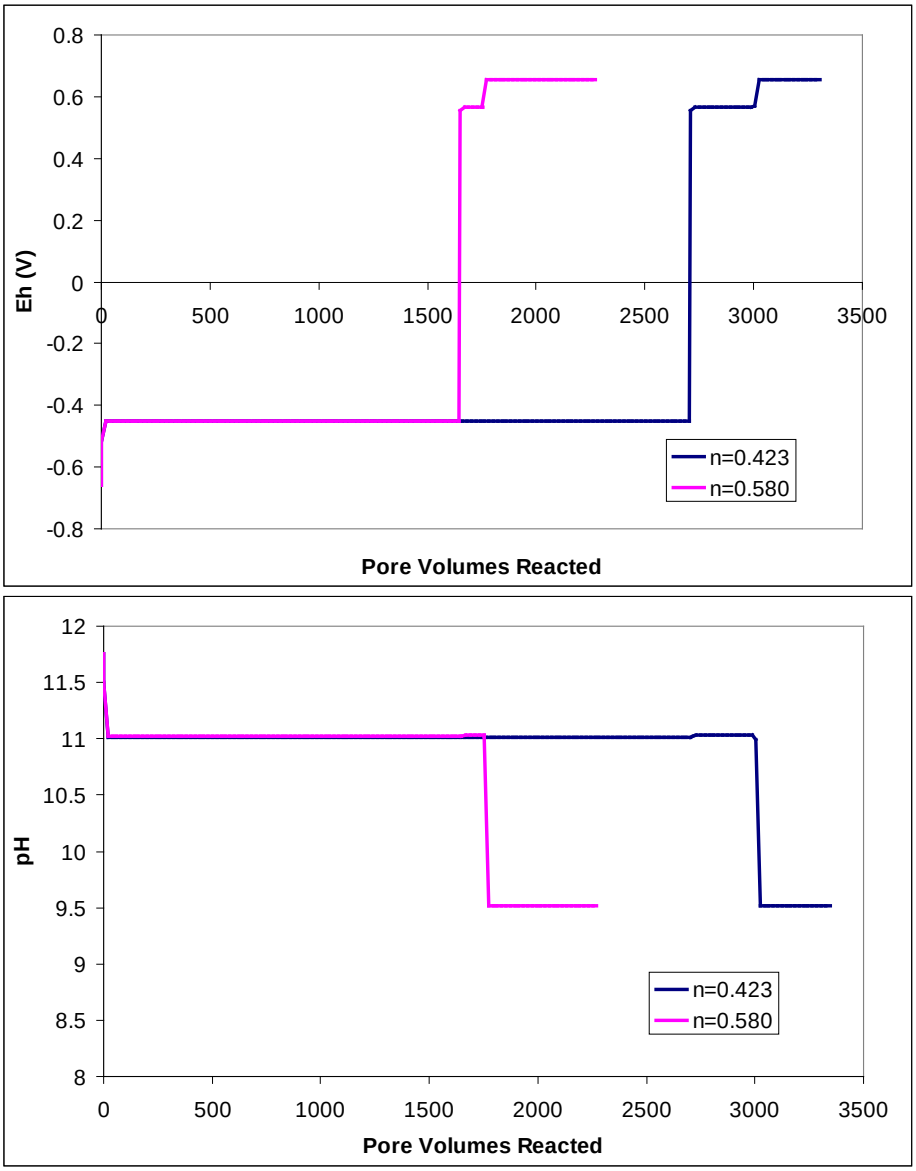

[Figure SP-8.3 in SRR-CWDA-2011-00044]

Since pH is not explicitly modeled within GoldSim, replacing the pH term in the relationship from Figure SP-12.1 with an equivalent number of pore flushes (based on the GWB modeling) provides a reasonable basis for modeling the change to the technetium solubility. For this analysis, three sets of assumed pore flush values were considered for estimating technetium solubility based on the Reduced/Young → Reduced/Moderate transition:

- Early: transition occurs at 10 pore flushes,
- Nominal: transition occurs at 25 pore flushes, and
- Conservative: transition occurs at 50 pore flushes.

Due to the low flow rates through saltstone during early periods of the simulation, it takes an unexpectedly long amount of time for this early transition to occur (see Table SP-12.2), based on the counting of pore flushes within GoldSim sensitivity modeling. Because the K_d values for a number of elements within the Reduced/Young chemical environment are considerably different from those in the Reduced/Middle chemical environment, this transition was also applied to the other radionuclides to determine the impact on total doses to the MOP at the 100-meter SDF boundary. These results were generated using modified versions of the GoldSim SDF Tc-99 Release Model and the GoldSim SDF All-Species Model (see Section 4.4.2 of the FY2014 SDF SA).

Table SP-12.2: Estimated Time to Complete Saltstone Transition from Reduced/Young → Reduced/Middle for Each SDU Type

SDU Type	Year of Transition		
	10 Pore Flushes (Early)	25 Pore Flushes (Nominal)	50 Pore Flushes (Conservative)
SDU 1	4,925	7,139	9,522
SDU 4	3,111	3,809	4,633
150-foot diameter SDUs	5,345	7,895	10,677
375-foot diameter SDUs	4,865	6,184	8,077

The peak doses are shown in Table SP-12.3. Figures SP-12.4 and SP-12.5 show the peak doses within 10,000 years and within 50,000 years, respectively.

Table SP-12.3: Peak Dose to the MOP at the 100-Meter SDF Boundary Using Reduced/Young Chemical Environment at Start of Simulation

Sector	Peak Dose for All Sectors							
	FY2014 SDF SA Evaluation Case [a]		10 Pore Flushes (Early)		25 Pore Flushes (Nominal)		50 Pore Flushes (Conservative)	
	Within 10,000 Years	Within 50,000 Years	Within 10,000 Years	Within 50,000 Years	Within 10,000 Years	Within 50,000 Years	Within 10,000 Years	Within 50,000 Years
Sector A	6.0	134	10.0	136	10.2	130	10.6	119
Sector B	11.7	256	17.9	262	18.3	250	**20.2**	230
Sector C	5.9	107	9.7	109	9.9	104	12.0	95.5
Sector D	3.1	50	5.9	50	6.1	48	7.0	43.8
Sector E	6.6	155	10.9	156	11.2	149	11.2	136
Sector F	3.4	74	6.3	74.5	6.5	71	6.5	65.1
Sector G	7.1	171	11.7	171	11.9	163	11.9	149
Sector H	11.2	273	17.5	272	17.8	260	17.8	239
Sector I	6.3	425	11.9	418	12.3	410	12.3	397
Sector J	8.6	**477**	15.3	**469**	15.8	**460**	15.8	**445**
Sector K	**12.7**	305	**19.7**	310	**20.1**	295	20.1	271
Sector L	7.6	166	12.5	171	12.8	163	12.8	150
Maximum	**12.7**	**477**	**19.7**	**469**	**20.1**	**460**	**20.2**	**445**

Note: (a) Values vary slightly from those presented in Section 5.5 of the FY2014 SDF SA because this simulation used the GoldSim results from the benchmarking analysis rather than the equivalent PORFLOW results.

Figure SP-12.4: Total Doses to the MOP for SP-12 Sensitivity Analysis (Within 10,000 Years)

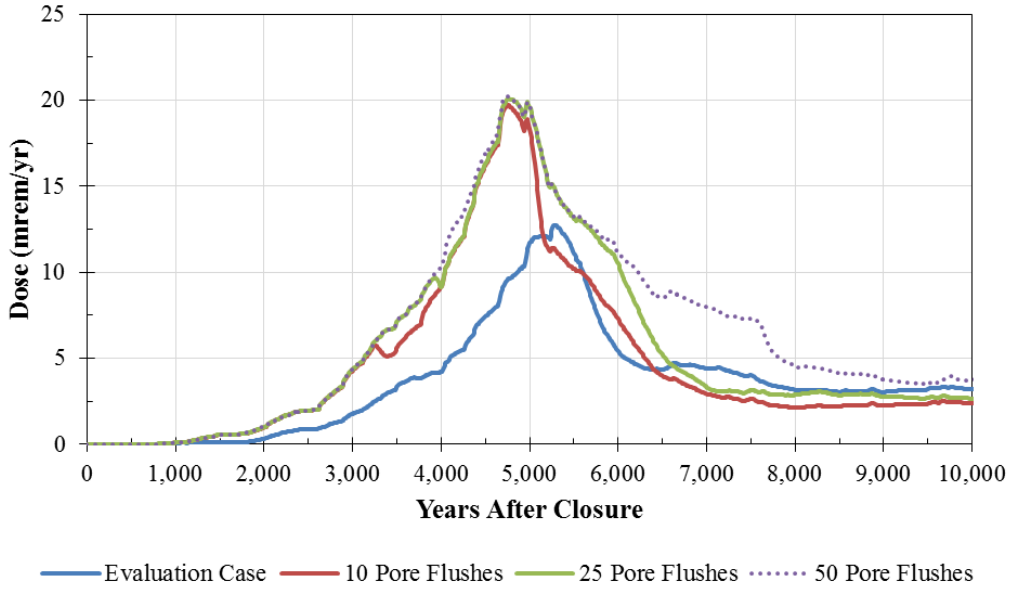

Figure SP-12.5: Total Doses to the MOP for SP-12 Sensitivity Analysis (Within 50,000 Years)

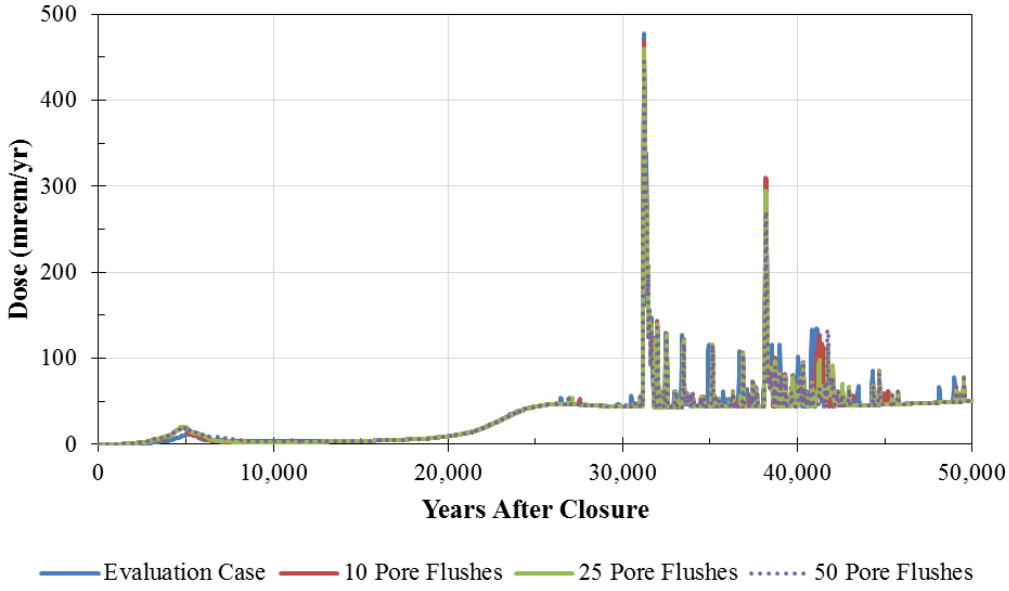

The 50,000-year dose peaks were slightly lower than those from the Evaluation Case, while the 10,000-year dose peaks were substantially higher. In the first 10,000 years, the lower iodine K_d for Reduced/Young cementitious materials (5 mL/g versus 9 mL/g) results in higher I-129 peaks which were coupled with the increased Tc-99 releases. Since Sector K is the dominant sector within 10,000 years, Figure SP-12.6 shows the two primary dose contributors (I-129 and Tc-99) for Sector K for each simulation.

Figure SP-12.6: Sector K Dose Contributions from I-129 and Tc-99 for SP-12 Sensitivity Analysis (Within 10,000 Years)

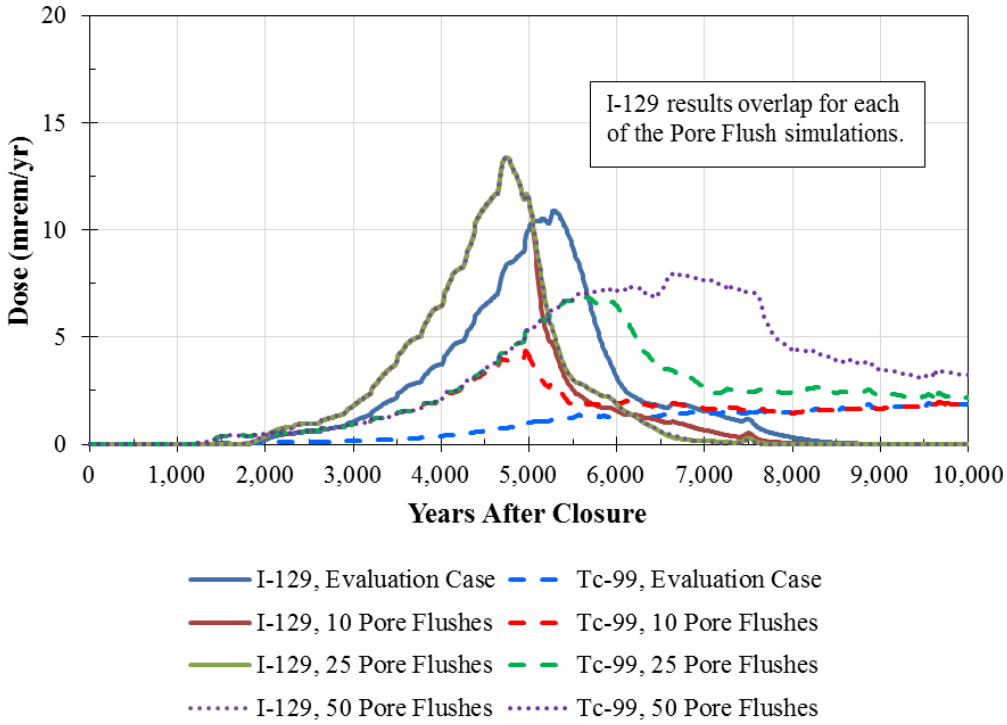

Although these doses within 10,000 years are higher than those presented within the FY2014 SDF SA, the peaks within 10,000 years remain below the 25 mrem/yr performance objective. Therefore, the conclusions in the FY2014 SDF SA are not affected. Future performance assessment modeling will consider alternate approaches for modeling the Reduced/Young chemical environment.

INFILTRATION AND EROSION CONTROL (IEC)

IEC-1

IEC-1	**Question:** Technical justification is needed for the expectation that future infiltration rates will be between the minimum and average values. In addition, information is needed about the status of the Hydrologic Evaluation of Landfill Performance (HELP) code replacement evaluation.
	Basis: Section 5.6.3.1 in the DOE FY14 SDF Special Analysis document included the following: "This referenced report [WSRC-STI-2008-00244] indicates that a number of conservatisms were assumed in the development of the HELP model used to generate these infiltration rates. Giving credit for these conservatisms, it is reasonable to expect that future infiltration rates would be between the minimum and average values. Therefore, a discrete distribution was applied in which the minimum infiltration rate was assigned a 40% probability, the average infiltration rate was assigned a 40% probability, and the maximum infiltration rate was assigned a 20% probability." However, expected conservatisms in the HELP code are not adequate justification given the concerns about the reliability of HELP for predicting performance without site-specific calibration. The NRC 2012 SDF TER includes the following: "Although the HELP code may be suitable for estimating long-term water balances, short-term events and trends may not be adequately represented [(U.S. Environmental Protection Agency (EPA) Report EPA-600-R-02-099, Bonaparte et al. (2002). That EPA report included:] '… the model will generally not be adequate for use in a predictive or simulation mode, unless calibration is performed using site-specific measured (not default) material properties and actual leachate generation data'. Since calibration data over the lifetime of the planned closure cap is unavailable, the use of an alternative code may provide more defensible infiltration estimates." The DOE document WSRC-STI-2007-00184, Rev.2 included that the HELP results were generally conservative, but page 59 of that DOE document included the following: "However as indicated in Section 8.7.1, the HELP model is not capable of appropriately considering the results of the probability based root penetration model which has been developed to evaluate root penetration of the [Geosynthetic Clay Liner (GCL)] through tensile stress cracks within the overlaying HDPE geomembrane. For this reason in the future other models will be evaluated as a replacement to the HELP model. The models to be considered may include but are not limited to FEHM, HYDRUS-2D, LEACHM, TOUGH-2, UNSAT-H, and VADOSE/W." Because of the importance of infiltration to the dose results, the NRC staff continues to monitor the hydraulic performance of the closure cap and needs information about the status of that DOE evaluation. The importance of infiltration rates to peak dose was seen in Figure 5.6.5-20 in the DOE FY14 SDF Special Analysis document, which presented a comparison of minimum, average, and maximum infiltration rates.
	Path Forward: Provide technical justification for the expectation that future infiltration rates will be between the minimum and average values**.** Provide the results or the status of the HELP

	code replacement evaluation.

DOE Response to IEC-1

Note that the deterministic Evaluation Case assumes the average infiltration rate. The discussion cited from Section 5.6.3.1 of the FY2014 SDF SA is only in reference to the assigned probability weightings used in the probabilistic GoldSim Model and should not be misconstrued as representing the modeling assumptions used for the deterministic Evaluation Case.

The performance capabilities of the closure cap, based on the current conceptual design, were developed via the HELP model. Therefore, it is reasonable to assign probabilities to the infiltration rates that are informed by inputs and assumptions used in the HELP model. Once a formal closure cap design has been finalized, such weightings will be reevaluated. The conservatisms (from WSRC-STI-2008-00244) which informed the assigned probabilities include, but are not limited to, the following:

- Evapotranspiration assumed a maximum evaporative depth of 22 inches due to the anticipated capillarity associated with the surficial soils and anticipated root depths.
- For conservatism, it was assumed that every HDPE geomembrane hole generated over time is penetrated by a root that subsequently penetrates the GCL, once significant roots are available to penetrate.
- The upper drainage layer, GCL, and HDPE layers will be conservatively modeled as being at the minimum depth, with each entire layer subject to root contact. This is conservative because root penetration is not considered possible below a depth of 12 feet (i.e., less than one-half of the HELP-modeled closure cap area can have an upper drainage layer, GCL, or HDPE subject to pine root penetration).
- The precipitation data included significant pulses of water, not just average values, by utilizing a range of daily precipitation from 0 inches up to 6.7 inches and an annual range from 29.8 inches to 68.6 inches.
- The maximum slope length of the closure cap (i.e., 825 feet) was used to determine both runoff and lateral drainage for the entire cap. A significant portion of the cap will have slope lengths less than 825 feet, resulting in more runoff.
- The erosion barrier is assumed to be infilled with a sandy soil; the use of a less permeable infill would reduce infiltration.
- No lateral drainage is assumed to occur over the erosion barrier; however such lateral drainage could occur, particularly if a low permeable infill were used.
- The initial saturated hydraulic conductivity of the GCL was taken as 5.0E-09 cm/s even though test results indicate that the value should be significantly lower.
- It has been assumed that the GCL saturated hydraulic conductivity increases to 5.0E-08 cm/s at the end of the 100-year institutional control period. This is not likely since infiltrating water at SRS should be very low in dissolved calcium and other divalent cations.

As described in WSRC-STI-2007-00184 (Section 8.7), since the HELP model cannot handle the probability based root penetration model, the model applied holes (i.e., Geomembrane Installation Defects) at discrete timesteps which penetrate through the combined HDPE/GCL layers starting as early as year 300 after closure (despite the root penetration modeling showing no penetrations before 560 years, per Section 8.7.1 of same report). By combining the HDPE and GCL layers and applying penetrations through the combined HDPE/GCL, with the number of holes increasing over time, the HELP model compensates for the model's inability to fully integrate the probability based root penetration model. Although the HELP model does not automatically integrate with the root penetration model, it does apply holes through the HDPE/GCL layers, which increase at discrete intervals.

SRNL evaluated computer codes that are used to predict percolation of water through the closure-cap and into the waste containment zone at DOE closure sites (SRNL-STI-2009-00572). This work compared the HELP model with alternative computer codes that use unsaturated flow (Richards' equation). The report provided a literature review of the HELP model and the proposed codes, which resulted in two recommended codes for further evaluation: HYDRUS-2D3D and VADOSE/W. This further evaluation involved performing actual simulations on a simple model and comparing the results of those simulations to those obtained with the HELP code and field data. The largest difference between the two codes is their approach to modeling evaporative transpiration. VADOSE/W uses a first principles approach while HYDRUS-2D3D uses empirical equations. HYDRUS-2D3D does not account for snow fall or melt-runoff. While snow is not a large factor at SRS, it may be a major concern at other sites across the DOE complex.

HYDRUS-2D3D was preferred over VADOSE/W for the following reasons:

- The HYDRUS family of codes is more widely known and used. Earlier versions of HYDRUS are available to the public free of cost. These may be important considerations to reviewers and other stakeholders.
- The licensing cost is much lower for HYDRUS-2D3D. Twenty perpetual network licenses for HYDRUS were purchased for approximately the same cost of one perpetual hardware key locked VADOSE/W license.
- As indicated by the name, HYDRUS-2D3D includes a 3D capability. While 2D is sufficient for most cover systems, analysis of discrete holes in HDPE and GCL liners may require 3D simulations.
- HYDRUS-2D3D is capable of simulating general multiphase flow and transport, whereas VADOSE/W simulates liquid flow.
- The Graphical User Interface (GUI) was more robust for HYDRUS-2D3D during the limited testing performed. The VADOSE/W GUI regularly exhibited a fatal error that prevented completion of numerical simulations.

HYDRUS-2D3D is the latest version in the HYDRUS family of codes. HYDRUS-2D3D is a software package that simulates water, heat and solute movement in either two- or three-dimensional variably saturated media and is currently under active development and use.

For a simple no-cover scenario (Sandy Clay soil type and grass cover), HYDRUS-2D3D produced an infiltration estimate of 17.6 in/yr. For a similar problem specification (United States Department of Agriculture Soil Classification soil and fair stand of grass), the HELP model produced an estimate of 9.8 in/yr. Both model predictions are within the range of infiltration estimates generated from field measurements and other modeling studies for similar conditions (WSRC-STI-2007-00184, Rev. 2, Table 9). As DOE continues to evaluate potential replacements, a decision will be made on the associated costs and benefits of replacing the HELP code and will be weighed with the priorities for risk reduction of other activities within the SRS Liquid Waste Program, including waste removal and treatment options.

The merits of using HYDRUS-2D3D over HELP for cover system scenarios are still uncertain at this point. Evaluation of additional scenarios and parameter settings would be needed to assess any systemic biases in HYDRUS-2D3D relative to HELP and/or field measurements for SRS applications. As of the preparation of this RAI response, the HELP model has not been replaced.

DISPOSAL STRUCTURE PERFORMANCE (DSP)

DSP-1

DSP-1	**Question:** The evaluation of a potential breach of High Density Polyethylene (HDPE) did not consider the potential impacts of a breach in the HDPE or HDPE seam welds in the closure cap or below the drainage layer above a disposal structure.
	Basis: During the February 2015 Onsite Observation Visit (see SDF-CY15-01 Report in ADAMS as ML15041A562), the DOE discussed that the observance of water in the leak detection system of SDS 3A was most likely caused by the failure of an extrusion weld. Although the observations of water in the leak detection system are consistent with the failure of an extrusion weld, the DOE evaluation did not rule out the possibility of an HDPE tear or a failure of a seam weld. The NRC staff is concerned that the evaluation only included the potential impacts of a breach in the HDPE around the disposal structure and did not evaluate the potential impact of a breach in the HDPE layer in either the closure cap or below the drainage layer above each disposal structure. The NRC staff understands that the HDPE seam welds are tested in the field during the construction phase. However, the NRC staff is not aware of longer-term tests of these seam welds after the initial testing period.
	Path Forward: Provide information to support the DOE assumption of longer-term performance of the HDPE and HDPE seam welds, in particular field welds on 100 mil HDPE. Examples of that type of information include: field studies of similar materials, accelerated laboratory studies on HDPE and HDPE seam welds, and confirmatory testing of welds that have been conducted after the initial construction testing. Alternatively, provide a revised dose estimate that includes an early failure of these materials.

DOE Response to DSP-1

While no studies are available on HDPE seam welds, existing modeling utilizes conservative HDPE properties for the Evaluation Case. The PORFLOW model provides the HDPE degradation over time for the HDPE above the SDU roof. This file includes initial holes of 550 mm^2/hectare (2.2 cm^2/acre), then increases by an additional 35,750 mm^2/hectare (145 cm^2/acre) at year 54. With respect to closure cap modeling, the HELP model assumes that there are initially 12 holes per acre in the HDPE (with a total area of 4 cm^2/acre).

In addition, *Scoping Study: High Density Polyethylene (HDPE) in Saltstone Service*, WSRC-TR-2005-00101, provides a HDPE permeability of 2.0E-13 cm/sec. PORFLOW modeling assumes a higher initial permeability of ~6.0E-10 cm/sec to account for construction and possible defects.

In addition, the response to RAI SP-5 included additional GoldSim modeling using both the GoldSim SDF Tc-99 Release Model and GoldSim SDF All-Species Model (described in the FY2014 SDF SA) to address the NRC's question regarding earlier onset to saltstone degradation by effectively setting the starting time to zero and with higher infiltration rates than predicted by the closure cap model and used in PORFLOW (see Figure SP-5.1). The results demonstrate that while removal of the degradation delay (including the HDPE) does shift the peak doses in the 10,000-year and 50,000-year windows to earlier times (1,600 years earlier and 960 years earlier,

respectively), the magnitude and shape of the peaks remain largely unchanged and the performance objective is still met. Therefore, the SP-5 simulation provides reasonable expectation/assurance that if saltstone degradation were to begin without a delay for all SDUs, the peak dose at the 100-meter SDF boundary would remain below 25 mrem/yr during the performance assessment period.

DSP-2

DSP-2	**Question:** Additional information is needed to support the delays before carbonation of the roof and floors of the disposal structures were modeled to begin.
	Basis: The DOE Evaluation Case delayed modeled carbonation of the floor and roof of the 150-foot and 375-foot disposal structures until 1,400 years after site closure[1]. The DOE FY14 SDF Special Analysis document attributed those delays to the performance of the HDPE-GCL layer. However, it is not clear to the NRC staff why carbonation would not occur due to diffusion of carbon dioxide gas from the unsaturated soil into the roofs and floors of the disposal structures. The DOE FY14 SDF Special Analysis document provided a projection of the hydraulic performance of the HDPE-GCL layers; but did not discuss their permeability to gas. Furthermore, the sides of the 375-foot disposal structures are in direct contact with soil that would serve as a source of carbon dioxide. Section 4.2.2.2 of the DOE FY14 SDF Special Analysis document showed the results of a mechanistic model of carbonation of disposal structure concrete performed with the CBP toolbox model LeachXS/Orchestra. The DOE determined that the analytical solution represented in the DOE Evaluation Case predicted a conservative carbonation rate compared to the numerical solution determined with LeachXS/Orchestra. However, the LeachXS/Orchestra solution did not support the assumption that carbonation would not begin until the complete degradation of the HDPE-GCL. Although degradation through sulfate attack of the roofs and floors of the 150-foot and 375-foot disposal structures was modeled as beginning at the time of closure, delaying the modeled onset of carbonation increased the total time needed for degradation. The time until complete degradation of the disposal structure roofs and floors, in turn, delayed the modeled onset of saltstone degradation. Earlier degradation of saltstone and disposal structure components could shift doses due to risk-significant radionuclides, such as I-129, earlier in the performance period and could contribute to moving doses from other radionuclides into the performance period.
	Path Forward: Provide support to the assumption that the HDPE and HDPE-GCL layers delay carbonation of disposal structure cementitious components or provide a revised analysis that demonstrates the effects of assuming disposal structure carbonation begins immediately after emplacement.

DOE Response to DSP-2

The response to RAI SP-5 presents the results of a GoldSim simulation (herein referred to as the SP-5 Simulation) in which the saltstone degradation delay is removed from both the GoldSim SDF Tc-99 Release Model and GoldSim SDF All-Species Model (described in the FY2014 SDF SA). Hence, the SP-5 Simulation effectively models saltstone degradation for each SDU as beginning at time zero. While the 10,000-year and 50,000-year peaks shift to earlier times (by 1,600 years and 960 years, respectively), the magnitude and shape of the peaks remain largely

[1] In the context of these RAIs and RAI responses, "site closure" refers to facility closure of the Saltstone Disposal Facility and not the closure of the Savannah River Site.

unchanged and the performance objective is still attained. Therefore, the SP-5 Simulation provides reasonable expectation/assurance that if saltstone degradation were to begin without a delay for all SDUs, the peak dose at the 100-meter SDF boundary would stay below 25 mrem/yr during the performance assessment period.

DSP-3

DSP-3	**Question:** Additional information is needed about I-129 sorption in and release from the walls, floors, and mud mats of the 375-foot and 150-foot disposal structures to support the conceptual model of the peak dose within 10,000 years.
	Basis: The DOE FY14 SDF Special Analysis document included the following: "Figure 5.5-4 shows I-129 climbing from about 2,000 years until it reaches the two peaks, at around 5,000 years and 5,300 years after closure. These peaks correspond to releases from [SDS 9 and SDS 7], respectively, as the modeled wall segments become oxidized (starting around 1,600 and completing 4,100 years after closure). As oxidation occurs, and as flow through the [disposal structure] saltstone increased due to degradation, I-129 is more readily transported." However, Table 4.1-4 in the DOE FY14 SDF Special Analysis document showed that I-129 is modeled with a higher K_d value under oxidized conditions as compared to reduced conditions (i.e., 15 mL/g under oxidized Region II conditions and 9 mL/g under reduced Region II conditions), which does not support the explanation of I-129 release due to a transition to oxidizing conditions. Figure 4.8-3 of the DOE FY14 SDF Special Analysis document showed the K_d values for I-129 in the lower and upper mud mats of the 375-foot disposal structures were greater than the K_d values in saltstone during a 20,000 year analysis period. That difference in K_d values may lead to modeled reconcentration of I-129 in the mud mats. Similarly, Figures 4.8.2 and 4.8.3 showed that, at different times during a 20,000 year analysis period, the walls and lower mud mat of the 150-foot disposal structures and wall segments of the 375-foot disposal structures have greater K_d values for I-129 than saltstone does. Iodine-129 is a key risk driver in the DOE FY14 SDF Special Analysis document. Information about iodine storage in and release from saltstone and the disposal structures is needed to support an accurate understanding of the conceptual and mathematical models of I-129 release.
	Path Forward: Provide intermediate model results that show the total concentration of I-129 in saltstone in the disposal structure walls, floor, and mud mats of both the 150-foot and 375-foot disposal structures as a function of time. If I-129 is shown to reconcentrate in the disposal structure walls, floors, or mud mats, justify whether that reconcentration is an intended part of the conceptual model. If necessary, clarify the description in Section 5.5.1.2 of the DOE FY14 SDF Special Analysis document related to the I-129 peaks in Figure 5.5-4.

DOE Response to DSP-3

While developing the response to RAI SP-11, it was determined that it was not the oxidation of the walls that drove the I-129 releases. The timings of the releases were very similar to the timings of the oxidation of the modeled wall segments, but in fact the I-129 releases were driven by the degradation of the barriers and the resulting increase in the volumetric flow through the saltstone.

Within the response to RAI SP-11, Figures SP-11.2, SP-11.3, and SP-11.4 show that I-129 doses very closely reflect the volumetric flow through saltstone, which is expected. Figure SP-11.2, in particular, demonstrates that concrete K_ds have a minimal impact, delaying the I-129 peak by

less than 500 years. As the volumetric flow through saltstone increases, the relative importance of the cementitious K_d values for iodine diminishes. This phenomenon is highlighted by Figures DSP-3.1 through DSP-3.11, which show I-129 concentrations (mol/L) for a cross section of a 375-foot diameter SDU at various times (up to 10,000 years) within the simulation. Note that after 10,000 years, most of the I-129 inventory has been released and significant dose impacts are no longer possible. This set of figures illustrates that no significant reconcentration of I-129 is occurring within the disposal structure walls, floors, or mud mats (i.e., the I-129 concentration within these features never exceeds the initial saltstone concentration of 3.38E-08 mol/L). Note that the upper and lower mud mats of the 375-foot diameter SDUs and the lower mud mat of the 150-foot diameter SDUs are initially assigned the hydraulic properties of the lower vadose zone (see Section 4.2.2 of the FY2014 SDF SA); therefore, no reconcentration of I-129 was expected within these barriers.

Figures DSP-3.12 through DSP-3.22 provide equivalent figures for a 150-foot diameter SDU.

Figure DSP-3.1: I-129 Concentrations in a 375-Foot Diameter SDU at 0 Years

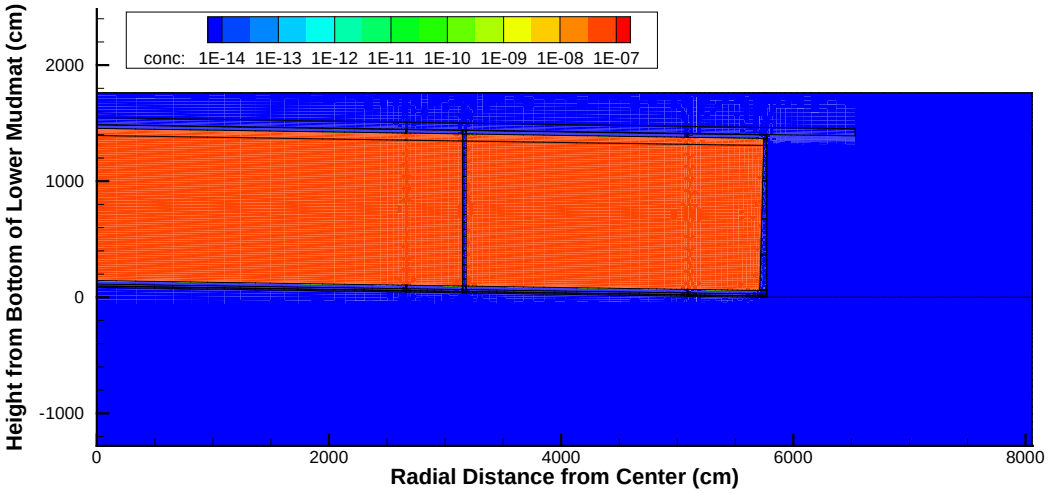

Figure DSP-3.2: I-129 Concentrations in a 375-Foot Diameter SDU at 1,000 Years

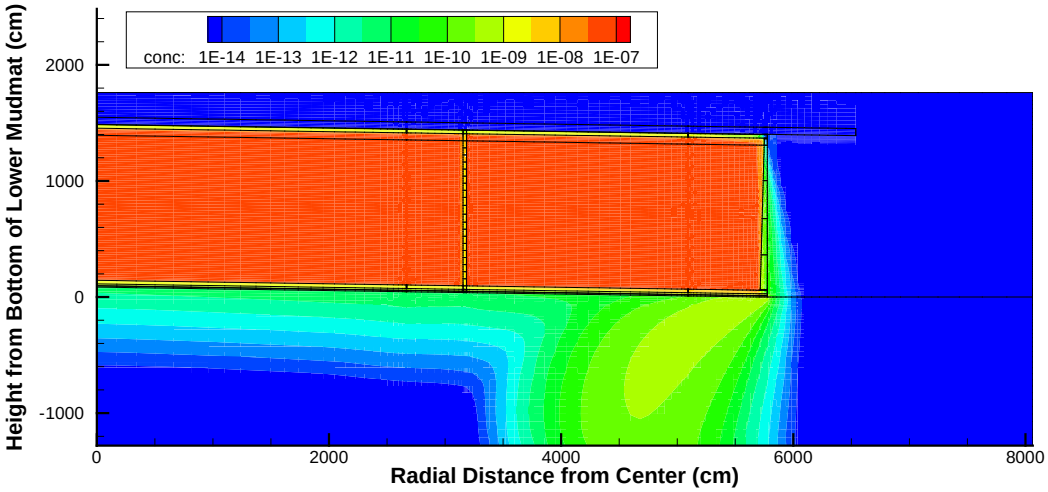

Figure DSP-3.3: I-129 Concentrations in a 375-Foot Diameter SDU at 2,000 Years

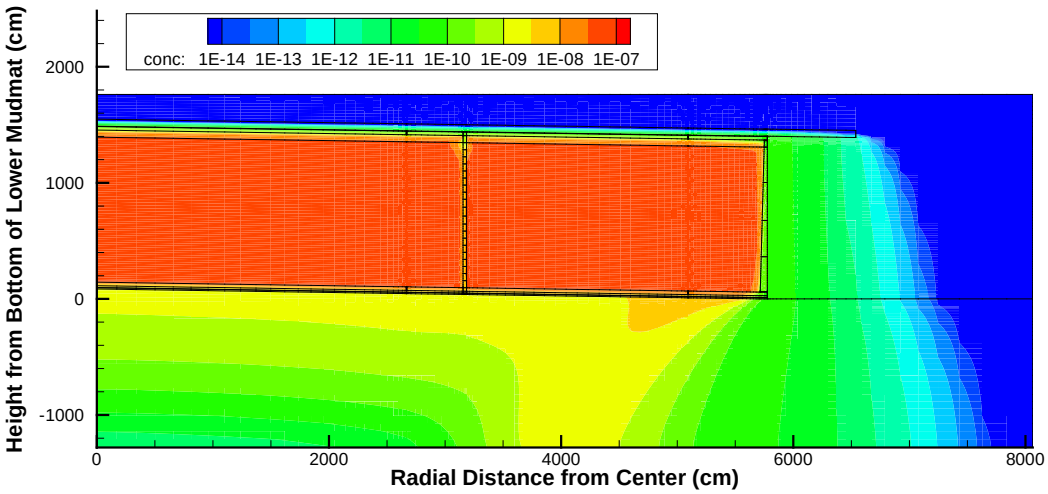

Figure DSP-3.4: I-129 Concentrations in a 375-Foot Diameter SDU at 3,000 Years

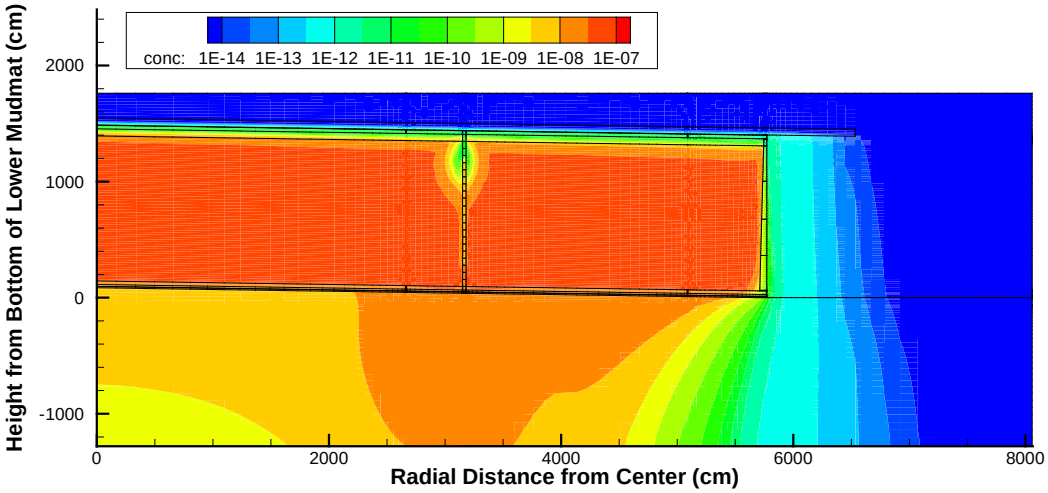

Figure DSP-3.5: I-129 Concentrations in a 375-Foot Diameter SDU at 4,000 Years

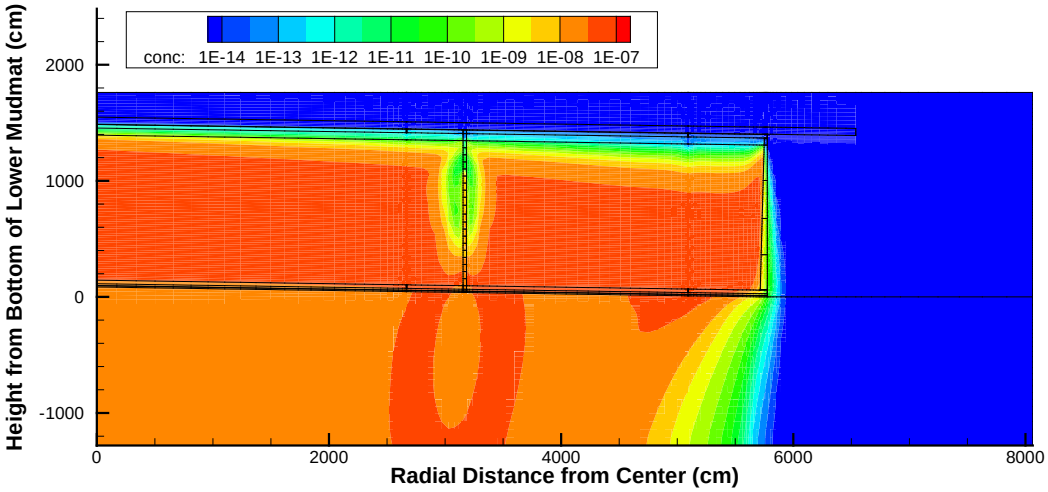

Figure DSP-3.6: I-129 Concentrations in a 375-Foot Diameter SDU at 5,000 Years

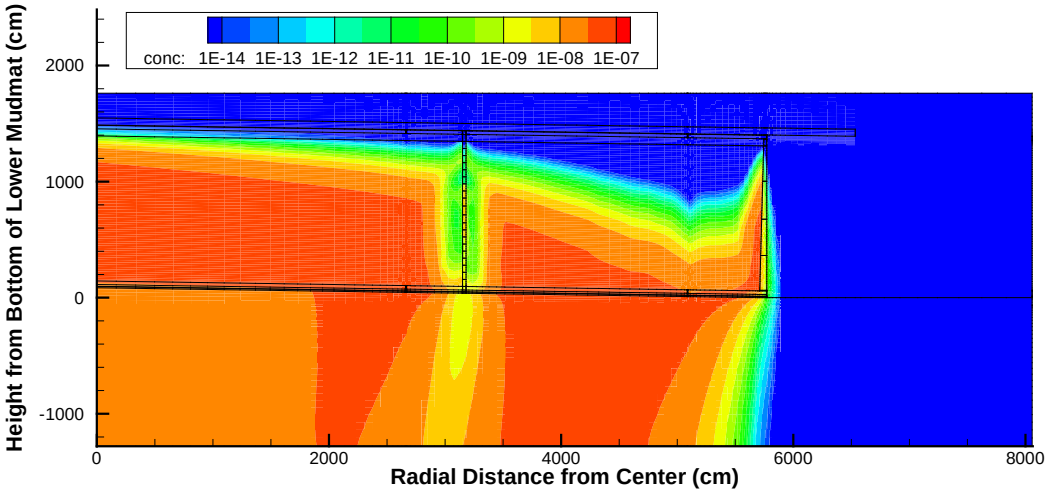

Figure DSP-3.7: I-129 Concentrations in a 375-Foot Diameter SDU at 6,000 Years

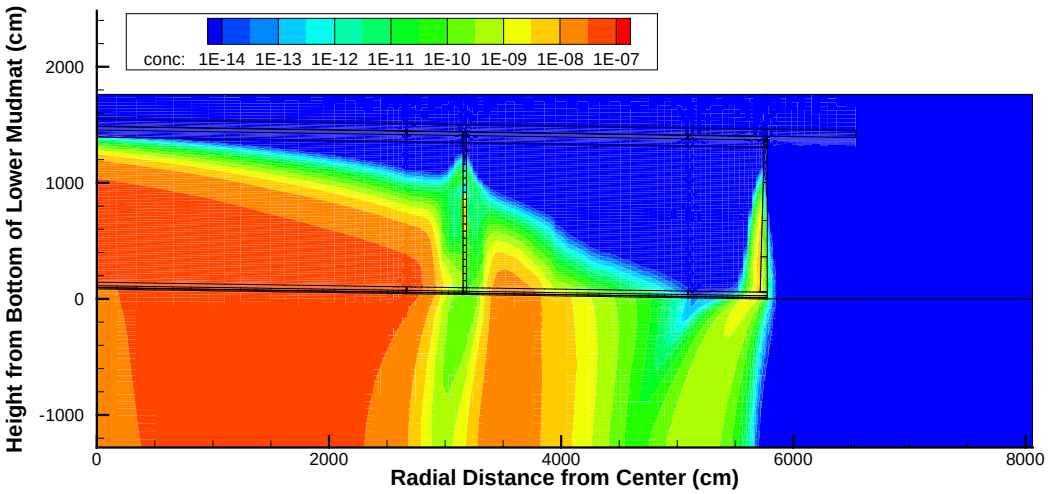

Figure DSP-3.8: I-129 Concentrations in a 375-Foot Diameter SDU at 7,000 Years

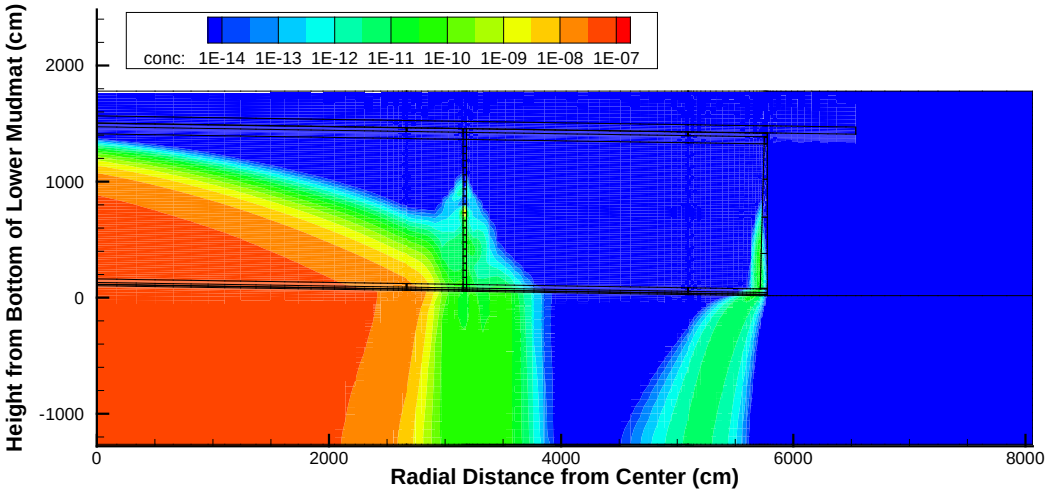

Figure DSP-3.9: I-129 Concentrations in a 375-Foot Diameter SDU at 8,000 Years

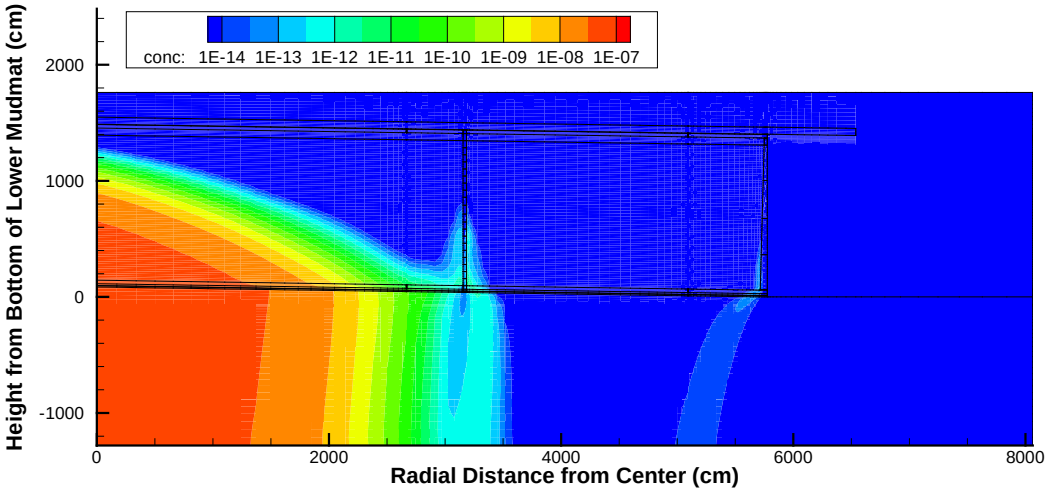

Figure DSP-3.10: I-129 Concentrations in a 375-Foot Diameter SDU at 9,000 Years

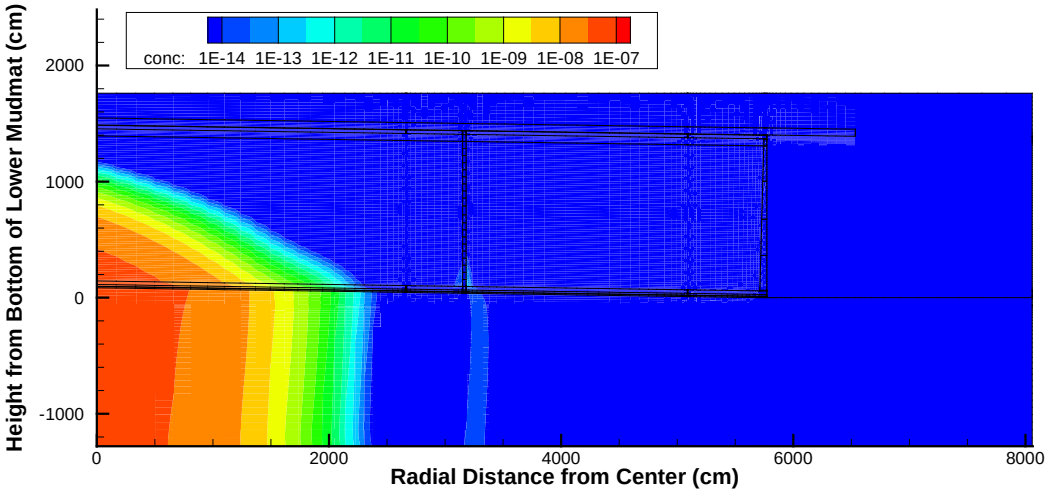

Figure DSP-3.11: I-129 Concentrations in a 375-Foot Diameter SDU at 10,000 Years

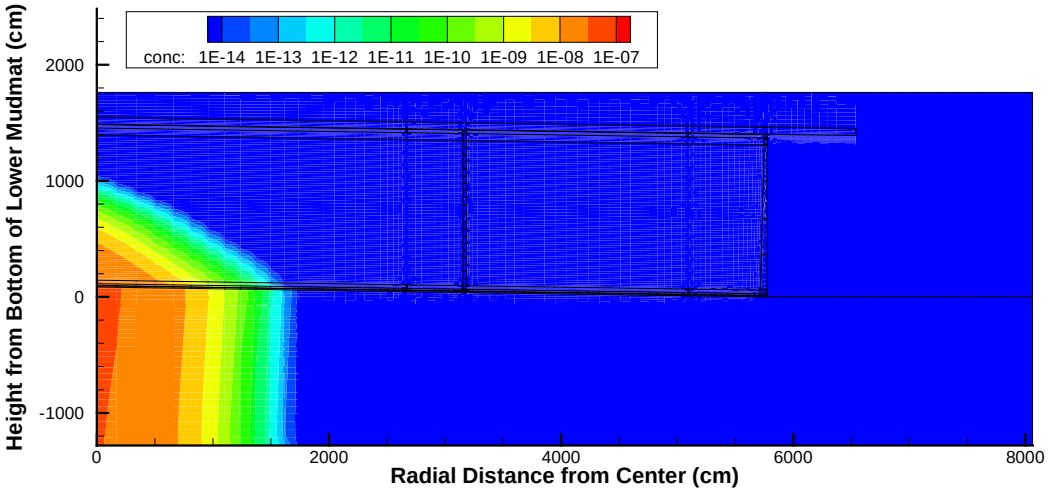

Figure DSP-3.12: I-129 Concentrations in a 150-Foot Diameter SDU at 0 Years

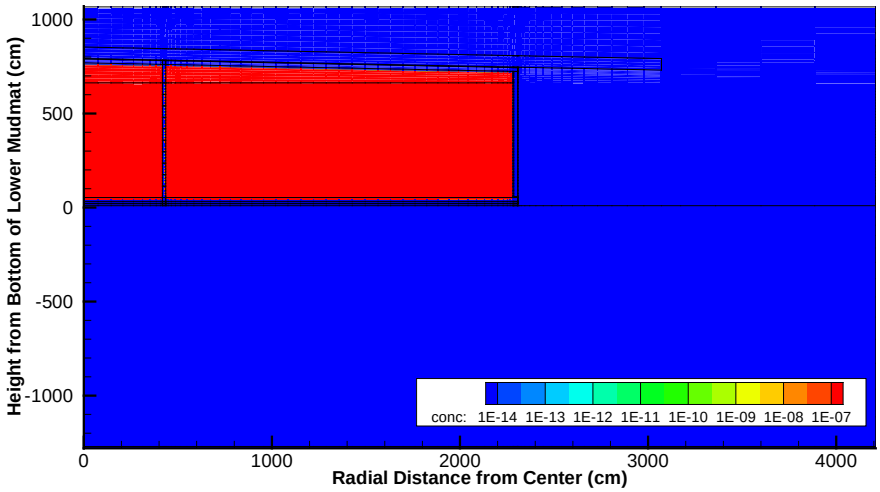

Figure DSP-3.13: I-129 Concentrations in a 150-Foot Diameter SDU at 1,000 Years

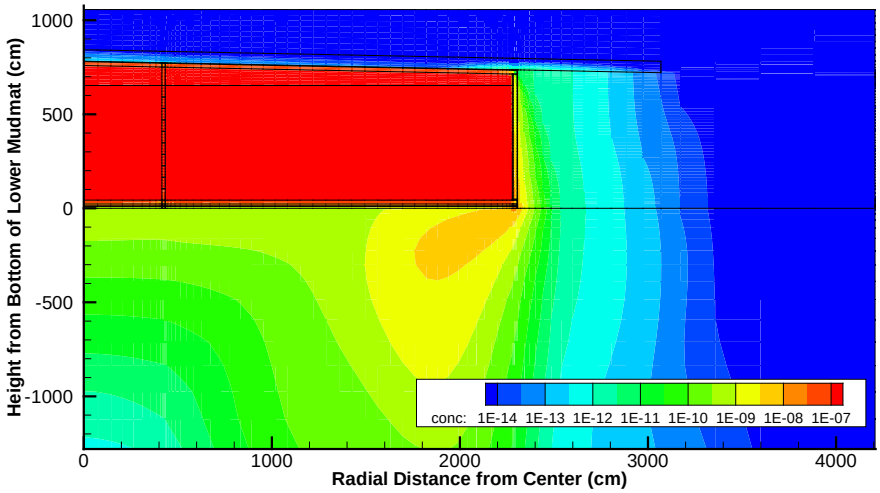

Figure DSP-3.14: I-129 Concentrations in a 150-Foot Diameter SDU at 2,000 Years

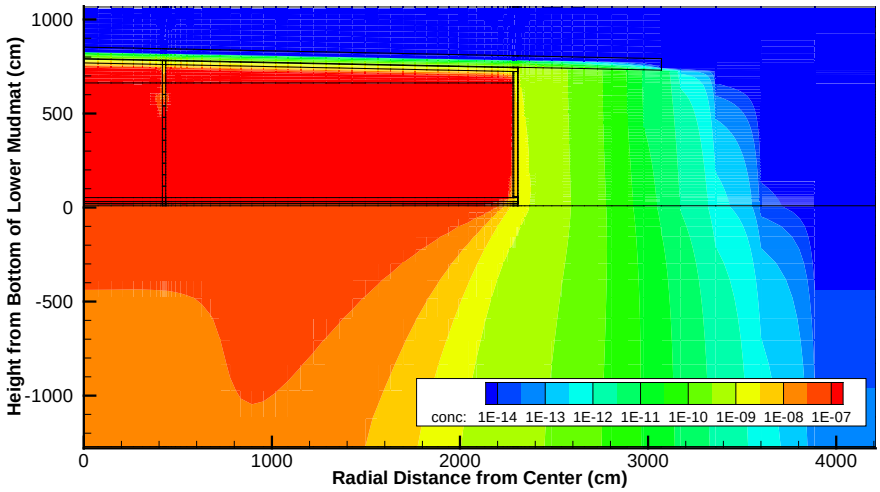

Figure DSP-3.15: I-129 Concentrations in a 150-Foot Diameter SDU at 3,000 Years

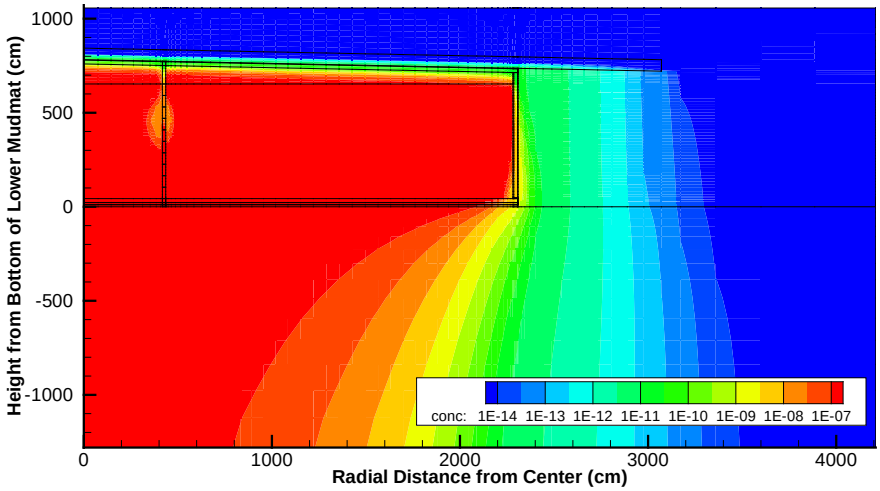

Figure DSP-3.16: I-129 Concentrations in a 150-Foot Diameter SDU at 4,000 Years

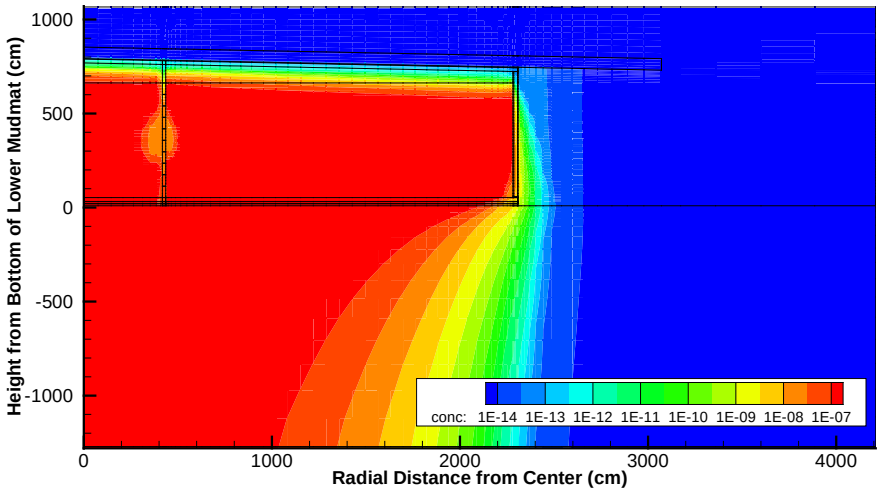

Figure DSP-3.17: I-129 Concentrations in a 150-Foot Diameter SDU at 5,000 Years

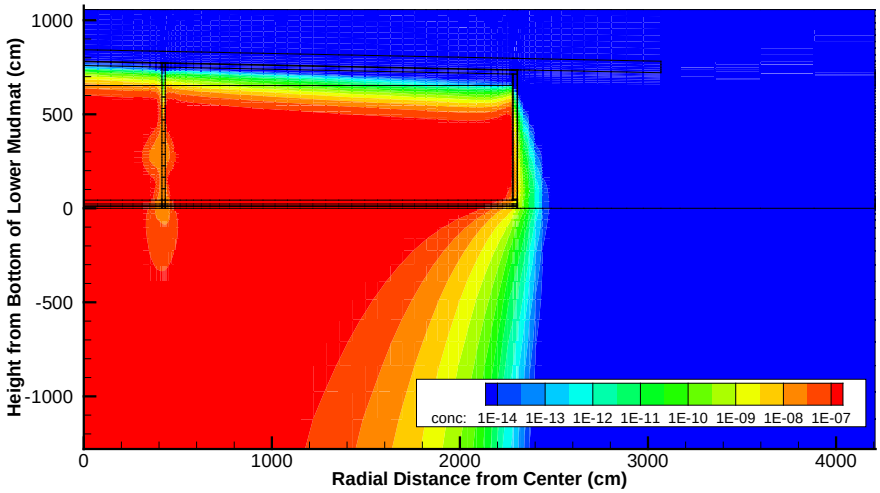

Figure DSP-3.18: I-129 Concentrations in a 150-Foot Diameter SDU at 6,000 Years

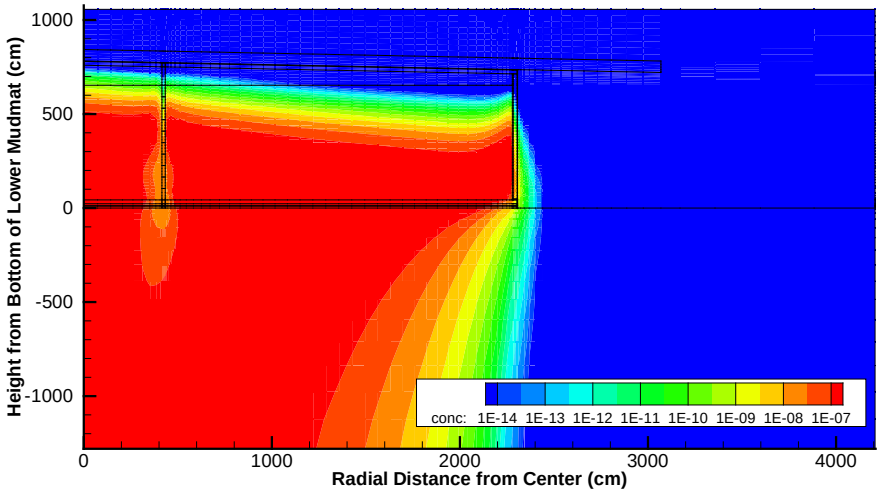

Figure DSP-3.19: I-129 Concentrations in a 150-Foot Diameter SDU at 7,000 Years

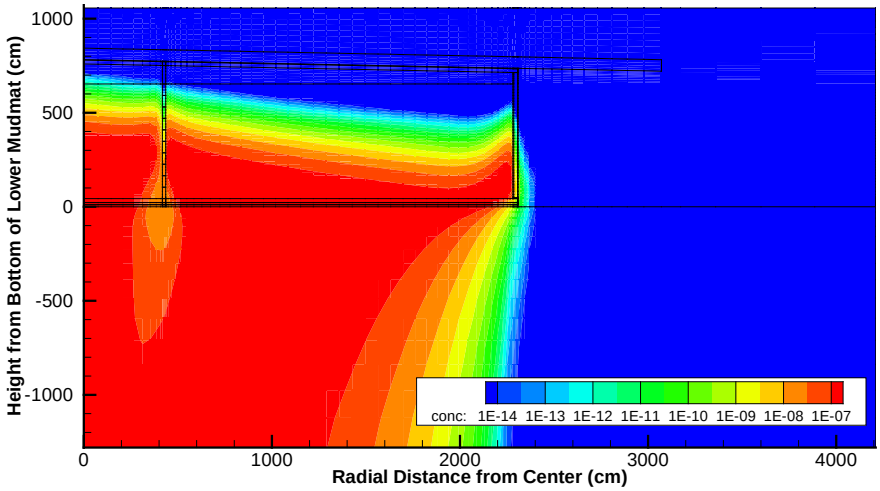

Figure DSP-3.20: I-129 Concentrations in a 150-Foot Diameter SDU at 8,000 Years

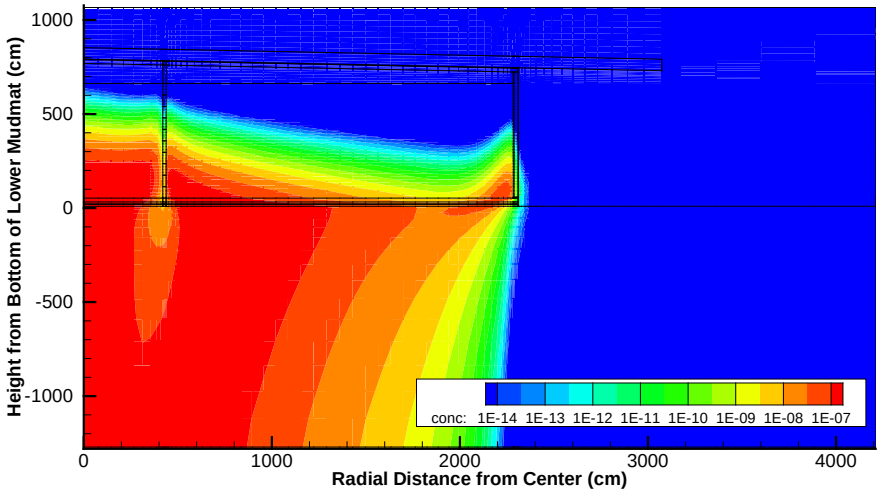

Figure DSP-3.21: I-129 Concentrations in a 150-Foot Diameter SDU at 9,000 Years

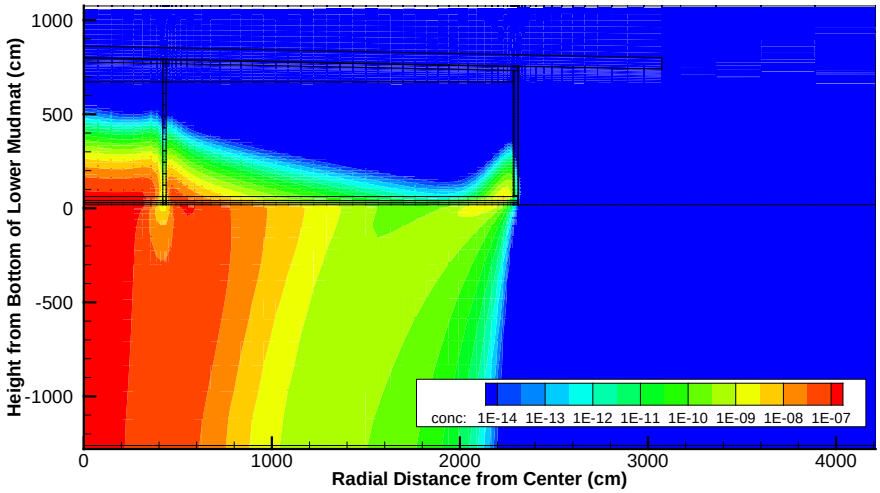

Figure DSP-3.22: I-129 Concentrations in a 150-Foot Diameter SDU at 10,000 Years

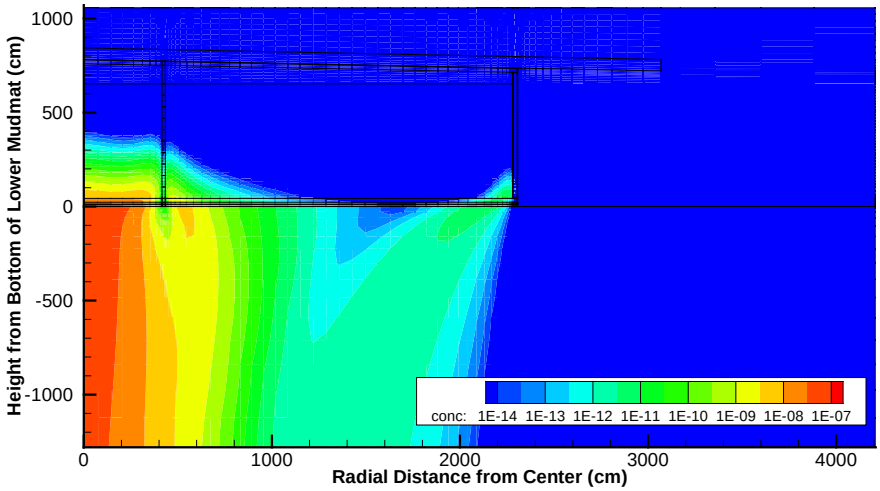

DSP-4

DSP-4	**Question:** Information is needed on the dose results of the PORFLOW sensitivity analysis for the roof slope of the 375-foot disposal structures.
	Basis: Section 5.6.7.1 of the DOE FY14 SDF Special Analysis document provided an analysis of the sensitivity of the projected volumetric flow through a 375-foot disposal structure to the slope of the roof. The analysis showed that changing the slope from 1.5% to 1.0% increased the projected flow through the disposal structure by 70% at approximately 4,000 years after site closure[1]. However, neither the release of I-129 nor the effect on dose is projected. The section also indicated that the dose from I-129, with a peak dose at approximately 5,300 years, was expected to arrive slightly earlier; but, not expected to increase significantly in magnitude. That result is unexpected to the NRC staff because increased flow is expected to increase the annual fractional release rate (i.e., sharpen the dose peak).
	Path Forward: Provide results for the sensitivity analysis of the slope of the roofs of the 375-foot disposal structures in terms of projected dose.

DOE Response to DSP-4

Radionuclide transport and the resulting doses were not explicitly modeled using the alternative roof slopes described in Section 5.6.7.1 of the FY2014 SDF SA. This stand-alone modeling only included a flow simulation. Release and dose was not simulated because the design margin analysis (Section 5.6.7.2 of the FY2014 SDF SA) included the 1.0% roof slope and provided the resulting doses. Despite a number of additional design conservatisms, the analysis still demonstrated that performance objectives were met. Although the reduced slope in the design analysis was not the only change applied in the design margin case (summarized in Table DSP-4.1), it effectively demonstrates the phenomenon described, in which an increase in flow at earlier times diminishes the available I-129 inventory such that the magnitude of the peak is not significantly increased.

[1] In the context of these RAIs and RAI responses, "site closure" refers to facility closure of the Saltstone Disposal Facility and not the closure of the Savannah River Site.

Table DSP-4.1: Summary of 375-Foot Diameter SDU Features Considered for the Design Margin Analysis

Parameter	Design	Design with Margin
Roof thickness (inches)	12	9
Roof and floor slope (%)	1.5	1.0
Floor thickness (inches)	12	9
Upper Mud Mat thickness (inches)	6	5
Lower Mud Mat thickness (inches)	4	3
Wall thickness (inches, tapered from bottom to top)	24 - 10	20 - 7
HDPE thickness (mil)	100	60

[Source: SRR-CWDA-2014-00006, Table 5.6.7-2]

Figures DSP-4.1 through DSP-4.7 show flows for a cross section of a 375-foot diameter SDU at various times within the simulation; arrows indicate the direction of flow and color contours indicate magnitude (in cm/yr) of downward flow. In each figure, the first panel (a) depicts flows from the Evaluation Case, where the roof slope is modeled at 1.5% and the second panel (b) depicts flows from the Sensitivity Case with the 1.0% roof slope.

Figures DSP-4.1 and DSP-4.2 show that within the first 2,000 years, the roof slope does not appreciably influence the flow system. At these relatively early times, the barriers are still mostly intact such that most flow is still diverted away from the SDU rather than moving through the SDU.

Figure DSP-4.1: Vertical Flow Through a 375-Foot Diameter SDU (1,265 to 1,400 Years)

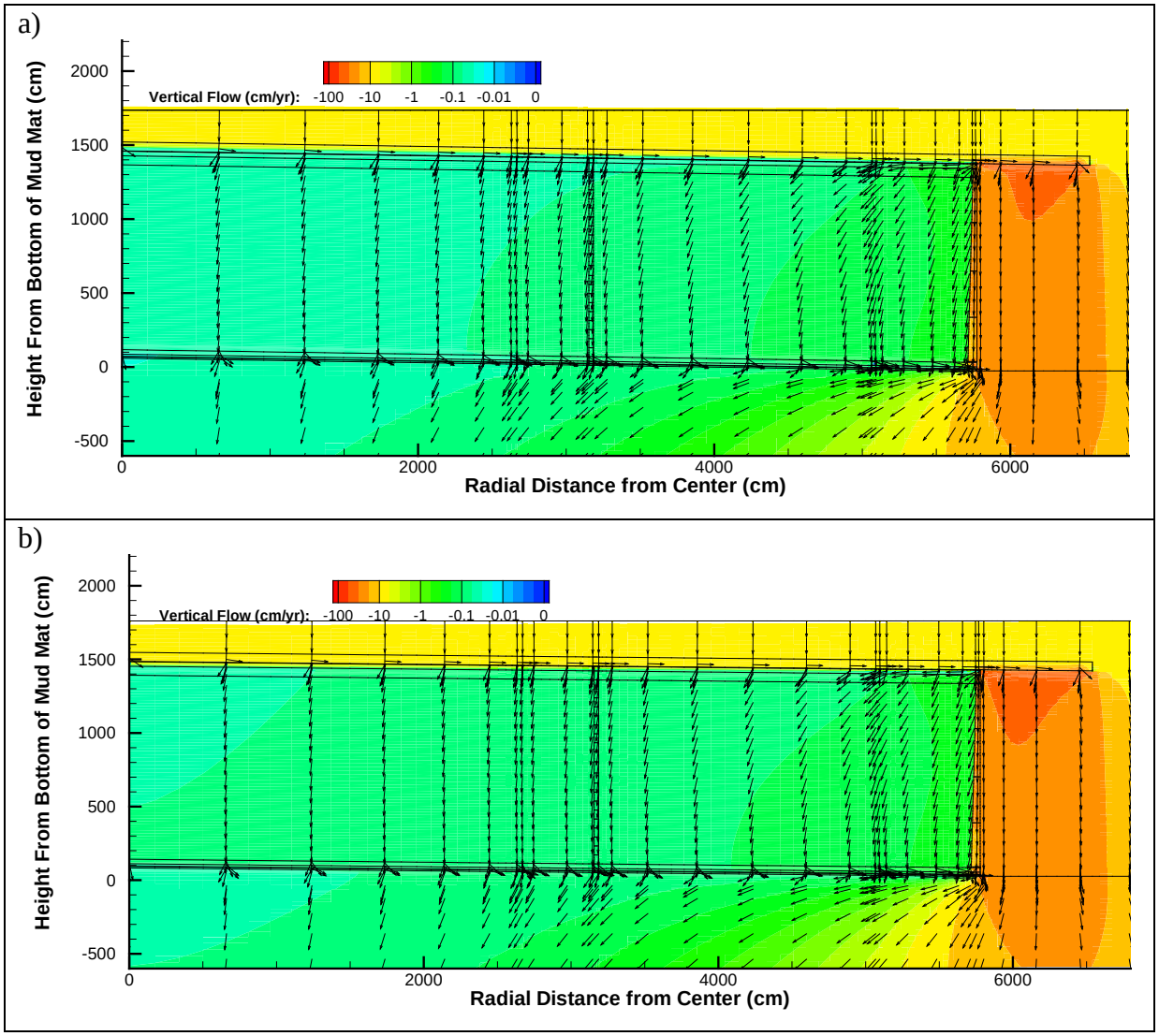

Notes: (a) Evaluation Case; Roof slope = 1.5%
(b) Sensitivity Case; Roof slope = 1.0%

Figure DSP-4.2: Vertical Flow Through a 375-Foot Diameter SDU (1,827 to 1,997 Years)

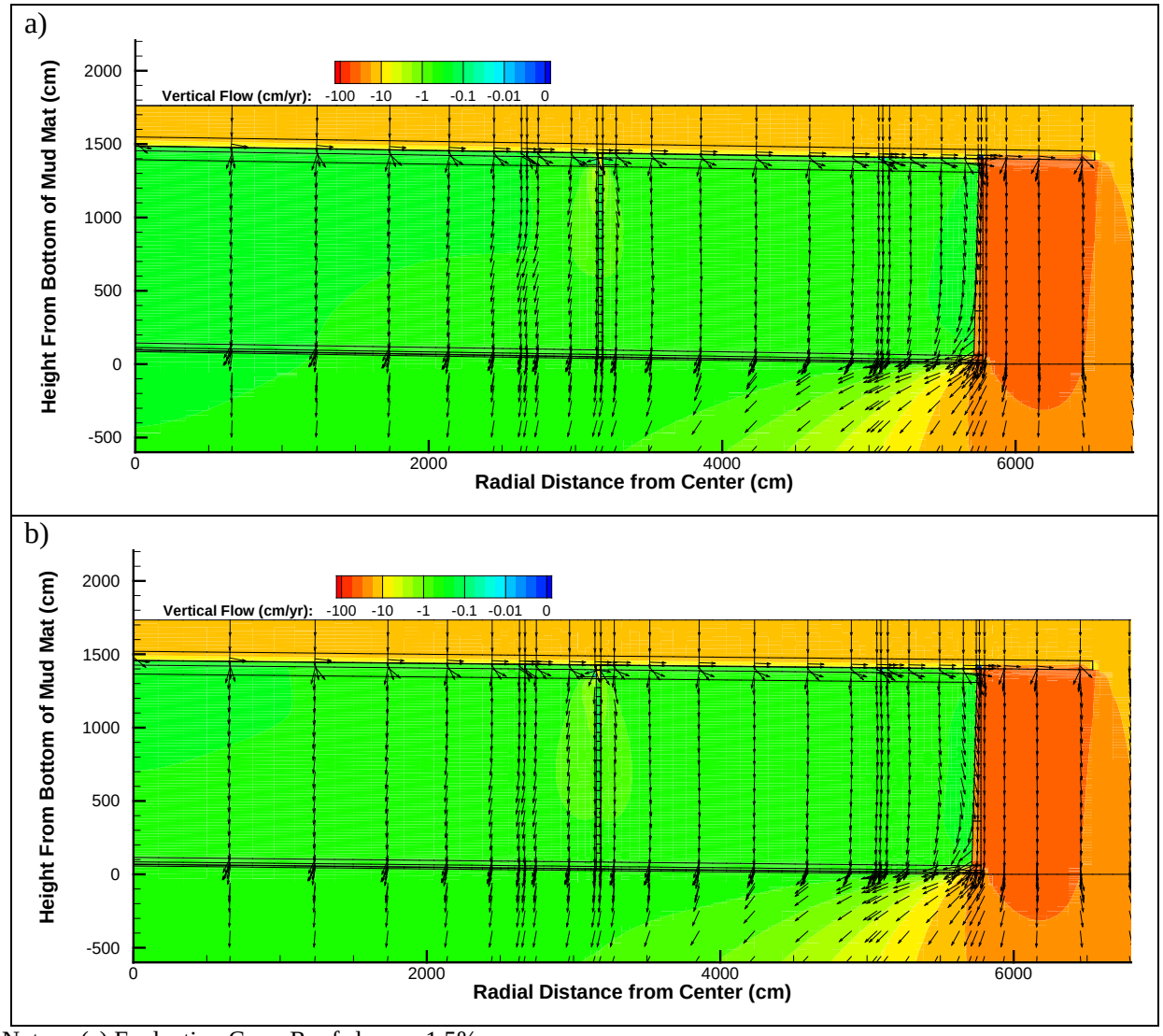

Notes: (a) Evaluation Case; Roof slope = 1.5%
(b) Sensitivity Case; Roof slope = 1.0%

Figures DSP-4.3 and DSP-4.4 show that between 2,000 years and 4,000 years, there is a more noticeable difference in the magnitudes of the flow; however, as a whole, these magnitudes are still relatively low (i.e., less than 10 cm/yr). By releasing more I-129 in this time frame, while the hydraulic conductivity of saltstone is still effective at slowing the rate of flow, a significant amount of the available I-129 inventory is released from the SDU without exceeding peak values.

Figure DSP-4.3: Vertical Flow Through a 375-Foot Diameter SDU (2,873 to 3,165 Years)

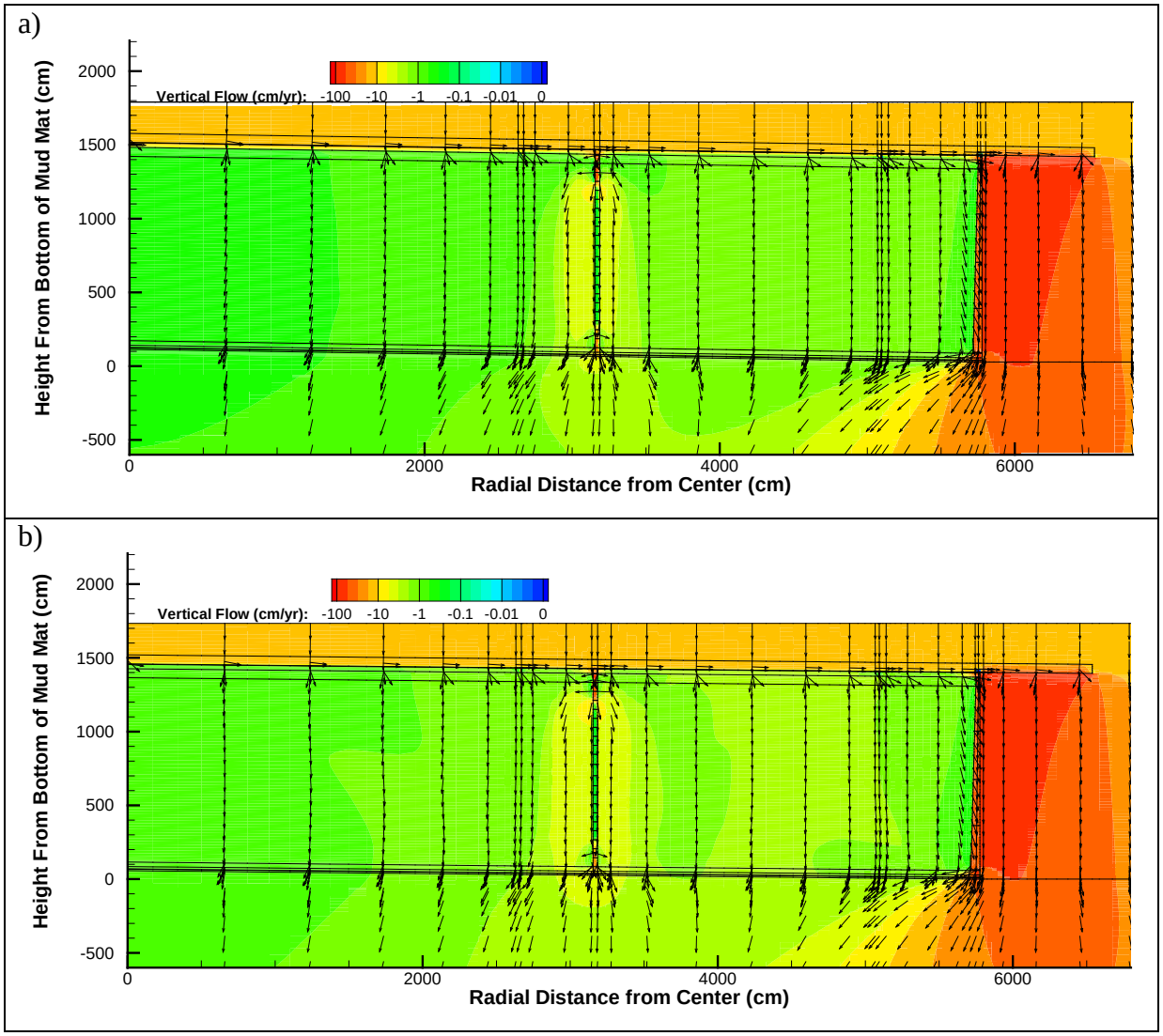

Notes: (a) Evaluation Case; Roof slope = 1.5%
(b) Sensitivity Case; Roof slope = 1.0%

Figure DSP-4.4: Vertical Flow Through a 375-Foot Diameter SDU (3,749 to 3,990 Years)

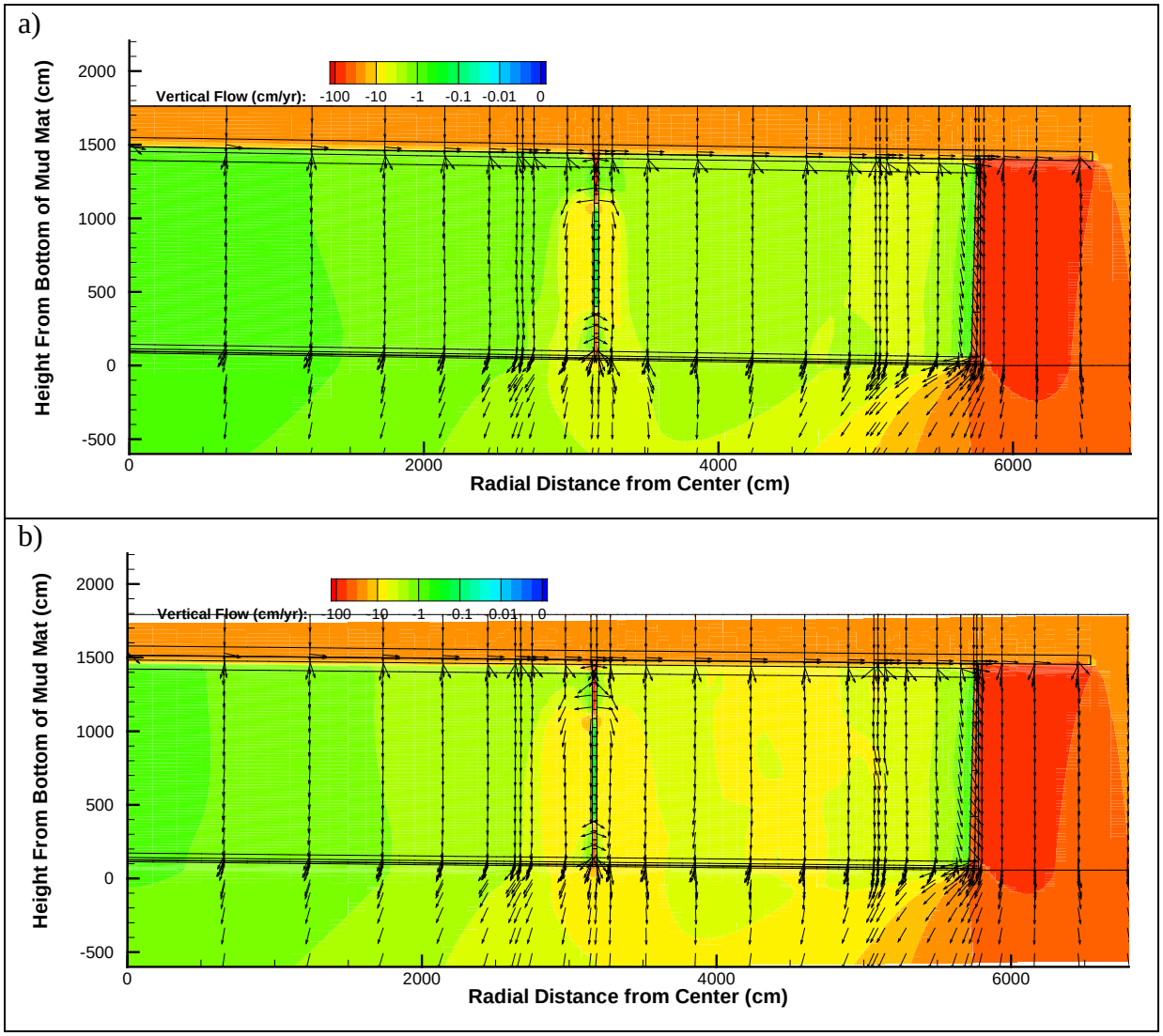

Notes: (a) Evaluation Case; Roof slope = 1.5%
(b) Sensitivity Case; Roof slope = 1.0%

Figures DSP-4.5 and DSP-4.6 show that between 4,000 years and 6,000 years, the flow rates begin to reach higher magnitudes (i.e., greater than 10 cm/yr). Although the 1.0% roof slope case shows significantly higher flows, there is less I-129 inventory available for release, due to the "bleed off" which occurred in the earlier time frames.

Figure DSP-4.5: Vertical Flow Through a 375-Foot Diameter SDU (4,333 to 4,625 Years)

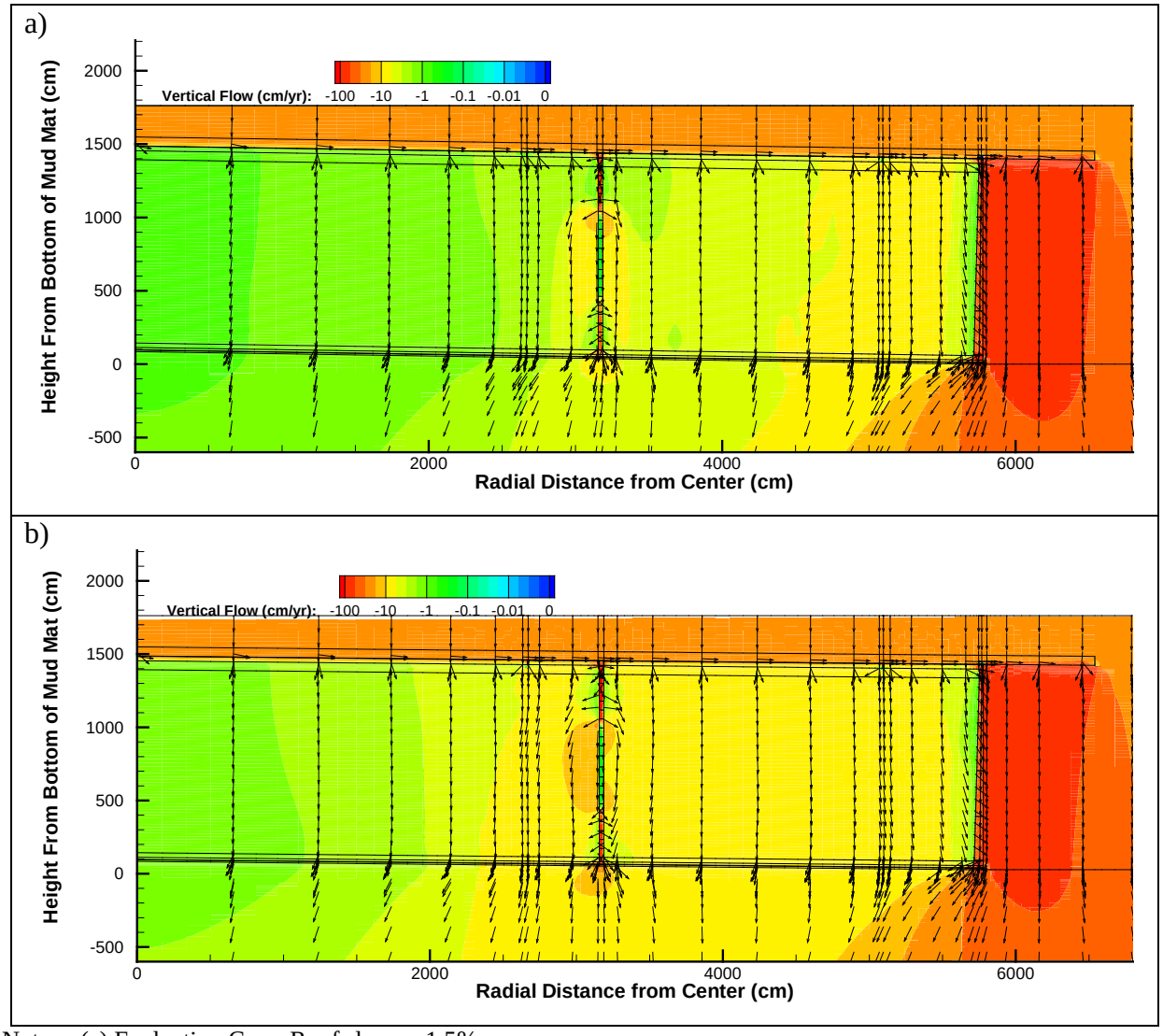

Notes: (a) Evaluation Case; Roof slope = 1.5%
(b) Sensitivity Case; Roof slope = 1.0%

Figure DSP-4.6: Vertical Flow Through a 375-Foot Diameter SDU (5,501 to 5,647 Years)

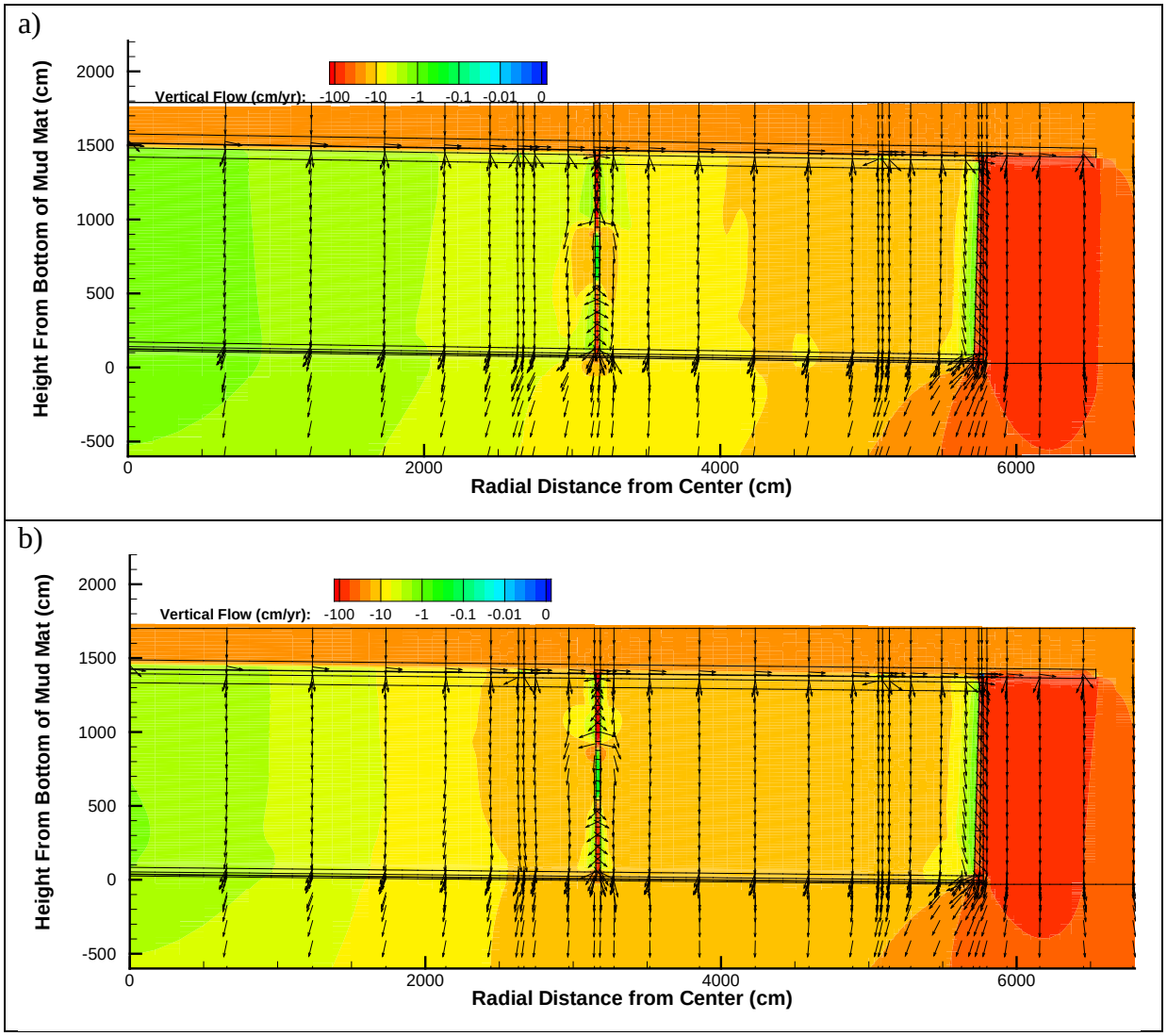

Notes: (a) Evaluation Case; Roof slope = 1.5%
(b) Sensitivity Case; Roof slope = 1.0%

To demonstrate this effect in more exaggerated terms, the GoldSim model was modified to use Flow Case F-13, which is identical to the Evaluation Case except the maximum infiltration rate is assumed (see Table 4.4-3 of the FY2014 SDF SA). Figure DSP-4.7 shows the resulting volumetric flow through saltstone for a 375-foot diameter SDU and compares it to the flows from the Evaluation Case (1.5% slope) and from the alternative 1.0% roof slope analysis. As shown, Flow Case F-13 provides a higher flow rate through saltstone over the time period considered within this figure.

Figure DSP 4-7: Volumetric Flow through 375-Foot Diameter SDU Saltstone for Select Cases

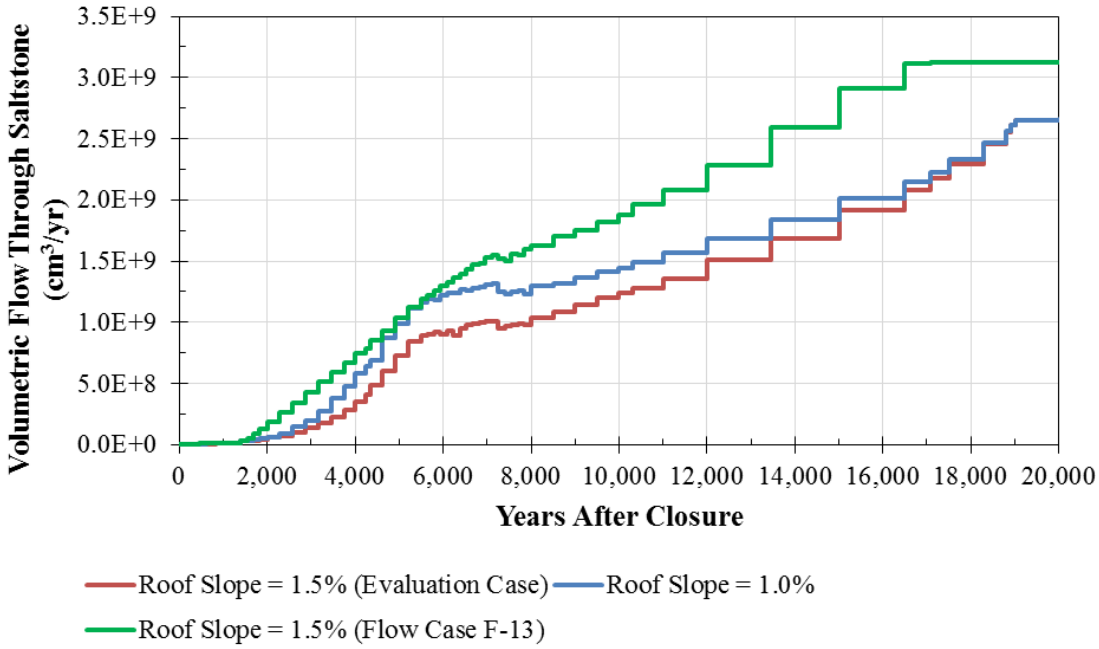

Using the GoldSim model, the I-129 doses from SDU 9 were determined for both the Evaluation Case and Flow Case F-13. Figure DSP.4-8 provides a clear picture of the effect being considered. The area under the curve for both of these doses is effectively the same; however, Flow Case-13 exhausts the available inventory of I-129 much earlier, while the saltstone material is less degraded. Accordingly, despite the increased flow, the magnitudes of the dose peaks are not significantly different.

Figure DSP 4-8: I-129 Dose from a 375-foot Diameter SDU, Using Average Infiltration (Evaluation Case) versus Maximum Infiltration (Flow Case F-13)

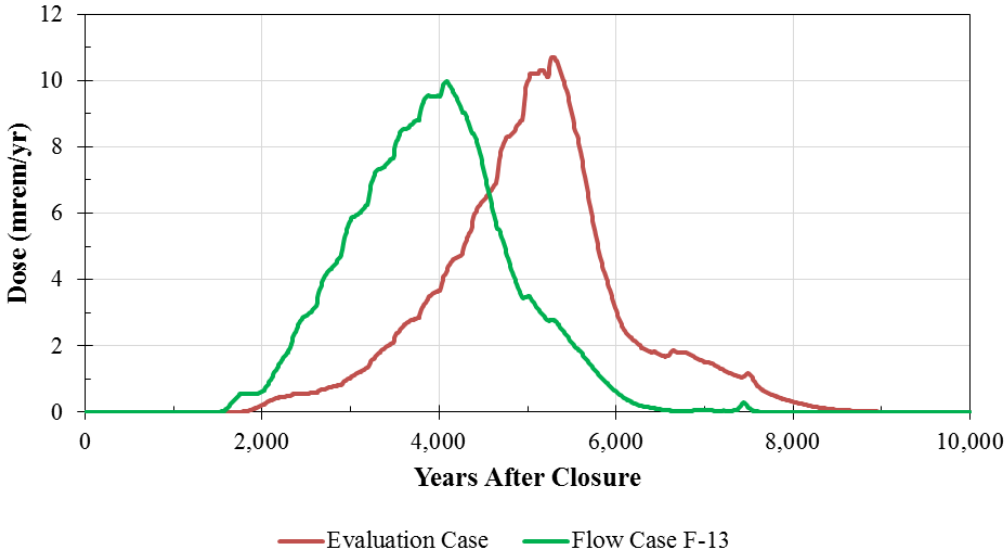

As indicated in the response to RAI SP-11, the release of I-129 relies heavily on the volumetric flow rates through saltstone (see Figures SP-11.2 through SP-11.4). By plotting both the volumetric flow rates through saltstone (left axis) and the I-129 doses (right axis) for the cases described above, this relationship is clearly depicted (Figure DSP.4-9).

Figure DSP 4-9: Volumetric Flow through 375-Foot Diameter SDU Saltstone with I-129 Doses (Select Cases)

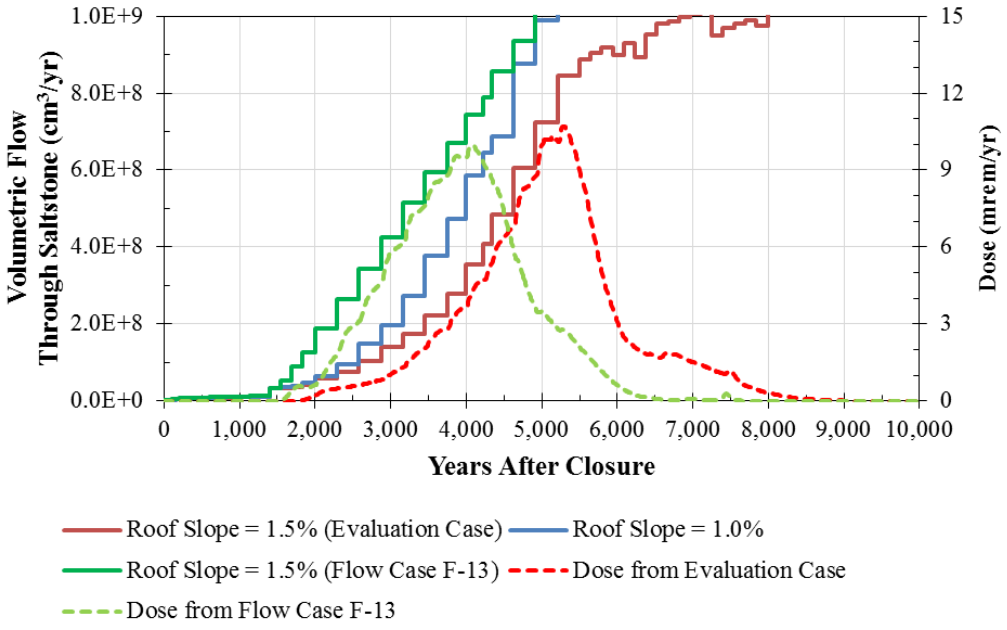

For the first 2,200 years, the flow rates from the 1.0% roof slope are similar to those from the Evaluation Case, so a similar dose would be expected during this early period. Between 2,200 years and 4,000 years, the flow rate from the 1.0% roof slope is approximately the same as Flow Case F-13, only delayed by 600 to 800 years. Therefore, the I-129 dose would be expected to follow a similar shaped curve during this intermediate period. Based on these volumetric flow rates, the peak dose from a 1.0% roof slope would very likely occur between 4,000 and 4,500 years and would be of similar magnitude to the Evaluation Case and the maximum infiltration flow case.

DSP-5

DSP-5	**Question:** Justifications are needed for the assumptions related to the lower lateral sand drainage layer as used in both the DOE FY13 and FY14 SDF Special Analysis documents.
	Basis: In the RAI Comments on the FY13 Special Analysis document, the NRC staff was concerned about several specific aspects of the closure cap design. The DOE 2015 Response to the NRC 2014 RAI Comments included the following: "There are key questions related to closure cap design and performance that could affect the results of the modeling (e.g., plugging of the drainage layer). However, the … parameters [that are] most sensitive to SDF performance are related to the saltstone waste form and the disposal [structures] themselves… As such, in the near term, resources are prioritized to support testing and modeling research activities related to key parameters of the saltstone waste form and the disposal [structures] ..." The NRC staff understands that the closure cap design has not been finalized by the DOE. However, the NRC staff is concerned about the practicality of the DOE achieving the final reduced saltstone infiltration rates. Despite the SDF closure cap design and installation being at least 20 years in the future, the NRC staff needs to have confidence that infiltration rates in the future will not exceed a rate that would endanger public health and safety. The importance of infiltration rates to peak dose are seen in Figure 5.6.5-20 in the DOE FY14 SDF Special Analysis document, which presented a comparison of minimum, average, and maximum infiltration rates. The lower lateral drainage layer, also known as the sand drain, diverts a significant percentage of the infiltrating water from the surface away from the disposal structures within 10,000 years. Although less water is drained in the DOE FY14 SDF Special Analysis document compared to that in the DOE 2009 SDF PA, the lower lateral drainage layer, together with the HDPE-GCL and the concrete roof, are a significant component of the system and requires strong bases. Regarding that NRC staff concern, the DOE assumptions in the DOE FY14 SDF Special Analysis document that need stronger supporting technical bases or information include the following: (a) *Assumption: The backfill overlying the sand drain below will remain relatively separate for thousands of years.* That assumption relies on relatively clean sand layers lying directly beneath clayey layers in natural geologic units tens of millions of years old. However, the backfill is not a natural geologic unit. Soil and material have been placed there by heavy equipment and therefore lack the natural depositional structures that link individual particles in natural clay units. (b) *Assumption: Clay from the backfill will accumulate in the sand drain from the bottom up and form a depositional layer at the bottom of the drainage layer similar to the formation of the B soil horizon as documented in the soil literature.* Although most literature described accumulation of clay that has either been deposited out of percolating waters or precipitated by chemical processes involving dissolved products of weathering, most did not discuss deposition from the bottom up. (c) *Assumption: Hydraulic properties of the material being deposited in the lower lateral drainage layer are similar to that of backfill.*

	Although the NRC staff expects that material deposited in the drainage layer would be clay, the parameter values used by the DOE were that of a backfill, which is considerably sandier than clay.
	Path Forward: Provide the technical bases or additional information to address the DOE assumptions listed in RAI Question DSP-5 in (a), (b), and (c) above.

DOE Response to DSP-5

(a) *Assumption: The backfill overlying the sand drain below will remain relatively separate for thousands of years.*

Although the closure cap construction is not equivalent to natural deposition, the closure cap structure utilizes geotextile filter fabric layers to segregate the drainage layers and backfill during construction. Over time as the closure cap structure compacts, the geotextile filter fabric barrier layers will continue to provide a mechanism for separating the backfill from the drainage layers although the effectiveness of the separation mechanism will lessen. The degree of influence on radionuclide release rates associated with this modification to closure cap integrity is difficult to quantify. But in general, implicit to the conceptual model of the SDUs, any decrease of the effectiveness of the closure cap over time will be reflected in a decrease in the time-delay assumed prior to initiation of saltstone degradation. As noted in the responses to RAIs SP-5 and DSP-2, disregarding the initial delay of saltstone degradation, will shift the release patterns of the radionuclide over time, but is unlikely to change any conclusions associated with dose-based risk.

(b) *Assumption: Clay from the backfill will accumulate in the sand drain from the bottom up and form a depositional layer at the bottom of the drainage layer similar to the formation of the B soil horizon as documented in the soil literature.*

As noted in Assumption (b), the reference to a "bottom up" accumulation of clays in the B-Horizon can be found in soil literature. Although the Buol et.al. 1973 (Buol, S. W., Hole, F. D., and McCracken, R. J. 1973, *Soil Genesis and Classification*, Iowa University Press, Ames) referenced in WSRC-STI-2008-00244, may be hard to find, Buol et.al. 2011 (Buol, S. W., Southard, R.J., Graham, R. C., and McDaniel, P. A. 2011, John Wiley & Sons) is accessible.

The 2011 reference discusses the plugging of voids by clays in deeper soil horizons. As noted in the 2011 reference the process causes clay to accumulate above the zones of lower permeability (which is a good analogue to the closure cap structure) initiating the phenomenon of clay layer growth from the bottom up. It also makes sense physically, if the colloidal clays can migrate through the less permeable backfill at the expected infiltration rates, they should also be able to migrate through the more permeable (and higher porosity) drainage layer until being influenced by the change in the flow regime near and/or at the contact of the drainage layer and lower permeability material below. The concept of bottom-up colloidal deposition in soils is also discussed in Hans Jenny's *Factors of Soil Formation: A system of quantitative pedology*, Dover Press, 1994. Jenny also references others (V. T. Aaltonen, 1939 and S. Mattson and Lonnemark, 1939) on the subject.

If the plugging mechanism worked from top down, a skin would be expected to form on top of the sand layer further inhibiting the downward flow of water. In addition, the sand layer itself,

and its low resistance to flow, would tend to stay effective for longer. Since these are conservative conditions pertaining to processes such as saltstone degradation and leaching of radionuclides from saltstone, the model, as presently constructed, is considered as adequate with respect to how it handles the time dependent effectiveness of the sand layer.

(c) *Assumption: Hydraulic properties of the material being deposited in the lower lateral drainage layer are similar to that of backfill.*

Like NRC, DOE assumes that the material deposited in the drainage layer would be clay, but DOE also assumes that the addition of clay to the sand matrix would result in a clayey-sand type material, which would exhibit parameter values similar to that of a backfill. Note that clayey-sand is typically used as backfill at SRS (WSRC-STI-2008-00244).

DSP-6

DSP-6	**Question:** Support is needed for the assumption that modeling features that extend beyond the footprint of the disposal structure walls as flush with outer edges of the disposal structure walls will not have a significant impact on projected flow fields.
	Basis: Without any explanation or justification, Section 3.3.1.2 of the DOE FY14 SDF Special Analysis document includes the following: " … except for the sand drainage layer above the roof, those parts of features that extend beyond the footprint of the [disposal structure] walls are ignored (e.g., the roof and mud mats are modeled as being flush with outer edges of the [disposal structure] walls)." In the DOE 2015 Response to the NRC 2014 RAI Comments (see RAI Comment DSP-6 in that document), the DOE indicated that velocity flow fields exhibit water moving in and out of the disposal structure components (e.g., water moves out of the components near the top and near the bottom of the disposal structure and water moves into disposal structure components between the top and bottom). Modeling the portions of the features that extend beyond the footprint of the disposal structure could change the velocity flow fields which could have an effect on the overall speed and direction of radionuclide transport.
	Path Forward: For a variety of conditions that could represent future environments (e.g., changes to infiltration rates, degradation rates, or soil properties), provide a technical basis that demonstrates whether modeling the roof and mud mats as being flush with outer edges of the disposal structure walls significantly changes projected flow fields.

DOE Response to DSP-6

DOE has prepared a sensitivity run using PORFLOW (vadose zone flow and transport), in which the floors and mud mats extend two feet beyond the walls and the roof five feet past the walls. Note that per construction and design of SDU 6, the roofs of the 375-foot diameter SDUs only extend nine inches past the walls. [C-CC-Z-00042] By extending the roof further than designed, any influence of potential flow effects may be exaggerated to provide greater insights. The vertical cross sections depicted in Figure DSP-6.1 provide a side-by-side comparison of these features.

Figure DSP-6.1: Configuration of Select Modeled Features for the 375-Foot Diameter SDUs

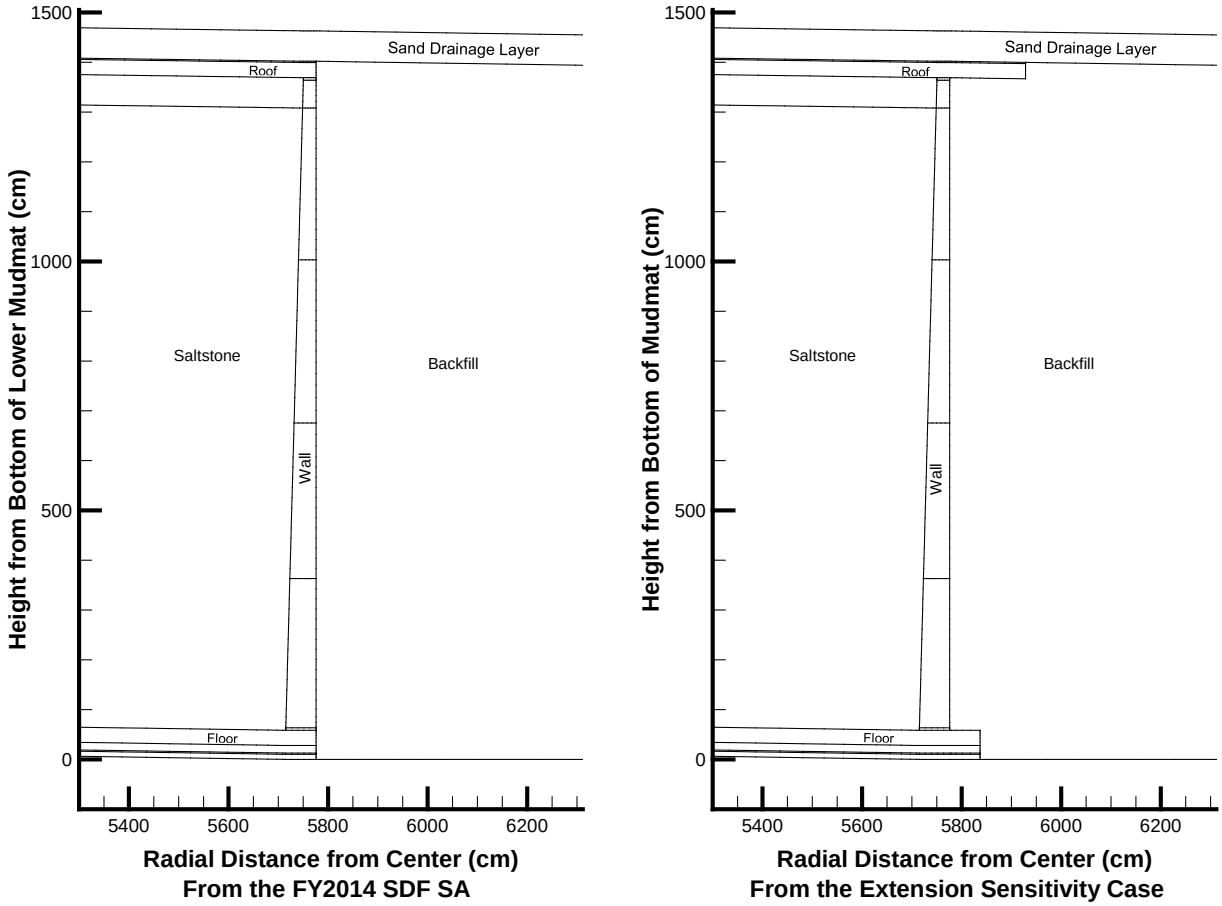

Note: The two-foot thick horizontal feature above the roof is the sand drainage layer. The two-foot thick horizontal feature below the roof is the upper two-feet of the saltstone monolith (in lieu of a two-foot clean cap).

Prior to the degradation of the HDPE above the roof (at 1,400 years), the Extension Sensitivity Case model shows slightly less total volumetric flow through saltstone (Figure DSP-6.2), relative to the Evaluation Case from the FY2014 SDF SA. During this time period, flow through saltstone is relatively low, such that the impact from this difference is negligible. After the HDPE fails, the differences are considerably less distinctive (Figure DSP-6.3).

Figure DSP-6.2: Comparison of Total Volumetric Flow Through Saltstone for the 375-Foot Diameter SDUs, Prior to Degradation of HDPE

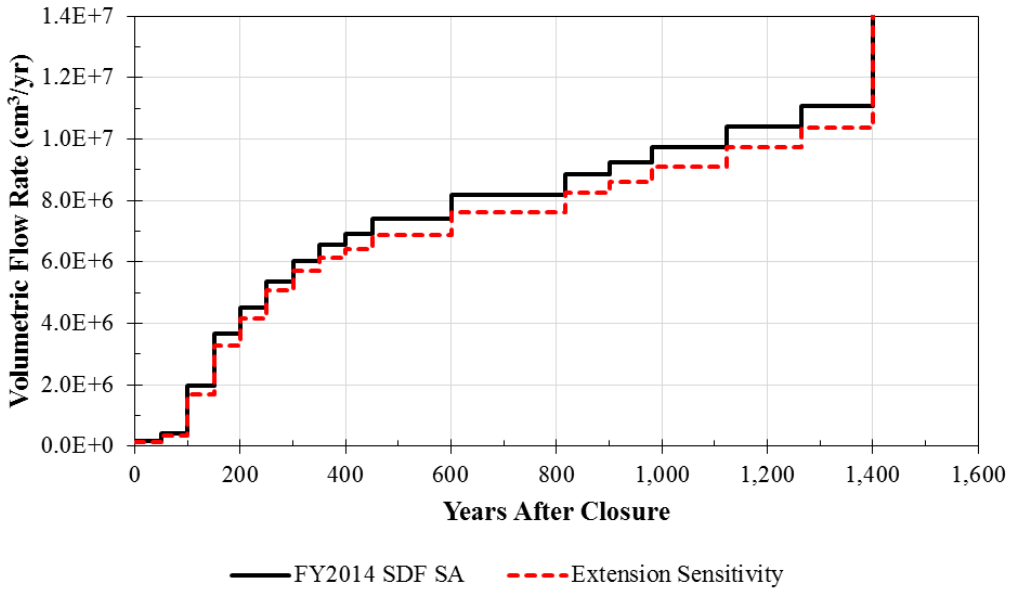

Figure DSP-6.3: Comparison of Total Volumetric Flow Through Saltstone for the 375-Foot Diameter SDUs, From 0 to 10,000 Years

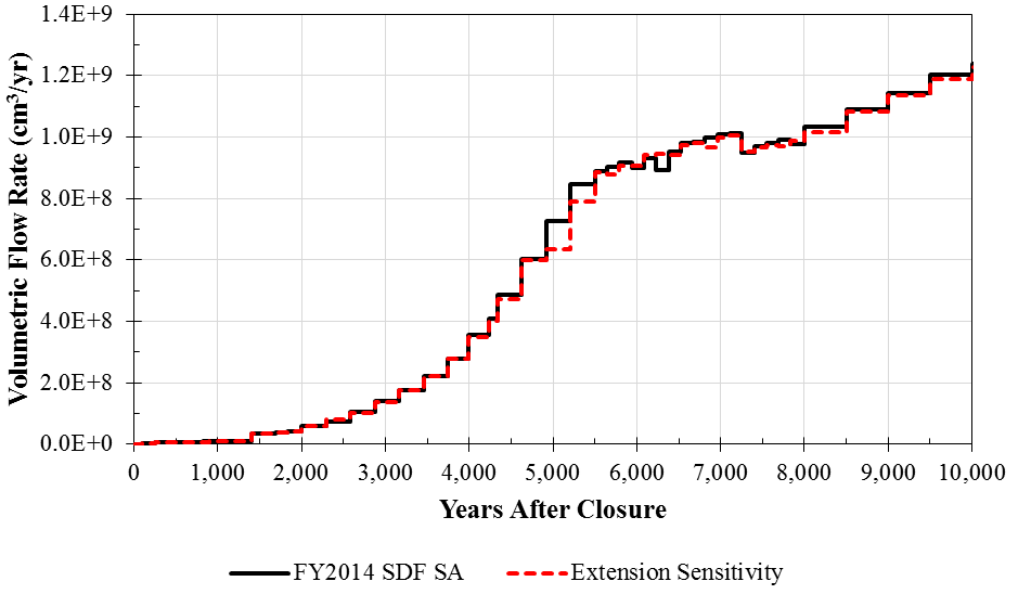

Due to these differences in flow being relatively minor, the resulting impacts to the doses are also minimal (Figure DSP-6.4). Note that the Extension Sensitivity Case only modeled five radionuclides (Cs-135, I-129, Ra-226, Th-230, and U-234). The dose comparison in Figure DSP-6.4 uses the doses contributions from only these radionuclides from the FY2014 SDF SA and the Extension Sensitivity Case.

Figure DSP-6.5 shows the respective dose contributions from Tc-99 only, which was simulated to 50,000 years to ensure that there were not any significant impacts relative to the Tc-99 releases.

As shown in Figures DSP-6.4 and DSP-6.5, the dose impacts due to extending the design features beyond the walls are not significant. Within 10,000 years and within 50,000 years, the timing of the resulting dose peaks does not change, and the magnitudes of these peaks are slightly lower. This indicates that the simplifying assumption in the Evaluation Case of the FY2014 SDF SA is slightly conservative and is reasonable.

Figure DSP-6.4: Comparison of Total Dose to the MOP from a 375-Foot Diameter SDU, From 0 to 10,000 Years (Sector K)

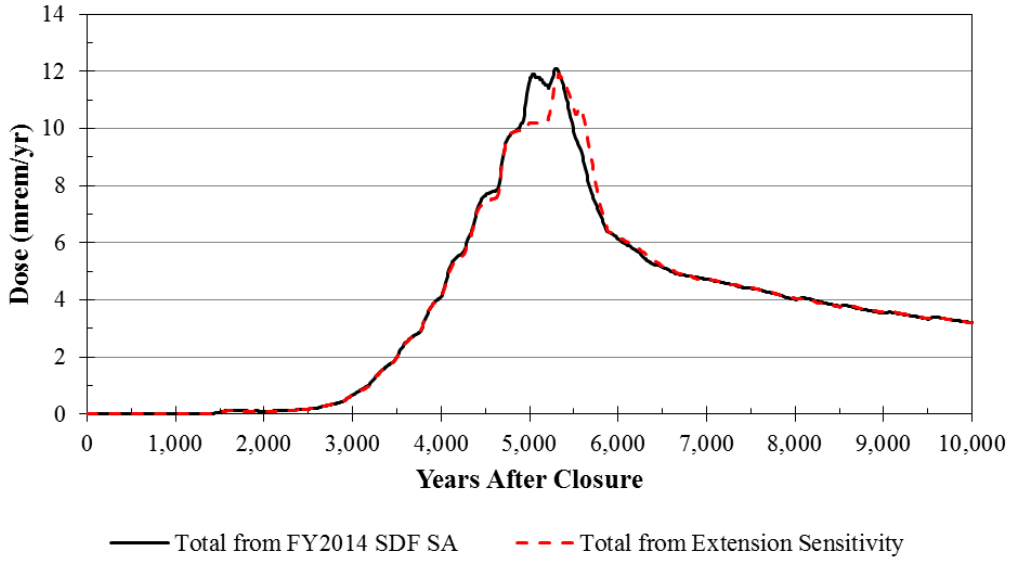

Note: These totals are slightly lower than the total reported in Section 5.5 of the FY2014 SDF SA because the totals shown here only sum Cs-135, I-129, Ra-226, Th-230, and U-234 contributions.

Figure DSP-6.5: Comparison of Tc-99 Dose to the MOP from a 375-Foot Diameter SDU, From 0 to 50,000 Years (Sector K)

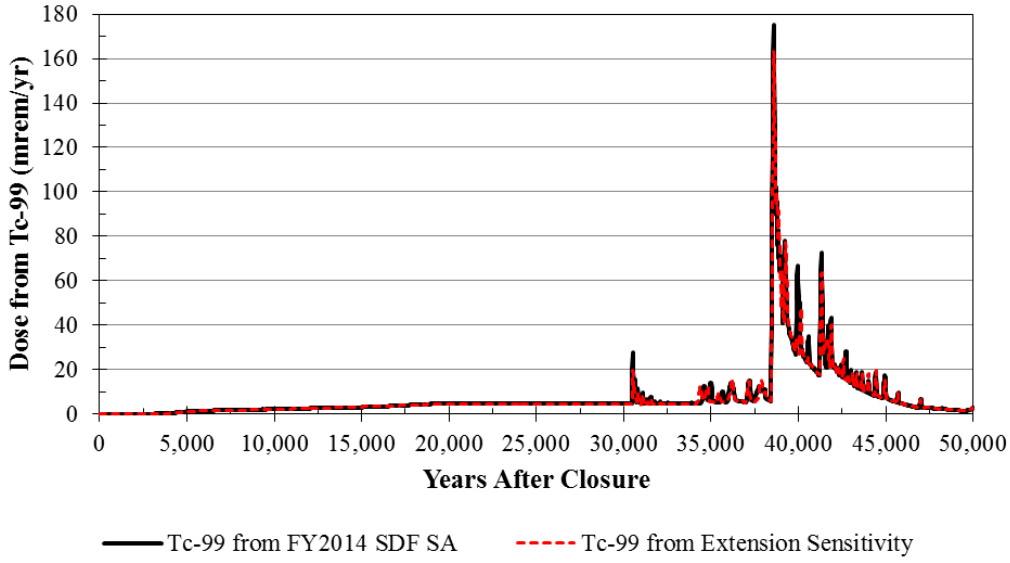

DSP-7

DSP-7	**Question:** Additional information is needed about how the GoldSim model captures horizontal advective radionuclide transport from the floor and the mud mats.
	Basis: Section 4.4.4.3 of the DOE FY14 SDF Special Analysis document includes the following: "Unlike the 150-foot diameter [disposal structures], the volumetric flows through the saltstone of the 375-foot diameter [disposal structures] are much more variable. This is because the walls of the larger [disposal structures] are not protected by a layer of HDPE liner and are, therefore, subject to more influence from horizontal flow." However, the DOE document, "Updates to the Saltstone Disposal Facility Stochastic Fate and Transport Model" SRR-CWDA-2013-00073, Rev. 2, includes the following: "Several simplifying assumptions are made in conjunction with the abstraction model used in the SDF GoldSim Model. With exception of the wall-to-floor joint cells in the FDCs, only vertical advection through the engineered barrier (and UZ) is considered in the model abstraction upon which the three [disposal structure] models are based." If horizontal advective transport of radionuclides into the backfill from the disposal structure floor and mud mats is not captured, then the dose and concentration results may be too low.
	Path Forward: Provide a description that demonstrates how the GoldSim model is capturing horizontal advective radionuclide transport from disposal structure components into the backfill.

DOE Response to DSP-7

The horizontal advective transport of radionuclides into the backfill from the disposal structure floor and mud mats is not explicitly modeled in GoldSim. As stated in the Executive Summary of the SDF GoldSim Model report (SRR-CWDA-2013-00073, Rev. 2), the "radionuclide transport modules of the two SDF GoldSim Models are simplified abstractions of the three-dimensional (3-D) SDF PORFLOW Model, allowing for a computationally efficient solution to the contaminant transport process, which is necessary for multi-realization runs." Section 5 of the SDF GoldSim Model report documents the benchmark testing performed to show that this abstraction of the SDF GoldSim Model is a valid surrogate for the 3-D SDF PORFLOW Model. During the testing, results from SDF GoldSim modeling and from SDF PORFLOW modeling were compared, and the results showed "that the abstraction can adequately approximate the trends and results produced by the SDF PORFLOW Model." [SRR-CWDA-2013-00073]

The benchmarking results presented in Section 5 of the SDF GoldSim Model report demonstrate that the GoldSim SDF Tc-99 Release Model and the GoldSim SDF All-Species Model provide an acceptable approximation of radionuclide releases from the SDUs to the saturated zone, and are capable of reproducing the trends found in the PORFLOW modeling results at the 100-meter and 1-meter points of assessment. Furthermore, these results demonstrate that for the most important dose contributors (i.e., I-129, Cs-135, Ra-226, and Tc-99), GoldSim predicts higher peak releases than PORFLOW (within 20,000 years for I-129, Cs-135, and Ra-226; within 50,000 years for Tc-99) for the 375-foot diameter SDUs. [Section 5.1.1.4 of SRR-CWDA-2013-00073]

Given the agreement in the benchmarking results between the GoldSim and PORFLOW SDF models it is concluded that while the horizontal advective transport of radionuclides into the backfill from the disposal structure floor and mud mats is not explicitly modeled in GoldSim, the overall effect on contaminant transport is sufficiently captured by the SDF GoldSim Models.

DSP-8

DSP-8	**Question:** Additional information is needed about how the parameters used to develop the flow cases were selected.
	Basis: In Section 3.1.4 of the DOE FY14 SDF Special Analysis document, the DOE identified that the sampling set of 36 flow cases was developed for the DOE FY13 SDF Special Analysis document to evaluate the effects on flow from varying the input values for selected parameters. Those input values that were varied were infiltration rates, cement degradation, initial hydraulic conductivity of grout, and moisture characteristic curves. The DOE FY13 Special Analysis document also evaluated roof slope. The DOE FY14 SDF Special Analysis document used infiltration rates, cementitious material degradation, and initial hydraulic conductivity of grout to obtain the flow cases, and described why the moisture characteristic curves were not varied in the DOE FY14 SDF Special Analysis document. However, neither the DOE FY13 nor the DOE FY14 SDF Special Analysis documents described how the five parameters that were varied were initially selected. For example, it is not clear to the NRC staff how the DOE determined that the volumetric flow rates were not sensitive to HDPE/GCL degradation, the shape of saltstone degradation (e.g., shrinking core, entire block, or from top down), or the hydraulic property of the adjacent backfill.
	Path Forward: Provide the criteria and basis for how the parameters that were varied to develop the sampling set of 36 flow cases were initially selected.

DOE Response to DSP-8

RAI DSP-8 questions "how the DOE determined that the volumetric flow rates were not sensitive to HDPE/GCL degradation, the shape of saltstone degradation (e.g., shrinking core, entire block, or from top down), or the hydraulic property of the adjacent backfill". It should be noted that DOE did not assume that the volumetric flow rates are insensitive to the above processes and/or parameters, but for practical reasons (i.e., for performance-based, risk-informed decision making) the DOE did not develop complex modeling to facilitate rigorous implementation of such processes (e.g., shrinking core, entire block, or from top down). Instead, the DOE chose to use simpler abstractions of the processes as long as the approach was conservative with respect to evaluating the risk associated with radionuclide release.

HDPE/GCL Degradation

The HDPE/GCL composite layers, used in SDUs at SDF, are assumed to degrade relatively quickly as holes form when implemented in the flow model. In the PORFLOW model, the roof HDPE/GCL is considered to behave like the overlying sand after a relatively short time, 1,400 years, and as clay accumulates in the sand layer the behavior of the HDPE/GCL continues to reflect the sand's transition to a clayey-sand, finally assuming backfill-like properties after greater than 19,000 years. Note that according to SRNL-STI-2009-00115, Appendix E, the HDPE/GCL layers should provide much more resistance to flow than sand and/or soil properties for well over 100,000 years. Similarly, the floor HDPE/GCL is considered to be fully degraded to backfill, at the end of 1,400 years.

Varying the HDPE/GCL degradation time would be expected to accelerate or delay arrival of the I-129 peak by less than 1,000 years, but have minimal effect on the magnitude of the peak I-129

dose. The peak dose of I-129 would still be expected to arrive at the 100-meter boundary within 10,000 years. The Tc-99 peak arrival would also be expected to shift in time, but would still occur well outside of 10,000 years, and perturbations to the Tc-99 contribution to total dose within 10,000 years would be relatively small.

An analysis presented in the response to RAI SP-5, which evaluates what would happen to doses if there was no delay prior to saltstone degradation, can provide insight as to what may happen if the HDPE/GCL fails earlier and carbonization of the roof occurs earlier.

Shape of the Saltstone Degradation Front

The choice of the saltstone degradation model used to determine maximum peak release rates for radionuclides was based on the decision that the additional complexity and associated computational effort inherent to the more rigorous shrinking core model was not warranted and a simpler abstraction could be used as long as the results were conservative with respect to risk.

A top-down decalcification process versus a shrinking-core process would produce similar releases except in the vicinity of the outer perimeter of an SDU. In the shrinking core conceptual model, diffusion and horizontal flow from the surrounding backfill can create a very thin zone of degraded saltstone adjacent to the wall from which radionuclides are released early. The degradation process within the bulk of the saltstone would be similar in both the top-down and shrinking-core developments of the degradation front. Further from the outer perimeter of the SDU, vertical movement of the decalcification front is the expected mode of the monolith's degradation. In both the top-down and shrinking core model degrading front concepts, the contrast in saturated hydraulic conductivity between the non-degraded saltstone ahead of the front (6.4E-09 cm/sec) and the degraded saltstone behind the front (4.1E-05 cm/sec) would tend to generate a horizontal component of flow behind the front. This horizontal component of flow would slowly expand (in the vertical direction), and would tend to bleed off mass in a more dispersed manner. This slow, vertical expansion would allow more mixing with infiltrating water flowing through the surrounding backfill as the mass approaches the saturated zone when compared to a conceptual model dominated by vertical flow.

The third conceptual saltstone degradation model noted is the one used in the FY2014 SDF SA which assumes that the entire saltstone monolith changes saturated hydraulic conductivity over time in a homogeneous fashion. This model is based on the concept that vertical flow dominates the release from the system. Although the top-down and shrinking core models are more consistent with the expected mode of a porous medium degrading by decalcification, a vertical-flow dominated system would tend to generate larger peak releases, especially considering the conservative (linear) manner in which the time-dependent saltstone saturated conductivity curve is derived (see the response to RAI SP-1). The vertical-flow dominated release of radionuclides would simulate earlier releases of radionuclides from the core of the saltstone monolith (as opposed to earlier low-level releases from the outside of the SDUs), with peak releases controlled by near-simultaneous release patterns across most of the floor. The vertical-flow dominated release of radionuclides represents a conservative assumption, consistent with the conceptual model of a flow system controlled by a ubiquitous set of vertically oriented shrinkage-joints.

The saltstone degradation mode used in which properties are smeared uniformly and varying linearly through time (see the response to RAI SP-1), practically bounds the range of potential behaviors on the conservative end of the distribution. Any sensitivity variations would improve dose performance.

Hydraulic Property of the Adjacent Backfill

Unless the infiltration rate surpasses the saturated hydraulic conductivity of the backfill, water approaching the SDU, or water bypassing the SDU along the structure's side, will flow straight downwards and the backfill will be unsaturated. The backfill itself is not a flow-limiting component of the system. Therefore, although changing the saturated hydraulic conductivity of the backfill would affect the saturation of the backfill, the change would have little effect on the water balance within the SDU.

DSP-9

DSP-9	**Question:** Additional justification is needed for the K_d values assumed for risk-significant and potentially risk-significant radionuclides in disposal structure concrete in the DOE Evaluation Case and the ranges of values used in sensitivity cases.
	Basis: The K_d values assumed for disposal structure concrete were identical to those assumed for saltstone. Therefore, the basis for this RAI Question is the same as the basis for RAI Question SP-11 above.
	Path Forward: Provide a justification for the K_d values assumed for I, Se, and Ra in disposal structure concrete and the ranges used in the sensitivity analyses included with the DOE FY14 SDF Special Analysis document. Alternately, perform sensitivity analyses that include the range of observed K_d values for those elements to determine the potential effect of those parameters on the projected dose or provide a revised analysis that uses more defensible values.

DOE Response to DSP-9

The response to SP-11 provides sensitivity analyses which evaluate wider ranges for the K_d values than those that were used in the FY2014 SDF SA.

These analyses demonstrated that I-129 dose contributions are sensitive to the iodine K_ds in saltstone (and concrete, to a much lesser degree), but the degree of this sensitivity is also dependent upon the volumetric flow through saltstone. Even under the very conservative modeling assumptions, the overall magnitude of the I-129 dose contribution is not expected to increase by more than 5 or 6 mrem/yr (see Figure SP-11.1). The SP-11 sensitivity analyses also demonstrated that Ra-226 is not a significant dose contributor within the first 10,000 years after SDF closure, regardless of the cementitious K_d values, and is relatively insignificant (when compared to Tc-99 dose contributions) beyond 10,000 years. Finally, the SP-11 sensitivity analyses also show that Se-79 is not expected to be a significant dose contributor, even under very conservative cementitious K_d assumptions. FFT-5 also addresses Se-79 K_d values and discusses additional SP-11 results for both cementitious and soil K_ds indicating Se-79 is not a significant dose contributor even under extreme conditions.

DSP-10

DSP-10	**Question:** Additional information is needed to demonstrate the effects of uncertainty in modeled chemical reducing capacity in disposal structure concrete.
	Basis: The NRC staff concerns about the quantification of reducing capacity in saltstone also apply to the quantification of reducing capacity in disposal structure concrete. Therefore, the basis for RAI Question SP-8 above also applies to this RAI question.
	Path Forward: Provide a sensitivity or uncertainty analysis demonstrating the effects of uncertainty in the reducing capacity of disposal structure concrete on projected dose from Tc-99. Because many of the factors that affect the available reducing capacity in disposal structure concrete are expected to apply to saltstone, the modeled reducing capacity in saltstone and disposal structure concrete should be correlated (see RAI Question SP-8 above). A justification of the sensitivity analysis values used or the probabilistic uncertainty range used should address the issues discussed in RAI Question SP-7 above as well as additional variability caused by inherent variability in slag reactivity and variable slag storage times and conditions.

DOE Response to DSP-10

The response to RAI SP-8 provides a sensitivity analysis which evaluates a broad range of concrete reducing capacity values, including the value used in the FY2014 SDF SA (i.e., 1.78E-01 meq e-/g).

This sensitivity analysis revealed that even under the unrealistically conservative conditions of Sensitivity Case 5E in which both saltstone and concrete have a reduction capacity equal to that of SRS Sandy Sediment (8.12E-02 meq e-/g), the maximum total dose at the 100-meter boundary is below 25 mrem/yr within 10,000 years after closure. Furthermore, it was demonstrated that even when a higher Tc solubility of 4.2E-08 mol/L (see SP-12 and Table SP-12.1 for details on selection of this value) was applied to Sensitivity Case 5E, the maximum total dose within 10,000 years after facility closure did not exceed 25 mrem/yr (Figure SP-8.3). Therefore, this sensitivity analysis provides reasonable expectation/assurance that the expected variability in saltstone and concrete reduction capacities will not hinder the SDF from meeting performance objectives. This conclusion is consistent with the results of the uncertainty analyses related to modeled reducing capacities and the release of Tc-99, as presented in the response RAI SP-2.

DSP-11

DSP-11	**Question:** Additional information is needed about the grid, saturation, and Darcy velocity fields for different time periods as well as for vertical and horizontal volumetric flow rates for the disposal structure components.
	Basis: The Closure System Modeling section in the "Analysis of Performance" in the DOE 2009 SDF PA had detailed cross-sectional figures from the PORFLOW model, including detailed close-ups of the grid, saturation, and Darcy velocity fields for 100, 1000, 5000, and 10,000 years. Such detailed cross-sectional figures were not included in same section in the DOE FY14 SDF Special Analysis document. The DOE 2015 Response to the NRC 2014 RAI Comments (see RAI Comment DSP-6 in that document) provided useful information, such as, cross-sectional views of flow rate transient and flow fields for different time periods and volumetric flow rates for the disposal structure components. The DOE 2015 Response to the NRC 2014 RAI Comments (see RAI Comment DSP-5 in that document) included the following: "A portion of the infiltrating water that initially bypasses saltstone via the sand drainage layer (and to a lesser extent the roof) is commonly observed to enter (or re-enter) the engineered structure through the side. As a result, the total flow through the engineered system tends to increase moving down the disposal [structure] starting a short distance below the roof." Based on the information in the DOE 2015 Response to the NRC 2014 RAI Comments (see RAI Comments DSP-5 and DSP-6 in that document), the NRC staff has the following additional specific questions and concerns: • Considering that that the HDPE in the wall still has a relatively low hydraulic conductivity value (6.44×10^{-7} cm/sec after 10,000 years) in comparison to the other components, how is the reentry flow into SDS 2 possible? • Most of the wall for SDS 6 has water flow into the disposal structure. However, most of the water appears to be exiting in a relatively small section at the bottom of the disposal structure. Considering that the HDPE extends up the side of the disposal structure, is embedded in the middle part of the floor, and still has a relatively low hydraulic conductivity value of 6.44×10^{-7} cm/sec after 10,000 years, why is there no bathtub effect above the floor HDPE/GCL of SDS 6? • Considering the horizontal component of water flow exiting in a relatively small vertical section at the bottom of SDS 6, has a floor slope evaluation of flow similar to the roof slope evaluation been performed for SDS 6 type disposal structures? • Why did the SDS 2 and SDS 6 roofs remain relatively unsaturated compared to the grout (See Figures DSP-6.6 and DSP-6.8 from the DOE 2015 Response to the NRC 2014 RAI Comments)? • In the DOE 2015 Response to the NRC 2014 RAI Comments (see RAI Comment DSP-1 in that document), the DOE response included: "DOE has modeled construction joints (with the hydraulic properties associated with gravel) that penetrate through the roof of the 375-foot diameter [disposal structures] (see Section 4.2.3 of the [DOE FY14 SDF Special Analysis document])." However, that information was not included in the DOE responses to RAI Comments DSP-5 and DSP-6 in that document. • To provide a more accurate understanding of the flow regime within a disposal structure

	at any particular time, both vertical and horizontal volumetric flow rates for each disposal structure component at different time steps is needed. The inflow and outflow of the backfill in relation to the disposal structure components needs to be included with vertical and horizontal volumetric flow rates. • Detailed cross-sectional views of the grid, saturation, and Darcy velocity fields for different time periods as well vertical and horizontal volumetric flow rates for the disposal structure components and the underlying vadose units are important and needed for understanding the how processes are being modeled and discovery risk significant features or processes.
	Path Forward: Provide information relevant to the NRC staff questions and concerns in this RAI Question.

DOE Response to DSP-11

The responses to each of the bulleted items within the basis of this RAI shall be addressed in the order in which they are listed, and identified as responses "a" through "g".

a) As the closure cap degrades and infiltration increases, more water is channeled radially outward (i.e., away from the SDU) via the sand drainage layer. Because the sand drainage layer extends past the roof of the 150-foot diameter SDUs, water shedding off of it is directed into the backfill that surrounds the SDU. This backfill has a horizontal hydraulic conductivity (7.60E-05 cm/sec) that is slightly higher than the vertical hydraulic conductivity (4.10E-05 cm/sec), such that the shedding water undergoes horizontal spreading within the backfill (both away from the sand drain and inward, back towards the SDU). Furthermore, the backfill hydraulic conductivity is orders of magnitude lower than the sand drain; therefore, some of the water that is shed off the sand drainage layer is actually flowing along the interface between the backfill and the sand drainage layer.

   Most of the water that backflows towards the SDU ends up flowing downward before penetrating into the HDPE layer. However, at 10,000 years the difference in the horizontal conductivity of the backfill (7.60E-05 cm/sec) is only about two orders of magnitude higher than the HDPE (6.44E-07 cm/sec), so some of the backflow does penetrate into the HDPE. This small amount of water that enters the outer edge of the HDPE is then channeled nearly directly inward because the vertical hydraulic conductivity of the HDPE (5.0E-15 cm/sec) is significantly lower than the horizontal hydraulic conductivity.

b) The 375-foot diameter SDUs are not modeled as having any HDPE barrier up the sides of the walls because the design and construction of the SDUs does not include any HDPE along the walls. Instead, the HDPE only extends half way up the side of the floor (i.e., it does not even reach the wall-to-floor joint). [C-CY-Z-00007] Therefore, any "bathtub" effect would be limited to the floor below the saltstone. Because saltstone has a lower hydraulic conductivity than the floor, the overflow would only exit the floor via the sides until the HDPE is degraded (at 1,400 years), at which point downward flow would become dominant. As a modeling simplification, the HDPE is only modeled as a horizontal layer between the lower mudmat and the upper mudmat.

As such, flow through the floor, through the waterstops in the floor, and through the wall-to-floor joint is not directly impeded by any HDPE barriers. These waterstops and joints are essentially modeled as gravel-filled gaps. Therefore, there is no "bathtub effect" because the flow out of the bottom of the disposal unit is not impeded enough to create such an effect.

c) The floor is modeled as having a 1.5% grade slope from the SDU center to the wall. No sensitivity modeling was performed to evaluate variation to the floor slope. Again, due to the waterstops through the floor and the joints at the wall-to-floor interface being modeled as gravel-filled gaps, minor changes to the slope of the floor are not expected to result in significant changes to flow.

d) The figures referenced from the *Response Matrix for U.S. Nuclear Regulatory Commission Staff Request for Additional Information on the Fiscal Year 2013 Special Analysis for the Saltstone Disposal Facility at the Savannah River Site* (Figures DSP-6.6 and DSP-6.8) show roof saturation at approximately 1,000 years after SDF closure. [SRR-CWDA-2014-00099] Initially, these roofs are completely (or nearly completely) saturated. Prior to HDPE liner failure, there is relatively little water infiltrating into the roof from above; however, the roof is degraded very quickly (e.g., by 1,000 years the roof of the 375-foot diameter SDU has a hydraulic conductivity of 3.1E-05 cm/sec). Without significant inflow, and without the ability to retain the available water, the roof loses saturation as water moves downward into the saltstone.

Note that this state of partial saturation is temporary. After the HDPE fails (at 1,400 years), the infiltration from above increases significantly, resulting in re-saturation of the roof.

e) As indicated in the NRC's RAI, the waterstops, the wall-to-roof joint, and the wall-to-floor joint for the 375-foot diameter SDUs are all conservatively modeled as having the hydraulic properties of gravel. Despite the conservative modeling approach, the DOE does not expect that these features would provide a significant pathway for air flow or atmospheric interaction due to the thickness of the assumed closure cap (i.e., greater than 10 feet) and because backfill will be compacted using vibratory rollers to at least 90% of the maximum dry density per the Modified Proctor Density Test or 95% per the Standard Proctor Density Test. [WSRC-STI-2008-00244] Including this information in the responses to DSP-5 or DSP-6 (from SRR-CWDA-2014-00099) would not have impacted the conclusions to these RAI responses.

f) Data files associated with the FY2014 SDF SA have been transmitted to the NRC. [SRR-CWDA-2014-00121] Consistent with similar data transmittals in the past, this transmittal included Tecplot files (*.lay). These files provide a graphical interface for examining the results from PORFLOW, including both the vertical and horizontal flow rates for each SDU over time. For example, the following file provides the relevant information for SDU 6, as modeled in the Evaluation Case:

.. \PORFLOW\VadoseSDU6\Flow\Case_sa\Plot.lay

g) Data files associated with the FY2014 SDF SA have been transmitted to the NRC. [SRR-CWDA-2014-00121] Consistent with similar data transmittals in the past, this

transmittal included Tecplot files (*.lay). These files provide a graphical interface for examining the results from PORFLOW, including cross-sectional views of the grid, saturation, and Darcy velocities for each SDU over time. For example, the following file provides the relevant information for SDU 6, as modeled in the Evaluation Case:

.. \PORFLOW\\VadoseSDU6\Flow\Case_sa\Plot.lay

FAR-FIELD TRANSPORT (FFT)

FFT-1

FFT-1	**Question:** In the DOE 2015 Response to the NRC 2014 RAI Comments (see RAI Comment FFT-1 in that document), the DOE referenced the DOE document SRR-CWDA-2014-00095. The NRC staff has concerns about information in that document and additional information is needed.
	Basis: Figure 2.1-8 in the DOE document SRR-CWDA-2014-00095 showed the dose within 50,000 years for various SZ and UZ thicknesses, including the importance of the leachate impact on K_d values in the UZ. However, considering that the transport of certain radionuclides were delayed by the thicker UZ, it is not clear to the NRC staff why the timing of the peaks in the case with the thinner SZ and thicker UZ are the same as those of the other cases. Additional information is needed to explain the match in timing of peaks between those cases. Table 2.1-1 in the DOE document SRR-CWDA-2014-00095 showed SZ thickness by taking the differences in elevation between the water table elevation and the elevation of the top of the Gordon Confining Unit or Green Clay. However, the Tan Clay Confining Zone (TCCZ) acts locally as an aquitard. For a better representation, the DOE should take the differences between the bottom elevation of the TCCZ (or the water table elevation if lower than the bottom of the TCCZ) and the top of the Gordon Confining Unit. Figure 2.2-1 in the DOE document SRR-CWDA-2014-00095 showed the importance of the dispersivity values in the SZ. To reduce potential uncertainty with regard to the potential significance of the dispersivity values used in Z-Area, the DOE could compare modeled plume results for the SDF against other plumes at the Savannah River Site (SRS), especially nearby plumes. The presence of structure and contours in the subsurface appears to have resulted in the unexpected narrowing and updip migration of a contaminant plume at P Reactor (see Cameron, González, et al., (2010)). Although the specific features at P Reactor may not be relevant to Z-Area, the DOE has observed subsurface structure in the TCCZ that could result in channeling of contaminants in the subsurface and similar structure could exist in the underlying stratigraphic layers. It is not clear to the NRC staff whether and how much those potential features could impact the dose results.
	Path Forward: Provide additional information on how the properties of radionuclides represented in Figure 2.1-8 in the DOE document SRR-CWDA-2014-00095 and the characteristics of the sediments beneath the disposal structures can explain the timing of the peak doses for the different cases. Provide the thickness between the bottom elevation of the TCCZ (or the water table elevation if lower than the bottom of the TCCZ) and the elevation of the top of the Gordon Confining Unit. Provide a description of what effect such saturated thicknesses would have on the dose results. Provide the results and the DOE interpretation of the significance of applied dispersivity values by comparing the DOE modeled plume results for the Z-Area against other plumes at SRS, especially nearby plumes.

DOE Response to FFT-1

The response to FFT-1 has two parts. The first part addresses the NRC's concern regarding Figure 2.1-8 from the *Saltstone Disposal Facility Sensitivity Modeling to Address Concerns*

Related to Saturated Zone Transport. [SRR-CWDA-2014-00095] The second part of the response addresses the remaining questions raised in FFT-1.

Explanation of Figure 2.1-8 from SRR-CWDA-2014-00095

Figure 2.1-8 from SRR-CWDA-2014-00095 shows total dose results from sensitivity modeling, which looked at various SZ thicknesses. The timing of the peaks was not affected by varying the thicknesses of the saturated zone, because Tc-99 is the dominant dose driver at the time of each peak. The K_ds for Tc-99 in soils are relatively small, such that it would require a much further travel distance to appreciatively influence the timing of the peaks. Effectively, once Tc-99 is released from the SDUs, it is almost instantaneously transported to the 100-meter boundary. The transport of the slower-moving radionuclides (e.g., Ra-226) was significantly influenced by the differences in saturated zone thicknesses and the overall impact (when considering total doses) was negligible. The Tc-99 doses, which control the timing of the peaks, were not significantly affected.

Response to Other FFT-1 Questions

Within the RAI, the NRC states that the Tan Clay Confining Zone (TCCZ) "acts locally as an aquitard" and "the DOE has observed subsurface structure in the TCCZ that could result in channeling of contaminants in the subsurface and similar structure could exist in the underlying stratigraphic layers."

The current model already includes the TCCZ as a locally significant feature. Figure FFT-1.1 shows a visualization of the three-dimensional aquifer transport model used by PORFLOW. Looking down at the model from above (i.e., XY rotation), the model appears to be relatively flat. However, by rotating the model to view it horizontally (i.e., YZ rotation, shown in Figure FFT-1.2), more detailed observations can be made. First, note that (as a point of reference) the brown line indicates the 100-meter boundary of the SDF and this depiction provides significant vertical exaggeration. Next, the mesh shows alternating sets of thinner layers and thicker layers. These correspond to the hydrologic features in the Z Area, where the thinner layers are the dense clay layers (e.g., the TCCZ) while the thicker layers are the less dense, sandier layers.

The DOE does plan to update the General Separations Area database and the resulting aquifer flow and transport PORFLOW modeling. This update will incorporate any new information with respect to Z-Area hydrology (e.g., the subsurface structure in the TCCZ) and site-specific plumes shall be reviewed to inform the assumed dispersivity values. However, as these updates are significant, this work is not expected to be available until the next SDF PA revision.

Figure FFT-1.1: Visualization of the 3-D PORFLOW Model Used for Aquifer Transport (XY Rotation)

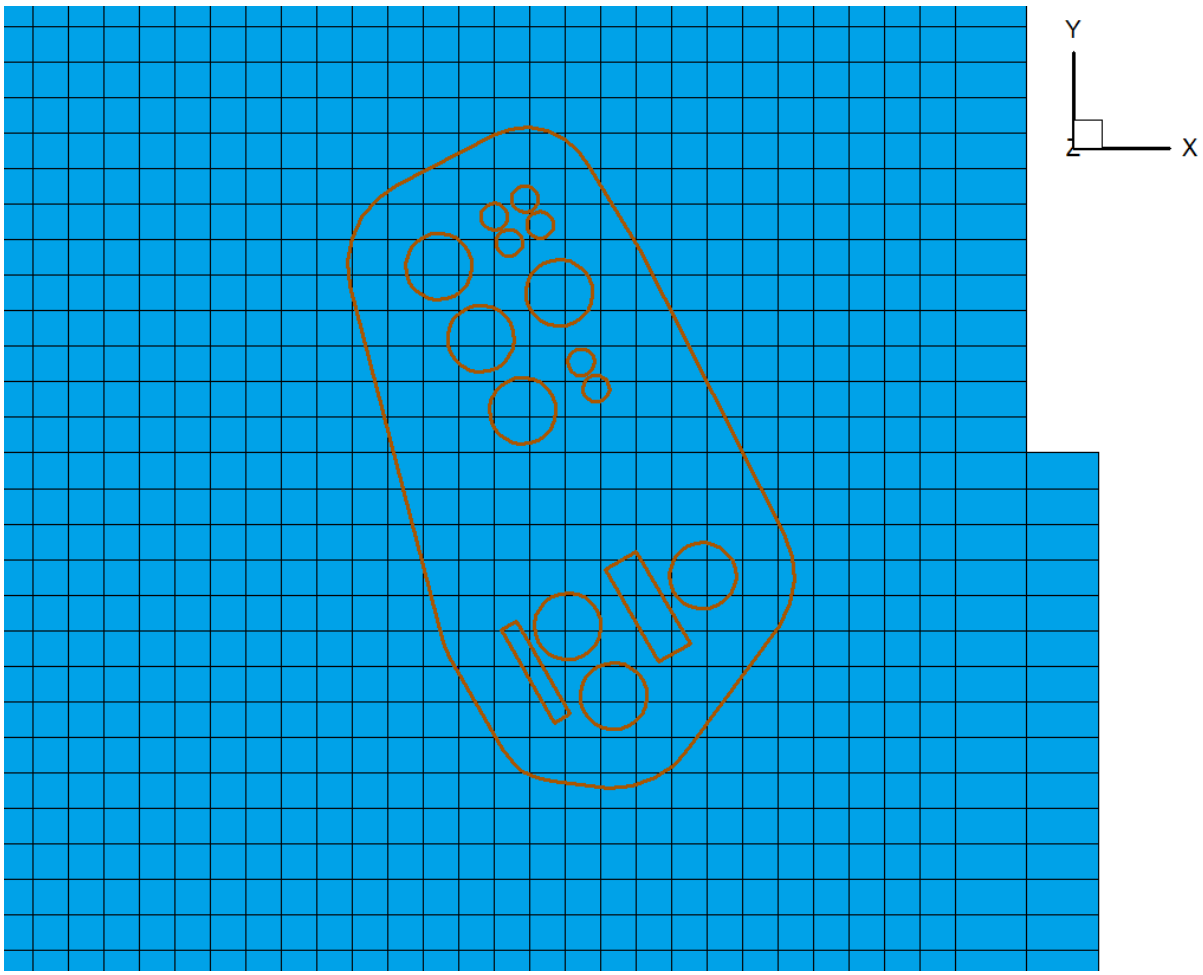

Figure FFT-1.2: Visualization of the 3-D PORFLOW Model Used for Aquifer Transport (YZ Rotation)

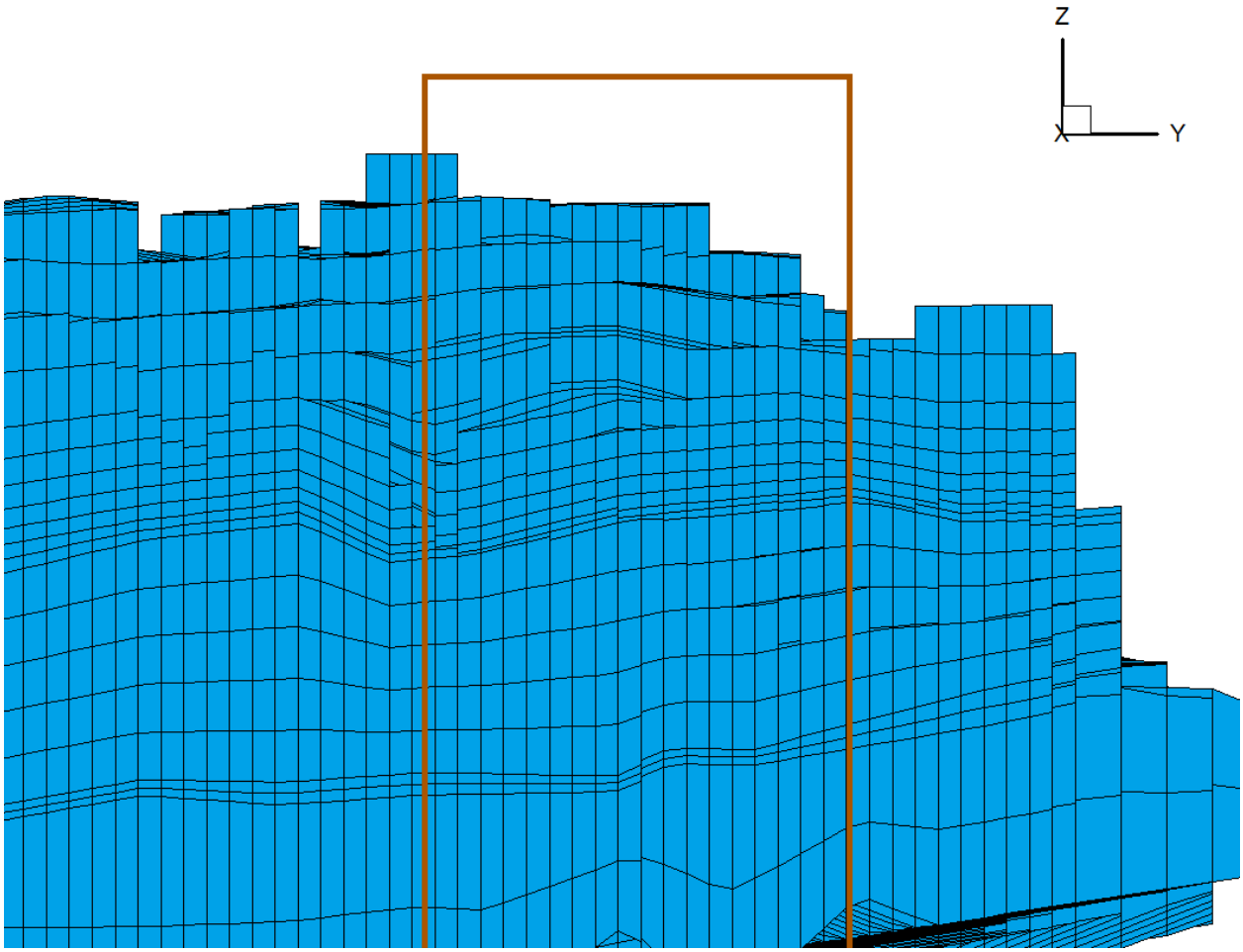

Through this layering, PORFLOW simulates three distinct aquifer zones (the Upper Aquifer Zone of the Upper Three Runs Aquifer [UAZ], the Lower Aquifer Zone of the Upper Three Runs Aquifer [LAZ], and the Gordon Aquifer). The appendices of both the SDF PA and the FY2014 SDF SA explicitly provided concentration results for contaminants within each of these aquifers, including the UAZ (i.e., the zone above the TCCZ).

Alternatively, the GoldSim model, which was used to generate the results described within the *Saltstone Disposal Facility Sensitivity Modeling to Address Concerns Related to Saturated Zone Transport* (SRR-CWDA-2014-00095), does not explicitly simulate the specific geologic units within Z Area. Instead, the GoldSim model is a simplified one-dimensional transport model that generically simulates a vadose zone (or UZ) beneath the SDUs (from the bottom of the SDUs to the water table) and a saturated zone (from the SDU footprint to the 100-meter boundary). Flow rates are determined based on spatially-averaged flow data from the PORFLOW simulation. As such, with respect to transport, the hydrologic layers are implicitly (not explicitly) included in the GoldSim model. The saturated zone thickness is a modeling parameter included in the GoldSim model to control plume-spreading calculations for saturated zone transport. Accordingly, the

process for determining the thickness of the saturated zone is not as important as the actual values used. The range of saturated zone thicknesses considered in the sensitivity modeling encompasses the difference between the bottom of the TCCZ and the top of the Gordon Confining Unit.

Figure 6-7 of the *Z Area Site Assessment* indicates that the bottom of the TCCZ is approximately 216 feet above mean sea level (MSL) (66 meters above MSL) while the top of the Green Clay (i.e., the Gordon Confining Unit) is 144 feet above MSL (44 meters above MSL). [DPST-86-426] Therefore, the thickness from the bottom of the TCCZ to the top of the Gordon Confining Unit was 72 feet (or 22 meters).

More recently, a number of geotechnical investigations identified SDU-specific elevations for various subsurface layers, as summarized in Table FFT-1.1.

Table FFT-1.1: Summary of Subsurface Elevations (Average Feet Above Mean Sea Level)

Document ID	SDU	Ground Surface [a]	Top of C2 [b]	Top of S3 [c]	Top of M1 [d]	Water Table
K-ESR-Z-00003	SDU 1	286	217	205	141	230
K-ESR-Z-00001	SDU 2	281	224	208	<140 [e]	225
K-ESR-Z-00002	SDU 3/5	269	225	219	145 [f]	220
K-ESR-Z-00005	SDU 6	278	235	226	146 [f]	215

Notes: (a) Value prior to excavation or construction.
(b) The C2 Layer is the engineering layer that is equivalent to the TCCZ.
(c) The S3 Layer is the engineering layer that is equivalent to the LAZ.
(d) The M1 Layer is equivalent to the Gordon Confining Unit.
(e) The M1 layer was not located during the geotechnical investigation of SDU 2, so the elevation of the bottom of the borehole depth is identified.
(f) The M1 layer was not located during the geotechnical investigation of SDU 3/5 or SDU 6, so the elevation of the next available unit (the Gordon Aquifer) is identified.

In Table FFT-1.1, the bottom of the TCCZ would be at the top of Layer S3. Similarly, the top of the Gordon Confining Unit would be at the top of Layer M1. Therefore, the difference between the bottom of the TCCZ and the top of the Gordon Confining Unit ranges from 64 feet to 81 feet (or 19 meters to 25 meters). These values are consistent with the 22 meters indicated in the *Z Area Site Assessment* report. [DPST-86-426] These values are also consistent with the range of saturated zone thickness values (i.e., 19 meters to 32 meters) considered in *Saltstone Disposal Facility Sensitivity Modeling to Address Concerns Related to Saturated Zone Transport*. [SRR-CWDA-2014-00095]

As stated above, the TCCZ acts locally as an aquitard; however, over the entire SDF area, the TCCZ does not significantly impede the downward mobility of groundwater across the TCCZ. Water table wells at the SDF respond to variation in the amounts of rainfall over time. Figure FFT-1.3 shows a comparison of water level readings over time for ZBG 2 to moving one-year average rainfall for the nearest rainfall monitoring station in H Area. As shown in the figure, the water table is usually above the top of the TCCZ and correlates with the changes in rainfall. Monitoring wells ZBG 3 through ZBG 5 (in the LAZ) are placed downgradient of SDU 4 and upgradient of ZBG 2. Figure FFT-1.4 compares the water levels in ZBG 2 to those in ZBG 3 through ZBG 5. As shown on the figure, there is a strong correlation between the water levels in

ZBG 2 and ZBG 3 through ZBG 5. This would indicate that water levels in ZBG 2 and ZBG 3 through ZBG 5 respond closely with rainfall. This correlation would not be the case if water was not moving freely between the UAZ and the LAZ at the SDF.

Figure FFT-1.5 shows a contour map of the water table surface from the third quarter of 2015 for the SDF from the *Z-Area Saltstone Disposal Facility Groundwater Monitoring Report for 2015*. [SRNS-TR-2015-00300] This map is compiled from monitoring well data for wells screened both above and below the TCCZ. The contours are very smooth and basically reflect topography, which is what would be expected of water table wells if the TCCZ was not a significant impedance to flow.

Figure FFT-1.6 provides a location map for a cross section through the SDF in Z Area. Figure FFT-1.7 is the cross section through the SDF from SRNS-TR-2015-00300. This cross section is perpendicular to groundwater flow. The figure shows how the water table, which is present at least 20 feet above the TCCZ on the left edge of the section (the southwest edge of Z Area) slowly descends to the right as it approaches McQueen Branch. The water table surface mimics the topography and passes across the TCCZ with little effect. It should be noted that although the cross section shows the TCCZ as a continuous clay horizon, this is not the case. Vertically, the TCCZ at the SDF varies significantly, consisting of interbedded layers of clay, sandy clay, clayey sand, and sand. Laterally, the horizon can be used for hydrogeologic correlation purposes, but does not impede the vertical movement of water on the scale of the SDF.

Table FFT-1.2 presents the water table elevations for ZBG 2 (UAZ) and ZBG002C (LAZ). The two wells are directly adjacent to each other. Vertically, there is approximately five feet of difference between the top and bottom of the two screen zones across the TCCZ; however, there is only 0.3 feet of difference in hydraulic head, indicating they represent the same aquifer.

Figure FFT-1.3: Plot of Historical Rainfall vs. Water Levels in ZBG 2

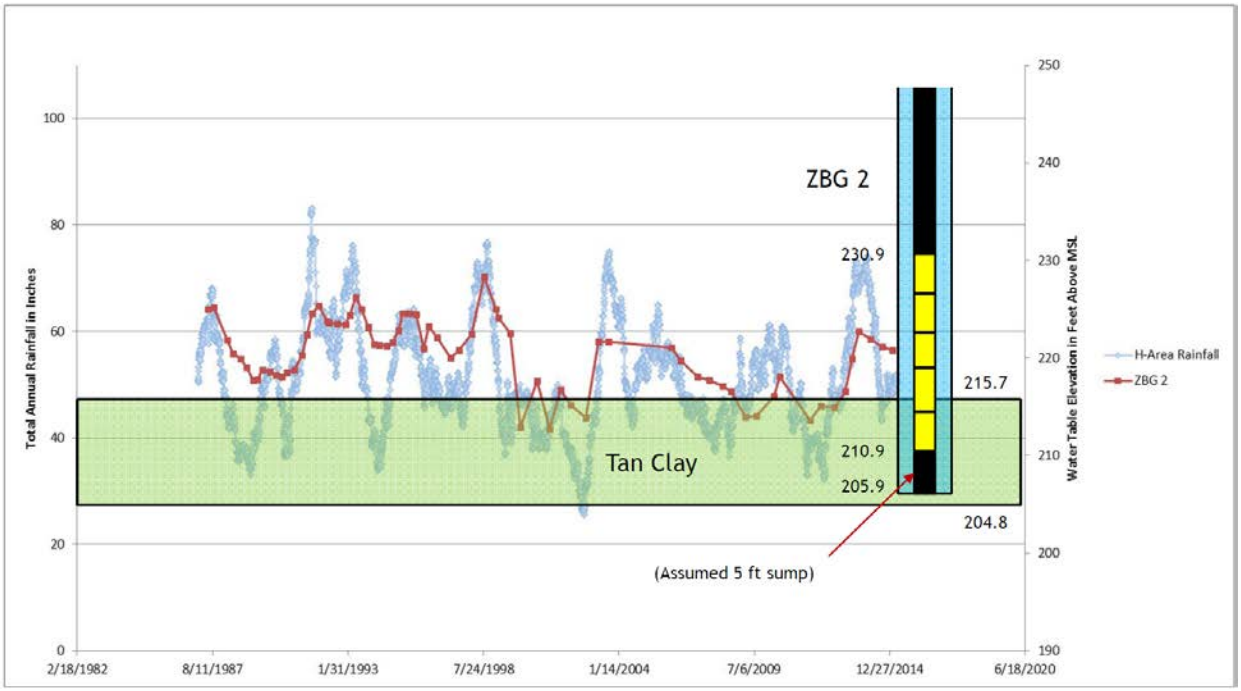

Figure FFT-1.4: Plot of Water Levels in ZBG 2 vs. ZBG 3 through ZBG 5

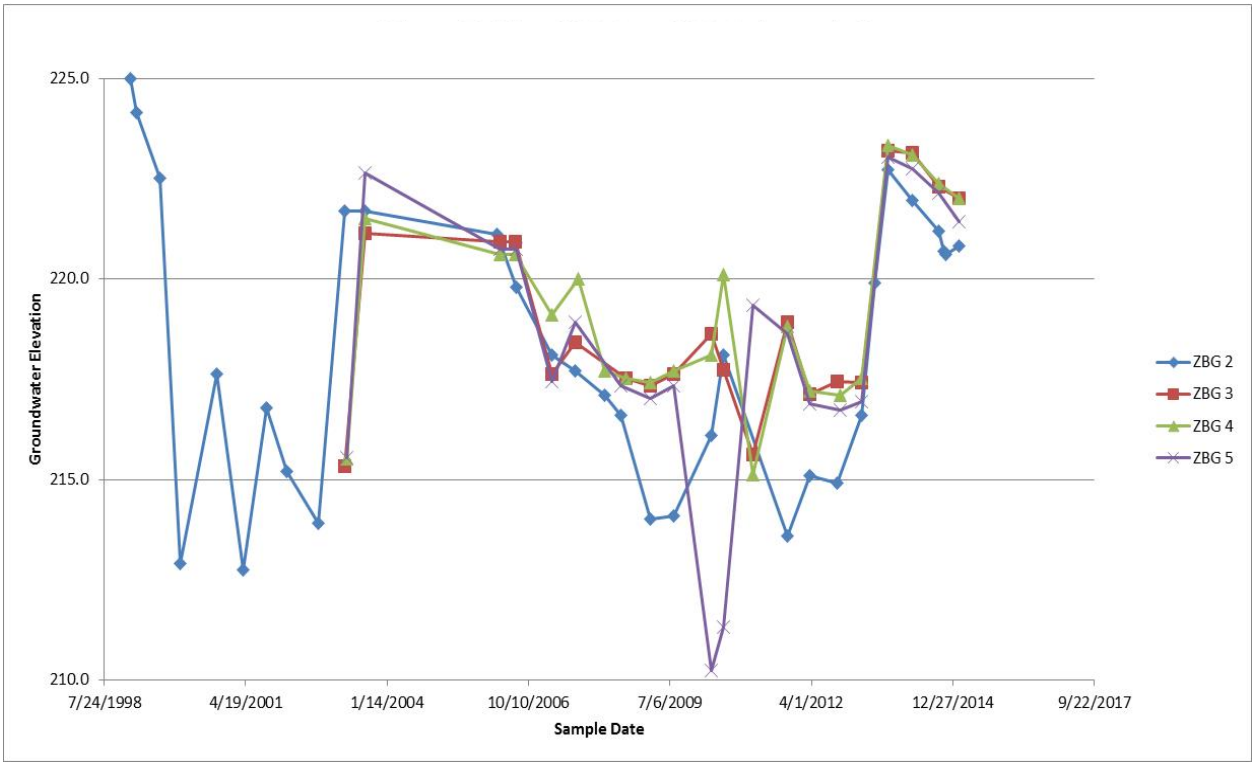

Figure FFT-1.5: Plot of Water Table Contours for the SDF (3Q15)

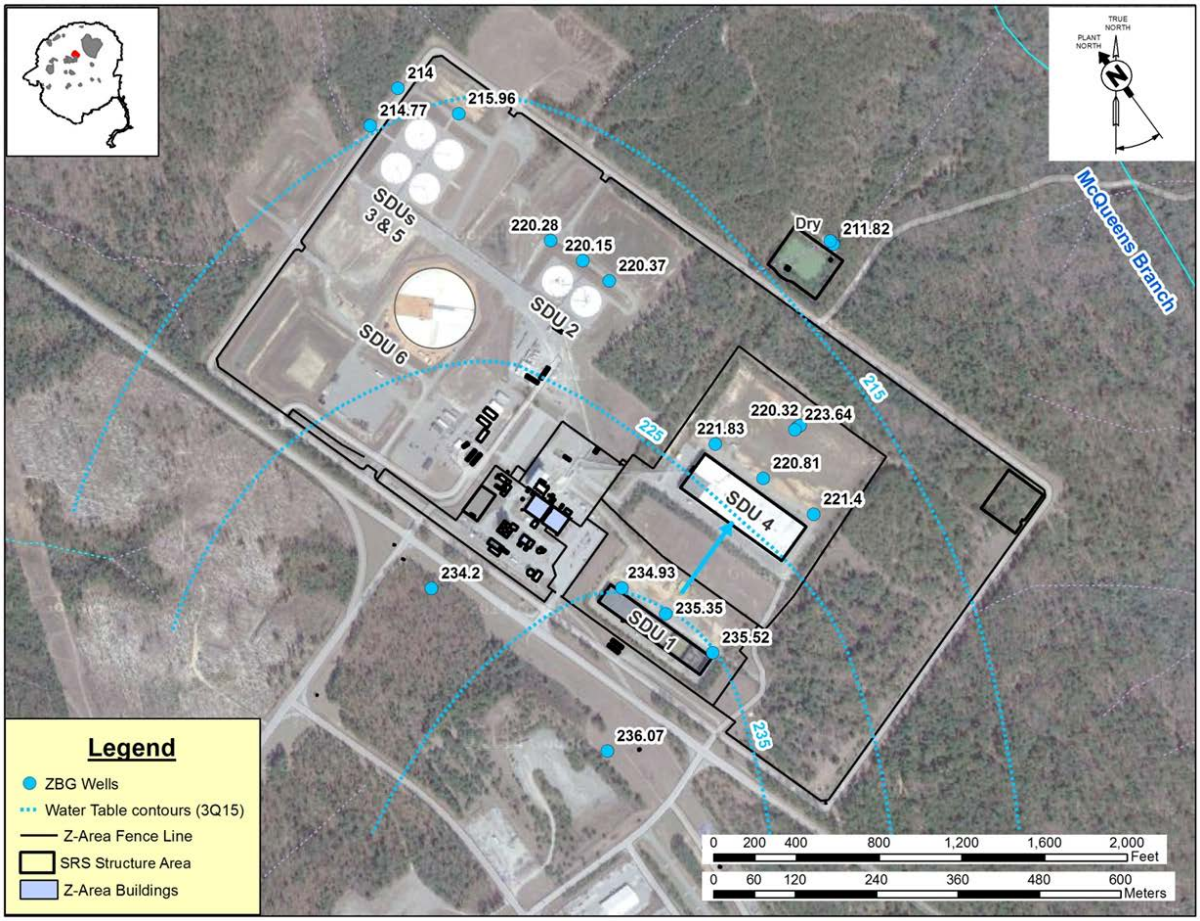

Figure FFT-1.6: Location of Cross Section A-A' in Z Area

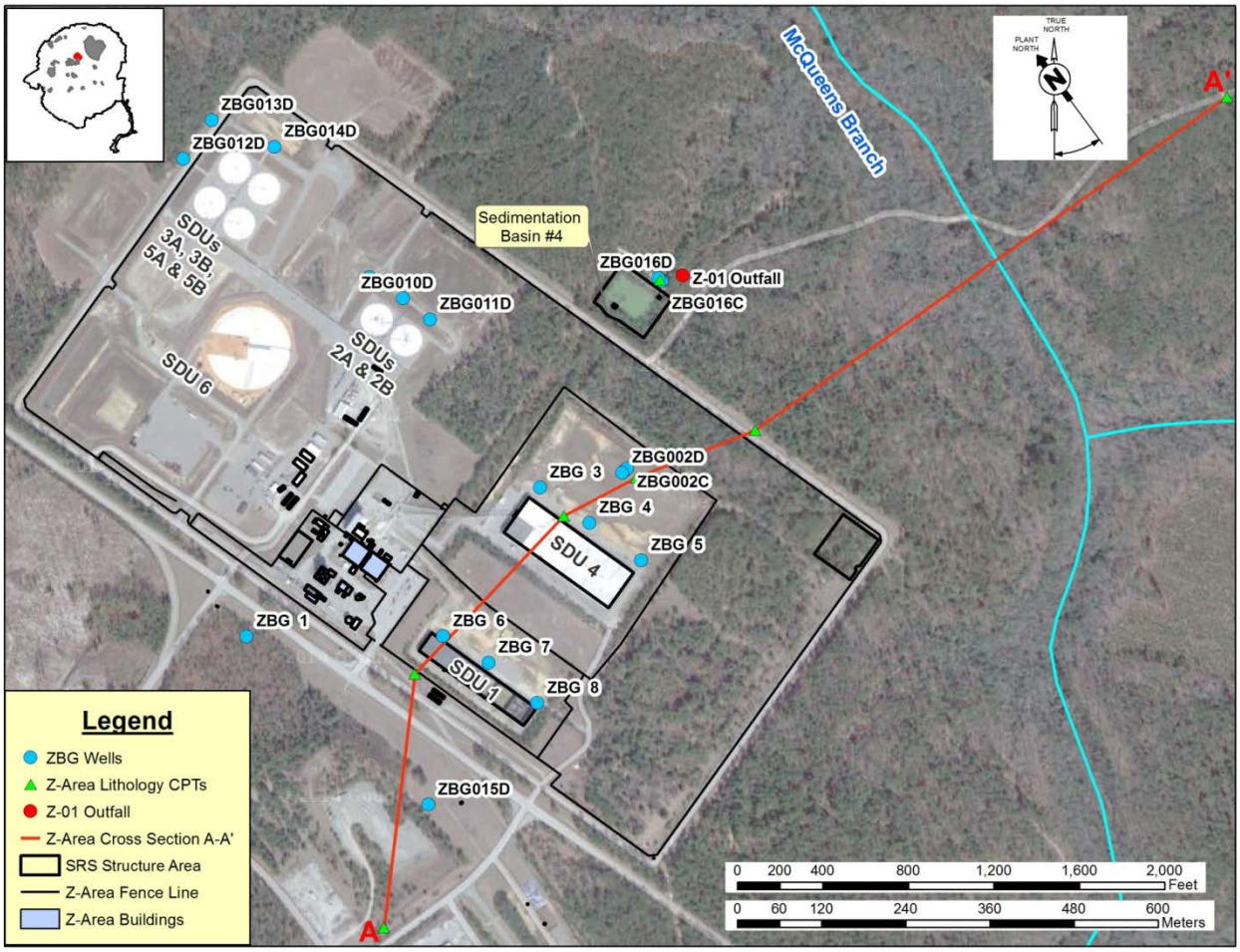

Figure FFT-1.7: Cross Section Through Z Area (Southwest to Northeast) with Contaminant Plume

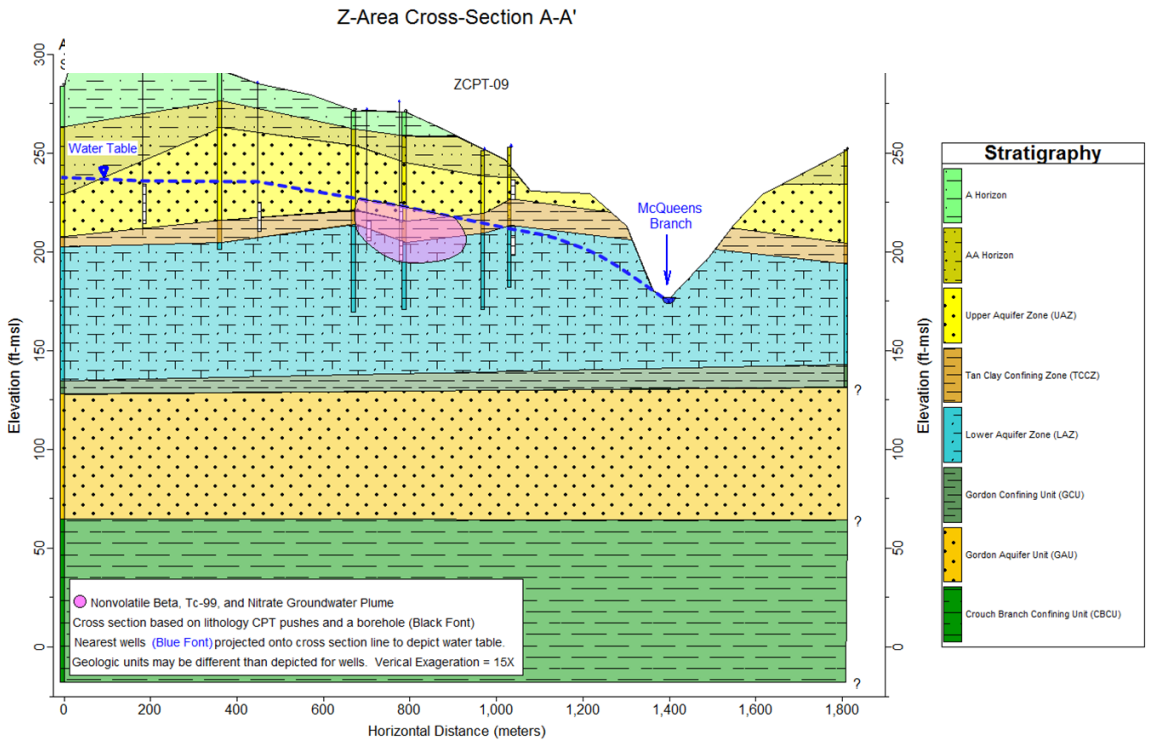

Table FFT-1.2: Water Elevations for Saltstone Monitoring Wells ZBG 2 and ZBG002C (from 1Q15)

Well	Reference Elevation (ft-msl)	Screen Zone Elevation (ft-msl)	Date	Water Depth (ft-bgs)	Water Elevation (ft-msl)	Aquifer
ZBG 2	278.10	210.9 – 230.9	2/9/15	57.3	220.8	UAZ
ZBG002C	278.56	195.8 - 205.8	2/9/15	58.0	220.5	LAZ

All of this information indicates there is hydraulic connectivity across the TCCZ, therefore, both the UAZ and LAZ should be treated as the saturated zone for SDF modeling purposes.

Currently, there is no known PORFLOW modeling in the vicinity of Z Area associated with known groundwater contaminant plumes. DOE is currently contemplating updating the GSA Database and will incorporate PORFLOW modeling. This update is future work. Future work may include comparisons of Z Area groundwater modeling to other areas in the GSA to ensure characteristics such as dispersity values are applied appropriately and consistently.

FFT-2

FFT-2	**Question:** Additional information is needed to support the values for the parameters used in the equation in Section 3.0 of the DOE document SRNS-TR-2014-00283.
	Basis: The value of the effective porosity was provided as 0.25% and that value was referenced to be from the DOE document WSRC-TR-2007-00283. However, the NRC staff could not find that value for that parameter in that document. Well ZBG 7 is screened in the upper zone of the Upper Three Runs (UTR) aquifer and Well ZBG 4 is screened in the lower zone of the UTR aquifer. Consequently, the head difference that DOE described was between two different aquifer zones with different hydraulic properties, separated by the TCCZ. The head difference should be between either two upper aquifer zone wells or two lower aquifer zone wells, unless the DOE shows that the influence of the TCCZ is minimal in that area (i.e., not a confining zone). The DOE showed that flow existed in the upper zone of the UTR aquifer (e.g., in Well ZGB 2). However, only the hydraulic conductivity value for the lower zone of the UTR aquifer was used (i.e., 13 ft/day rather than 10 ft/day). In addition, prior to 2013 the assumed hydraulic conductivity was 1.7 ft/day (see the DOE document SRR-ESH-2012-00066). In the 2013 Groundwater Monitoring report (see the DOE document SRNS-TR-2013-00275), the hydraulic conductivity was revised to 13 ft/day. That report indicated that parameters were changed to be consistent with the PA modeling data in the SRS General Separations Area. However, it is not clear to the NRC staff why it was appropriate for the DOE to change parameter values from the field-derived values to the model results. If the higher hydraulic conductivity value is not supported, then the model could be adding unrealistic dilution.
	Path Forward: Provide the original reference for the assumed effective porosity. Explain the use of the head difference between two different aquifer zones (i.e., Wells ZBG 7 and ZBG 4). Provide justification for why the as-modeled hydraulic conductivity of the aquifer was used in the DOE FY14 SDF Special Analysis document rather than the value that appears to be field-derived. If the field-derived value is more defensible, then provide a revised dose estimate using the field-derived hydraulic conductivity.

DOE Response to FFT-2

The effective porosity used in Section 3.0 of SRNS-TR-2014-00283 (25%) has an asterisk indicating the source of the value is from the SDF PA (SRR-CWDA-2009-00017), not WSRC-TR-2007-00283. The text referencing WSRC-TR-2007-00283 is an F-Area Tank Farm (FTF) document and is incorrect. The effective porosity used in the SDF PA is 25%. This SDF PA porosity value is referenced from Section 5.6.1 of *Hydraulic Property Data Package for the E-Area and Z-Area Soils, Cementitious Materials, and Waste Zones* (WSRC-STI-2006-00198). Note that the text on page 2 of SRNS-TR-2014-00283 states that the effective porosity (n) value is 25 percent. The second bullet on page 2 stating that the effective porosity is "0.25%" is a typographical error and should be "25%".

The TCCZ at the Savannah River Site is designated a "confining zone" versus a "confining unit" because the impact of the TCCZ on water movement can be significant on a small scale, but is regionally minimal. Monitoring well ZBG 2 is located in the upper aquifer zone of the UAZ and ZBG 4 is screened in the LAZ. However, water levels in wells screened both above and below

the TCCZ respond to rainfall in the same manner, indicating that they have significant hydraulic connectivity and therefore can be used to determine hydraulic gradients.

The hydraulic conductivity in the 2013 Groundwater Monitoring report (SRNS-TR-2013-00275) was updated to be 13 feet/day to reflect the values used in the GSA Database and the value used in the modeling for the 2009 SDF PA, along with the H-Area Tank Farm (HTF) and FTF PAs. The SDF groundwater monitoring reports provided prior to 2013 used the 1.7 feet/day value for hydraulic conductivity; however, there was no basis provided for the value.

The GSA Database uses field-derived hydraulic conductivity values, mostly from slug tests, from hundreds of sample locations around the GSA and are more representative of the overall hydraulic conductivity of the Upper Three Runs Aquifer in the SDF. PORFLOW modeling is based on inputs from the GSA Database.

FFT-3

FFT-3	**Question:** Additional information is needed to support assumptions about potential saturated conditions in the upper zone of the UTR aquifer in Z-Area and potential contamination in the upper zone of the UTR aquifer in Z-area.
	Basis: The DOE document SRNS-TR-2014-00283 in Section 7 included: "The two samples collected at ZBG002C in 2014 indicate no contamination is migrating through the TCCZ." That indicated to the NRC staff that contaminates may flow horizontally on top of the TCCZ rather than solely through the TCCZ. However, contamination remaining in water from the upper zone of the UTR aquifer and serving as the main source of water to a receptor well was not considered as an alternative conceptual model. Only seven wells are screened in the upper zone of the UTR aquifer (i.e., ZBG 1, ZBG 2, ZBG 6, ZBG 7, ZBG 8, ZBG 15D, ZBG 16D). Except for Well ZBG 2, most of those wells are located in one area of Z-Area. However, other areas have been shown to have water present above the TCCZ, as seen in Figures 2, 3, and 4 in the DOE document K-ESR-Z-00001. Most wells are located in either the TCCZ or the lower zone of the UTR aquifer. Therefore, water level measurements from those wells showed the potentiometric surface rather than the UTR upper zone water table level, as indicated in Figure 3 in the DOE document SRNS-TR-2014-00104.
	Path Forward: Provide information on the extent and thickness of water in the upper zone of the UTR aquifer over an extended time period in the entire Z-Area. As an alternative conceptual model, the water in the upper zone of the UTR aquifer could be a primary source of radionuclides for a receptor well. Either provide justification that the alternative conceptual model is invalid or provide the dose estimates using that alternative conceptual model.

DOE Response to FFT-3

As discussed in the response to RAI FFT-1, Figure FFT-1.6 is a cross section through the SDF from the *Z-Area Saltstone Disposal Facility Groundwater Monitoring Report for 2015*. [SRNS-TR-2015-00300] This cross section is perpendicular to groundwater flow. The figure shows how the water table, which is present at least 20 feet above the TCCZ on the left edge of the section (at the southwest edge of Z Area) gradually descends as it approaches McQueen Branch. The water table surface mimics the topography and passes across the TCCZ with little effect. It should be noted that although the cross section shows the TCCZ as a continuous clay horizon, this is a simplified representation. Vertically, the TCCZ at the SDF varies significantly, consisting of interbedded layers of clay, sandy clay, clayey sand, and sand. Laterally, the horizon can be used for hydrogeologic correlation purposes, and may impede vertical flow at a very localized scale; however, the TCCZ does not impede the vertical movement of water when observing groundwater flow on the scale of the SDF.

Figure FFT-1.3 shows how the water table varies over time with changes in rainfall. Also, Figure FFT-1.4 shows how wells ZBG 3 through ZBG 5 (all screened below the TCCZ) respond to rainfall in a similar fashion to ZBG 2, indicating the TCCZ is not a significant impedance to the vertical migration of groundwater.

Groundwater monitoring results for ZBG 2 have indicated the presence of a contaminant plume containing Tc-99, non-volatile Beta, and nitrates since 2012. This monitoring well was installed above the TCCZ. However, an additional monitoring well (ZBG002C) was installed at the same location as ZBG 2, but with a screen zone below the TCCZ, in the LAZ. Monitoring results for ZBG002C, as well as ZBG 3 through ZBG 5, reported in SRNS-TR-2015-00300 for both the first and third quarter 2015 monitoring periods contain detectable Tc-99, non-volatile Beta, and nitrates, although at levels less than in ZBG 2. This would indicate that the contaminant plume associated with SDU 4 is moving through the TCCZ with only a slight delay in timing (2 to 3 years). These results show that even though the TCCZ is present in the vicinity of SDU 4, it is not a significant impedance to the movement of contaminants from the UAZ into the LAZ.

In addition, as shown on Figure FFT-3.1, cone penetrometer test (CPT) lithologic pushes ZCPT-04 through ZCPT-06 are located adjacent and directly downgradient of ZBG 2. ZCPT-12 is located approximately 200 feet upgradient of ZBG 2, in the direction of SDU 4. Figures FFT-3.2 through FFT-3.5 provide the lithologic CPT logs for ZCPT-04 through ZCPT-06, and ZCPT-12, respectively. The stratigraphic location of the TCCZ is defined in red on each of these four figures. ZCPT-04 through ZCPT-06 are all collected at a ground elevation of approximately 269 feet above MSL. The contours in Figure FFT-3.1 indicate a slight depression in the structural contour surface of the TCCZ. This depression is in the direction of regional groundwater flow and detected groundwater contamination is moving parallel to the depression and with the regional water table flow. [SRNS-RP-2015-00902]

Table FFT-3.1 summarizes the horizons within the TCCZ that are classified as “clay” from the column on the far right on the CPT logs in Figures FFT-3.2 through FFT-3.5. The majority of the TCCZ on these CPT logs is not characterized as “clay”, but as “sandy silt” to “silty sand”. The TCCZ represents a hydrostratigraphic horizon for correlation, but it is not a continuous and significant clay layer to impede the vertical movement of groundwater between the UAZ and the LAZ.

Figure FFT-3.1: CPT Locations on Top of Refined TCCZ Contours

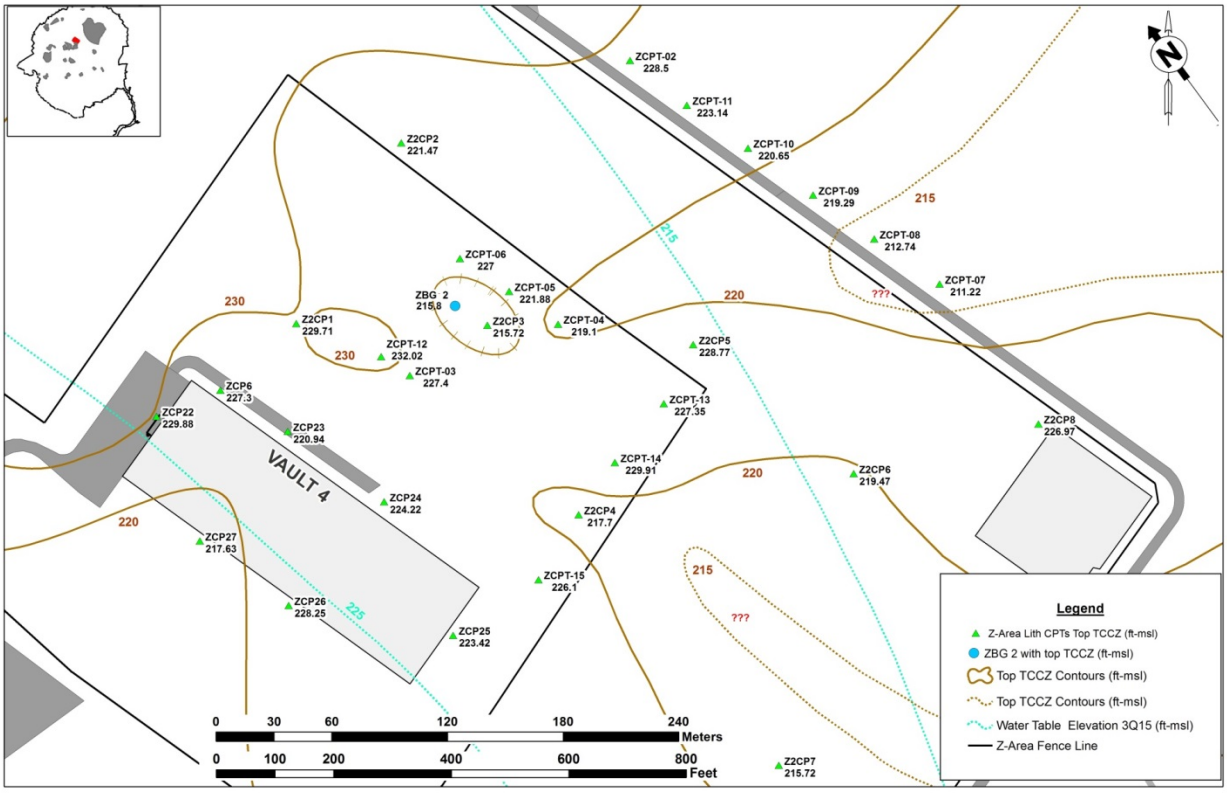

[SRNS-RP-2015-00902]

Figure FFT-3.2: ZCPT-04 Lithologic Strip Log

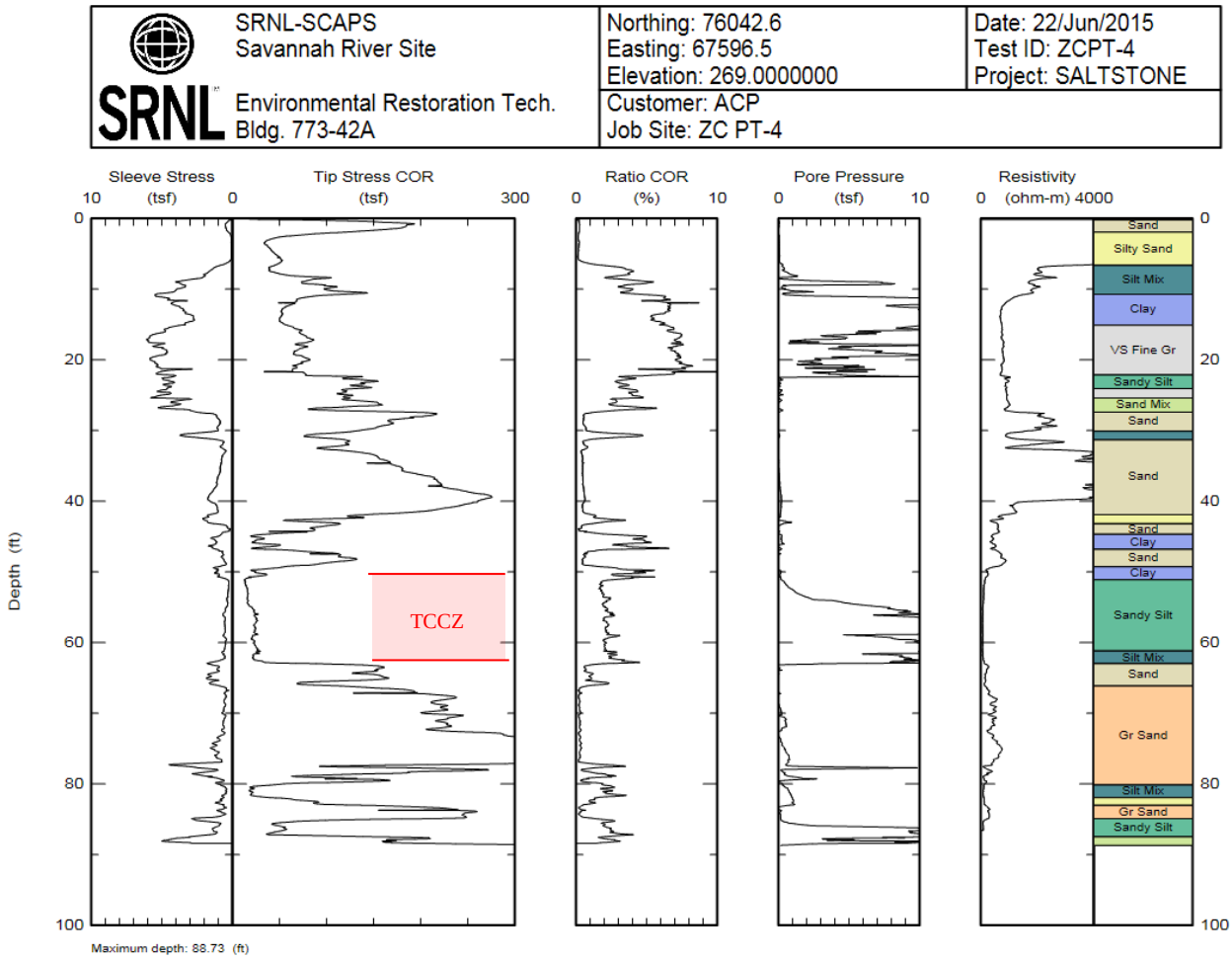

[SRNS-RP-2015-00902]

Figure FFT-3.3: ZCPT-05 Lithologic Strip Log

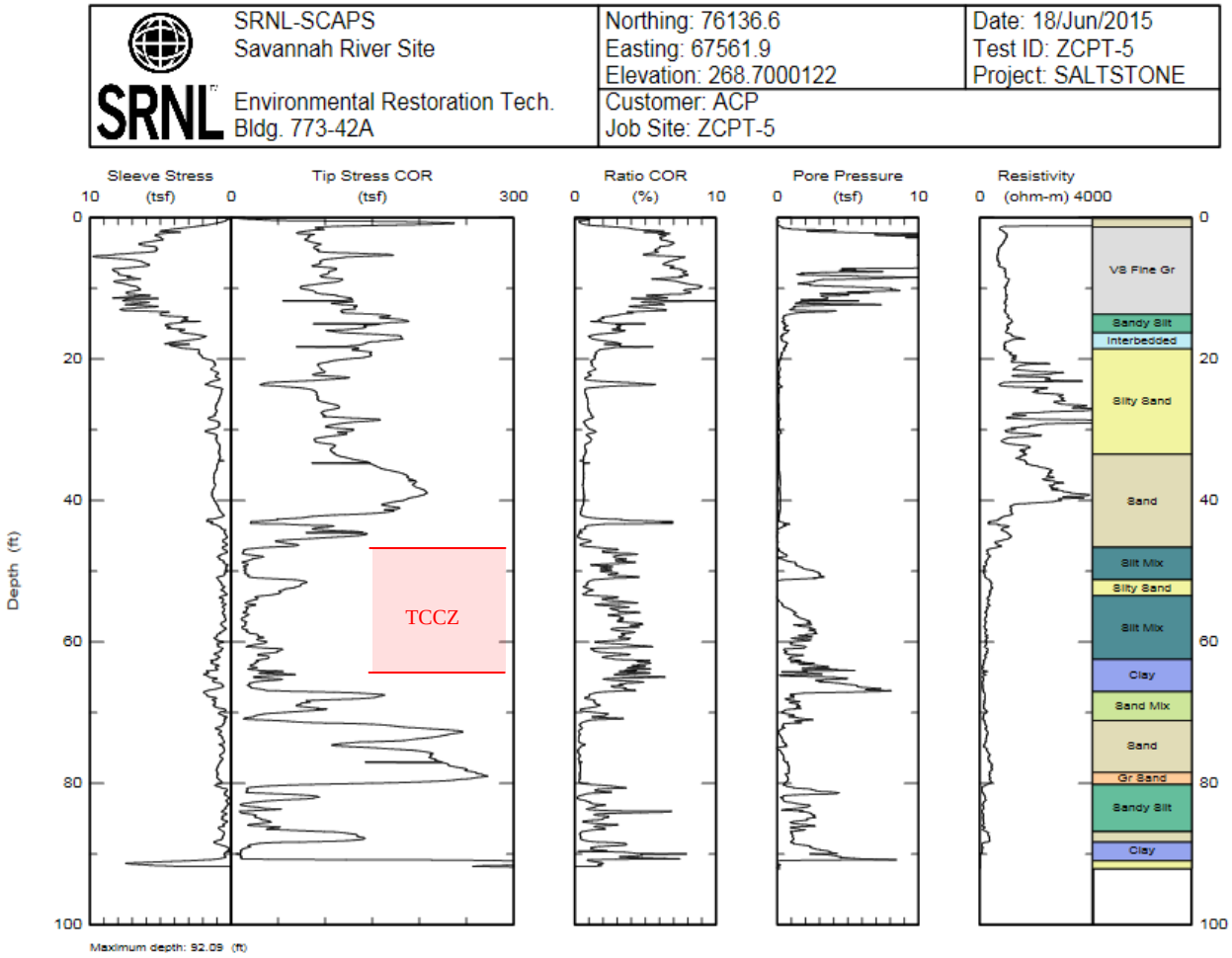

[SRNS-RP-2015-00902]

Figure FFT-3.4: ZCPT-06 Lithologic Strip Log

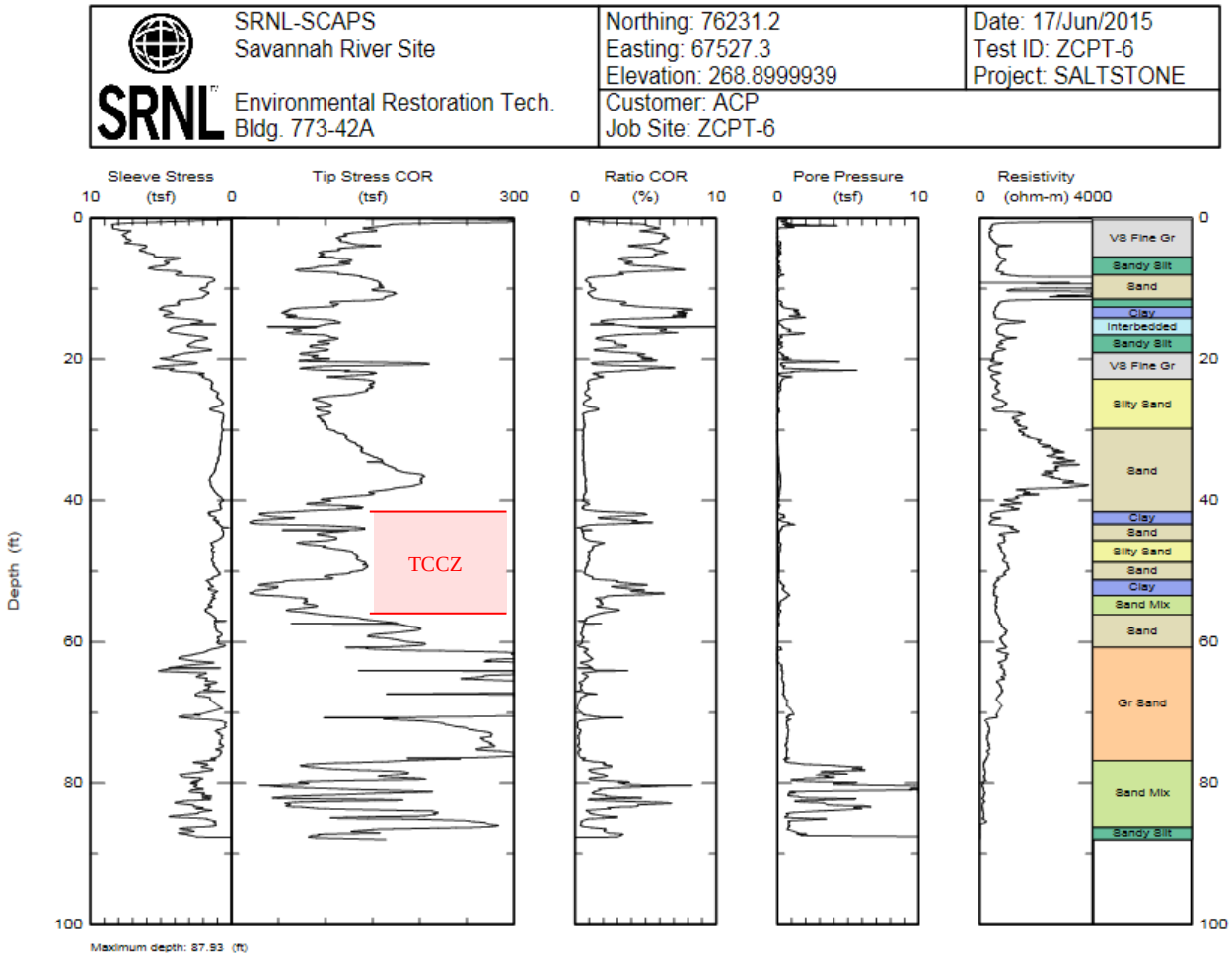

[SRNS-RP-2015-00902]

Figure FFT-3.5: ZCPT-12 Lithologic Strip Log

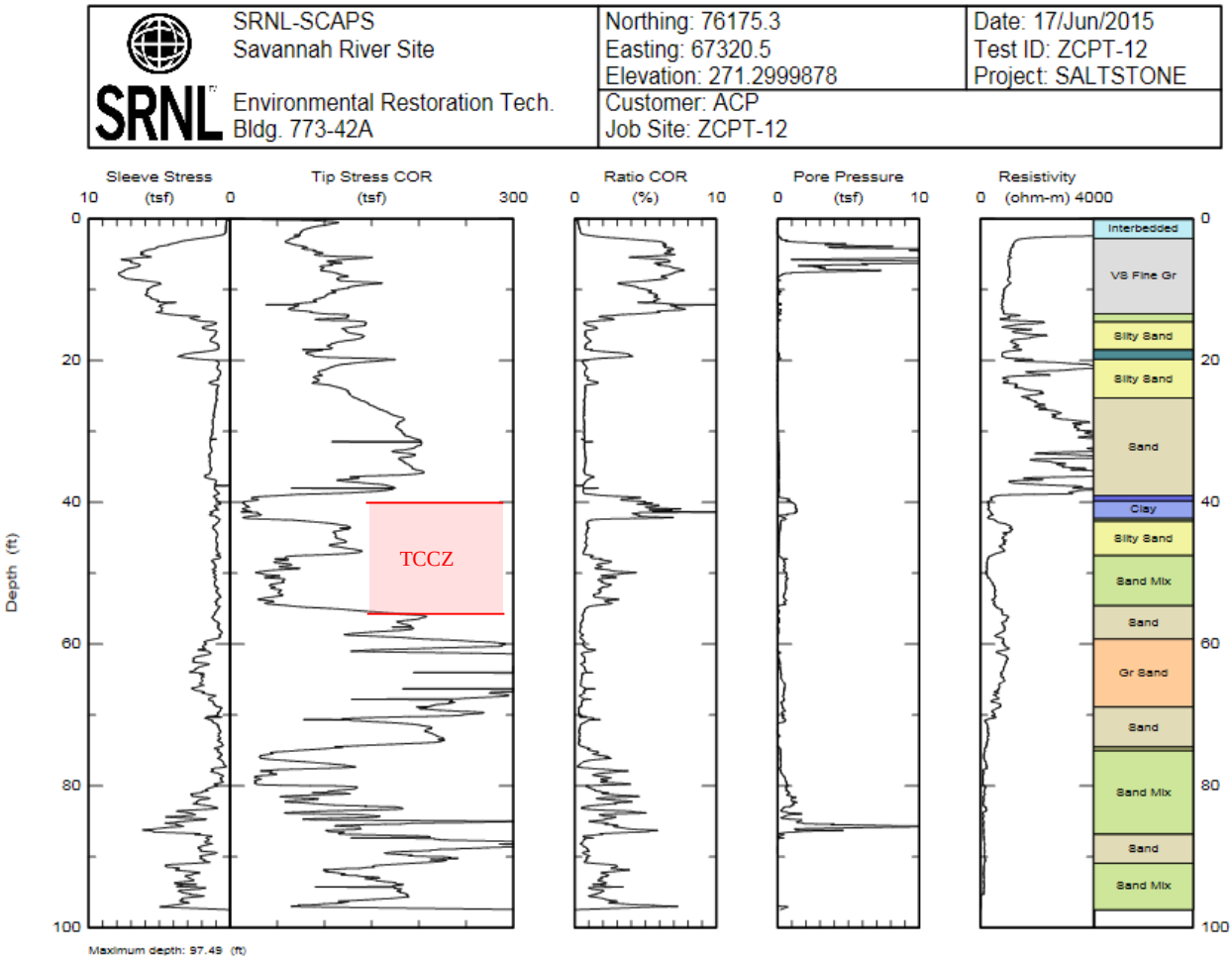

[SRNS-RP-2015-00902]

Table FFT-3.1: Selected CPT Logs Downgradient of SDU 4 Presenting Clay Intervals within the Tan Clay Confining Zone

CPT	TCCZ (feet above MSL)	TCCZ Thickness (feet)	Upper Clay Layer (feet above MSL)	Upper Clay Thickness (feet)	Lower Clay Layer (feet above MSL)	Lower Clay Thickness (feet)
ZCPT-04	219 - 207	12	219 - 218	1	Absent	N/A
ZCPT-05	222 - 202	10	Absent	N/A	206 - 202	4
ZCPT-06	227 - 214	13	227 - 226	1	218 - 217	1
ZCPT-12	232 - 216	16	232 - 230	2	Absent	N/A

In the FY2014 SDF SA, the 100-meter peak groundwater pathway dose is determined as the highest radionuclide concentration within the vertical computational meshes used from each of the three distinct aquifers modeled (UAZ, LAZ, and the Gordon Aquifer). The aquifer with the highest dose is considered the primary source of the radionuclide for the receptor well. As such, the Base Case already considers the potential contributions from concentrations in the UAZ, but as a model conservatism, only uses the concentrations from whichever aquifer showed the highest values, regardless of the aquifer in which it occurs.

FFT-4

FFT-4	**Question:** Additional information is needed about the extent and thickness of the TCCZ in the entire Z-Area and how it was modeled in PORFLOW.
	Basis: Section 3.1.5.2 in the DOE 2009 SDF PA included the following: "Contained within the Dry Branch Formation, the hydrostratigraphic unit, known (at SRS) as the [TCCZ], is of particular interest because it acts locally as an aquitard, supporting a water table and retarding the downward flow of groundwater. The presence or absence, thickness, and extent of this unit are important inputs into groundwater flow and transport models that are in turn used to demonstrate expected compliance with applicable groundwater regulatory requirements." The NRC staff agrees with the importance of the TCCZ. However, the extent, thickness, and properties of the TCCZ are not fully known. For example, the vertical gradient of the water in and around the TCCZ, which is significant for radionuclide transport through the TCCZ, is not well known. The DOE document SED-GTE-2008-002 included the following: "… interpretation indicates that the TCCZ is present in every borehole and [Cone Penetrometer Test] evaluated at the Saltstone site, ranging from 4.7 to 14.8 feet thick, with an average thickness of 10 feet." Figures 3 and 5 from the DOE document K-ESR-Z-0002 showed the TCCZ to be entirely missing in a section of the disposal structure area. The DOE document SED-GTE-2008-002 relied on borehole SDS21A in Table 2 to conclude that the TCCZ was present in every borehole. However, borehole SDS21A was previously examined in a U.S. Geological Survey (USGS) report (see WRI Report 88-4221) and Figure 10 in that USGS report showed that the TCCZ was missing in that part of Z-Area. The TCCZ in Z-Area is not well defined and the dose implications are not clear to the NRC staff because of uncertainty regarding lateral transport and sorption due to that layer. Due to the importance of the TCCZ, the DOE should provide additional documentation on how the TCCZ is modeled in PORFLOW, including either input values with output results or effects of the unit.
	Path Forward: Provide information on the extent and thickness of TCCZ in the entire Z-Area, and, if saturated, information on the vertical gradient within the TCCZ. Provide additional documentation on how the TCCZ is modeled in PORFLOW.

DOE Response to FFT-4

As stated in the response to RAI FFT-2, the TCCZ at the SRS is designated a "confining zone" versus a "confining unit" because the impact of the TCCZ on water movement can be impactive on a small scale, but is regionally minimal. Also, as noted in the response to RAI FFT-1, monitoring well ZBG 2 is located in the UAZ and ZBG 4 is screened in the LAZ, below the TCCZ. Figure FFT-1.3 shows a comparison of water level readings over time for well ZBG 2 to moving one-year average rainfall for the nearest rainfall monitoring station in H Area. As shown in Figure FFT-1.3, the water table is usually above the top of the TCCZ and correlates well with the changes in rainfall. Water levels in wells screened both above and below the TCCZ respond

to rainfall in the same manner (as shown in Figure FFT-1.4), indicating that they have a significant hydraulic connectivity and therefore can be used to determine hydraulic gradients. RAI FFT-1 provides additional information on how the TCCZ is addressed within the PORFLOW modeling.

Although the TCCZ is present at the SDF, it is not strictly clay. The "confining zone" consists of interbedded layers of clay, sandy clay, silt, and sand. In addition, the TCCZ appears at various elevations across the SDF. In some instances the bottom of the TCCZ is higher in elevation than the top of the TCCZ in nearby wells.

Groundwater moving toward UTR on the north flank of the GSA (including Z Area) leaks through the TCCZ into the LAZ or discharges to surface streams where they incise the TCCZ. [PIT-MISC-0124] In the *Saltstone Disposal Unit 6 Geotechnical Characterization Report*, K-ESR-Z-00005, the TCCZ, or "C2 Layer" as reported in the characterization, is part of the Dry Branch Formation. The TCCZ consists of medium dense clayey fine sand interlayered with stiff silty clay. A series of CPTs were performed during the characterization for SDU 6. For an example of a typical CPT, Figure FFT-4.1 provides the various geotechnical parameters collected at location Z-SDU6-01. The TCCZ ("C2" horizon) has been assigned on this strip log to be 7 feet thick at an elevation of 226 to 233 feet above MSL. As can be seen on the log, the 226 to 233 foot interval only contains two intervals of clay, each no more than one foot in thickness. On Figure FFT-4.2, the same interval from 226 to 233 feet above MSL is interpreted to consist mostly of sand mixtures of silty sand to sandy silt (light green),interbedded with minor sand clay to clayey sand (dark green, and minor layers of clay to silty clay [dark blue]). This interbedding is typical of the TCCZ across the SDF.

Figure FFT-4.3 is taken from the *Saltstone Disposal Cells No. 3 and 5 Geotechnical Investigation Report*, K-ESR-Z-00002. This figure provides the results from 5 CPT pushes. The cross section indicates that the TCCZ ("C2" horizon) is at basically the same elevation across the figure, for correlation purposes. However, there is a significant thinning of the horizon from right to left across the section, with the C2 horizon nonexistent in the two CPTs on the left side of the section, indicating little to no clay within the TCCZ at those locations.

This data supported construction of the GSA Database, which contains elevation and location information on hydrostratigraphic units, including the TCCZ. As stated in RAI FFT-2, the GSA Database uses field-derived hydraulic conductivity values, mostly from slug tests, from hundreds of sample locations around the GSA and is more representative of the overall hydraulic conductivity of the Upper Three Runs Aquifer in the SDF. PORFLOW modeling is based on three-dimensional inputs from the GSA Database. The TCCZ along with the other aquifers and confining horizons are defined in the database to provide three-dimensional hydrostratigraphic intervals for correlation and modeling purposes.

Figure FFT-4.1: CPT Characterization Log for Z-SDU6-C01

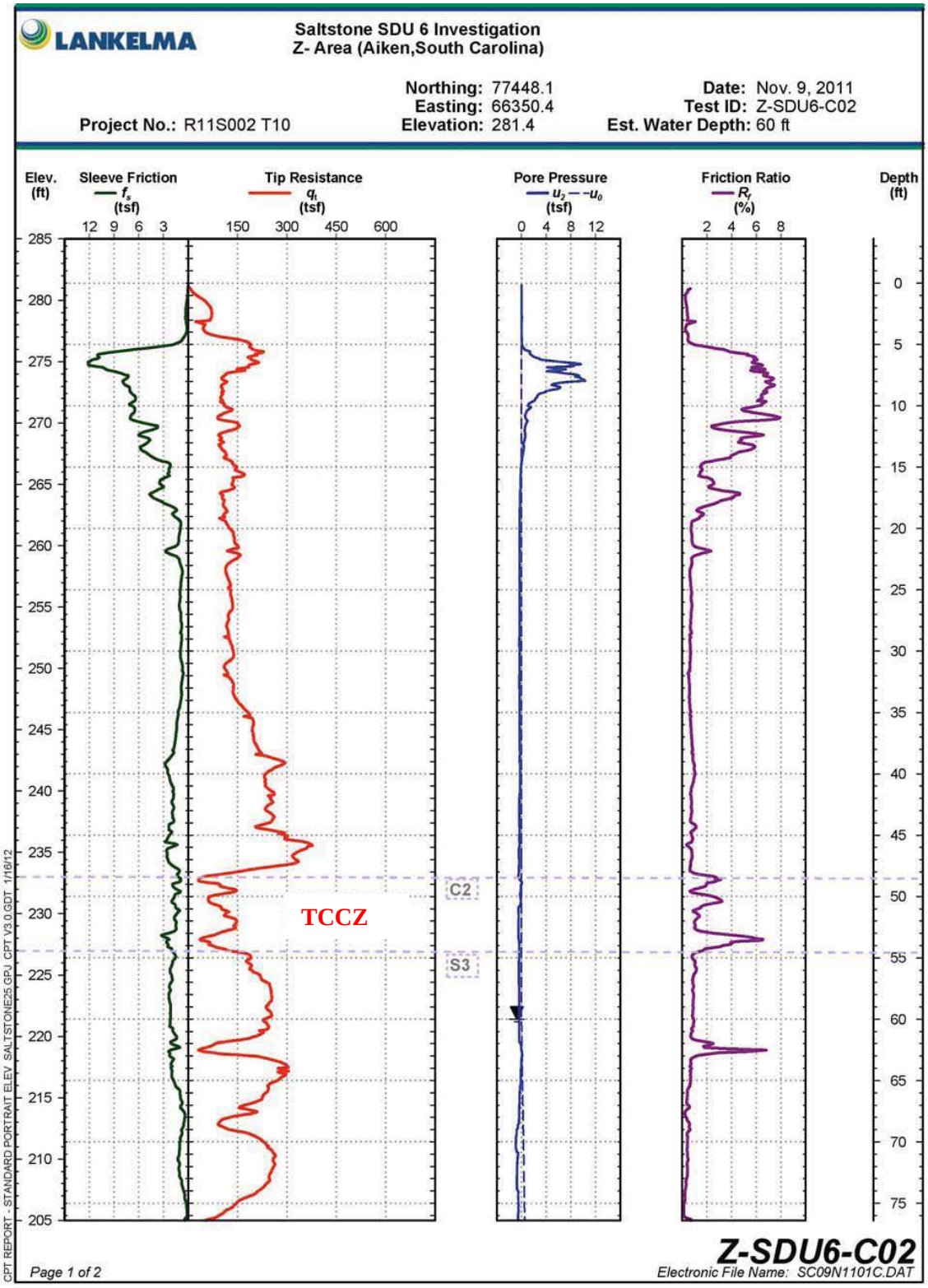

Figure FFT-4.2: CPT Characterization Log for Z-SDU6-C01 with Geologic Interpretation

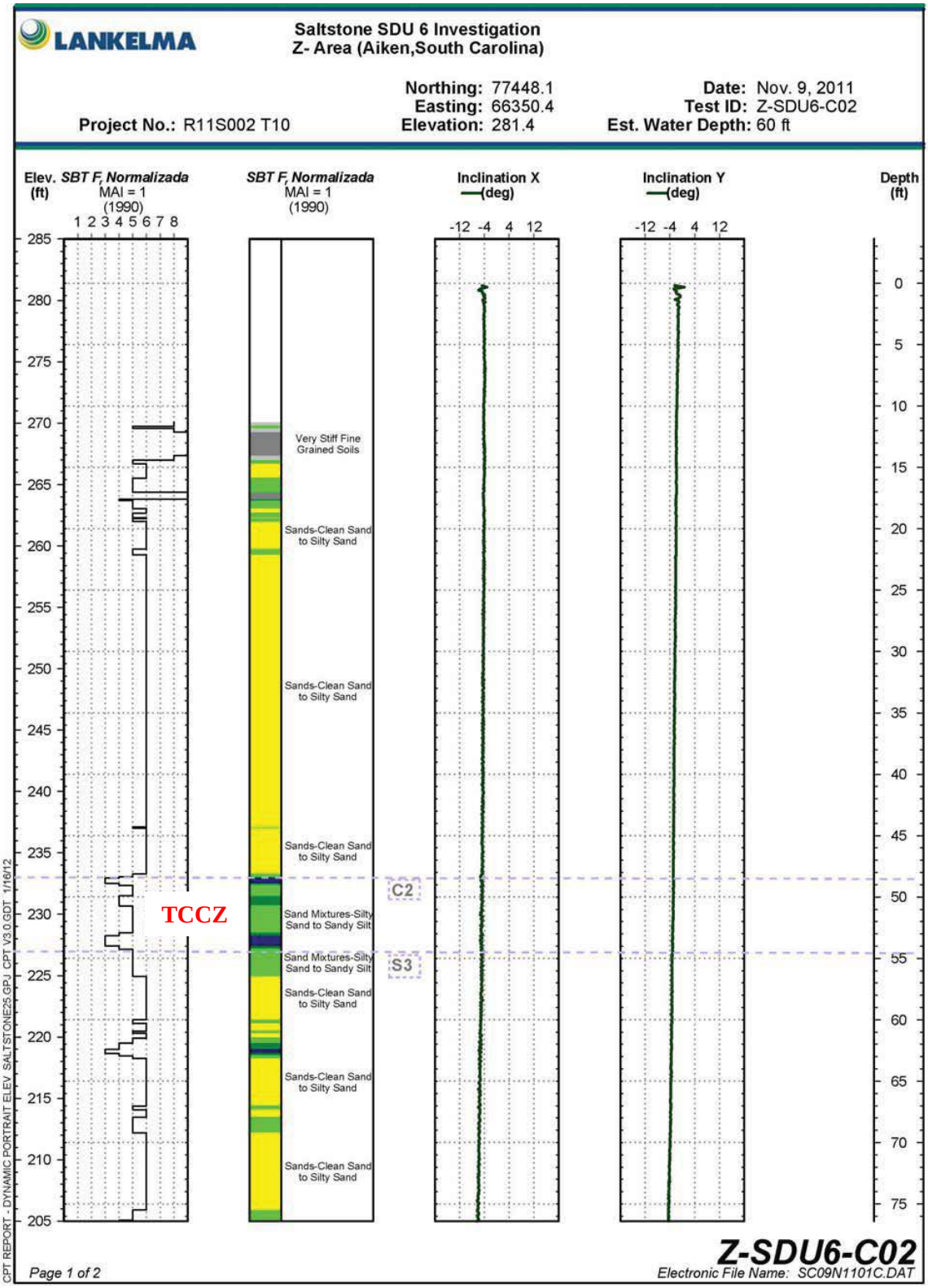

Figure FFT-4.3: Cross Section through SDUs 3A and 3B

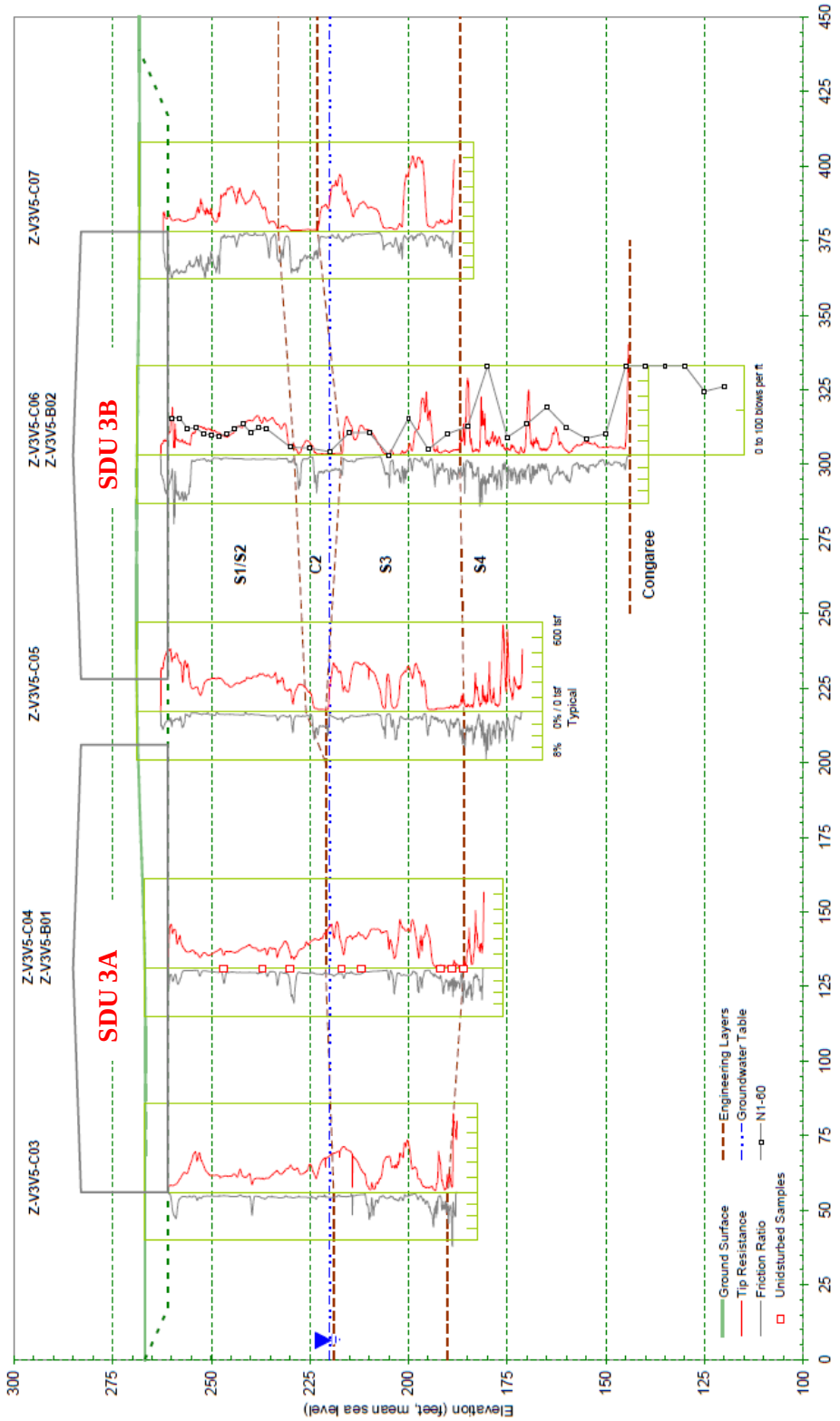

FFT-5

FFT-5	**Question:** Additional justification is needed for the soil K_d values for Se assumed in the DOE FY14 SDF Special Analysis document.
	Basis: This is the same NRC staff concern as in NRC RAI Comment FFT-2 on the DOE FY13 SDF Special Analysis document and the basis is the same as before. In the DOE document SREL Doc. R-13-0005, the measured K_d values for Se on SDF soil that has been impacted by leachate from cementitious materials were reported. Those measured values ranged from 1 to 41 milliliters per gram (mL/g). Those values are much less than the values assumed in the DOE FY14 SDF Special Analysis document (i.e., 1,400 mL/g for both clayey and sandy soils). In addition, as described in the 2012 SDF NRC TER, the measurements that the assumed Se soil K_d values are based on may have been affected by experimental errors, which could have resulted in an overestimation of the K_d values. In the DOE 2015 Response to the NRC 2014 RAI Comments (see RAI Comment FFT-2 in that document), the DOE referenced a sensitivity analysis included in the DOE FY14 SDF Special Analysis document. In that sensitivity analysis, the K_d value for sandy soil was reduced from 1,000 to 500 mL/g and the K_d value for leachate impacted sandy soil was reduced from 1,400 to 20 mL/g. It is not clear to the NRC staff that the value of 500 mL/g appropriately considered the uncertainty in the K_d value for Se for sandy soil. The high values measured for the soil K_d for Se under low pH conditions appear to be due to solubility limitation instead of sorption. Those values may not reflect the behavior of Se in the subsurface if the conditions in the experiments were not consistent with the conditions in the subsurface. For example, if the concentration of Se in the experiments was higher than the concentration in the subsurface, then the real system may not reach a solubility limit as quickly. Also, if the pH in the experiments differed from the pH in the saturate zone, then the experimental values may not be applicable to the real system. Previously, the DOE indicated that the estimated Se K_d values will decrease sharply as the pH increases above a pH of 6 and will decrease an order of magnitude as the pH value approaches 7 (see DOE document SRR-CWDA-2011-00044). If the pH of the groundwater in the saturated zone is higher than the pH in the experiments, then the experimental results may over-represent the amount of sorption. Additionally, the value of 20 mL/g for the K_d value for leachate impacted sandy soil did not capture the range of values measured for leachate impacted soils (i.e., 1 to 41 mL/g).
	Path Forward: Provide additional justification for the values assumed for the soil K_d values for Se or provide an evaluation of the potential impact on the projected dose due to the assumption of high values for the K_d for Se for soil that incorporates the full range of experimental values measured. That evaluation should include a consideration of the combined effect of the soil and cementitious material K_d values.

DOE Response to FFT-5

The response to SP-11 provides sensitivity analyses which evaluate wider ranges for the K_d values than those that were used in the FY2014 SDF SA.

The analyses described in the response to SP-11 assumed that selenium was un-retarded in cementitious materials (i.e., concrete and saltstone had K_ds of 1E-30 mL/g) and applied the minimum K_d for selenium in leachate-impacted sandy soils (i.e., 1.0 mL/g). Despite these

various conservatisms, the peak dose contribution from Se-79 within 10,000 years was less than 1 mrem/yr and within 50,000 years was less than 2 mrem/yr (see Figure SP-11.8). Therefore, the DOE does not consider Se-79 to be a significant dose contributor.

FFT-6

FFT-6	**Question:** Additional information is needed for the leachate impacted K_d values for clayey and sandy soil listed in Table 4.1-3 of the DOE FY14 SDF Special Analysis document.
	Basis: In the NRC RAI Comments on the DOE FY13 SDF Special Analysis document (see RAI Comment FFT-3 in that document), the NRC requested additional information for the assumed K_d values for leachate impacted clayey and sandy soil. The DOE response to RAI Comment FFT-3 in that document was minimal and the basis for those values in the DOE response is not clear to the NRC staff. In many cases, the DOE assumed values differed significantly from the values assumed for soil that was not leachate-impacted and those values are potentially significant to the projected dose. For example, the K_d for leachate-impacted sandy soils for Ra was identified as a sensitive parameter in the DOE probabilistic sensitivity analysis performed as part of the FY14 SDF Special Analysis document. In the DOE 2015 Response to the NRC 2014 RAI Comments (see RAI Comment FFT-3 in that document), the DOE referenced future research, but did not respond to the entire specific concern raised by the NRC staff. That information is needed to support DOE assumptions about radionuclide transport in the UZ at the SDF.
	Path Forward: Provide an explanation of the origin of the leachate impacted K_d values listed in Table 4.1-3 of the DOE FY14 SDF Special Analysis document, including the original reference(s).

DOE Response to FFT-6

For greater clarity, Table 4.1-3 of the FY2014 SDF SA should have included note "g" for every single leachate-impacted K_d value except neptunium (Np) and protactinium (Pa). This note reads: Multiplied the "cement leachate impact factor" from SRNL-STI-2009-00473 to the "without leachate" value. Specifically, this cement leachate impact factor comes from the 10th column of Table 13 of the *Geochemical Data Package for Performance Assessment Calculations Related to the Savannah River Site*. [SRNL-STI-2009-00473] These values are reproduced here as Table FFT-6.1.

The development of these cement leachate impact factors is described in Sections 4.2.4 and 4.2.5 of SRNL-STI-2009-00473. Briefly, the factors were developed based on measured differences between cementitious-leachate impacted and non-impacted K_d values for the Hanford PAs, as cited in the *Geochemical Processes Data Package for the Vadose Zone in the Single-Shell Tank Waste Management Areas at the Hanford Site*. [PNNL-16663]

To determine each specific leachate-impacted K_d value, the non-impacted K_d value was simply multiplied by the corresponding cement leachate impact factor from Table FFT-6.1. The two exceptions are for neptunium and protactinium, which applied a cement leachate impact factor of 20 (instead of 1.5 from SRNL-STI-2009-00473, Table 13), based on the neptunium sorption test data presented in the *Estimated Neptunium Sediment Sorption Values as a Function of pH and Measured Barium and Radium K_d Values*. [SRNL-STI-2011-00011]

Table FFT-6.1: Cement Leachate Impact Factors

Element	Cement Leachate Impact Factor (unitless)		Element	Cement Leachate Impact Factor (unitless)
Ac	1.5		Lu	1.5
Ag	3.2		Mn	1.4
Al	1.5		Mo	1.4
Am	1.5		N	0.1
Ar	1		Na	1
As	1.4		Nb	1.4
At	0.1		Ni	3.2
Ba	3		Np	20 [a]
Bi	1.5		Pa	20 [a]
Bk	1.5		Pb	3.2
C	5		Pd	3.2
Ca	3		Po	2
Cd	3		Pt	3.2
Ce	1.5		Pu	2
Cf	1.5		Ra	3
Cl	0.1		Rb	1
Cm	1.5		Re	0.1
Co	3.2		Rn	1
Cr	1.4		Sb	1.4
Cs	1		Se	1.4
Cu	3.2		Sm	1.5
Eu	1.5		Sn	3
F	0.1		Sr	3
Fe	1.5		Tc	0.1
Fr	1		Te	1.4
Gd	1.5		Th	2
H	1		Tl	1
Hg	3.2		U	3
I	0.1		Y	1.5
K	1		Zn	3
Kr	1		Zr	2

[Source: SRNL-STI-2009-00473, Table 13]
Note: (a) Based on SRNL-STI-2011-00011.

Table FFT-6.2 shows the clayey soil K_d values, identifies the source for those values, and shows the corresponding cement leachate impact factor. The product of the clayey soil K_d and the cement leachate impact factor is displayed as the leachate-impacted clayey soil K_d. Table FFT-6.3 provides this equivalent data for sandy soil K_ds. These K_d values reflect the data in Table 4.1-3 of the FY2014 SDF SA which were rounded to the nearest tenth. This reflects the level of precision used in the GoldSim modeling. For the PORFLOW modeling, the inputs for the K_d values were rounded to the nearest hundredth.

Table FFT-6.2: K_d Values for Clayey Soils

Element	K_d (mL/g)	Reference	Location in Reference	Cement Leachate Impact Factor (unitless)	Leachate-Impacted K_d (mL/g)
Ac	8,500	SRNL-STI-2009-00473	Table 16	1.5	12,750
Ag	30	SRNL-STI-2010-00493	Table 9	3.2	96
Al	1,300	SRNL-STI-2009-00473	Table 16	1.5	1,950
Am	8,500	SRNL-STI-2009-00473	Table 16	1.5	12,750
As	200	SRNL-STI-2009-00473	Table 16	1.4	280
At	0.9	SRNL-STI-2009-00473	Table 16	0.1	0.09
Ba	101	SRNL-STI-2011-00011	Table 2-2	3	303
Bk	8,500	SRNL-STI-2009-00473	Table 16	1.5	12,750
C	400	SRNL-STI-2009-00473	Table 16	5	2,000
Cd	30	SRNL-STI-2009-00473	Table 16	3	90
Ce	8,500	SRNL-STI-2009-00473	Table 16	1.5	12,750
Cf	8,500	SRNL-STI-2009-00473	Table 16	1.5	12,750
Cl	8	SRNL-STI-2010-00493	Table 9	0.1	0.8
Cm	8,500	SRNL-STI-2009-00473	Table 16	1.5	12,750
Co	100	SRNL-STI-2009-00473	Table 16	3.2	320
Cr	400	SRNL-STI-2010-00493	Table 9	1.4	560
Cs	50	SRNL-STI-2009-00473	Table 16	1	50
Cu	70	SRNL-STI-2009-00473	Table 16	3.2	224
Eu	8,500	SRNL-STI-2009-00473	Table 16	1.5	12,750
Fe	400	SRNL-STI-2009-00473	Table 16	1.5	600
Fr	50	SRNL-STI-2009-00473	Table 16	1	50
Gd	8,500	SRNL-STI-2009-00473	Table 16	1.5	12,750
H	0	Assigned a value of zero.			
Hg	1,000	SRNL-STI-2009-00473	Table 16	3.2	3,200
I	3	SRNL-STI-2012-00518	page iv	0.1	0.3
K	25	SRNL-STI-2009-00473	Table 16	1	25
Mn	200	SRNL-STI-2009-00473	Table 16	1.4	280
N	0	Assigned a value of zero.			
Na	25	SRNL-STI-2009-00473	Table 16	1	25
Nb	900	ML073510127	Section 2.4.5	1.4	1,260
Ni	30	SRNL-STI-2009-00473	Table 16	3.2	96
Np	9	SRNL-STI-2009-00473	Table 16	20	180
Pa	9	SRNL-STI-2009-00473	Table 16	20	180
Pb	5,000	SRNL-STI-2009-00473	Table 16	3.2	16,000

Table FFT-6.2: K_d Values for Clayey Soils (continued)

Element	K_d (mL/g)	Reference	Location in Reference	Cement Leachate Impact Factor (unitless)	Leachate-Impacted K_d (mL/g)
Pd	30	SRNL-STI-2009-00473	Table 16	3.2	96
Pm	0	Assigned a value of zero.			
Po	5,000	SRNL-STI-2009-00473	Table 16	2	10,000
Pr	0	Assigned a value of zero.			
Pt	30	SRNL-STI-2009-00473	Table 16	3.2	96
Pu	5,950	SRNL-STI-2009-00473	Table 16	2	11,900
Ra	185	SRNL-STI-2011-00011	Table 2-2	3	555
Rb	50	SRNL-STI-2009-00473	Table 16	1	50
Re	1.8	SRNL-STI-2009-00473	Table 16	0.1	0.18
Rh	0	Assigned a value of zero.			
Rn	0	Assigned a value of zero.			
Ru	0	Assigned a value of zero.			
Sb	2,500	SRNL-STI-2009-00473	Table 16	1.4	3,500
Se	1,000	SRNL-STI-2009-00473	Table 16	1.4	1,400
Sm	8,500	SRNL-STI-2009-00473	Table 16	1.5	12,750
Sn	5,000	SRNL-STI-2009-00473	Table 16	3	15,000
Sr	17	SRNL-STI-2011-00011	Table 2-2	3	51
Tc	1.8	SRNL-STI-2009-00473	Table 16	0.1	0.18
Te	1,000	SRNL-STI-2009-00473	Table 16	1.4	1,400
Th	2,000	SRNL-STI-2009-00473	Table 16	2	4,000
U	400	SRNL-STI-2010-00493	Table 8	3	1,200
V	0	Assigned a value of zero.			
Y	8,500	SRNL-STI-2009-00473	Table 16	1.5	12,750
Zn	30	SRNL-STI-2009-00473	Table 16	3	90
Zr	2,000	SRNL-STI-2009-00473	Table 16	2	4,000

Table FFT-6.3: K_d Values for Sandy Soils

Element	K_d (mL/g)	Reference	Location in Reference	Cement Leachate Impact Factor (unitless)	Leachate-Impacted K_d (mL/g)
Ac	1,100	SRNL-STI-2009-00473	Table 16	1.5	1,650
Ag	10	SRNL-STI-2010-00493	Table 9	3.2	32
Al	1,300	SRNL-STI-2009-00473	Table 16	1.5	1,950
Am	1,100	SRNL-STI-2009-00473	Table 16	1.5	1,650
As	100	SRNL-STI-2009-00473	Table 16	1.4	140
At	0.3	SRNL-STI-2009-00473	Table 16	0.1	0.03
Ba	15	SRNL-STI-2011-00011	Table 2-2	3	45
Bk	1,100	SRNL-STI-2009-00473	Table 16	1.5	1,650
C	10	SRNL-STI-2009-00473	Table 16	5	50
Cd	15	SRNL-STI-2009-00473	Table 16	3	45
Ce	1,100	SRNL-STI-2009-00473	Table 16	1.5	1,650
Cf	1,100	SRNL-STI-2009-00473	Table 16	1.5	1,650
Cl	1	SRNL-STI-2010-00493	Table 9	0.1	0.1
Cm	1,100	SRNL-STI-2009-00473	Table 16	1.5	1,650
Co	40	SRNL-STI-2009-00473	Table 16	3.2	128
Cr	1,000	SRNL-STI-2010-00493	Table 9	1.4	1,400
Cs	10	SRNL-STI-2009-00473	Table 16	1	10
Cu	50	SRNL-STI-2009-00473	Table 16	3.2	160
Eu	1,100	SRNL-STI-2009-00473	Table 16	1.5	1,650
Fe	200	SRNL-STI-2009-00473	Table 16	1.5	300
Fr	10	SRNL-STI-2009-00473	Table 16	1	10
Gd	1,100	SRNL-STI-2009-00473	Table 16	1.5	1,650
H	0	Assigned a value of zero.			
Hg	800	SRNL-STI-2009-00473	Table 16	3.2	2,560
I	1	SRNL-STI-2012-00518	page iv	0.1	0.1
K	5	SRNL-STI-2009-00473	Table 16	1	5
Mn	15	SRNL-STI-2009-00473	Table 16	1.4	21
N	0	Assigned a value of zero.			
Na	5	SRNL-STI-2009-00473	Table 16	1	5
Nb	160	ML073510127	Section 2.4.5	1.4	224
Ni	7	SRNL-STI-2009-00473	Table 16	3.2	22.4
Np	3	SRNL-STI-2009-00473	Table 16	20	60
Pa	3	SRNL-STI-2009-00473	Table 16	20	60
Pb	2,000	SRNL-STI-2009-00473	Table 16	3.2	6,400

Table FFT-6.3: K_d Values for Sandy Soils (continued)

Element	K_d (mL/g)	Reference	Location in Reference	Cement Leachate Impact Factor (unitless)	Leachate-Impacted K_d (mL/g)
Pd	7	SRNL-STI-2009-00473	Table 16	3.2	22.4
Pm	0	Assigned a value of zero.			
Po	2,000	SRNL-STI-2009-00473	Table 16	2	4,000
Pr	0	Assigned a value of zero.			
Pt	7	SRNL-STI-2009-00473	Table 16	3.2	22.4
Pu	650	SRNL-STI-2011-00672	Section 5.0	2	1,300
Ra	25	SRNL-STI-2011-00011	Table 2-2	3	75
Rb	10	SRNL-STI-2009-00473	Table 16	1	10
Re	0.6	SRNL-STI-2009-00473	Table 16	0.1	0.06
Rh	0	Assigned a value of zero.			
Rn	0	Assigned a value of zero.			
Ru	0	Assigned a value of zero.			
Sb	2,500	SRNL-STI-2009-00473	Table 16	1.4	3,500
Se	1,000	SRNL-STI-2009-00473	Table 16	1.4	1,400
Sm	1,100	SRNL-STI-2009-00473	Table 16	1.5	1,650
Sn	2,000	SRNL-STI-2009-00473	Table 16	3	6,000
Sr	5	SRNL-STI-2011-00011	Table 2-2	3	15
Tc	0.6	SRNL-STI-2009-00473	Table 16	0.1	0.06
Te	1,000	SRNL-STI-2009-00473	Table 16	1.4	1,400
Th	900	SRNL-STI-2009-00473	Table 16	2	1,800
U	300	SRNL-STI-2010-00493	Table 8	3	900
V	0	Assigned a value of zero.			
Y	1,100	SRNL-STI-2009-00473	Table 16	1.5	1,650
Zn	15	SRNL-STI-2009-00473	Table 16	3	45
Zr	900	SRNL-STI-2009-00473	Table 16	2	1,800

CLARIFYING COMMENTS (CC)

CC-1

CC-1	**Comment:** Please clarify which direction (i.e., into or out of the disposal structures) the water is flowing through the construction joints. In the first 2,000 years after site closure[1], the volumetric flowrate through the joints and floor is essentially equivalent for those two different materials. It is not clear to the NRC staff if that is a coincidence or if there is another explanation (e.g., water flowing up through the construction joints and then down through the floor).
	Basis: Not provided.
	Path Forward: Not provided.

DOE Response to CC-1

Figure 4.4-12 of the FY2014 SDF SA shows the volumetric flow rates for various features of the 375-foot diameter SDUs. For this discussion, this SA figure has been modified to show the flows for only the floor and the joint materials within the first 2,000 years of the simulation (Figure CC-1.1). As noted in the comment, the two are very similar.

[1] In the context of these RAIs and RAI responses, "site closure" refers to facility closure of the Saltstone Disposal Facility and not the closure of the Savannah River Site.

Figure CC-1.1: Total Volumetric Flow Rates through the 375-Foot Diameter SDUs for Floor and Joint Materials (2,000 Years)

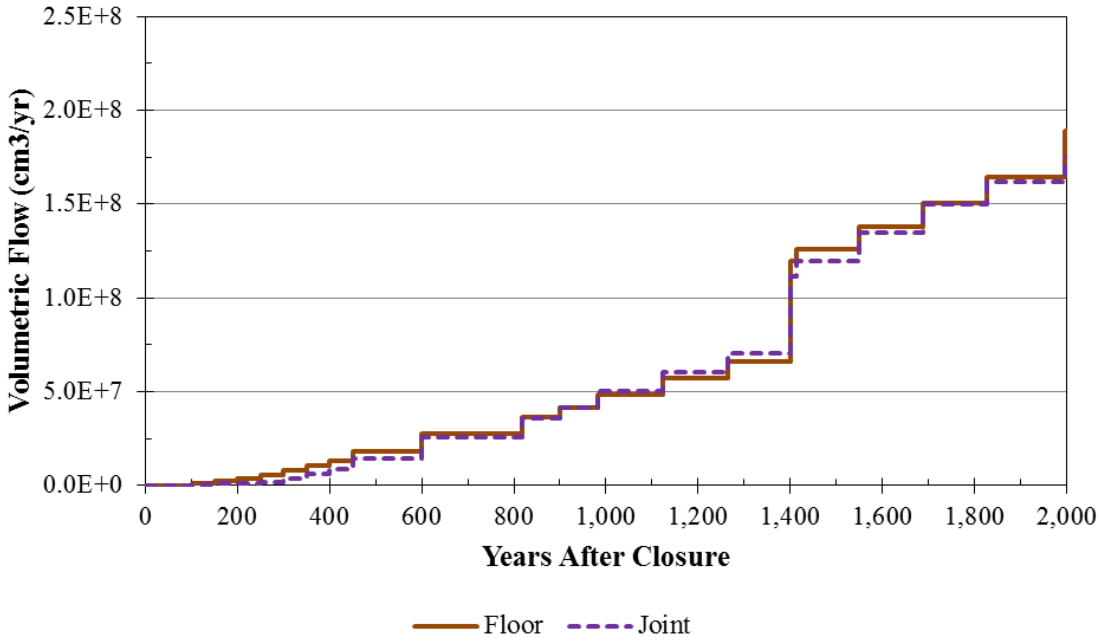

In PORFLOW, the joint material properties are assigned to the roof-to-wall joint, the floor-to-wall joint, the roof waterstops and the floor waterstops. The volumetric flow through the joint material, as depicted in Figure CC-1.1, combines all volumetric flow through these various features. Because the floor represents a much larger area and the joint material represents a more conductive material, it is coincidental that the two volumetric flows are so similar.

During the first 1,400 years of the simulation, water generally flows radially inward through the roof-to-wall joint, radially outward through the floor-to-wall joint, and downward through the waterstops. After the first 1,400 years, flow through the roof-to-wall and floor-to-wall joints reverse direction to flow radially outward and radially inward, respectively. There is no significant upward flow through the joint material or the floor.

Throughout the rest of this RAI response, close-up vertical cross-sections are provided to depict flow through select SDU features at various time periods. Figure CC-1.2 presents an example of a vertical cross-section of a 375-foot diameter SDU, in full view. Effectively, this figure shows the face of a wedge sliced from the center of the SDU (left axis of figure) and extending into the backfill beyond the walls (right side of figure).

Figure CC-1.2: Example of the Vertical Cross-Section of a 375-Foot Diameter SDU

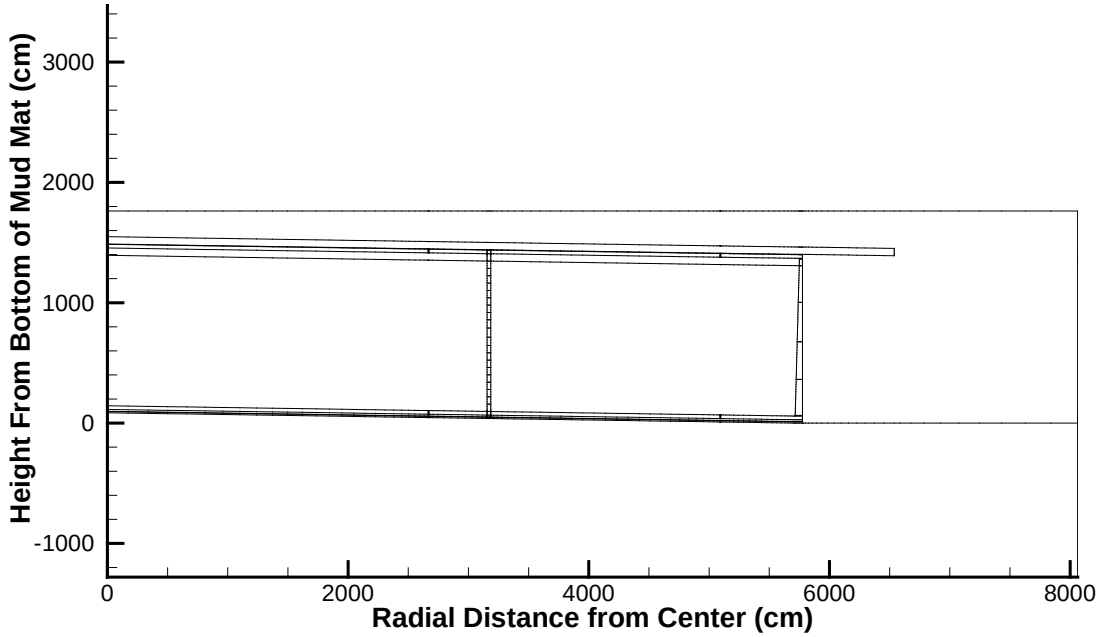

Figure CC-1.3 provides a more detailed view of the outer edge of the SDU and identifies a number of the modeled features.

Figure CC-1.3: Features Near the Outer Edge of a Vertical Cross-Section of an SDU

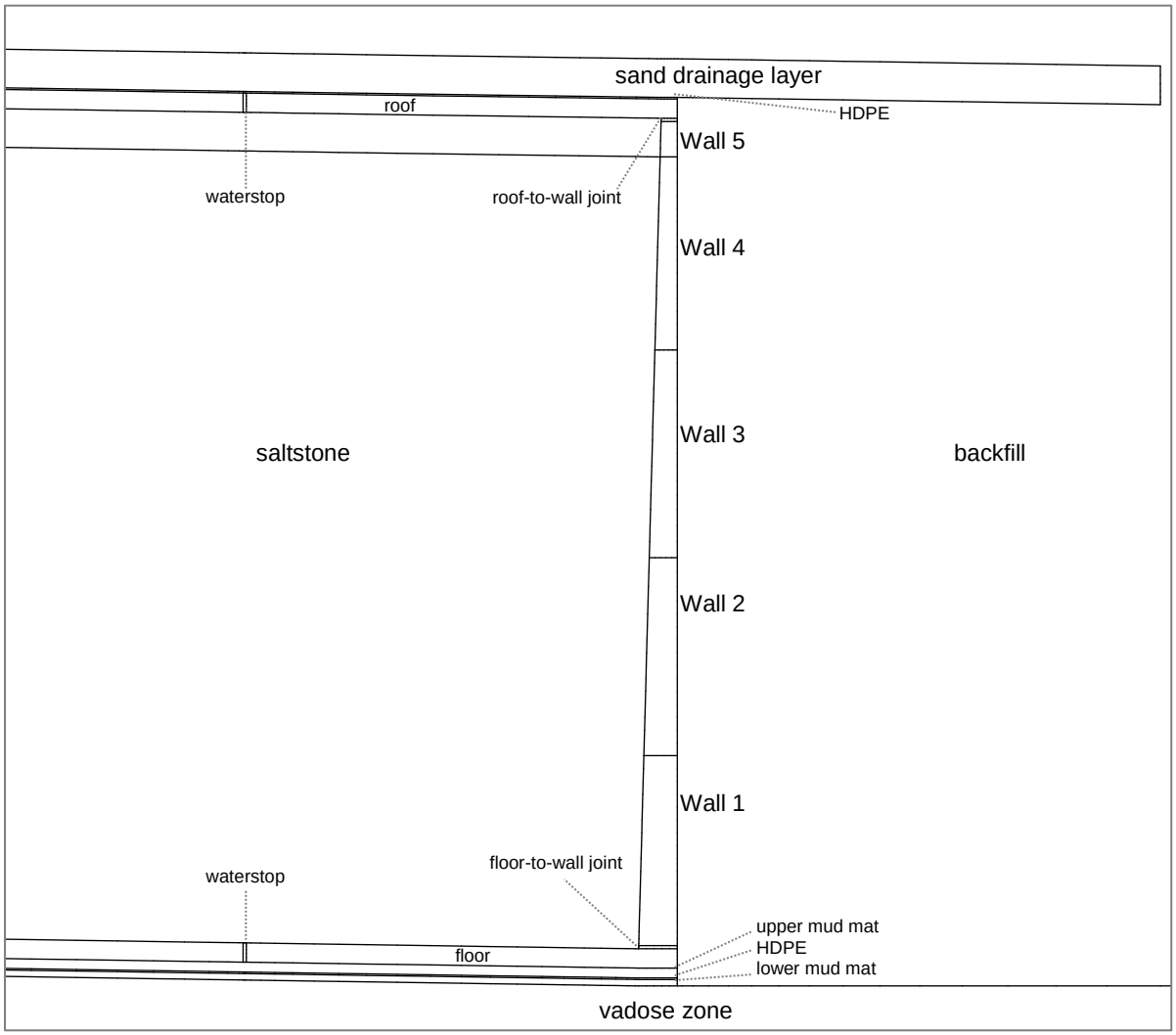

Flow through a number of these features is more closely examined in the following discussions. Arrows within these figures indicate the direction of flow through the feature during the select time period. The coloring within each figure indicates the magnitude of flow velocity in the horizontal direction, where red indicates relatively high velocity flow in a radially outward direction, green indicates extremely low flow rates, and dark blue indicates relatively high velocity flow in a radially inward direction.

Roof-to-Wall Joint

From 0 years to 250 years the flow direction through the roof-to-wall joint is predominantly inward (Figures CC-1.4 and CC-1.5). From 250 years to 1,400 years the flow shifts to predominantly downward flow (with some inward flow) (Figures CC-1.5 and CC-1.6). At 1,400 years, flow transitions to a predominantly outward direction (with some downward flow) (Figure CC-1.7). The direction of flow remains relatively constant for the remainder of the simulation.

Figure CC-1.4: Flow Direction Through the Roof-to-Wall Joints of the 375-Foot Diameter SDUs (Time Interval 01: 0 to 50 Years)

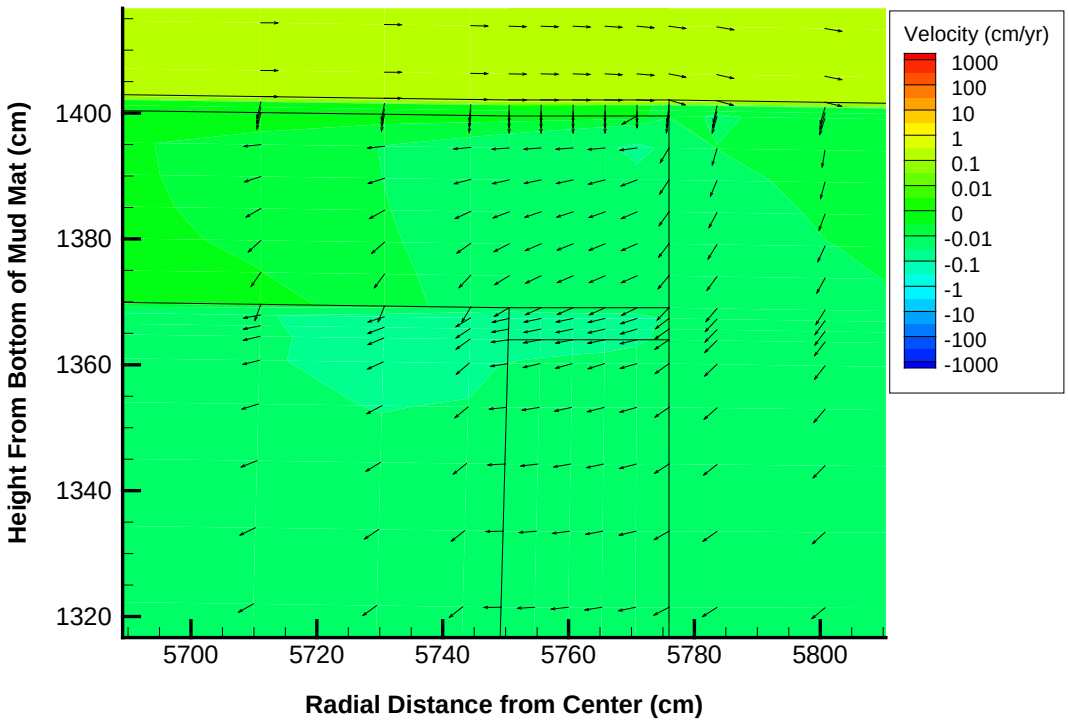

Figure CC-1.5: Flow Direction Through the Roof-to-Wall Joints of the 375-Foot Diameter SDUs (Time Interval 05: 200 to 250 Years)

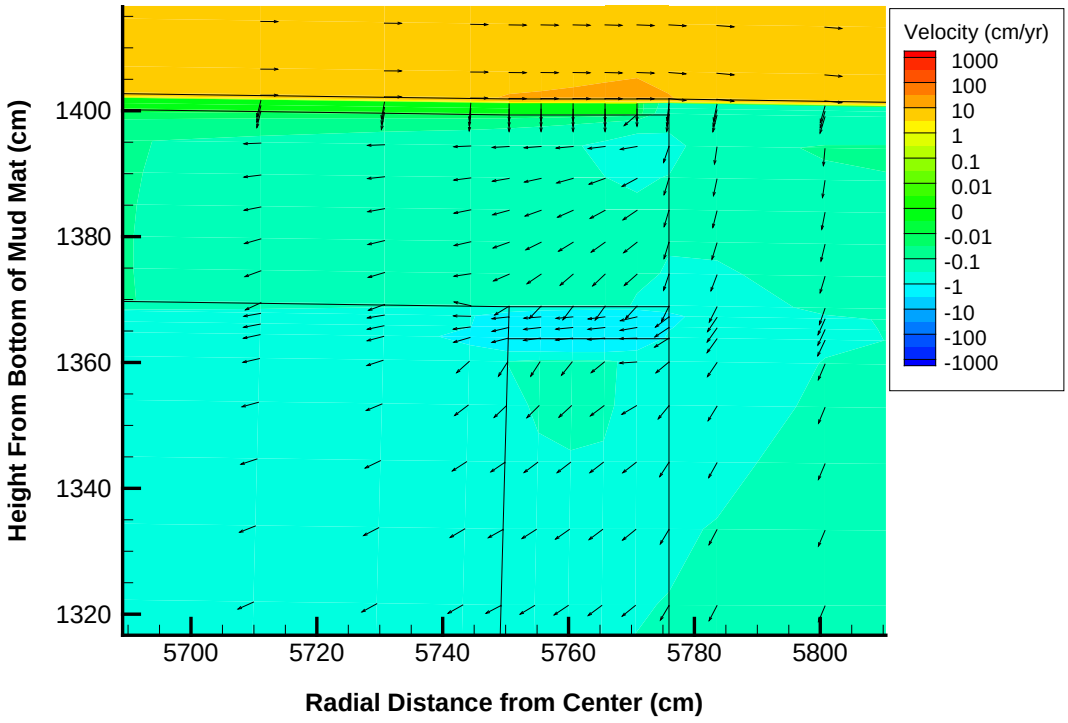

Figure CC-1.6: Flow Direction Through the Roof-to-Wall Joints of the 375-Foot Diameter SDUs (Time Interval 16: 1,265 to 1,400 Years)

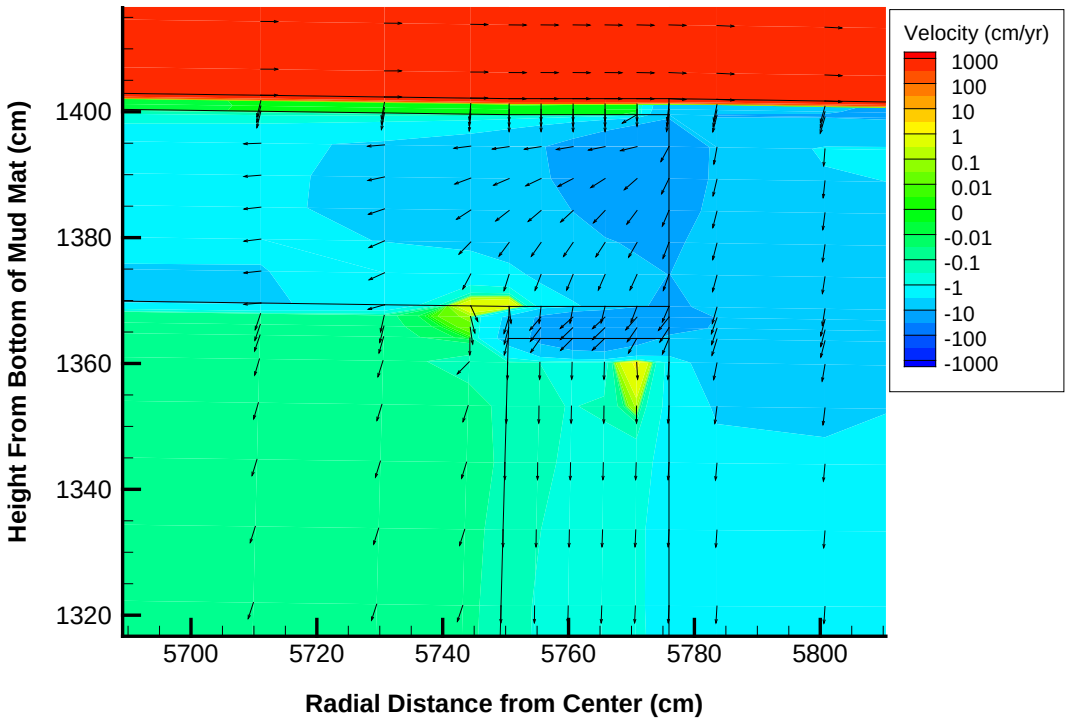

Figure CC-1.7: Flow Direction Through the Roof-to-Wall Joints of the 375-Foot Diameter SDUs (Time Interval 17: 1,400 to 1,413 Years)

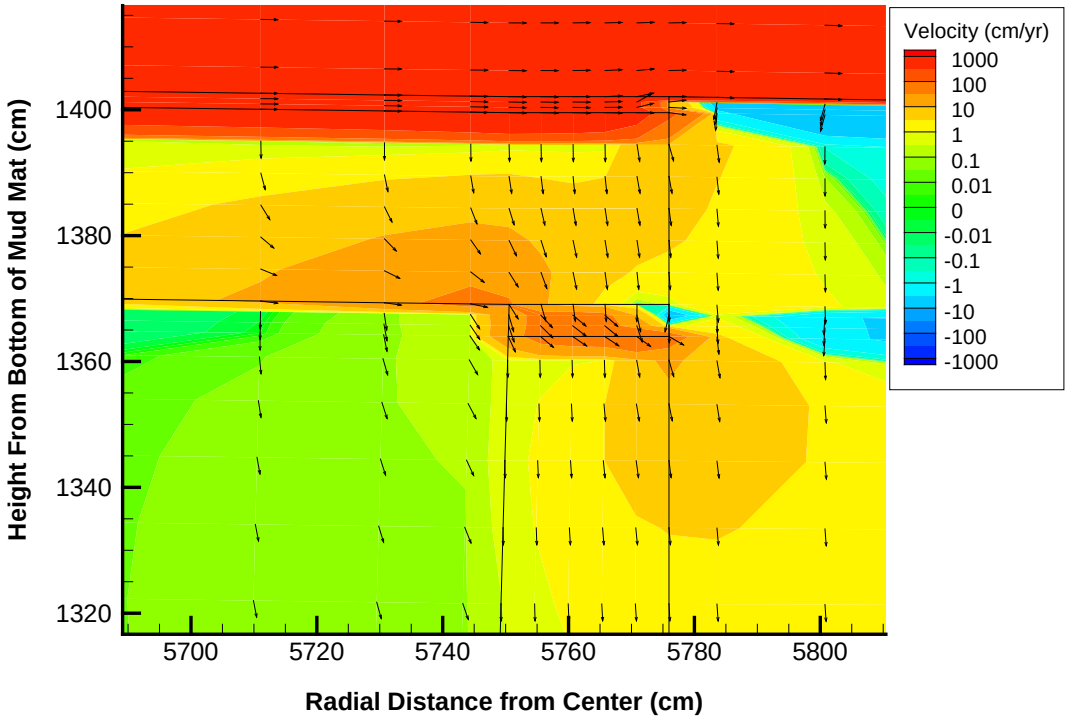

Floor-to-Wall Joint

From 0 years to 350 years the flow direction through the floor-to-wall joint is predominantly outward (Figures CC-1.8 and CC-1.9). From 350 years to 1,400 years the flow shifts to predominantly downward flow (with some inward flow) (Figure CC-1.9 and CC-1.10). At 1,400 years, the flow transitions to predominantly inward flow (with some downward flow) (Figure CC-1.11). The direction of flow remains relatively constant for the remainder of the simulation.

Figure CC-1.8: Flow Direction Through the Floor-to-Wall Joints of the 375-Foot Diameter SDUs (Time Interval 01: 0 to 50 Years)

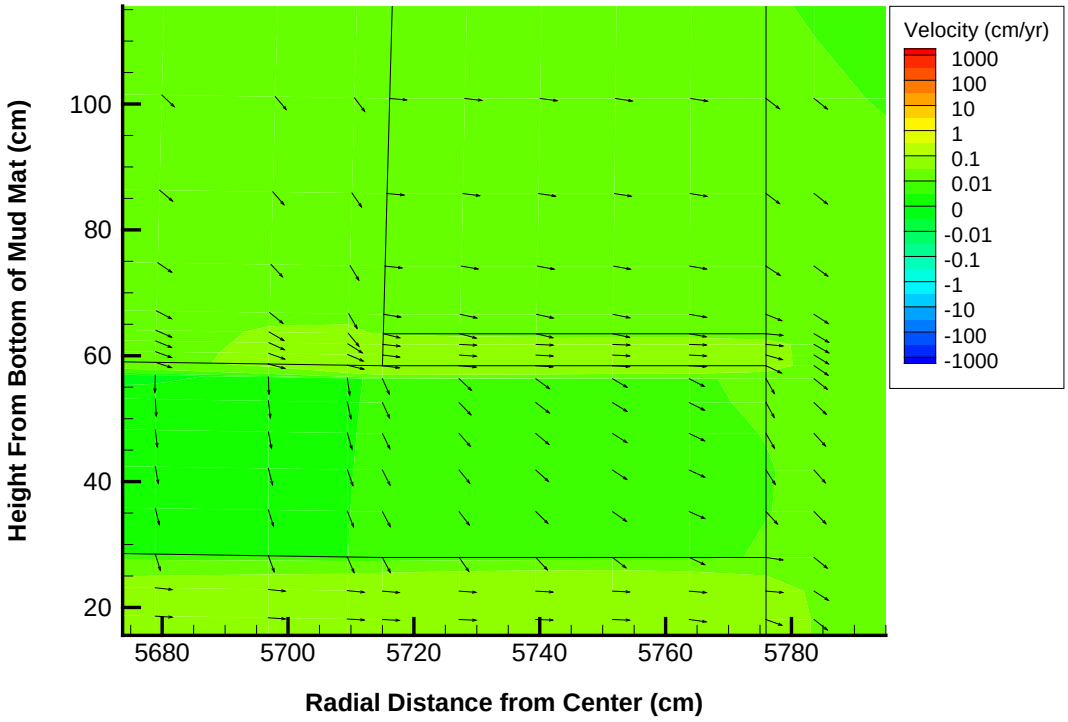

Figure CC-1.9: Flow Direction Through the Floor-to-Wall Joints of the 375-Foot Diameter SDUs (Time Interval 07: 300 to 350 Years)

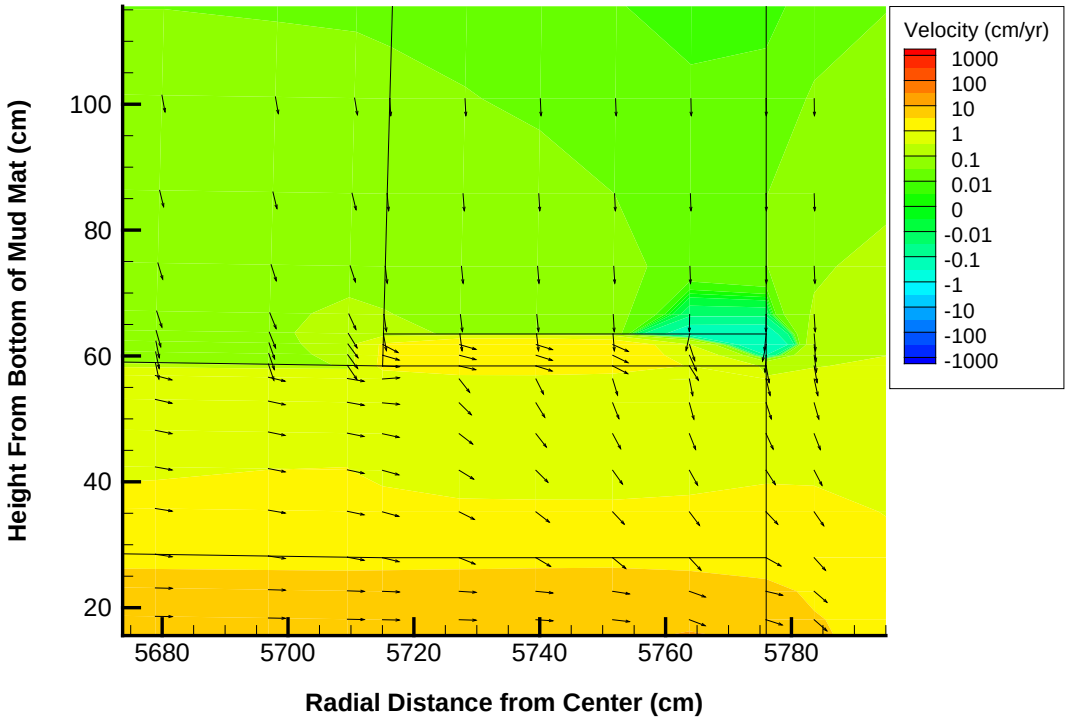

Figure CC-1.10: Flow Direction Through the Floor-to-Wall Joints of the 375-Foot Diameter SDUs (Time Interval 16: 1,265 to 1,400 Years)

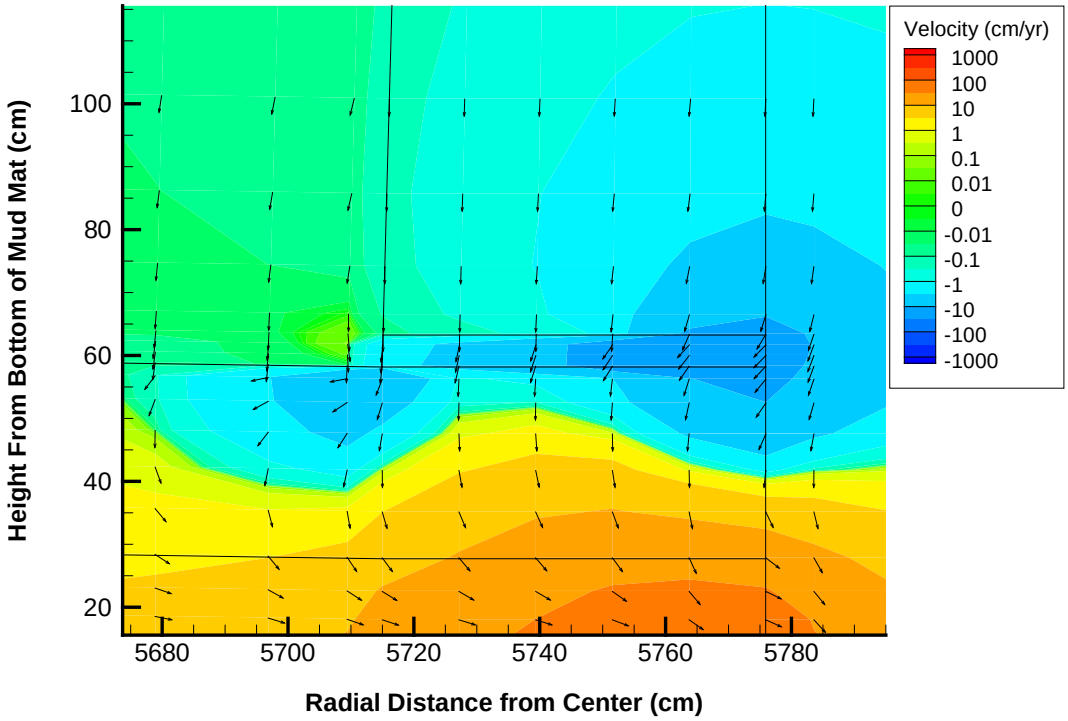

Figure CC-1.11: Flow Direction Through the Floor-to-Wall Joints of the 375-Foot Diameter SDUs (Time Interval 17: 1,400 to 1,413 Years)

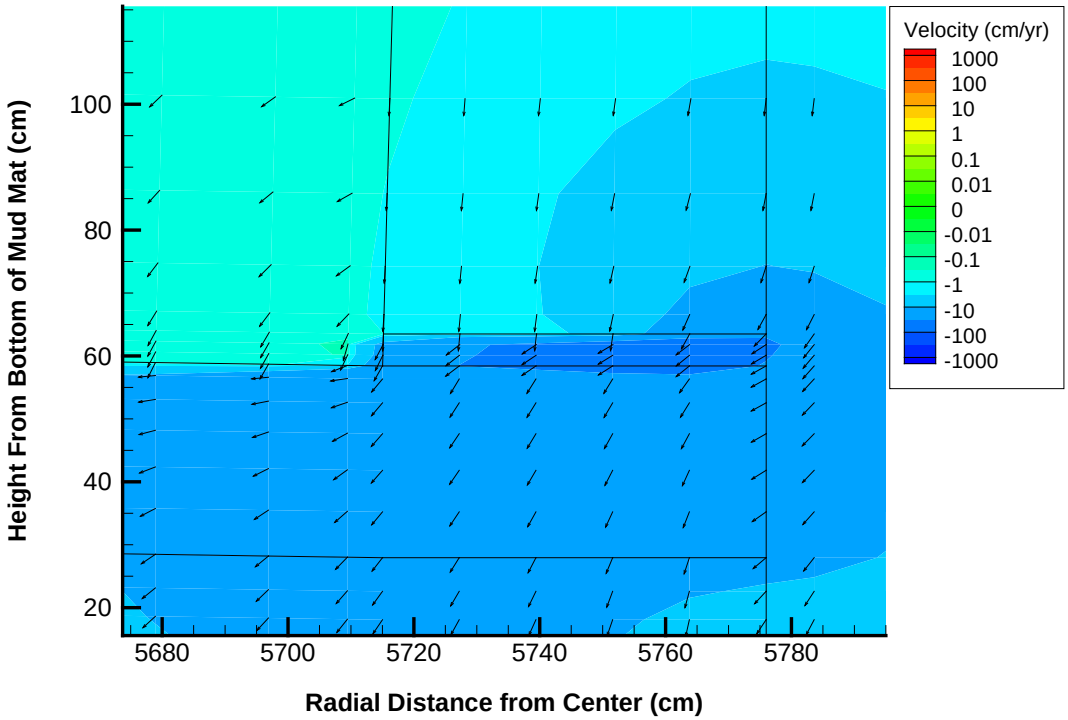

Roof Waterstops

As a modeling simplification, there are two waterstops in the roof (an interior waterstop, between the center of the SDU and the roof support column, and an exterior waterstop, between the roof support column and the wall of the SDU). Throughout the simulation, both roof waterstops exhibit similar behavior; however, the interior waterstop showed greater downward flow and less influence from interactions with the distinctive flow patterns at the outer edges of the SDU. Therefore, the following discussions (and figures) only pertain to the exterior roof waterstop.

From 0 years to 150 years the flow direction through the waterstop in the roof is predominantly inward (Figures CC-1.12 and CC-1.13). From 150 years to 600 years the flow shifts to predominantly downward flow (with some inward flow) (Figures CC-1.13 and CC-1.14). From 600 years to 1,400 years the flow shifts back to inward with some downward (Figures CC-1.14 and CC-1.15). At 1,400 years the flow shifts to predominantly downward with some outward flow (Figure CC-1.16). After 1,400 years the direction of flow gradually turns more downward, until flow through the waterstop is almost entirely downward (Figures CC-1.16 and CC-1.17).

Figure CC-1.12: Flow Direction Through the Roof Waterstop of the 375-Foot Diameter SDUs (Time Interval 01: 0 to 50 Years)

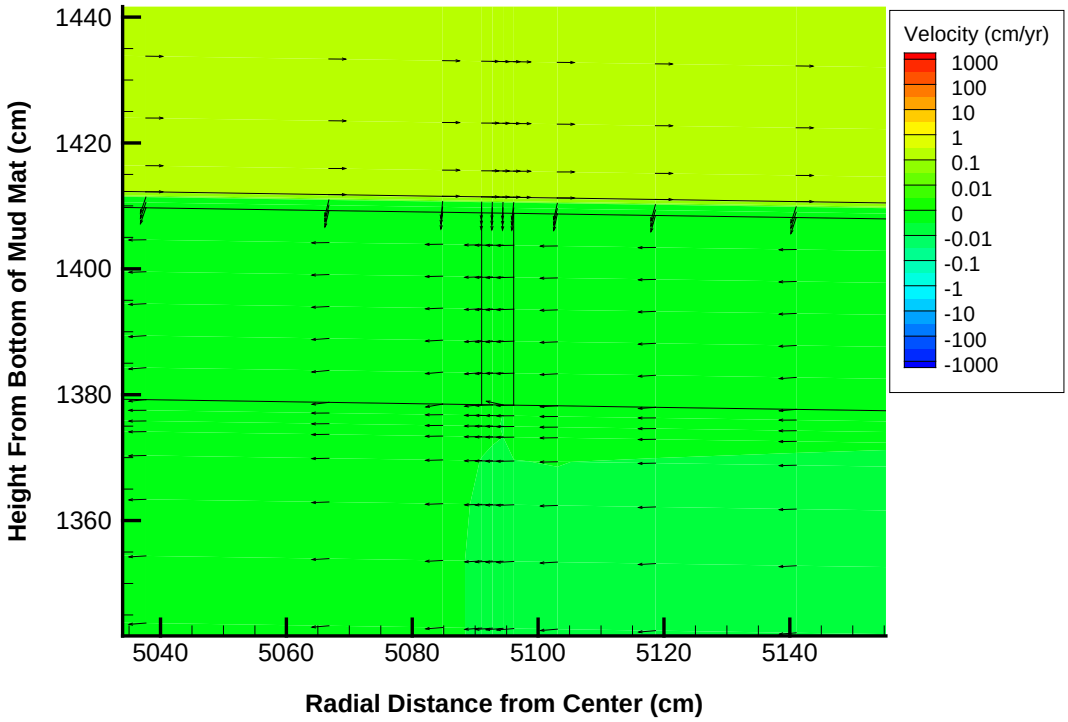

Figure CC-1.13: Flow Direction Through the Roof Waterstop of the 375-Foot Diameter SDUs (Time Interval 04: 150 to 200 Years)

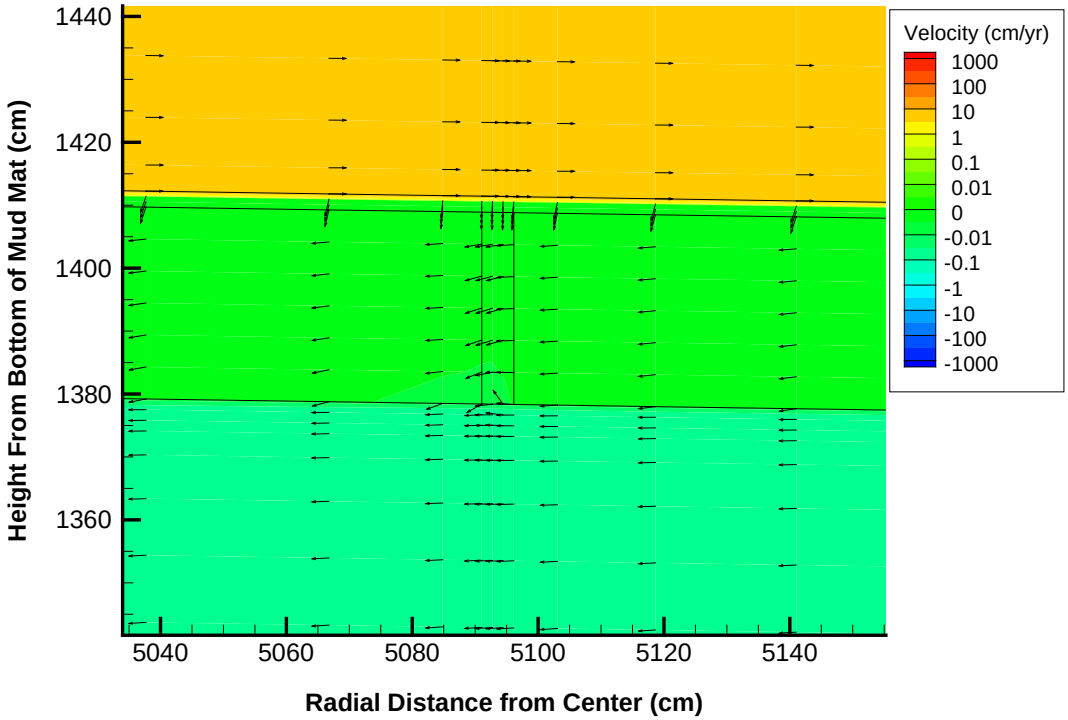

Figure CC-1.14: Flow Direction Through the Roof Waterstop of the 375-Foot Diameter SDUs (Time Interval 10: 450 to 600 Years)

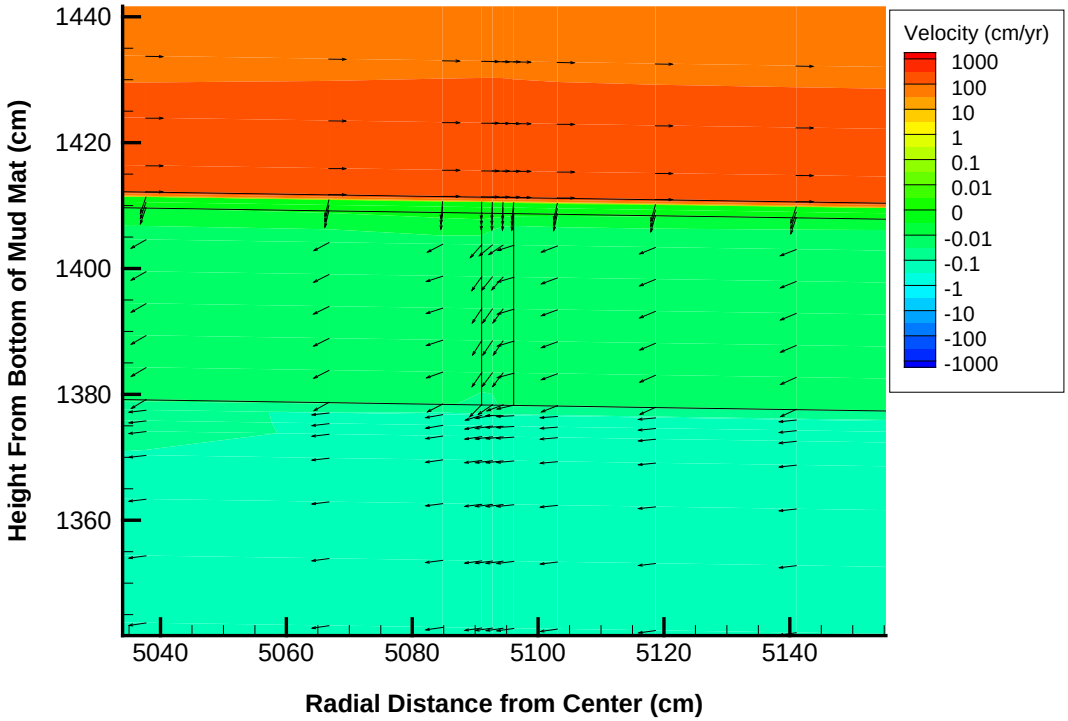

Figure CC-1.15: Flow Direction Through the Roof Waterstop of the 375-Foot Diameter SDUs (Time Interval 16: 1,265 to 1,400 Years)

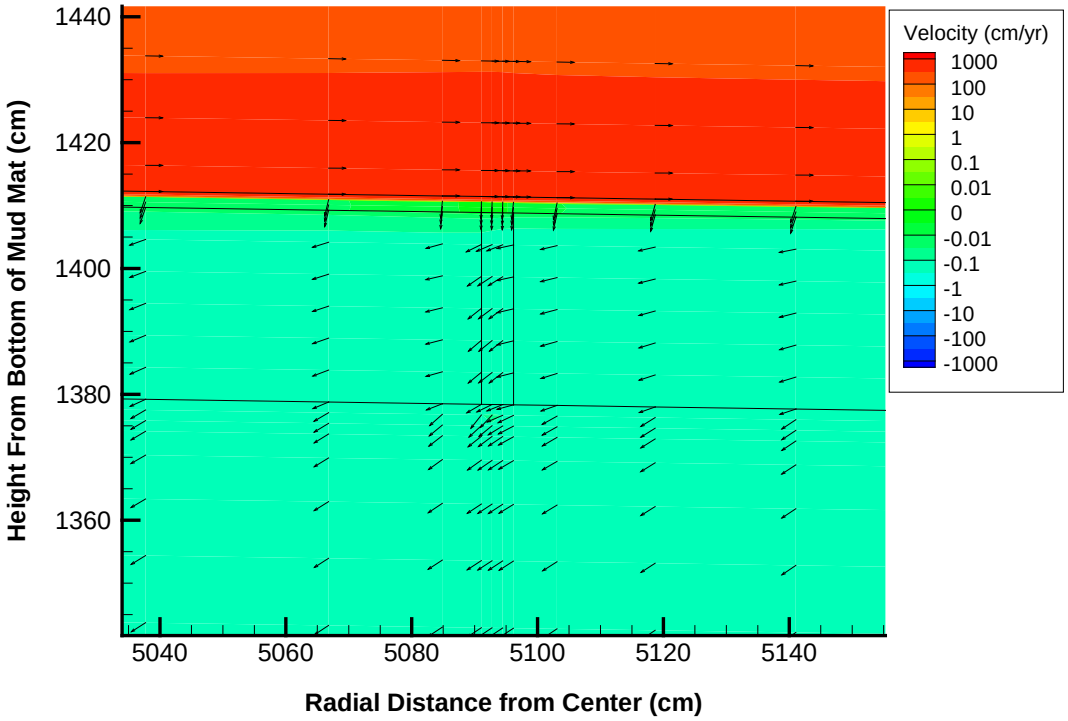

Figure CC-1.16: Flow Direction Through the Roof Waterstop of the 375-Foot Diameter SDUs (Time Interval 17: 1,400 to 1,413 Years)

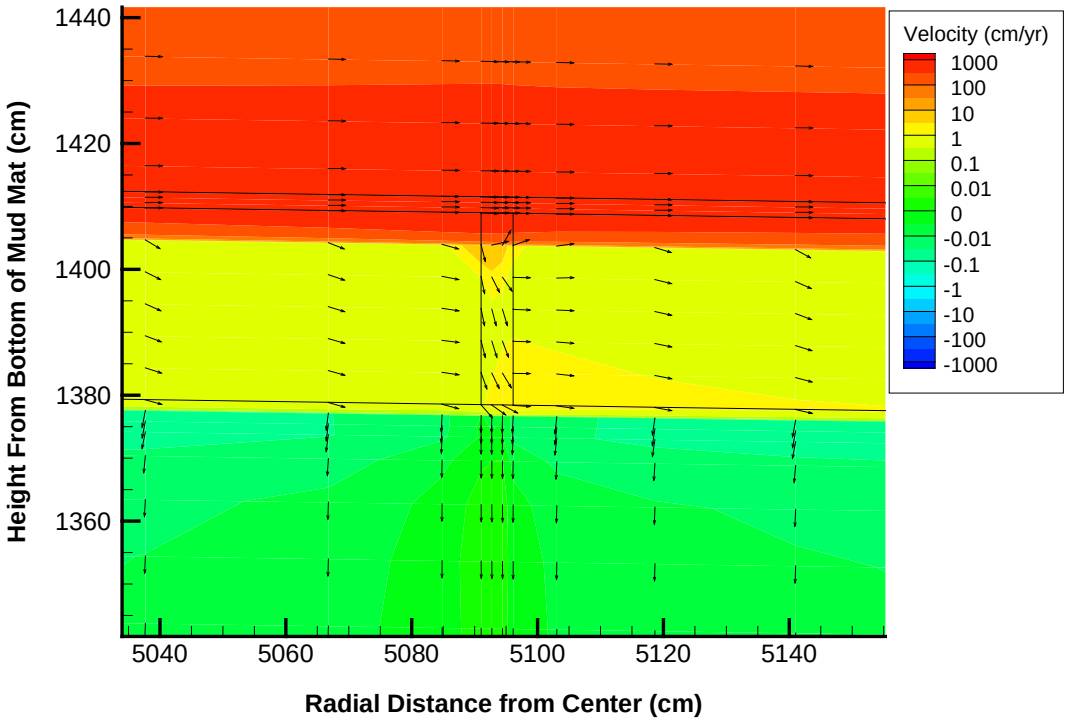

Figure CC-1.17: Flow Direction Through the Roof Waterstop of the 375-Foot Diameter SDUs (Time Interval 26: 3,165 to 3,457 Years)

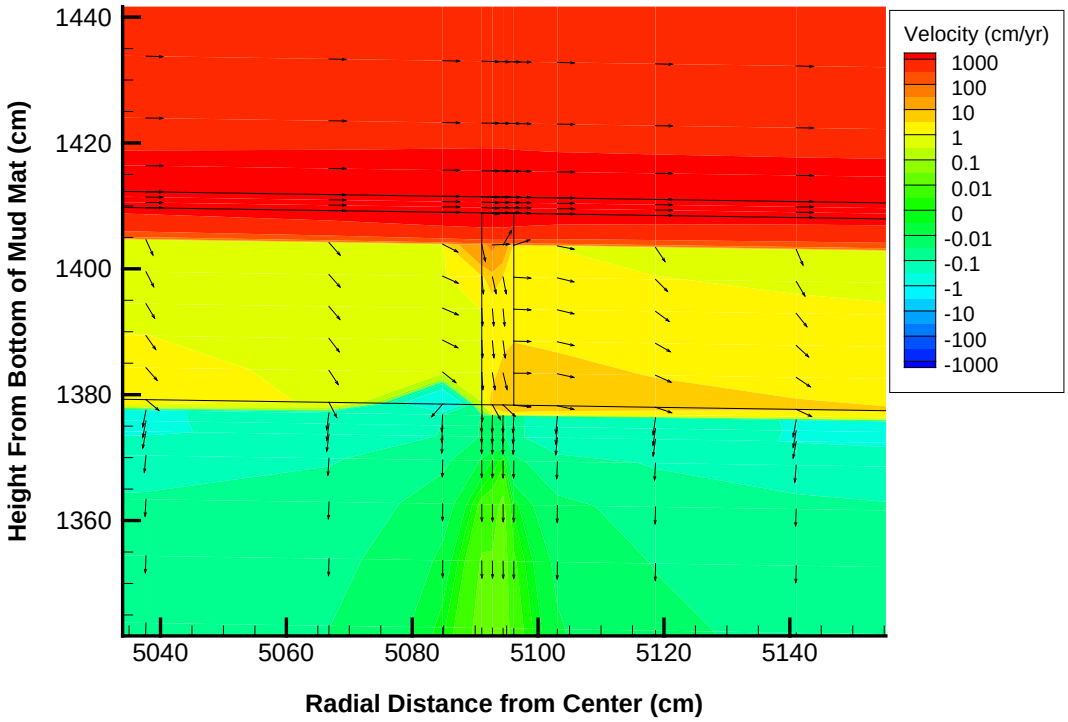

Floor Waterstops

As with the roof waterstops, the interior floor waterstop showed greater downward flow and less influence from the exterior flow patterns; therefore, the following discussions (and figures) only pertain to the exterior floor waterstop.

From 0 years to 150 years the flow direction through the waterstop in the floor is predominantly downward (Figure CC-1.18). From 150 years to 1,400 years the flow shifts towards the outward direction with some downward flow (Figures CC-1.19 and CC-1.20). At 1,400 years, the flow transitions to predominantly downward flow (with some inward flow) (Figure CC-1.21). After 1,400 years the direction of flow gradually becomes more downward (Figures CC-1.21 and CC-1.22).

Figure CC-1.18: Flow Direction Through the Floor Waterstop of the 375-Foot Diameter SDUs (Time Interval 01: 0 to 50 Years)

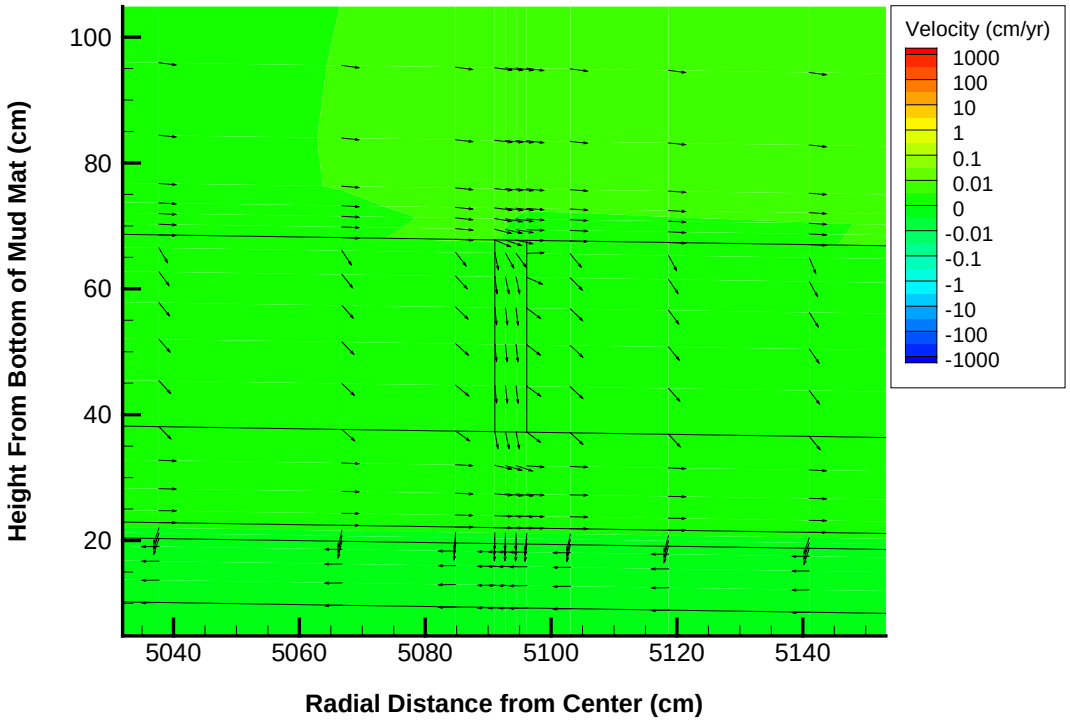

Figure CC-1.19: Flow Direction Through the Floor Waterstop of the 375-Foot Diameter SDUs (Time Interval 04: 150 to 200 Years)

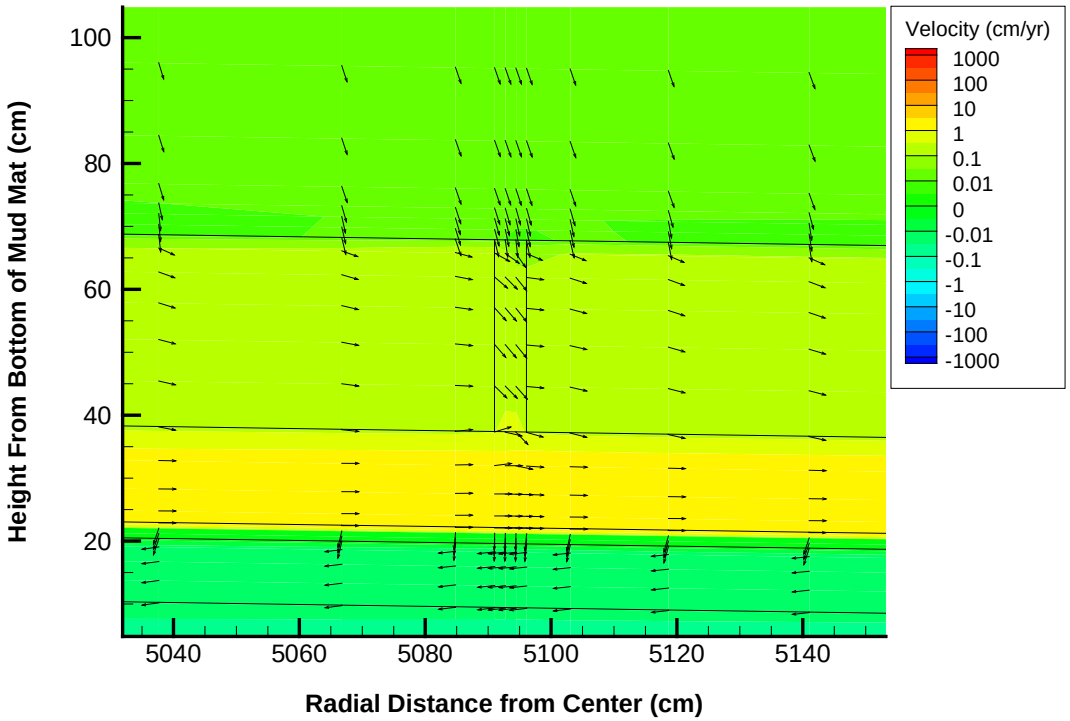

Figure CC-1.20: Flow Direction Through the Floor Waterstop of the 375-Foot Diameter SDUs (Time Interval 16: 1,265 to 1,400 Years)

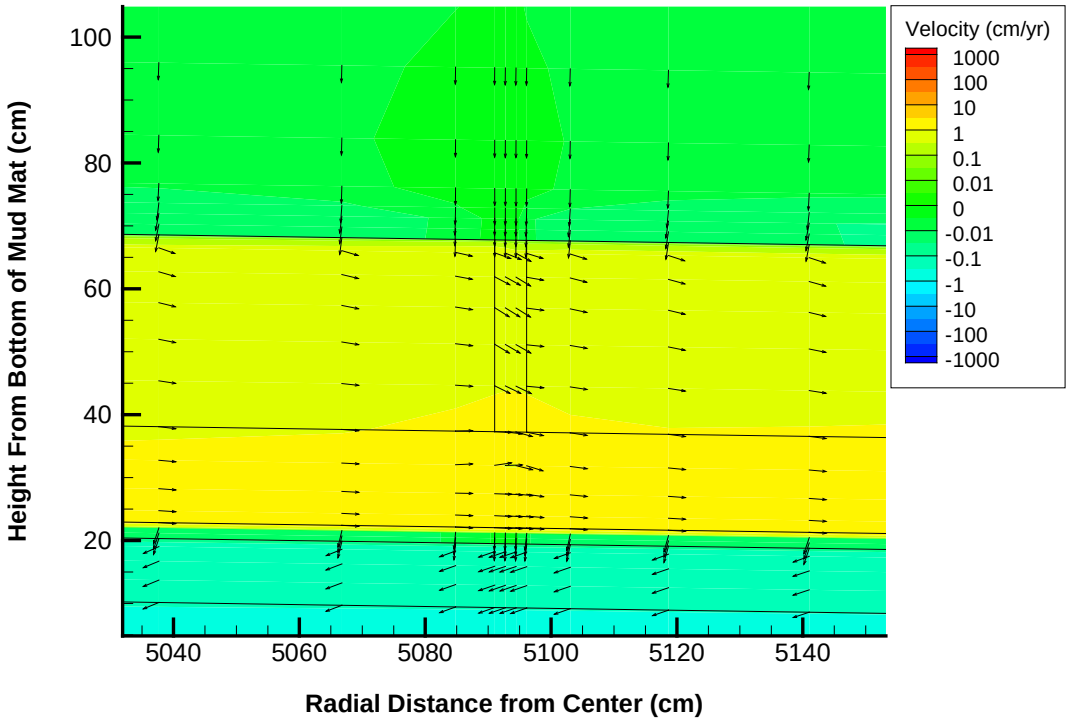

Figure CC-1.21: Flow Direction Through the Floor Waterstop of the 375-Foot Diameter SDUs (Time Interval 17: 1,400 to 1,413 Years)

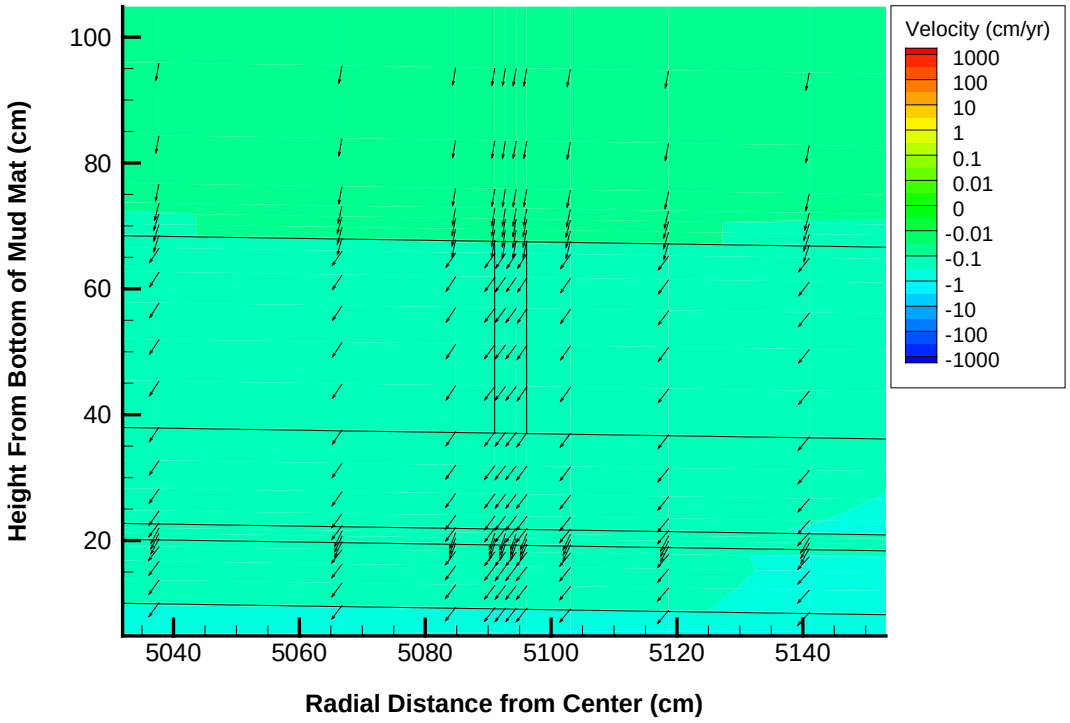

Figure CC-1.22: Flow Direction Through the Floor Waterstop of the 375-Foot Diameter SDUs (Time Interval 26: 3,165 to 3,457 Years)

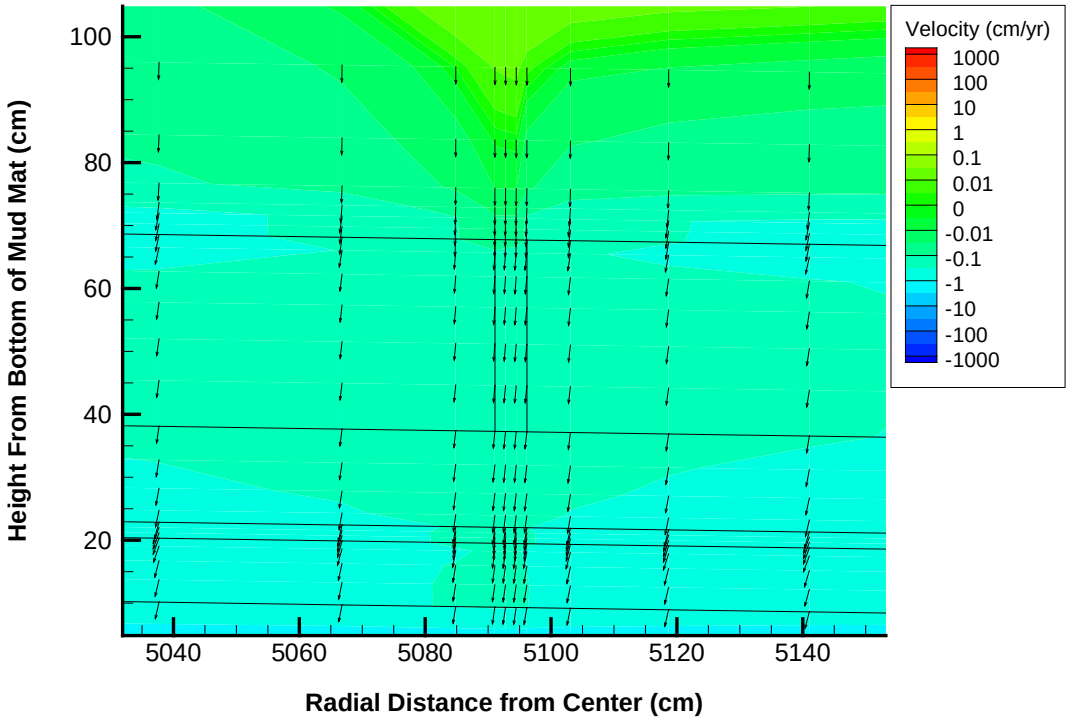

CC-2

CC-2	**Comment:** Section 5.6.3 of the DOE FY14 SDF Special Analysis document referenced the DOE 2009 SDF PA for the description for how the parameters were selected for inclusion in the probabilistic uncertainty analysis. That selection process was described as being based on "modeling experience informed by the basis for the selected values and available generic and site-specific data." Please clarify the role that the availability of generic and site-specific data played in the selection of parameters selected for inclusion in the probabilistic uncertainty analysis. Were parameters more likely to be included if data was scarce? Were parameters excluded from the uncertainty analysis on the basis that there was insufficient data available to generate a probabilistic distribution for the parameter value?
	Basis: Not provided.
	Path Forward: Not provided.

DOE Response to CC-2

Each model parameter was considered independently with respect to inclusion in the probabilistic uncertainty analysis (i.e., there was no strict methodology applied for parameter selection). In general:

- If a parameter was well understood (or currently known) and was unlikely to exhibit variability (e.g., the floor thickness of SDU 4), a reasonable value was applied.
- If a parameter was well understood (or currently known), was likely to exhibit variability, and was expected to have a significant impact on dose results, then an informed distribution was applied (see the parameters listed in Table CC-2.1).
- If a parameter was well understood (or currently known), was likely to exhibit variability, and was not expected to have a significant impact on dose results, then either an informed distribution was applied (see the parameters listed in Table CC-2.1) or a conservative value was assumed (e.g., the geometry factor for exposure from swimming).
- If a parameter was not well understood (or currently unknown) and was unlikely to exhibit variability (e.g., the fill height for future SDUs), then a conservative value was assumed.
- If a parameter was not well understood (or currently unknown), was likely to exhibit variability, and was not expected to have a significant impact on dose results (e.g., the moisture content of shower air), a reasonable value was assumed.
- If a parameter was not well understood (or currently unknown), was likely to exhibit variability, and was expected to have a significant impact on dose results (e.g., the hydraulic conductivity of fully degraded cementitious materials), a conservative value was assumed.

All parameters with assigned probabilistic distributions were sampled during the probabilistic GoldSim simulations. As such, all of these parameters were included in the probabilistic

uncertainty analysis provided in Section 5.6.4 of the FY2014 SDF SA. Similarly, all of these parameters provided some degree of influence on the dose results that were statistically analyzed as part of the probabilistic sensitivity analysis in Section 5.6.5 of the FY2014 SDF SA. However, as explained in Section 5.6.5.2 of the FY2014 SDF SA, due to computational limitations, not all of these parameters were included in the statistical analysis of parameter sensitivities. Appendix D of the FY2014 SDF SA provided the bases for selecting which variables were included in the probabilistic sensitivity analyses and which were excluded.

Future revisions of the Performance Assessment will consider a more formal approach to the selection of parameters for uncertainty sampling.

Table CC-2.1: Uncertainty Parameters in the FY2014 SDF SA GoldSim Model

Count	GoldSim Element Name	GoldSim Navigation Path	Basis for Distribution
1	SDU2_SatWidth	\DisposalUnits\VaultData	Described in SRR-CWDA-2009-00017, Section 5.6.3.8
2	SDU6_SatWidth	\DisposalUnits\VaultData	Described in SRR-CWDA-2009-00017, Section 5.6.3.8
3	UZthicknessDist	\DisposalUnits\VaultData	Described in SRR-CWDA-2009-00017, Section 5.6.3.5
4	Vault1_SatWidth	\DisposalUnits\VaultData	Described in SRR-CWDA-2009-00017, Section 5.6.3.8
5	Vault4_SatWidth	\DisposalUnits\VaultData	Described in SRR-CWDA-2009-00017, Section 5.6.3.8
6	CropIrrigationTimeUncert	\Dose_Parameter_Calculations\DoseParameters\CropParameters	Described in SRR-CWDA-2013-00058, Section 7.5.2
7	GardenSizeUncert	\Dose_Parameter_Calculations\DoseParameters\CropParameters	Described in SRR-CWDA-2013-00058, Section 7.5.2
8	RetentionUncert	\Dose_Parameter_Calculations\DoseParameters\CropParameters	Described in SRR-CWDA-2013-00058, Section 7.5.2
9	TillDepthUncert	\Dose_Parameter_Calculations\DoseParameters\CropParameters	Described in SRR-CWDA-2013-00058, Section 7.5.2
10	YieldUncert	\Dose_Parameter_Calculations\DoseParameters\CropParameters	Described in SRR-CWDA-2013-00058, Section 7.5.2
11	AirMassLoadingSoil_Uncert	\Dose_Parameter_Calculations\DoseParameters\ExposureAndInhalationParams	Described in SRR-CWDA-2013-00058, Section 7.4
12	ARF_Uncert	\Dose_Parameter_Calculations\DoseParameters\ExposureAndInhalationParams	Described in SRR-CWDA-2013-00058, Section 7.4
13	FractionUncertDrilling	\Dose_Parameter_Calculations\DoseParameters\ExposureAndInhalationParams	Described in SRR-CWDA-2013-00058, Section 7.4
14	FractionUncertGarden	\Dose_Parameter_Calculations\DoseParameters\ExposureAndInhalationParams	Described in SRR-CWDA-2013-00058, Section 7.4
15	FractionUncertShower	\Dose_Parameter_Calculations\DoseParameters\ExposureAndInhalationParams	Described in SRR-CWDA-2013-00058, Section 7.4
16	FractionUncertSwimming	\Dose_Parameter_Calculations\DoseParameters\ExposureAndInhalationParams	Described in SRR-CWDA-2013-00058, Section 7.4
17	UncertMultiplier_AirUptake	\Dose_Parameter_Calculations\DoseParameters\HumanUptakeParameters	Described in SRR-CWDA-2013-00058, Section 7.2.1
18	UncertMultiplier_FishUptake	\Dose_Parameter_Calculations\DoseParameters\HumanUptakeParameters	Described in SRR-CWDA-2013-00058, Section 7.2.1
19	UncertMultiplier_MeatUptake	\Dose_Parameter_Calculations\DoseParameters\HumanUptakeParameters	Described in SRR-CWDA-2013-00058, Section 7.2.1
20	UncertMultiplier_MilkUptake	\Dose_Parameter_Calculations\DoseParameters\HumanUptakeParameters	Described in SRR-CWDA-2013-00058, Section 7.2.1
21	UncertMultiplier_ProduceUptake	\Dose_Parameter_Calculations\DoseParameters\HumanUptakeParameters	Described in SRR-CWDA-2013-00058, Section 7.2.1
22	UncertMultiplier_SoilUptake	\Dose_Parameter_Calculations\DoseParameters\HumanUptakeParameters	Described in SRR-CWDA-2013-00058, Section 7.2.1

Count	GoldSim Element Name	GoldSim Navigation Path	Basis for Distribution
23	UncertMultiplier_WaterUptake	\Dose_Parameter_Calculations\DoseParameters\HumanUptakeParameters	Described in SRR-CWDA-2013-00058, Section 7.2.1
24	FracLocalEgg_IHI	\Dose_Parameter_Calculations\DoseParameters\LocalFractionParameters	Described in SRR-CWDA-2013-00058, Section 7.6
25	FracLocalEgg_MOP	\Dose_Parameter_Calculations\DoseParameters\LocalFractionParameters	Described in SRR-CWDA-2013-00058, Section 7.6
26	FracLocalFished	\Dose_Parameter_Calculations\DoseParameters\LocalFractionParameters	Described in SRR-CWDA-2013-00058, Section 7.6
27	FracLocalMeat_IHI	\Dose_Parameter_Calculations\DoseParameters\LocalFractionParameters	Described in SRR-CWDA-2013-00058, Section 7.6
28	FracLocalMeat_MOP	\Dose_Parameter_Calculations\DoseParameters\LocalFractionParameters	Described in SRR-CWDA-2013-00058, Section 7.6
29	FracLocalMilk_IHI	\Dose_Parameter_Calculations\DoseParameters\LocalFractionParameters	Described in SRR-CWDA-2013-00058, Section 7.6
30	FracLocalMilk_MOP	\Dose_Parameter_Calculations\DoseParameters\LocalFractionParameters	Described in SRR-CWDA-2013-00058, Section 7.6
31	FracLocalPlants_IHI	\Dose_Parameter_Calculations\DoseParameters\LocalFractionParameters	Described in SRR-CWDA-2013-00058, Section 7.6
32	FracLocalPlants_MOP	\Dose_Parameter_Calculations\DoseParameters\LocalFractionParameters	Described in SRR-CWDA-2013-00058, Section 7.6
33	FracLocalPoultry_IHI	\Dose_Parameter_Calculations\DoseParameters\LocalFractionParameters	Described in SRR-CWDA-2013-00058, Section 7.6
34	FracLocalPoultry_MOP	\Dose_Parameter_Calculations\DoseParameters\LocalFractionParameters	Described in SRR-CWDA-2013-00058, Section 7.6
35	UncertMult_MEATFodderFraction	\Dose_Parameter_Calculations\DoseParameters\OtherUptakerParameters	Described in SRR-CWDA-2013-00058, Section 7.2.3
36	UncertMult_MILKFodderFraction	\Dose_Parameter_Calculations\DoseParameters\OtherUptakerParameters	Described in SRR-CWDA-2013-00058, Section 7.2.3
37	UncertMultiplier_FoddertoMEAT	\Dose_Parameter_Calculations\DoseParameters\OtherUptakerParameters	Described in SRR-CWDA-2013-00058, Section 7.2.2
38	UncertMultiplier_FoddertoMILK	\Dose_Parameter_Calculations\DoseParameters\OtherUptakerParameters	Described in SRR-CWDA-2013-00058, Section 7.2.2
39	UncertMultiplier_WatertoMEAT	\Dose_Parameter_Calculations\DoseParameters\OtherUptakerParameters	Described in SRR-CWDA-2013-00058, Section 7.2.2
40	UncertMultiplier_WatertoMILK	\Dose_Parameter_Calculations\DoseParameters\OtherUptakerParameters	Described in SRR-CWDA-2013-00058, Section 7.2.2
41	IrrigationRateUncert	\Dose_Parameter_Calculations\DoseParameters\SoilBuildupParameters	Described in SRR-CWDA-2013-00058, Section 7.5.1
42	SoilDensityUncert	\Dose_Parameter_Calculations\DoseParameters\SoilBuildupParameters	Described in SRR-CWDA-2013-00058, Section 7.5.1
43	WeatheringDecayConstUncert	\Dose_Parameter_Calculations\DoseParameters\SoilBuildupParameters	Described in SRR-CWDA-2013-00058, Section 7.5.1
44	SoilToPlant_Ratio_Uncert	\Dose_Parameter_Calculations\DoseParameters\TransferFactors	Described in SRR-CWDA-2013-00058, Section 7.3.1
45	TransferFactorFish_Uncert	\Dose_Parameter_Calculations\DoseParameters\TransferFactors	Described in SRR-CWDA-2013-00058, Section 7.3.4
46	TransferFactorMeat_Uncert	\Dose_Parameter_Calculations\DoseParameters\TransferFactors	Described in SRR-CWDA-2013-00058, Section 7.3.2
47	TransferFactorMilk_Uncert	\Dose_Parameter_Calculations\DoseParameters\TransferFactors	Described in SRR-CWDA-2013-00058, Section 7.3.3
48	WellDepth_Uncert	\Dose_Parameter_Calculations\DoseParameters\WellDepthParameters	Described in SRR-CWDA-2013-00058, Section

Count	GoldSim Element Name	GoldSim Navigation Path	Basis for Distribution
			7.5.3
49	Solubility	\GlobalModel_Input\Stochastic	Described in SRR-CWDA-2013-00062, Section 4.4.2.3
50	FlowFieldSampler	\GlobalModel_Input\Stochastic\FlowFieldByParameter	Described in SRR-CWDA-2014-00006, Section 5.6.3.1
51	InventoryUncertaintyCs135	\Inventory\InventoryUncertainty\FDCUncert	Described in SRR-CWDA-2009-00017, Section 5.6.3.2
52	InventoryUncertaintyI129	\Inventory\InventoryUncertainty\FDCUncert	Described in SRR-CWDA-2009-00017, Section 5.6.3.2
53	InventoryUncertaintyTc99	\Inventory\InventoryUncertainty\FDCUncert	Described in SRR-CWDA-2009-00017, Section 5.6.3.2
54	C14u	\Inventory\InventoryUncertainty\Vault1Uncert	Described in SRR-CWDA-2009-00017, Section 5.6.3.2
55	Cs137u	\Inventory\InventoryUncertainty\Vault1Uncert	Described in SRR-CWDA-2009-00017, Section 5.6.3.2
56	I129u	\Inventory\InventoryUncertainty\Vault1Uncert	Described in SRR-CWDA-2009-00017, Section 5.6.3.2
57	Np237u	\Inventory\InventoryUncertainty\Vault1Uncert	Described in SRR-CWDA-2009-00017, Section 5.6.3.2
58	Otheru	\Inventory\InventoryUncertainty\Vault1Uncert	Described in SRR-CWDA-2009-00017, Section 5.6.3.2
59	Pu239u	\Inventory\InventoryUncertainty\Vault1Uncert	Described in SRR-CWDA-2009-00017, Section 5.6.3.2
60	Sr90u	\Inventory\InventoryUncertainty\Vault1Uncert	Described in SRR-CWDA-2009-00017, Section 5.6.3.2
61	Tc99u	\Inventory\InventoryUncertainty\Vault1Uncert	Described in SRR-CWDA-2009-00017, Section 5.6.3.2
62	U238u	\Inventory\InventoryUncertainty\Vault1Uncert	Described in SRR-CWDA-2009-00017, Section 5.6.3.2
63	C14u	\Inventory\InventoryUncertainty\Vault4Uncert	Described in SRR-CWDA-2009-00017, Section 5.6.3.2
64	Cs137u	\Inventory\InventoryUncertainty\Vault4Uncert	Described in SRR-CWDA-2009-00017, Section 5.6.3.2
65	I129u	\Inventory\InventoryUncertainty\Vault4Uncert	Described in SRR-CWDA-2009-00017, Section 5.6.3.2
66	Np237u	\Inventory\InventoryUncertainty\Vault4Uncert	Described in SRR-CWDA-2009-00017, Section 5.6.3.2
67	Otheru	\Inventory\InventoryUncertainty\Vault4Uncert	Described in SRR-CWDA-2009-00017, Section 5.6.3.2
68	Pu239u	\Inventory\InventoryUncertainty\Vault4Uncert	Described in SRR-CWDA-2009-00017, Section

Count	GoldSim Element Name	GoldSim Navigation Path	Basis for Distribution
			5.6.3.2
69	Sr90u	\Inventory\InventoryUncertainty\Vault4Uncert	Described in SRR-CWDA-2009-00017, Section 5.6.3.2
70	Tc99u	\Inventory\InventoryUncertainty\Vault4Uncert	Described in SRR-CWDA-2009-00017, Section 5.6.3.2
71	U238u	\Inventory\InventoryUncertainty\Vault4Uncert	Described in SRR-CWDA-2009-00017, Section 5.6.3.2
72	FDCIndexer	\Inventory\Tank_to_FDC\TankAndFDCRandomization\FDCRandomizerLoop	Described in SRR-CWDA-2014-00006, Section 5.6.3.2
73	TankIndexer	\Inventory\Tank_to_FDC\TankAndFDCRandomization\TankRandomizerLoop	Described in SRR-CWDA-2014-00006, Section 5.6.3.2
74	Kd_Dist	\Materials\ClayeySoilKds	Described in SRR-CWDA-2009-00017, Section 5.6.3.3
75	Kd_Dist	\Materials\ClayeySoilKds_LeachateImpacted	Described in SRR-CWDA-2009-00017, Section 5.6.3.3
76	Kd_Dist	\Materials\Concrete_Kds_Oxidizing\middle_concrete_kds_ox	Described in SRR-CWDA-2009-00017, Section 5.6.3.3
77	SaltstoneKd_Dist_Sr	\Materials\Concrete_Kds_Oxidizing\middle_concrete_kds_ox	Described in SRR-CWDA-2009-00017, Section 5.6.3.3
78	SaltstoneKd_Dist_Tc	\Materials\Concrete_Kds_Oxidizing\middle_concrete_kds_ox	Described in SRR-CWDA-2009-00017, Section 5.6.3.3
79	Kd_Dist	\Materials\Concrete_Kds_Oxidizing\old_concrete_kds_ox	Described in SRR-CWDA-2009-00017, Section 5.6.3.3
80	Kd_Dist	\Materials\Concrete_Kds_Oxidizing\young_concrete_kds_ox	Described in SRR-CWDA-2009-00017, Section 5.6.3.3
81	SaltstoneKd_Dist_Sr	\Materials\Concrete_Kds_Oxidizing\young_concrete_kds_ox	Described in SRR-CWDA-2009-00017, Section 5.6.3.3
82	SaltstoneKd_Dist_Tc	\Materials\Concrete_Kds_Oxidizing\young_concrete_kds_ox	Described in SRR-CWDA-2009-00017, Section 5.6.3.3
83	Kd_Dist	\Materials\Concrete_Kds_Reducing\middle_concrete_kds_red	Described in SRR-CWDA-2009-00017, Section 5.6.3.3
84	SaltstoneKd_Dist_Sr	\Materials\Concrete_Kds_Reducing\middle_concrete_kds_red	Described in SRR-CWDA-2009-00017, Section 5.6.3.3
85	SaltstoneKd_Dist_Tc	\Materials\Concrete_Kds_Reducing\middle_concrete_kds_red	Described in SRR-CWDA-2009-00017, Section 5.6.3.3
86	Kd_Dist	\Materials\Concrete_Kds_Reducing\old_concrete_kds_red	Described in SRR-CWDA-2009-00017, Section 5.6.3.3
87	Kd_Dist	\Materials\Concrete_Kds_Reducing\young_concrete_kds_red	Described in SRR-CWDA-2009-00017, Section 5.6.3.3
88	SaltstoneKd_Dist_Sr	\Materials\Concrete_Kds_Reducing\young_concrete_kds_red	Described in SRR-CWDA-2009-00017, Section

Count	GoldSim Element Name	GoldSim Navigation Path	Basis for Distribution
			5.6.3.3
89	SaltstoneKd_Dist_Tc	\Materials\Concrete_Kds_Reducing\young_concrete_kds_red	Described in SRR-CWDA-2009-00017, Section 5.6.3.3
90	Kd_Dist	\Materials\SandySoilKds	Described in SRR-CWDA-2009-00017, Section 5.6.3.3
91	Kd_Dist	\Materials\SandySoilKds_LeachateImpacted	Described in SRR-CWDA-2009-00017, Section 5.6.3.3
92	SatThickness	\Transport\WaterTransport	Described in SRR-CWDA-2013-00062, Section 5.6.3
93	SatZoneDarcyVelDist	\Transport\WaterTransport	Described in SRR-CWDA-2009-00017, Section 5.6.3.8 Note: Most of the uncertainty associated with the saturated zone Darcy velocity is attributed to variability in conditions related to the flow fields. Therefore, when the flow field sampling was introduced (which resulted in flow field-specific Darcy velocities), the sampling distribution for this multiplier was revised to reduce the range of variability (i.e., instead of a standard deviation of 0.5, the standard deviation is now 0.1). In preparation of this RAI response, it was determined that this update to the model had not been captured in the associated model reports.

CC-3

CC-3	**Comment:** The DOE document SRR-CWDA-2013-00073 Rev. 2, described the column-by-column calculation of radionuclide transport through saltstone and the disposal structure in the GoldSim model. That document described that the analysis implicitly assumed that transport was due only to vertical advection. To simulate horizontal diffusion, Equation 3.2-1 in that document allowed the user to specify a percentage of a mixing cell's mass to be released to the UZ at cell-specific transition times. However, that document did not indicate the basis for Equation 3.2-1. In addition, it is not clear to the NRC staff whether that provision was used in the model runs in the DOE FY14 SDF Special Analysis document. If that provision was used by the DOE, then it is not clear to the NRC staff what range of values were used and the justification for those values. Provide the basis for Equation 3.2-1 in the DOE document SRR-CWDA-2013-00073. Clarify whether that provision in the DOE document SRR-CWDA-2013-00073 was used in the model runs in the DOE FY14 SDF Special Analysis document. If that provision was used in those model runs, then provide the DOE assumed percentage of mass transferred through diffusion and provide justification for that value.
	Basis: Not provided.
	Path Forward: Not provided.

DOE Response to CC-3

The GoldSim based Tc-99 release model, utilizes the GoldSim *Direct Transfer Mass Flux Link*, to implement a fractional release of Tc-99 in each cell near the outer perimeter of the saltstone monolith. This release is a conservative substitute for a fully radial or cross-sectional implementation of advective and diffusive transport, taking advantage of the dominance of vertical flow in the release of Tc-99 to the accessible environment. The fractional transfer rate (FTR) of Tc-99, described by Equation 3.2-1 (SRR-CWDA-2013-00073) is designed to release to the unsaturated zone a specified percentage of the mass in solution during the time step that the Tc-99 stored as a precipitate, dissolves during the transition from reducing conditions to oxidizing conditions. Equation 3.2-1 is similar to the first order decay rate used to implement a radionuclide half-life.

The definition of a first order decay rate (λ) for a radionuclide, can be written in the form:

$$\lambda = \frac{ln2}{T_{1/2}} \quad (1)$$

where $T_{1/2}$ is the half-life. The basis for Equation (1) is as follows:

$$e^{-\lambda t} = \frac{1}{2} \quad (2)$$

or inverting both sides of the equation

$$e^{\lambda t} = 2 \quad (3)$$

Taking the natural log of both sides of Equation (3) redefines the equation as

$$\lambda t = ln2 \quad (4)$$

and dividing both sides by t,

$$\lambda = \frac{ln2}{t} \quad (5)$$

Finally, when time (t) is equal to the half-life ($T_{1/2}$), then the decay rate (λ) defines how long it takes for one-half the mass to decay away

$$\lambda = \frac{ln2}{T_{1/2}} \quad (6)$$

Similarly, Equation (2) can be generalized and written in the form:

$$e^{-\lambda t} = \frac{1}{x} \quad (7)$$

where x is any number. Following the logic presented in Equations (3) – (6) a general decay rate for any fractional remainder ($1/x$) can be written as:

$$\lambda = \frac{lnx}{t} = \frac{lnx}{T_{1/x}} \quad (8)$$

with $1/x$ representing the fraction remaining. The form of the decay rate used in the GoldSim model can be written as:

$$FTR = \lambda = \frac{\ln \frac{1}{(100\% - \%_{Transferred})/100\%}}{T_{step}} \quad (9)$$

The natural log argument defines the inverse of the fraction of the mass remaining in the cell (i.e., ½, ¼, etc.) after a time step has passed. For example if the user wants to remove 25% of the mass in a mixing cell over the specific time step when the transition from reducing to oxidizing conditions occurs, the user inputs 25% into GoldSim and the argument of the natural log term in Equation (9) becomes 4/3. The time term (T_{step}) defines the time step over which the mass is removed. The model sets the decay rate to zero prior to and after the mass is removed during the time step when the transition time occurs. The decay rate is implemented in the GoldSim model using GoldSim's *Direct Transfer Mass Flux Link* as described in the *GoldSim Contaminant Transport Module User's Guide*. [GTG-2010e]

The *Direct Transfer Mass Flux Link* was implemented to allow mass to be released from the saltstone at or near the saltstone perimeter and at or near the fast zones within the saltstone. The logic for the percent released allows a fraction of the mass to be immediately removed from the SDU while a fraction remains and is still subject to advective migration. This immediate removal is not intended to accurately simulate diffusion, but provides a conservative release of mass to the UZ from the outer zones of saltstone and from the saltstone adjacent to the fast release zones at the time of the transition from the reducing to the oxidizing environment. The value used is 50%, based on the assumption that at the time of transition, the instantaneous mass release to the water would send a diffusive pulse in all directions, and the maximum portion of the newly exposed mass diffusing towards the exposed boundary would be approximately 50%. Peaks observed in benchmarking runs indicate that this is a reasonable assumption (see Section 5.6.2 of the FY2014 SDF SA).

Also note that this version of the model was developed with the intention of minimizing the computational effort involved in representing the non-linear processes of importance and still reasonably approximate the conceptual model. Single realization PORFLOW runs with all processes considered, can take well over a week to run.

The only instance within the FY2014 SDF SA in which the GoldSim model was modified to allow a different percentage of mass to be transferred was within the sensitivity analysis in Section 5.6.6.2. In this analysis, not only were various percentages applied (0%, 25%, 50%, 75%, and 100%), but the logic was also modified. Where the Evaluation Case (and all other GoldSim modeling cases) only applied the instantaneous mass-transfer logic to the model cells undergoing oxidation at the periphery of the saltstone, this analysis applied the instantaneous mass-transfer to all of the model cells undergoing oxidation, regardless of location within the SDU. This approach provided a simplified evaluation of oxygen-controlled release of precipitated Tc-99 and the subsequent release of dissolved Tc-99 from a highly fractured system.

CC-4

CC-4	**Comment:** The DOE document SRR-CWDA-2013-00073 Rev. 2, described that the transition time for Tc oxidation was calculated by the FORTRAN dynamic link library (DLL). That document indicated that the DLL: (1) calculated the time required for oxidation due to vertical flow, (2) calculated the time required for oxidation due to horizontal flow, and (3) used the minimum of those two values as the transition time. It appears to the NRC staff that both horizontal and vertical flow would occur and the transition time would be calculated from the combination of those two factors, not the minimum of each separately considered factor. Please clarify how the process the DLL used to calculate the Tc transition times accounted for the combined effects of horizontal and vertical flow.
	Basis: Not provided.
	Path Forward: Not provided.

DOE Response to CC-4

As described in SRR-CWDA-2013-00073, Rev. 2, the GoldSim SDF Tc-99 Release Model is comprised of two components, (1) a GoldSim module, which evaluates the migration of Tc-99 transport through the individual SDUs, and (2) a FORTRAN dynamic link library (DLL) which evaluates the oxygen front movement through the SDUs and the associated oxidation of slag to develop cell-by-cell solubility-control mechanism transition times.

The data requirements of the GoldSim SDF Tc-99 Release model include the cell-specific transition times associated with oxidation of reducing slag. For each cell, the transition time represents the time at which all of the slag in the cell has been oxidized. These times can be generated by PORFLOW, but the length of time needed for PORFLOW to calculate each simulated realization limits the number of realizations that can be considered. For instance, the PORFLOW Tc-99 release simulations (for all SDUs) took approximately 24 days to complete. To allow for a reasonable number of samplings for parameters that influence transition times such as flow fields, a FORTRAN DLL, *TransitionTime.dll* (Version 1.0), which evaluates cell-by-cell solubility-control transition times was developed.

The DLL, *TransitionTime.dll*, is based upon the assumption that advection controls the oxygen front propagation. The transition time calculations proceed by following the oxygen front through each modeled cell (vertically then horizontally) and choosing the minimum time needed to go through a cell, by either of the two processes, as the transition time. In the vertical direction, the oxygen front positions are determined by assuming purely advective retarded transport from cell to cell from the top of the saltstone to the bottom of the floor (or floor and upper mud mat [UMM] layers). In the horizontal direction, the oxygen front positions are determined by assuming purely advective retarded transport from cell to cell proceeding from the outside of the wall into the saltstone and from the column zone (or crack/fracture zone) edges towards the inside and outside of the zone. The saltstone grout and concrete retardation values are based upon the ratios of the O_2 saturation to the saltstone and concrete reducing capacities.

The GoldSim model is a simplification of the PORFLOW model -- which is why benchmarking is important to demonstrate that the simplification is still an adequate representation despite not

rigorously representing all physical processes. In order to abstract a computationally efficient version of a complex (multi-dimensional) nonlinear system the process of flow was directionally decoupled. Assuming a one-dimensional (advection-only) process, the nonlinear aspects of the system can be replaced by using the relationship between oxygen solubility and reducing capacity to generate a factor which increases the storage capacity of a set of cells linked in series. From a one-dimensional perspective this is mathematically equivalent to increasing the length of each cell (segment of the pathway) and retaining the same velocity. It is then easy to calculate the time it takes to go from one cell face to the next at a specified velocity. The geometry of each string of cells reflects the structure of the discretized PORFLOW model. As the NRC correctly points out, this does not provide the mixing numerically approximated by a more rigorous model such as a finite difference model where mass moving to and from surrounding cells is mixed together to determine the concentration in each cell. On the other hand this does alleviate the need for dealing with the nonlinearity associated with the time-variant decrease in reducing capacity. This spatial decoupling could have a non-conservative influence on the calculated transition times relative to a model where full mixing takes place in a cell. To help offset the non-conservative nature of the calculations, two approximations were added to the calculations. First, in calculating the transition times based on vertical flow, the horizontal component of flow is assumed to add oxygen (at the solubility limit) to a cell during the time period that the reducing capacity is depleted. The second approximation is applied during the horizontal pathway calculations. This approximation compares the previously calculated (from the vertical pathway) transition time in a cell to the newly calculated value and uses the earliest time as a starting time for the downgradient cell calculation. Note that full mixing in a cell would generate numerical dispersion and a potentially conservative error. The degree of error was examined by comparing results from the GoldSim/DLL model with PORFLOW.

As can be seen in Figure CC-4.1 (Figure 5.6.2-31, SRR-CWDA-2014-00006, Rev. 2), the timing of the release of Tc-99 to the saturated zone for the 150-foot diameter SDUs for the GoldSim modeling closely matches the timing of the PORFLOW modeling. Much of the difference between the GoldSim and PORFLOW results can be attributed to the different manner in which the release from storage at a transition time (for the GoldSim model) or during a span of time (for the PORFLOW model), takes place. Figure CC-4.2, showing a comparison of the total release of Tc-99 over time, eliminates some of the differences attributable to the release methods and as can be seen, indicates that the total releases by the two models are similar. Therefore, selecting the minimum transition time for either vertical or horizontal flow from GoldSim provides an acceptable representation of the Tc-99 release.

Figure CC-4.1: SDU 3A Tc-99 Release to the Saturated Zone

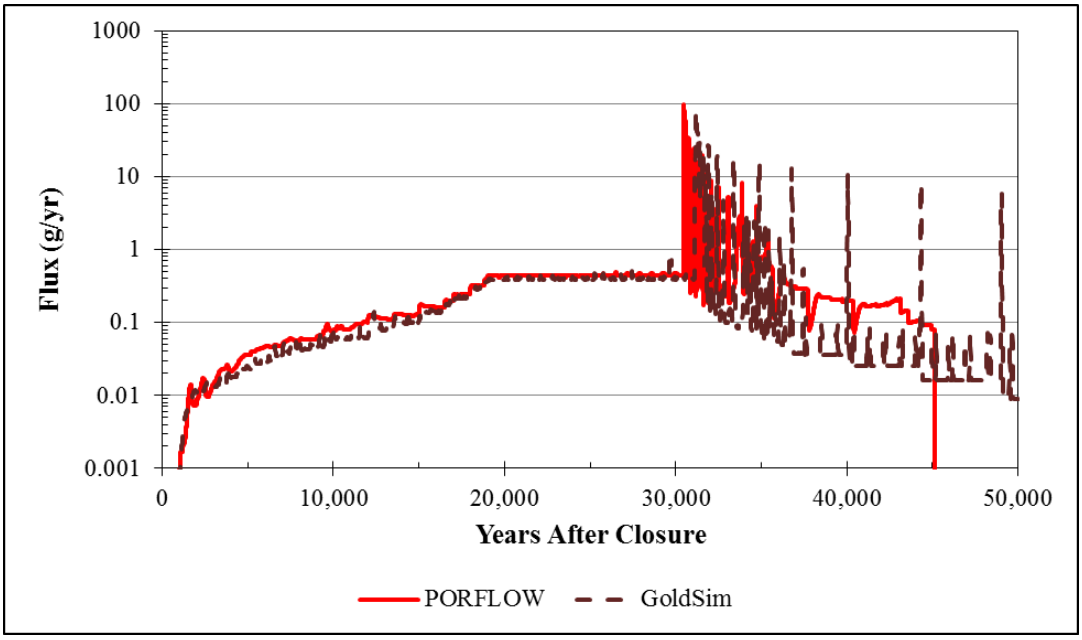

Figure CC-4.2: SDU 3A Tc-99 Release to the Saturated Zone

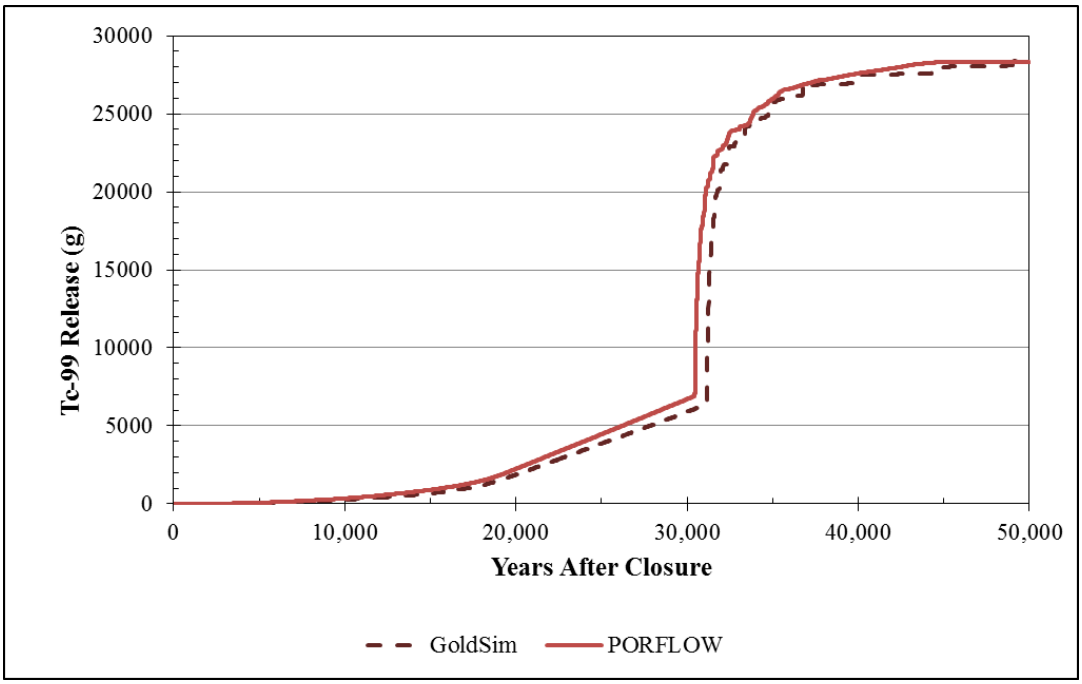

CC-5

CC-5	**Comment:** Additional information is needed about the configuration of the waterstop in the floor shown in Figure 3.3-6 of the DOE FY14 Special Analysis document. That figure showed that the floor segment above the waterstop has two joints (i.e., the concrete segment above the waterstop is separated from the main floor by the joints). It is not clear to the NRC staff how that piece of the floor is connected to the rest of the disposal structure. Please clarify as to whether all joints around waterstops in the disposal structure have two joints on one side and one joint on the other side of the waterstop, or if the joints around the waterstops in the floor are an exception.
	Basis: Not provided.
	Path Forward: Not provided.

DOE Response to CC-5

Figure 3.3-6 of the FY2014 SDF SA should have shown only a vertical joint extending above and below the waterstop. Figure CC-5.1 shows the design drawing of the waterstops for the floor of SDU 6. [C-CC-Z-00044] The trapezoidal shape above the waterstop was intended to define a step within the pouring process (ensuring that the concrete is placed up to the vertical mid-plane of the water stop). However, the bold lines outlining the floor slab indicate that the entire floor segment is created as a single pour with only the vertical joint extending above and below the waterstops. Figure CC-5.2 shows the actual placement of a waterstop in a floor joint during the construction of SDU 6. Slabs with waterstops for the roof and walls for SDU 6 were constructed in a similar manner.

Figure CC-5.1: Construction Design of Waterstops for Floor of SDU 6

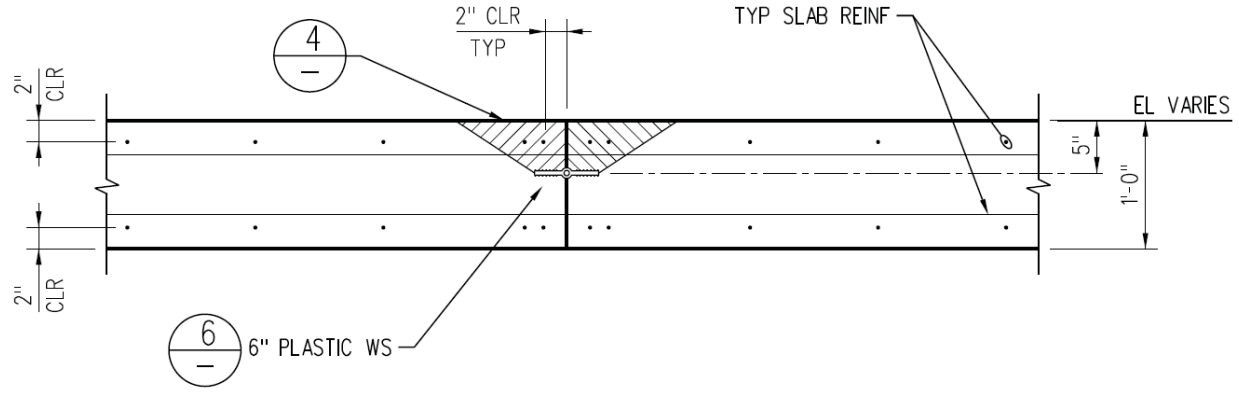

[C-CC-Z-00044]

Figure CC-5.2: Detail of SDU 6 Floor Construction with Waterstops

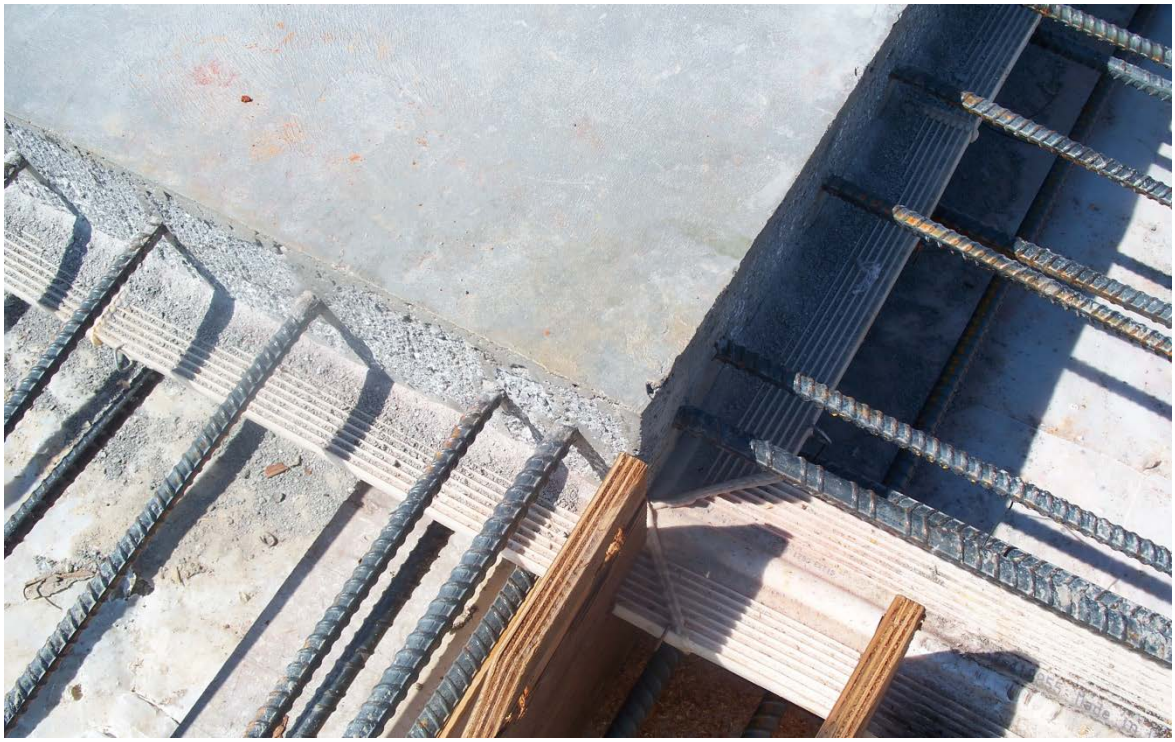

In PORFLOW, the waterstops are modeled as vertical joints (i.e., essentially modeled as vertical gaps in the concrete, filled with gravel and having the hydraulic properties of gravel). The walls of the SDU are connected to the floor of the SDU via vertical tensioning rods. These vertical rods, along with the horizontal wire wrapping are designed to put the unit under tension to minimize any potential cracks or releases through water stops.

CC-6

CC-6	**Comment:** Table 23 in the DOE document SRNL-STI-2009-00473 indicated that the leachate impacted values for iodine should be 0.1 for clay and 0.0 for sand. However, Table 4.1-3 in the DOE FY14 SDF Special Analysis document has K_d values of 0.3 for clay and 0.1 for sand. Please clarify how and why those values have changed.
	Basis: Not provided.
	Path Forward: Not provided.

DOE Response to CC-6

As described in Sections 4.2.4 and 4.2.5 of the *Geochemical Data Package for Performance Assessment Calculations Related to the Savannah River Site* (SRNL-STI-2009-00473), the leachate-impacted K_d values are determined as the product of the non-impacted K_d values and the cement leachate impact factors. (See the RAI response to FFT-6 for more detail.) Table 13 of SRNL-STI-2009-00473 indicated that the "Best" iodine K_d values for sand and clay are 0.3 mL/g and 0.9 mL/g, respectively. The table also indicates that the cement leachate impact factor for iodine is 0.1. Therefore, based on SRNL-STI-2009-00473, the leachate-impacted iodine K_d values for sand and clay were actually 0.03 mL/g and 0.09 mL/g, respectively. Table 23 displayed these values to the nearest tenth, such that the reported values for the leachate-impacted iodine K_d values for sand and clay are 0 mL/g and 0.1 mL/g, respectively.

Table 4.1-3 of the FY2014 SDF SA shows that the recommended, non-leachate impacted sandy soil and clayey soil K_d values for iodine have been updated. Rather than referencing SRNL-STI-2009-00473, data from a more recent site-specific iodine study, *Radioiodine Geochemistry in the SRS Subsurface Environment*, is referenced in the table. [SRNL-STI-2012-00518] This new reference indicates that for iodine in SRS soils, the best sandy soil K_d is 1.0 mL/g and the best clayey soil K_d is 3.0 mL/g. The cement leachate impact factor was not updated. Therefore, the resulting leachate-impacted K_d values for sand and clay are 0.1 mL/g and 0.3 mL/g, respectively.

CC-7

CC-7	**Comment:** Table 4.1-3 in the DOE FY14 Special Analysis document showed distribution coefficients for sandy and clayey soils. Please clarify whether the information below, which the NRC staff understands to be true, is correct for the DOE modeling effort: • Values for no leachate impacted clayey soils were applied to the saturated portion of the TCCZ and the Green Clay (Gordon Confining Unit). • Values for leachate impacted clayey soils were applied to the unsaturated portion of the TCCZ and the surrounding backfill. • Values for no leachate impacted sandy soils were applied to the saturated portion of the UTR Aquifer. • Values for leachate impacted sandy soils were applied to the unsaturated portion of the UTR Aquifer.
	Basis: Not provided.
	Path Forward: Not provided.

DOE Response to CC-7

PORFLOW simulates transport via the near field model (i.e., "vadose zone transport") and the far field model (i.e., the "aquifer transport"). Both models apply a discrete set of K_d values for sandy soil (native soil) and clayey soil (backfill).

The PORFLOW vadose zone transport model applies the leachate-impacted K_d values to the backfill and native soil everywhere. The leachate-impact assignments are made without consideration of geologic formation or saturation state, as the majority of the model only contains backfill (clay) or vadose zone soil (sand). For example, if the TCCZ is present in the vadose zone model then it gets a leachate-impacted K_d for clay.

The PORFLOW aquifer transport model uses the non-leachate-impacted K_d values everywhere, including the unsaturated zone (where no contamination resides because sources are placed beneath the water table). Moving from a disposal unit toward McQueen Branch through the TCCZ, the non-leachate-impacted K_ds are used over the entire distance in the aquifer model, even if the TCCZ rises above the water table.

For the GoldSim model, all of the bullets above are correct, with the exception of the TCCZ portion of the second bullet. The water table is a single specified depth above the TCCZ in the GoldSim model.

It should be noted that the leachate-impacted values for sands and clays only apply when the saltstone remains in Reduced Region II conditions; however, this transition from Reduced Region II to Oxidized Region II does not occur until well beyond 10,000 years.

CC-8

CC-8	**Comment:** The NRC staff understands that volumetric flow is a key factor in determining if distribution coefficients are considered leachate impacted. The SZ is not considered impacted due the quantity of water that dilutes the leachate. Please clarify the criterion or cutoff value for a medium to be considered impacted by leachate (e.g., any unit containing leachate that is less than saturated is considered leachate impacted). Please clarify the criterion for making that determination and the basis for that criterion.
	Basis: Not provided.
	Path Forward: Not provided.

DOE Response to CC-8

For the assignment of leachate impacted distribution coefficients versus non-leachate impacted distribution coefficients, the assignments were based on specific modeling domains and the chemical environment within the overlying saltstone. As stated in the response to CC-7, within PORFLOW's vadose zone transport model, any soil material above the water table horizon (whether it be sand or clay) is assumed to be leachate impacted at the start of the simulation. As described in Section 4.1.2 of the FY2014 SDF SA, fluid that passes through the saltstone becomes chemically altered to be a high pH leachate. This same fluid infiltrates through the floor, the mud mats, and into the underlying vadose zone soils. Therefore, the leachate-impacted conditions are imparted onto the vadose zone soils and held until the overlying saltstone monolith transitions from middle aged (Oxidized Region II) to old aged (Oxidized Region III). This saltstone transition does not occur within the performance period or within the simulation period, so this change is not observed within the results of the FY2014 SDF SA.

CC-9

CC-9	**Comment:** Section 5.6.2.3.1 of the DOE FY14 SDF Special Analysis document included that: "Because of the influences of the column zone on the saltstone flow domain, the saltstone is divided into two rectangles (central and outer) for [SDS 1 and SDS 4] and two cylinders (inner and outer cylinder) for the other [disposal structures]." Please clarify the DOE basis for modeling SDS1 with two rectangles (central and outer), even though there are no columns in SDS 1.
	Basis: Not provided.
	Path Forward: Not provided.

DOE Response to CC-9

The next to the last sentence in the third paragraph of Section 5.6.2.3.1 of the FY2014 SDF SA has an error in it and should read "To represent the influences of columns as potential vertical fast flow pathways in the saltstone flow domain, the saltstone in SDU 4 is divided into two rectangles with a column zone sandwiched between. Like SDU 4, the saltstone in SDU 1 is divided into two rectangles, but the zone sandwiched between represents either saltstone or a crack/fracture zone to allow the model to be used to evaluate the potential influence of a vertical fast flow pathway if desired. The other SDU's are based on a cylindrical design, with the 150-foot diameter and 375-foot diameter SDUs divided into two cylinders (an inner and outer cylinder) with a column zone sandwiched between. "

CC-10

CC-10	**Comment:** Section 03740 in document C-SPP-Z-00008, Rev. 3 contained information about "Crack Repair Epoxy Injection Grouting." Please provide further details under what circumstances that epoxy injection grouting might occur.
	Basis: Not provided.
	Path Forward: Not provided.

DOE Response to CC-10

Per C-SPP-Z-00008, Rev. 3, Crack Repair Epoxy Injection Grouting is used to repair visible cracks in containment structures during SDU construction that are 0.005 inch wide and wider, cracks that leak, spalls, chips, embedded debris, sand streaks, mortar leakage from form joints, deviations in formed surface that exceed specified tolerances and include but are not limited to fins, form pop-outs, and other projections. Epoxy Injection Grouting is also used to repair surface defects that include honeycomb, rock pockets, indentations, and surface voids smaller than 3/8 inch deep and greater than 3/16 inch deep, surface voids greater than 5/8 inch and smaller than 1 inch in diameter.

During construction of SDU 6, these methods were employed primarily on construction related imperfections noted above and surface defects intentionally caused to support construction activities (e.g., nail holes, drill holes etc.).

CC-11

CC-11	**Comment:** Section 3.3.1.2 of the DOE FY14 SDF Special Analysis document indicated that the 375-foot disposal structures will have 2-inch thick bearing pads made out of neoprene and sponge rubber positioned between the floor and the wall. The NRC staff expects that the weight of the wall and roof will compress the bearing pads to a smaller thickness. It is not clear to the NRC staff how the potential effects on the structural integrity of the wall due to settlement caused by decreasing thickness of the bearing pads was evaluated and incorporated into the DOE projections of SDF performance. Please clarify what the DOE has done in the past and what the DOE intends to do in the future regarding this.
	Basis: Not provided.
	Path Forward: Not provided.

DOE Response to CC-11

The structural integrity of the walls is not expected to be compromised by the compression of the bearing pad. Compression is part of the design of the 375-foot diameter SDU. Construction of the walls includes vertical post-tensioning, which is intended to maintain the structural integrity of the walls prior to roof emplacement. [C-SPP-Z-00008; C-CC-Z-00042] After wall and roof construction, a liquid tightness test shall confirm that the integrity of the walls has not been compromised. [C-CC-Z-00039]

REFERENCES FOR COMMENT RESPONSES

10 CFR 61, *Licensing Requirements for Land Disposal of Radioactive Waste*, U.S. Nuclear Regulatory Commission, Washington DC, December 22, 2011.

Buol, S.W., et al., (Copyright) *Soil Genesis and Classification*, Iowa University Press, Ames, 1973.

Buol S.W., et al. (Copyright) *Soil Genesis and Classification*, Iowa University Press, Ames, 2011.

C-CC-Z-00039, *Z-Area Saltstone Disposal Site SDU6 Tank Design Concrete Foundation Plan*, Savannah River Site, Aiken, SC, Rev. 0, November 9, 2012.

C-CC-Z-00042, *Z-Area Saltstone Disposal Site SDU6 Tank Design Concrete Wall Column Section Details*, Savannah River Site, Aiken, SC, Rev. 0, November 9, 2012.

C-CC-Z-00044, *Z Area Saltstone Disposal Site SDU6 Tank Design Concrete Sections and Details*, Savannah River Site, Aiken, SC, Rev. 0, November 9, 2012.

C-CY-Z-00007, *Z Area Saltstone Disposal Site SDU6 Tank Design Civil Leakage Detection and Settlement Monitoring Section and Details*, Savannah River Site, Aiken, SC, Rev. 0, November 9, 2012.

C-SPP-Z-00008, *Saltstone Disposal Site - SDU6 Procurement Specification*, Savannah River Site, Aiken, SC, Rev. 3, September 9, 2013.

DHEC-OS-08-28-2013-01, *Savannah River Site Liquid Waste Milestones*, Letter C.B. Templeton (SCDHEC) to Dr. E. Moniz, (Secretary U.S. DOE) dated August 28, 2013), South Carolina Department of Health and Environmental Control, Columbia, SC, August 28, 2013.

DOE M 435.1-1, Change 1, *Radioactive Waste Management Manual*, U.S. Department of Energy, Washington DC, June 19, 2001.

DOE O 435.1, Change 1, *Radioactive Waste Management*, U.S. Department of Energy, Washington DC, August 28, 2001.

DOE O 458.1, Chg. 3, *Radiation Protection of the Public and the Environment*, U.S. Department of Energy, Washington DC, January 15, 2013.

DOE/EIS-0082-S2, *Savannah River Site Salt Processing Alternatives Supplemental Environmental Impact Statement*, U.S. Department of Energy, Washington DC, June 2001.

DOE/EIS-0082-S2-SA-01, *Supplement Analysis, Salt Processing Alternatives at the Savannah River Site*, U.S. Department of Energy, Washington DC, January 2006.

DOE-HDBK-1215-2014, *DOE Handbook, Optimizing Radiation Protection of the Public and the Environment for Use with DOE O 458.1, ALARA Requirements*, U.S. Department of Energy, Washington DC, October 31, 2014.

DPST-86-426, *Z Area Site Assessment*, Savannah River Site, Aiken, SC, May 8, 1986.

GTG-2010e, (Copyright), *GoldSim User's Guide, GoldSim Containment Transport Module*, Version 6.0, GoldSim Technology Group LLC, Issaquah, WA, December 2010.

ISBN: 0-13-365312-9, (Copyright), Freeze, R.A. and Cherry, J.A., *Groundwater*, Prentice Hall, Englewood Cliffs, NJ, 1979.

Jenny, H., (Copyright), *Factors of Soil Formation: A System of Quantitative Pedology*, Dover Press, 1994.

K-ESR-Z-00001, *Saltstone Vault No. 2 Geotechnical Investigation Report*, Savannah River Site, Aiken, SC, Rev. 0, April 2006.

K-ESR-Z-00002, *Saltstone Disposal Cells No. 3 and 5 Geotechnical Investigation Report*, Savannah River Site, Aiken, SC, July 2009.

K-ESR-Z-00003, *Saltstone Disposal Unit No. 1 Updated Settlement Analysis Report*, Savannah River Site, Aiken, SC, Rev. 0, December 2010.

K-ESR-Z-00005, *Saltstone Disposal Unit 6 Geotechnical Investigation Report*, Savannah River Site, Aiken, SC, Rev. 0, April 2012.

Lukens, W.W., et al., (Copyright) *Evolution of Technetium Speciation in Reducing Grout*, Environ. Sci. Technol. 39:8064-8070, 2005.

Manual E7-1, Procedure DE-DP-384, *ALARA Design Considerations and Reviews*, Savannah River Site, Aiken, SC, Rev. 1, November 20, 2008.

Manual SCD-6, *SRS ALARA Program*, Savannah River Site, Aiken, SC, Rev. 4, October 2, 2007.

ML073510127, *Recommended Site-Specific Sorption Coefficients for Reviewing Non-High-Level Waste Determinations at the Savannah River Site and Idaho National Laboratory*, U.S. Nuclear Regulatory Commission, Washington DC, October 2007.

ML14148A153, *U.S. Nuclear Regulatory Commission Staff Comments and Requests for Additional Information on the Fiscal Year 2013 Special Analysis for the Saltstone Disposal Facility at the Savannah River Site, SRR-CWDA-2013-00062, Revision 2*, U.S. Nuclear Regulatory Commission, Washington, DC, June 13, 2014.

ML15161A541, *U.S. Nuclear Regulatory Commission Staff Comments and Requests for Additional Information on the Fiscal Year 2014 Special Analysis for the Saltstone Disposal Facility at the Savannah River Site, SRR-CWDA-2014-00006, Revision 2*, U.S. Nuclear Regulatory Commission, Washington, DC, June 26, 2015.

N-CLC-Z-00027, Broome, M.A., *Saltstone Disposal Unit (SDU) 6 Dose Rate and Bulk Shielding Evaluation*, Savannah River Site, Aiken, SC, Rev. 0, July 2013.

NCRP-160, (Copyright), *Ionizing Radiation Exposure of the Population of the United States: Recommendations of the National Council on Radiation Protection and Measurements*, Bethesda, MD, March 2009.

NDAA_3116, *Public Law 108-375, Ronald W. Reagan National Defense Authorization Act for Fiscal Year 2005, Section 3116, Defense Site Acceleration Completion*, October 28, 2004.

NRC_01-01-2011, *Biological Effects of Radiation*, U.S. Nuclear Regulatory Commission, Washington DC, January 2011.

PIT-MISC-0124, Aadland, R.K., et al., *Hydrogeologic Framework of West-Central Savannah River Area, South Carolina and Georgia*, Savannah River Site, Aiken, SC, December 1995.

PNNL-16663, Cantrell, K.J., et al, *Geochemical Processes Data Package for the Vadose Zone in the Single-Shell Tank Waste Management Areas at the Hanford Site*, Pacific Northwest National Laboratory, Richland, WA, Rev. 0, September 2007.

SREL Doc. R-13-0005, Seaman, J.C. and Chang, H., *Impact of Cementitious Leachate on Se, Nb and Ra Partitioning*, Savannah River Ecology Laboratory, Aiken, SC, Rev. 1, September 2013.

SREL Doc R-16-004, Seaman, J.C., *SREL FY16 Test Plan: Chemical and Physical Properties of ^{99}Tc-Spiked Saltstone*, University of Georgia, Savannah River Ecology Laboratory, Ver. 1.0, 2015.

SRNL-STI-2009-00115, Flach, G.P., et al., *Numerical Flow and Transport Simulations Supporting the Saltstone Disposal Facility Performance Assessment*, Savannah River Site, Aiken, SC, Rev. 1, June 17, 2009.

SRNL-STI-2009-00473, Kaplan, D.I., *Geochemical Data Package for Performance Assessment Calculations Related to the Savannah River Site*, Savannah River Site, Aiken, SC, Rev. 0, March 15, 2010.

SRNL-STI-2009-00572, Whiteside, T., et al, *Evaluation of HELP Model Replacement Codes*, Savannah River Site, Aiken, SC, Rev. 0, July 2009.

SRNL-STI-2009-00637, Roberts, K.A. and Kaplan, D.I., *Reduction Capacity of Saltstone and Saltstone Components*, Rev. 0, Savannah River National Laboratory, Aiken, SC, November 2009.

SRNL-STI-2010-00493, Seaman, J.C. and Kaplan, D.I., *Chloride, Chromate, Silver, Thallium, and Uranium Sorption to SRS Soils, Sediments, and Cementitious Materials*, Savannah River Site, Aiken, SC, Rev. 0, September 29, 2010.

SRNL-STI-2011-00011, Kaplan, D.I., *Estimated Neptunium Sediment Sorption Values as a Function of pH and Measured Barium and Radium K_d Values*, Savannah River Site, Aiken, SC, Rev. 0, January 23, 2011.

SRNL-STI-2011-00672, Almond, P.M., et al., *Variability of K_d Values in Cementitious Materials and Sediments*, Savannah River Site, Aiken, SC, Rev. 0, January 2012.

SRNL-STI-2012-00518, Kaplan, D.I., et al, *Radioiodine Geochemistry in the SRS Subsurface Environment*, Savannah River Site, Aiken, SC, Rev. 0, May 2013.

SRNL-STI-2012-00769, Kaplan, D.I. and Dien, L., *Solubility of Technetium Dioxides (TcO2-c, TcO2 1.6H2O and TcO2 2H2O) in Reducing Cementitious Material Leachates: A Thermodynamic Calculation*, Savannah River Site, Aiken, SC, Rev. 1, February 1, 2013.

SRNL-STI-2013-00541, Langton, C.A. and Almond, P.M., *Cast Stone Oxidation Front Evaluation: Preliminary Results for Samples Exposed to Moist Air*, Rev. 0, Savannah River National Laboratory, Aiken, SC, November 2013.

SRNL-STI-2014-00083, Flach, G.P. *PORFLOW Modeling Supporting the FY14 Saltstone Special Analysis*, Savannah River Site, Aiken, SC, Rev. 1, April 2014.

SRNS-RP-2015-00902, *Z-Area Groundwater Characterization Data Report*, Savannah River Site, Aiken, SC, Rev. 0, January 2016.

SRNS-STI-2008-00045, *Saltstone and Concrete Interactions with Radionuclides: Sorption (Kd), Desorption, and Reduction Capacity Measurements*, Rev. 0, Savannah River National Laboratory, Aiken, SC, October 2008.

SRNS-TR-2013-00275, *Z-Area Saltstone Disposal Facility Groundwater Monitoring Report for 2013*, Savannah River Site, Aiken, SC, January 2014.

SRNS-TR-2014-00283, *Z-Area Saltstone Disposal Facility Groundwater Monitoring Report for 2014*, Savannah River Site, Aiken, SC, January 2015.

SRNS-TR-2015-00300, *Z-Area Saltstone Disposal Facility Groundwater Monitoring Report for 2015*, Savannah River Site, Aiken, SC, January 2016.

SRR-CWDA-2009-00017, *Performance Assessment for the Saltstone Disposal Facility at the Savannah River Site*, Savannah River Site, Aiken, SC, Rev. 0, October 29, 2009.

SRR-CWDA-2011-00044, *Comment Response Matrix for Nuclear Regulatory Commission RAI-2009-02 Second Request for Additional Information (RAI) on the Saltstone Disposal Facility Performance Assessment (SRR-CWDA-2009-00017, Revision 0, dated October 29, 2009)*, Savannah River Site, Aiken, SC, Rev. 1, August 25, 2011.

SRR-CWDA-2013-00058, Hommel, S., *Dose Calculation Methodology for Liquid Waste Performance Assessments at the Savannah River Site*, Savannah River Site, Aiken, SC, Rev. 1, July 2014.

SRR-CWDA-2013-00062, *FY2013 Special Analysis for the Saltstone Disposal Facility at the Savannah River Site*, Savannah River Site, Aiken, SC, Rev. 2, October 3, 2013.

SRR-CWDA-2013-00073, Lester, B., *Updates to the Saltstone Disposal Facility Stochastic Fate and Transport Model*, Savannah River Site, Aiken, SC, Rev. 2, August 2014.

SRR-CWDA-2014-00006, *FY2014 Special Analysis for the Saltstone Disposal Facility at the Savannah River Site*, Savannah River Site, Aiken, SC, Rev. 2, September 2014.

SRR-CWDA-2014-00095, *Saltstone Disposal Facility Sensitivity Modeling to Address Concerns Related to Saturated Zone Transport*, Savannah River Site, Aiken, SC, Rev. 1, January 2015.

SRR-CWDA-2014-00099, *Comment Response Matrix for U.S. Nuclear Regulatory Commission Staff Request for Additional Information on the Fiscal Year 2013 Special Analysis for the Saltstone Disposal Facility at the Savannah River Site*, Savannah River Site, Aiken, SC, Rev. 1, January 2015.

SRR-CWDA-2014-00121, *Dataset for the FY2014 SDF Special Analysis Modeling*, Savannah River Site, Aiken, SC, January 8, 2015.

SRR-SDU-2012-00052, *ALARA Design Review for SDU 6 CD-2/3*, Savannah River Site, Aiken, SC, September 6, 2012.

WSRC-RP-2005-01674, Kaplan, D.I., et. Al., *Estimated Duration of the Reduction Capacity within a High-Level Waste Tank*, Rev. 0, Savannah River Site, Aiken, SC, August 2005.

WSRC-STI-2006-00198, *Hydraulic Property Data Package for the E-Area and Z-Area Soils, Cementitious Materials, and Waste Zones,* Savannah River Site, Aiken, SC, September 2006.

WSRC-STI-2007-00184, *FTF Closure Cap Concept and Infiltration Estimates,* Savannah River Site, Aiken, SC, Rev. 2, October 15, 2007.

WSRC-STI-2008-00244, *Saltstone Disposal Facility Closure Cap Concept and Infiltration Estimates*, Savannah River Site, Aiken, SC, Rev. 0, May 30, 2008.

WSRC-TR-2005-00101, *Scoping Study: High Density Polyethylene (HDPE) in Saltstone Service,* Savannah River Site, Aiken, SC, Rev. 0, February 18, 2005.

WSRC-TR-2007-00283, Millings, M.R. and Flach, G.P., *Hydrogeologic Data Summary In Support of the F-Area Tank Farm (FTF) Performance Assessment (PA),* Savannah River Site, Aiken, SC, Rev. 0, July 2007.

X-ESR-H-00665, Smith, T.E., *Engineering Evaluation of the Next Generation Solvent Demonstration,* Savannah River Site, Aiken, SC, Rev. 0, May 26, 2014.

X-SD-Z-00001, *Waste Acceptance Criteria for Aqueous Waste Sent to the Z-Area Saltstone Production Facility,* Savannah River Site, Aiken, SC, Rev. 15, January 4, 2016.